
**Water quality and pollutant dynamics in the Three Gorges
Reservoir on the Yangtze River, China**

~~~~~

**Wasserqualität und Schadstoffdynamik im Drei-  
Schluchten-Reservoir am Yangtze, China**

---

Zur Erlangung des akademischen Grades eines

DOKTORS DER NATURWISSENSCHAFTEN

von der Fakultät für

Bauingenieur-, Geo- und Umweltwissenschaften

des Karlsruher Instituts für Technologie (KIT)

genehmigte

DISSERTATION

von

Diplom-Geoökologe Andreas Holbach

aus Karlsruhe

Tag der mündlichen Prüfung: 17.11.2015

Referent: PD Dr. Stefan Norra

Korreferent: Prof. Dr. Jörg Schäfer

Karlsruhe den 01.02.2016

---

**für Rachel und Amelie**

---

## **Erklärung**

---

Hiermit erkläre ich, dass ich die vorliegende Dissertation, abgesehen von der Benutzung der von mir vollständig und genau bezeichneten Hilfsmittel, selbstständig verfasst und die Grundsätze des Karlsruher Instituts für Technologie (KIT) zur Sicherung guter wissenschaftlicher Praxis in ihrer aktuell gültigen Fassung beachtet habe.

Karlsruhe den 01.02.2016

---

gez. Andreas Holbach

## Die Sprache des Wassers — The language of water

---

Stille Wasser sind tief,  
tiefe Wasser nicht unbedingt still.  
Doch ihre uns fremde Sprache verhallt,  
findet unverstanden kein Gehör.  
Darum übersetzen wir mit vollem Einsatz!  
Und letztendlich bleibt doch nur dieses einzige einfache Wort.  
Muss ich *Hilfe!* in fremder Sprache wirklich kennen  
um es zu verstehen?

~~~~~

Still waters run deep,
deep waters not implicitly still.
Their foreign language fading away,
opaquely and unable to be heard.
This is why we're translating with total commitment!
And finally remaining, there is this simple single word.
Do I really need to know *Help!* in a foreign language
to understand?

Andreas Holbach, February 2015

Abstract

The Three Gorges Reservoir (TGR) on the Yangtze River in China is a widely known and most controversial engineering mega-project. In 1992, the Chinese government finally decided to build the Three Gorges Dam (TGD) though being aware of its enormous socio-economic and environmental impacts. The TGD is operating since 2003. Besides its intended benefits for flood-control, power generation, and navigation, ecosystem services of the TGR are also utilized for drinking water extraction, fisheries, and agriculture on the semi-terrestrial soils of its water level fluctuation zone. In terms of its dimensions (175 m dam height, $39.3 \times 10^9 \text{ m}^3$ storage capacity), mean water residence time of 30 days, 30 m annual water level fluctuation, and its eutrophic state, the TGR is not only ecologically complex but globally unique. Consequently, previously prepared environmental impact assessments are very uncertain and in depth monitoring of processes within the TGR is of specific scientific and ecological interest. Eutrophication and algal blooms have become an obviously underestimated and primary threat to drinking water safety, whilst long-term accumulation of pollutants in sediments, soils, agricultural products, and food webs of the TGR would pose invisible but equally serious risks. This was the initial point of my dissertation, which aims to provide a substantial scientific contribution to a sustainable management of this highly vulnerable newly created ecosystem along the TGR on the Yangtze River in China.

During nine fieldtrips, in total 15 weeks, I have analyzed selected TGR water bodies in spatial and temporal resolution, primarily with the in situ and online underwater multi-sensor system MINIBAT. As part of my work, I have considerably contributed to technically advance the MINIBAT and extend its applicability to field conditions in China. To appropriately account for the multi-dimensionality of MINIBAT datasets, I have adapted monitoring methods and utilized existing geostatistical methods to create novel approaches of spatio-temporal data modelling. Chemical analyses that I performed in the labs at KIT-Institute of Mineralogy and Geochemistry revealed concentrations of numerous water constituents. So far, comprehensive evaluations of the resulting have been published in six research papers and one extended abstract their major findings being summarized in the following.

Generally, the Yangtze River main stream carries higher concentrations of nutrients and higher loads of heavy metals than its tributary backwaters. At confluence zones of TGR tributary backwaters with the Yangtze River main stream, water mass interactions are strongly driven by discharge and water level dynamics in the reservoir. Upstream transport from the Yangtze River main stream into its tributary backwaters is a critical nutrient source for these water bodies tainted with algal blooms. Due to regionally differing thermal stratification properties of the water bodies, vertically circulating density current cells can form between the Yangtze River main stream and its tributary backwaters as

such amplifying lateral pollutant transport distances many times over. In particular, tributary backwaters of the TGR develop a distinct seasonal sequence of water quality characteristics and their underlying dominating processes. During spring and summer, prevailing thermal surface stratification promotes algae to grow, their photosynthetic activity in turn dominating water quality characteristics and dynamics. In autumn and winter, a much weaker thermal stratification is mainly attributed to the middle and bottom water layers. Water quality characteristics in these seasons are mainly driven by water mass exchanges and pollutant transport processes. Urban discharges and their effects have also been studied. Urban contaminants distribute specifically according to prevailing hydrologic conditions. Vast summer discharges in the Yangtze River main stream are capable of diluting large amounts of pollutants to uncritical levels. However, under low discharge conditions in winter or when being transported into tributary backwaters, nutrients can expectably promote algal growth while discharged heavy metals accumulate in algae. Merely taking local flow paths into account when discharge locations are being established can alter pollutant distributions and mitigate corresponding effects. In the long-term, also sedimentation of polluted particles and biomagnification of pollutants across food webs could turn out as serious environmental hazards. It was also verified that most TGR sediments host bacteria communities capable to degrade chlorinated organic compounds which are also typical anthropogenic environmental pollutants.

In summary, anthropogenic environmental impacts feedback on utilized ecosystem services of the TGR. Tributary backwaters turned out to be much more relevant to physico-bio-chemical processes in the TGR ecosystem than the Yangtze River main stream. Concentrations of dissolved pollutants are mainly not critical with respect to drinking water but eutrophic nutrition states of the TGR promote extensive algal growth. Recently, blooms of toxin producing cyanobacteria are the most serious threat to drinking water. Transport, bioaccumulation, and biomagnification processes of pollutants (e.g. heavy metals and pesticides) in the TGR ecosystem pose a long-term health risk to organisms and, in particular, to local residents. They rely on the production and consumption of local agricultural and fisheries products. In this respect, the capability of microbes in TGR sediments to degrade pollutants is, indeed, beneficial for all utilized ecosystem services.

This dissertation provides scientific basics that substantially enhance the eclectic understanding of environmental threats in the TGR water bodies. Based on this effective local mitigation measures can be derived. Further, these locally acquired results also contribute to a deeper understanding of (artificial) aquatic ecosystems in general, and thus to improve planning processes and environmental impact assessments of other future dam projects. Despite all gained new and important scientific-technical aspects about water quality characteristics and pollutant dynamics in the TGR, not only scientists agree that in the long-term a simple reduction of pollutant inputs is the best and most effective way to mitigate these and other environmental challenges.

Zusammenfassung

Das Drei-Schluchten-Reservoir am Yangtze in China ist weltweit bekannt und ein international äußerst umstrittenes Mega-Bauprojekt. Nach jahrzehntelangen Kontroversen beschloss die chinesische Regierung im Jahr 1992 definitiv den Bau der Drei-Schluchten-Talsperre, welche im Jahr 2003 schließlich in Betrieb genommen wurde. Massive Folgen für Sozio-Ökonomie und Umwelt waren den Entscheidungsträgern durchaus bewusst, wurden aber in Anbetracht der erstrebten Vorteile des Projektes in Kauf genommen. Neben Hochwasserschutz, Energiegewinnung und verbesserter Schiffbarkeit, dienen die Gewässer des Drei-Schluchten-Reservoirs auch der Trinkwasserversorgung und Fischerei. Die semiterrestrischen Böden im Bereich der Wasserspiegelschwankungen werden außerdem großflächig landwirtschaftlich genutzt und durch Sedimente des Drei-Schluchten-Reservoirs mit geprägt. Das Drei-Schluchten-Reservoir ist in Bezug auf seine Größe (175 m Höhe der Talsperre, $39,3 \cdot 10^9 \text{ m}^3$ max. Stauvolumen), mittlere hydrologische Verweilzeit des Wassers von 30 Tagen, jährliche Wasserspiegelschwankung von 30 m sowie seinen eutrophen Zustand ökologisch nicht nur äußerst komplex sondern weltweit einzigartig. Deshalb war eine genauere Vorhersage seiner Umweltauswirkungen im Rahmen von Umweltfolgenabschätzungen im Vorfeld deutlich erschwert wenn nicht sogar unmöglich. Umso wichtiger und von besonderem naturwissenschaftlichem und ökologischem Interesse sind daher detaillierte Untersuchungen der im Reservoir selbst ablaufenden Vorgänge, nachdem die Talsperre im Jahr 2003 geschlossen worden war. Direkt erkennbare Eutrophierungserscheinungen, wie ausgeprägte Algenblüten, wiesen auf ein äußerst akutes und offensichtlich stark unterschätztes Umweltproblem hin, was mit einer realen Gefahr für die lokale Trinkwasserversorgung einhergeht. Weniger sichtbar, aber mindestens ebenso relevant, ist die langfristige Gefahr von Schadstoffanreicherungen in den dortigen Sedimenten, Böden, Landwirtschaftsprodukten und Nahrungsnetzen. Dies war der Ausgangspunkt meiner hier vorliegenden Dissertation, mit der ich einen naturwissenschaftlich nachgewiesenen und fundierten Beitrag zur nachhaltigen Bewirtschaftung des neu geschaffenen aber auch bedrohten Ökosystems am Yangtze Drei-Schluchten-Reservoir in China leisten will.

Die hier dargestellten Forschungsergebnisse konnte ich im Rahmen des deutsch-chinesischen Forschungsverbundes ‚Yangtze-Project‘ (BMBF Projektnummer FKZ_02WT1131) gewinnen. Im Verlauf von neun Feldaufenthalten über insgesamt ca. 15 Wochen am Drei-Schluchten-Reservoir habe ich Messungen von Wasserqualitätsparametern und auch Wasserprobenahmen durchgeführt. Das dafür eingesetzte Unterwasser Multisensor System MINIBAT ermöglichte in situ und online Messungen von bis zu neun Wasserqualitätsparametern sowohl in horizontaler Verteilung (GPS-Signal) als auch durch manuelle Steuerung tiefen- und durch Mehrfachmessungen zeitaufgelöst. Ich leistete einen maßgeblichen Beitrag bei der technischen Weiterentwicklung dieses Systems (z.B.

Entwicklung eines ferngesteuerten Probensammlers sowie Optimierung der Steuerelektronik) und zur Erweiterung seines Einsatzbereiches in Bezug auf die Bedingungen am Drei-Schluchten-Reservoir. Der geographische Fokus meiner Arbeit richtete sich speziell auf die aufgestauten Nebenflusstäler des Daning River sowie des Xiangxi River und dort vorwiegend auf deren Mündungsbereiche in den Yangtze-Hauptstrom, weil sich insbesondere hier interessante Messergebnisse erzielen ließen. Ich habe mit angepassten Monitoring-Methoden und im Rahmen geostatistischer Verfahren neuartige Datenmodelle erstellt, die den MINIBAT-Messungen in ihrer Multidimensionalität Rechnung trugen. Die vor Ort gesammelten Wasserproben wurden in den Laboren des Instituts für Mineralogie und Geochemie mittels Anionen-Chromatographie sowie Massenspektrometrie mit induktiv gekoppeltem Plasma auf gelöste und partikuläre Inhaltsstoffe untersucht, um diese im Zusammenhang mit den MINIBAT Daten zu interpretieren. Die umfassend ausgewerteten Ergebnisse wurden in bislang sechs Forschungsartikeln sowie in einem erweiterten Konferenz-Abstract schriftlich publiziert. Die darin dargestellten zentralen Erkenntnisse sind im Folgenden zusammengefasst:

Im Allgemeinen beinhaltet der Wasserkörper im Yangtze-Hauptstrom des Drei-Schluchten-Reservoirs höhere Nährstoff- und Schwermetallgehalte als seine aufgestauten Nebenflusstäler. In den entsprechenden Mündungsbereichen werden Wasseraustauschprozesse hauptsächlich durch Dynamiken des Abflussverhaltens sowie des Wasserstandes im Reservoir angetrieben. Insbesondere der stromaufwärts gerichtete Transport vom Yangtze-Hauptstrom hinein in seine aufgestauten Nebenflusstäler stellt eine entscheidende Nährstoffquelle für diese, inzwischen stark von Algenblüten belasteten, Wasserkörper dar. Außerdem können sich zwischen dem Yangtze-Hauptstrom und seinen aufgestauten Nebenflüssen vertikal zirkulierende Dichteströmungen ausbilden, welche durch regionale Unterschiede in der thermischen Schichtung hervorgerufen und angetrieben werden. Diese wiederum sorgen für ein massives Anwachsen der horizontalen Transportdistanzen von Schadstoffen.

Insbesondere in den aufgestauten Nebenflusstälern des Drei-Schluchten-Reservoirs wurde eine ausgeprägte saisonale Abfolge von Wasserqualitätseigenschaften und der hierfür zugrunde liegenden Prozesse im Gewässer festgestellt. Während des Frühlings und des Sommers finden sich, aufgrund von vorherrschender oberflächennaher thermischer Schichtung, günstige Bedingungen für Algen, welche durch ihre Photosynthese-Aktivität die herrschenden Bedingungen und damit auch die Dynamik der Wasserqualität maßgeblich bestimmen. Im Laufe des Herbstes und Winters hingegen zeigt sich eine weit schwächer ausgeprägte thermische Stratifikation und diese dann vorwiegend in den mittleren bis tiefen Gewässerschichten. In diesen Zeiträumen finden, vor allem durch die instabilere Schichtung und den Wasserspiegelanstieg im Reservoir ausgelöst, die überwiegenden Wasseraustausch- und Schadstofftransportprozesse statt, welche die Bedingungen der aktuellen Wasserqualität bestimmen.

Städtische Einträge ins Drei-Schluchten-Reservoir und deren Auswirkungen wurden hier auch untersucht. Das Augenmerk dieser Arbeit liegt bei der räumlichen Ausdehnung sowie dem zeitlichen Verlauf der Verteilung städtischer Schadstoffe, welche durch die herrschenden hydrologischen Bedingungen im Reservoir bedingt werden. Enorme Durchflüsse des Yangtze im Sommer sind in der Lage große Mengen an Schadstoffen auf unkritische Konzentrationen zu verdünnen. Bei Bedingungen mit geringerem Abfluss im Winter, oder durch die untersuchten Transportprozesse in aufgestaute Nebenflusstäler hinein, verstärken eingeleitete städtische Nährstoffe erwartungsgemäß das Algenwachstum und auch eingeleitete Schwermetalle können durch Bioakkumulation in Algen angereichert werden. Es konnte hier allerdings gezeigt werden, dass alleine die Berücksichtigung von lokalen Fließwegen bei der Wahl von Einleitungsstellen sich massiv auf Verteilungsmuster von Schadstoffen auswirkt und somit lokal für deutliche Verbesserungen der Bedingungen sorgen kann. Auf lange Sicht ist auch die Sedimentation von kontaminierten Partikeln und die Anreicherung von Schadstoffen innerhalb des Nahrungsnetzes ein potentiell aber dann sehr ernst zu nehmendes Umweltproblem. Verifiziert wurde aber auch, dass sich in vielen Sedimentkörpern des Drei-Schluchten-Reservoirs Gemeinschaften von dehalogenierenden Bakterien finden, die in der Lage sind, typisch anthropogene chlorierte Schadstoffe effektiv abzubauen.

Zusammenfassend wird ein deutliches Feedback anthropogener Umwelteinflüsse auf die wiederum vom Menschen in Anspruch genommenen Dienstleistungen des Ökosystems am Drei-Schluchten-Reservoir festgestellt. Eine sehr wichtige Erkenntnis dieser Arbeit ist, dass sich im Vergleich zum Yangtze-Hauptstrom insbesondere die aufgestauten Nebenflusstäler als viel relevantere Wasserkörper in Bezug auf physiko-bio-chemische Prozesse herausstellten. Die Gehalte an den analysierten gelösten Schadstoffen sind meist unkritisch in Bezug auf die Nutzung als Trinkwasser, allerdings sind die Nährstoffgehalte im deutlich eutrophen Bereich und daher Grundlage für extensives Algenwachstum. Allerdings sind vor allem Blüten von Toxin freisetzenden Cyanobakterien in aufgestauten Nebenflusstälern momentan die größte akute Gefahr für die Sicherheit der Trinkwasserversorgung. Ich konnte wichtige Quellen, Transportpfade und Auswirkungen von Nähr- und Schadstoffen im Ökosystem des Drei-Schluchten-Reservoirs identifizieren und beschreiben. Daraus ableitend bilden Transport, Bioakkumulation, und Biomagnifikation von z.B. Schwermetallen und Pestiziden im Ökosystem des Drei-Schluchten-Reservoirs eine langfristige Gefahr für Organismen und letzten Endes auch für die lokale Bevölkerung. Diese hängt grundlegend von der Produktion und vom Konsum der regional erzeugten Agrar- und Fischereiprodukte ab. Die erfreulicherweise festgestellte Fähigkeit des Ökosystems, selbstständig Schadstoffe im Sediment abzubauen, wirkt sich in jedem Fall vorteilhaft auf die menschliche Nutzung aus.

In dieser Dissertation stelle ich umfassende wissenschaftliche Ergebnisse dar, die als Grundlage für ein vielschichtiges Verständnis von Umweltproblemen in den Gewässern des Drei-Schluchten-

Reservoirs von großer Bedeutung sind. Ausgehend von einem besseren Verständnis der Zusammenhänge im Ökosystem könnten künftig effektive Maßnahmen zur Verbesserung der dortigen Umweltbedingungen entwickelt werden. Außerdem erweitern die hier lokal erlangten Erkenntnisse ganz allgemein das Verständnis von Prozessen in (künstlichen) aquatischen Ökosystemen und dienen so auch der Verbesserung von Planungsvorgaben und Umweltfolgenabschätzungen künftiger Damm-Projekte. Neben aller neuen und wichtigen wissenschaftlich-technischen Erkenntnisse meiner Arbeit über Charakteristika der Wasserqualität und Schadstoffdynamik im Drei-Schluchten-Reservoir, sind sich allerdings nicht nur Wissenschaftler einig, dass langfristig ganz trivial eine Reduktion der Schadstoffeinträge die beste und effektivste Lösung dieser und anderer Umweltproblematiken ist.

Table of contents

Erklärung	2
Die Sprache des Wassers — The language of water.....	3
Abstract.....	4
Zusammenfassung	6
Table of contents	10
List of Figures.....	12
List of Tables.....	13
1 Context of this dissertation	14
1.1 The ‘Yangtze-Hydro Project’	15
1.2 Large dams and reservoirs—decades of global controversies.....	16
1.3 Classification approaches for reservoirs.....	20
1.4 The Three Gorges Reservoir—history and characteristics of a unique study area	21
1.4.1 Intended benefits of the Three Gorges Dam	26
1.4.2 Environmental threats related to the Three Gorges Dam	27
1.4.3 The Daning River backwater.....	29
1.4.4 The Xiangxi River backwater	30
1.5 The MINIBAT multi-sensor system for in situ and online water quality measurements.....	31
1.6 Performed fieldwork and chemical analytics.....	32
2 First author scientific publications	33
2.1 Water mass interaction in the confluence zone of the Daning River and the Yangtze River— a driving force for algal growth in the Three Gorges Reservoir	33
2.2 Three Gorges Reservoir: Density Pump Amplification of Pollutant Transport into Tributaries	35
2.3 Environmental water body characteristics in a major tributary backwater of the unique and strongly seasonal Three Gorges Reservoir, China	37
2.4 Urban Pollutant Plumes around Wushan and Dachang City in the Three Gorges Reservoir	39

Table of contents

2.5	Integrated water quality monitoring and modeling in the Three Gorges Reservoir, China ..	41
2.6	Dilution of pollution? Processes affecting water quality in the river-style Three Gorges Reservoir	43
3	Co-authored related scientific publications	45
3.1	An integrated approach to model the biomagnification of organic pollutants in aquatic food webs of the Yangtze Three Gorges Reservoir ecosystem using adapted pollution scenarios	45
3.2	Dechlorination and organohalide-respiring bacteria dynamics in sediment samples of the Yangtze Three Gorges Reservoir	47
3.3	The Yangtze-Hydro Project: a Chinese–German environmental program	49
4	Synoptic conclusion.....	51
4.1	Utilized ecosystem services—water body processes and feedbacks from anthropogenic impacts	52
4.1.1	Drinking water	52
4.1.2	Fisheries	53
4.1.3	Agriculture.....	54
4.2	Relevance of tributary backwaters in the newly created ecosystem along the Three Gorges Reservoir	56
4.3	Applicability and implications of the results	59
	Acknowledgement.....	61
	References.....	63
A	Appendix—Full papers of first author scientific publications	68
A.1	Water mass interaction in the confluence zone of the Daning River and the Yangtze River—a driving force for algal growth in the Three Gorges Reservoir	68
A.2	Three Gorges Reservoir: Density Pump Amplification of Pollutant Transport into Tributaries	80
A.3	Environmental water body characteristics in a major tributary backwater of the unique and strongly seasonal Three Gorges Reservoir, China	113
A.4	Urban Pollutant Plumes around Wushan and Dachang City in the Three Gorges Reservoir	131

A.5	Integrated water quality monitoring and modeling in the Three Gorges Reservoir, China	143
A.6	Dilution of pollution? Processes affecting water quality in the river-style Three Gorges Reservoir	151
B	Appendix—Full papers of co-authored scientific publications.....	154
B.1	An integrated approach to model the biomagnification of organic pollutants in aquatic food webs of the Yangtze Three Gorges Reservoir ecosystem using adapted pollution scenarios	154
B.2	Dechlorination and organohalide-respiring bacteria dynamics in sediment samples of the Yangtze Three Gorges Reservoir.....	173
B.3	The Yangtze-Hydro Project: a Chinese–German environmental program	185

List of Figures

Figure 1:	Statistics of scientific publications on the topic ‘water quality dam reservoir’. Mean publications/year displayed as numbers; ratio of the total number of scientific publications displayed as bars. *Search results from Thomson Reuters ‘Web of Science’ (Thomson Reuters, 2014).....	19
Figure 2:	The Three Gorges Reservoir area within China and the specific study areas of the following publications in the Daning River and Xiangxi River backwaters.....	22
Figure 3:	Properties of worldwide dams and reservoirs with dam heights > 100 m and storage capacities > 20*10 ⁹ m ³ . In comparison, the TGR and the Itaipú Reservoir have exceptionally low mean water residence times. Numbers refer to Table 2. (ICOLD, 2014; Lehner et al., 2011; Berggren and Wallmann, 2012; CHINCOLD, 2014; Gong and Wan, 2006; World Bank, 1987). Reproduced from Holbach et al., 2015 (section 2.3, Appendix A.3) with permission from The Royal Society of Chemistry.	23
Figure 4:	Seasonal hydrology of the TGR derived from daily inflow, outflow and water level data from 01.2010-04.2014. Data source: CTGC, 2014.	25
Figure 5:	‘Little Three Gorges’ in the Daning River backwater of the TGR. Photo: A. Holbach, 25.08.2011.....	29
Figure 6:	Downstream view from Xiakou along the Xiangxi River backwater of the TGR. Photo: A. Holbach, 13.09.2012.....	30
Figure 7:	The MINIBAT in the water around Wushan in January 2013. Photo: A. Holbach, 15.01.2013.	31
Figure 8:	Timeline of the fieldwork conducted within the ‘KIT-IMG’ sub-project of the ‘Yangtze-Hydro Project’. Note: in April 2011 the fieldwork was done without a MINIBAT. In August and December	

2011 we could apply an old MINIBAT system. The newly developed MINIBAT system could be applied from June 2012 on. Data obtained from fieldtrips in black font are subject of the scientific publications cumulated in this dissertation.32

Figure 9: Extensive agriculture on semi-terrestrial soils of the TGR water level fluctuation zone around Kaixian at the Xiaojiang River in April 2011. Photo: A.Holbach, 04.2011.51

Figure 10: Qualitative conceptual model of anthropogenic impact on processes within the Three Gorges Reservoir ecosystem as well as corresponding consequences for utilized ecosystem services. Specific contributions of the cumulated scientific publication of this dissertation to the understanding of the complex system are marked according to the legend.55

Figure 11: Spatial scheme of water body processes and external impact factors within the newly created ecosystem along the TGR.58

List of Tables

Table 1: Combined classification approach of reservoirs based on throughflow, mixing, and trophic classes. (modified from Straškraba and Tundisi, 1999)20

Table 2: Properties of selected dams and reservoirs worldwide with dam heights > 100 m and storage capacities > 20*10⁹ m³. The TGR and the Itaipú Reservoir have exceptionally low mean water residence times (MWRT). The TGR has by far the largest water level fluctuation (WLF). Reprinted from Holbach et al. (submitted to Journal) in section 2.3 and Appendix A.3.24

1 Context of this dissertation

The Three Gorges Reservoir (TGR) on the Yangtze River in China is a widely known and most controversial engineering mega-project (Stone, 2008). After decades-long debates within China and being aware that there would be enormous corresponding socio-economic and environmental impacts, in 1992 the Chinese government finally decided to build the Three Gorges Dam (TGD) (Ponseti and López-Pujol, 2006). In this context this dissertation aims to provide a substantial scientific contribution to a sustainable management of the highly vulnerable newly created ecosystem forming along the TGR on the Yangtze River in China since TGD operation in 2003.

This dissertation is based on the cumulation of nine scientific publications (sections 2.1 - 2.6 and 3.1 - 3.3). For six of these publications (sections 2.1 - 2.6), I am the first and the corresponding author. The six first-authorships include four research papers, one extended conference abstract, and one concluding conference report, whereas the co-authorships include two research papers and one commentary article with a project description. The research papers are all based on fieldwork, chemical analytics, mathematical modeling, and experiences that were performed and gained within the frame of the joint 'Yangtze-Hydro Project' funded by the 'Federal Ministry of Education and Research of Germany' (BMBF) as well as the 'Ministry of Science and Technology of China' (MOST). This project is highlighted in the following section 1.1. Within section 1.2, large dams and reservoirs as well as their consequences are put into a global context. Classification approaches for impounded reservoirs are dealt with in section 1.3 before the Three Gorges Reservoir (TGR) on the Yangtze River in China, dedicated study area of this work, is specifically characterized in section 1.4. The 'MINIBAT' described in section 1.5 was the main analytical and sampling instrument used throughout the executed fieldwork (section 1.6) of this project.

Within this dissertation, the term *water quality* is a key aspect and requires definition:

Water quality can be defined as an ensemble of physical, chemical, and biological characteristics of the given water. Which characteristics are considered important depends on the intended use of the corresponding water. (Straškraba and Tundisi, 1999)

According to this definition *water quality* is a term strongly dependent on the taken up point of view. In the first place, the current state and environmental quality of a water body consists of a number of measurable and neutral stand-alone figures such as temperature, pH, electrical conductivity, element contents, and so forth. Weightings, valuations, correlations, and judgments of and in-between these values are then all subject to specific interests behind the *water quality* data evaluation. In most

cases *water quality* is judged with respect to the anthropogenic utilization of ecosystem services of specific water bodies. From this perspective, possible subjective points-of-view to judge *water quality* could be for example: suitability of water for swimming, drinking, and fishing; suitability of water as habitat for biological species; environmental guiding principles and target values; closeness to natural state and anthropogenic impacts; identification of environmental processes and trends. Any point-of-view leads to another assessment of *water quality* parameters and thus to differing conclusions and guidance. In the cumulated publications of this dissertation, I have tried to evaluate *water quality* from different perspectives with focus on environmental processes that possibly affect the anthropogenic utilization of ecosystem services from the TGR on the Yangtze River in China.

1.1 The ‘Yangtze-Hydro Project’

Both the ‘Yangtze-Hydro Project’ (section 3.3) and the ‘Yangtze-Geo Project’ form the wider ‘Yangtze-Project’ with its stated aim to contribute to a sustainable management of the newly created ecosystem along the TGR on the Yangtze River in China. The Yangtze-Project is a joint research and development project formed by a Sino-German scientific consortium and bilaterally funded by BMBF and MOST. It includes experts from various environmental scientific disciplines and numerous German as well as Chinese research institutions. The ‘Yangtze-Hydro Project’ focuses on water body related threats arising from the impoundment of the TGR, whilst the ‘Yangtze-Geo Project’ is working on corresponding geohazards.

Within the ‘Yangtze-Hydro Project’, the sub-project ‘Spatio-temporal resolved in situ and online monitoring of the dynamics of water body relevant parameters by means of a towed underwater multi-sensor system (MINIBAT) and numerical modeling of pollutant transport dynamics’ (BMBF Grant Number: FKZ_02WT1131) was designed and supervised by PD Dr. Stefan Norra at the ‘KIT-Institute of Mineralogy and Geochemistry (IMG)’. MSc. Wei Hu and I acted as the corresponding executing scientists at the ‘KIT-IMG’. The preceding project proposal was written by PD Dr. Stefan Norra from the KIT-IMG in collaboration with our direct project partners Prof. Binghui Zheng and Dr. Lijing Wang from the Chinese Research Academy of Environmental Sciences (CRAES) in Beijing, China. Thus, these three people are the founders of the basic idea to develop and apply a MINIBAT system within the TGR to study spatio-temporal characteristics of water quality and pollutants. Further, PD Dr. Stefan Norra finally raised the necessary funds from BMBF for staff, equipment, and travel costs all being necessary to execute the ideas of this project. These crucial contributions of PD Dr. Stefan Norra, Prof. Binghui Zheng, and Dr. Lijing Wang to the ‘KIT-IMG’ sub-project of the ‘Yangtze-Hydro Project’, alone, justify their co-authorship of all publications derived from the corresponding scientific work.

The official project duration of the ‘Yangtze-Hydro Project’ was from August 2010 till July 2014. Personally, I was involved in the project from February 2011 on until the end. My responsibilities mainly focused on the in situ and online monitoring (MINIBAT) part of the ‘KIT-IMG’ sub-project and primarily included the following tasks: 1.) Technically advance the MINIBAT and extend its applicability to field conditions in China, particularly in the TGR; 2.) Management, preparation, and organization of fieldwork in the TGR; 3.) performance of the MINIBAT measurements and water sampling in water bodies of the TGR under different seasonal and hydrologic conditions; 4.) laboratory analytics of dissolved and particulate water constituents using digestions, anion chromatography (IC), as well as inductively coupled plasma mass spectrometry (ICP-MS) techniques; 5.) adaptation and execution of statistical and geostatistical methods for novel approaches of spatio-temporal MINIBAT data evaluation and modelling; 6.) scientific evaluation, interpretation, presentation and publication of the derived datasets, particularly considering their environmental relevance.

1.2 Large dams and reservoirs—decades of global controversies

Freshwater is an essential resource for human life. Since thousands of years, people are building dams on the world’s rivers to sustain drinking and irrigation water. In modern times, also hydropower and industrial utilization of water have become major purposes of building dams (WCD, 2000). The numbers and magnitudes of dams, however, have altered enormously in the course of the 20th century. From 1950 till 2000, around 40,000 large dams (height > 15 m) have been built in countries all over the world and were added upon the formerly only around 5,000 large dams that were concentrated on industrialized countries (WCD, 2000). Originally, dams have been seen as symbols of development and economic strength. However, step by step people started seeing negative socio-economic and ecological impacts of dams and reservoirs thus blurring the bright vision of a purely beneficial engineering achievement. Today, dams regulate more than half of the world’s large river systems; their corresponding reservoir volumes account for more than 15% of the global river runoff (Nilsson et al., 2005). It was only in 1997, when the controversial debate about costs and benefits of dams and reservoirs evolved from regional to international context and resulted in the formation of the world commission on dams (WCD) in 1998 (WCD, 2000). The first independent and global review “dams and development” was finally compiled in 2000 providing a “new framework for decision-making” (WCD, 2000). Among others, the basis for this compilation was formed by a fundamental review on impacts of large dams and reservoirs on ecosystems (McCartney et al., 2001). Negative socio-economic effects of dams are, indeed, equally important but these are beyond the scope of this work. Generally, effects of dams on ecosystems happen in both upstream

and downstream directions and can be summarized as follows (modified from McCartney et al., 2001):

A considerable change of **hydrology** and **hydrodynamics** is of course intended by building dams. However, the ecosystems attached to dams and reservoirs are adapted to specific seasonal discharge, flow velocity, and water level patterns which are disrupted and even sometimes inverted by dams. Irrigation dams and shallow reservoirs in warm climates are strongly affected by water abstraction and evaporation. The total annual discharge in the downstream reaches can thus decline considerably and cause a net loss of water in the connected ecosystems.

The **thermal regime** of both upstream and downstream water bodies will be affected by dams and reservoirs. An impounded water body is characterized by slower flow velocities and it is likely that lake-like thermal stratification patterns develop. Further, the vertical position of the dam's spillway intake causes selective discharge from specific layers in the water body. In turn, the downstream river section can either receive warmer water from dams with surface water release or colder water when the spillway intake is located near the reservoir bottom. The increased absorption of thermal energy by the reservoir water body as well as the cooling effect of evaporation can even impact the local and regional meteorological regimes (Wu et al., 2012).

Sedimentation within reservoir water bodies will increase due to reduced flow velocities. The ratio of trapped sediments in reservoirs varies strongly according to the reservoir properties. Impact factors are size and characteristics of the catchment area (e.g. area, geology, topography, soils, and vegetation), the ratio of storage capacity and discharge, as well as temporal variability of discharge (e.g. seasonality). In the long-term the composition of sediments will change considerably due to the different properties of settling particles. Further, sedimentation will modify the bathymetry within inundated valleys and can cause considerable losses of reservoir water storage capacities over time. It is obvious, that intense sedimentation within a reservoir will cause sediment deficiency in the downstream reaches of a dammed river. Downstream reaches of dammed rivers thus frequently change from formerly sedimentary to erosional regimes afterwards. Riverbanks may destabilize, river deltas can erode, and inhabiting flora and fauna can be severely affected by fundamental changes of their former habitats.

The increased surface area of reservoir water bodies leads to increasing **evaporation**. The magnitude of this effect is highly dependent on regional climatic settings and the reservoir

morphology. Especially reservoirs with large surface areas in hot and arid climates are strongly affected by evaporation. This effect can cause considerable loss of water and enrichment of dissolved contents leading to high salinity. It can even strongly affect the local and regional climate, particularly air temperature, humidity, and precipitation (Wu et al., 2012).

Recently, the emission of **greenhouse gases** from reservoirs became a serious scientific issue. Hydropower, widely presented as clean energy in terms of climate change and global warming might, in many cases, turn out as the opposite. Large amounts of greenhouse gases (mainly CO₂ and CH₄) are emitted from reservoirs due to decomposition of biomass. Thus, the greenhouse gas emissions of numerous reservoirs related to their hydropower yield in g/kWh are estimated to exceed those of comparable amounts of fossil fuel combustion (Hertwich, 2013).

Water quality of reservoir water bodies is affected by numerous interacting physical, chemical, and biological processes which are in turn all dependent on the regional settings enclosing the reservoir. Nutrient influxes from point (e.g. urban sewage plants) and non-point (e.g. wash out of agricultural fertilizers) pollution sources can cause severe eutrophication. When there is an additional stratification in reservoir water bodies, algal blooms can occur and the exchange of dissolved matter between the epilimnion and hypolimnion layers is limited. This can for example lead to anoxic conditions near the bottom and trigger a sequence of pH and redox related reactions such as mobilization of nutrients and redox-sensitive toxic substances (e.g. PO₄³⁻, As and Hg) from sediments. Subsequently, these substances can further increase eutrophication, have ecotoxic effects on the aquatic biocenoses, accumulate across the food web, and finally reach humans via food (e.g. contaminated fish and agricultural crops) and/or drinking water consumption. All these processes can of course also occur in natural lakes. However, the sudden inundation of large amounts of biomass and potentially contaminated urban and/or industrial areas by reservoirs enhances the risk of intense oxygen depletion and pollutant release near the bottom. The downstream reaches of a dammed river are fed by water discharged from the reservoir. Compared to its original runoff, this water is likely of very different quality mainly according to temperature, oxygen saturation, turbidity, and pollutant contents. In case of a dam with surface water release warmer and well oxygenated water with little sediment load will be contributed to the downstream reaches, whereas bottom water outlets likely supply

colder, oxygen depleted water with frequently extremely high sediment loads when sediment sluicing is practiced by the dam management.

Riverine water bodies and riparian wetlands are characterized by specific *biocenoses* and thus *biodiversity*. These communities of plants and animals are adapted to the environmental characteristics of their habitats. As seen above, the hydrological, hydrodynamic, water quality, sedimentation, and pollution conditions of habitats will change considerably after dam construction and reservoir impoundment in both up and downstream directions. Further, migratory routes of animal species (e.g. anadromous and catadromous fishes) are often obstructed by dams. All this will inevitably lead to severe changes of biocenoses and biodiversity within the areas affected by the dam and reservoir. Especially in river basins with high rates of endemism dams and reservoirs can consequently cause extinction of biological species and irreversible loss of biodiversity.

To sum it up, there are numerous and enormous impacts of dams and reservoirs on adjacent ecosystems, particularly on the affected water bodies. Thus, among scientists, studies on water quality in dams and reservoirs also became an emerging research field. From 2010 on till today, there are on average 70 publications each year on this topic listed in Thomson Reuters 'Web of Science' (Thomson Reuters, 2014) compared to only 6 publications per year from 1990 till 1994 (Figure 1). Also the ratio of publications on this topic related to the total number of publications listed in 'Web of Science' (Thomson Reuters, 2014) has enormously grown (Figure 1). Obviously, there was an emerging international scientific interest and relevance of water quality studies related to dams and

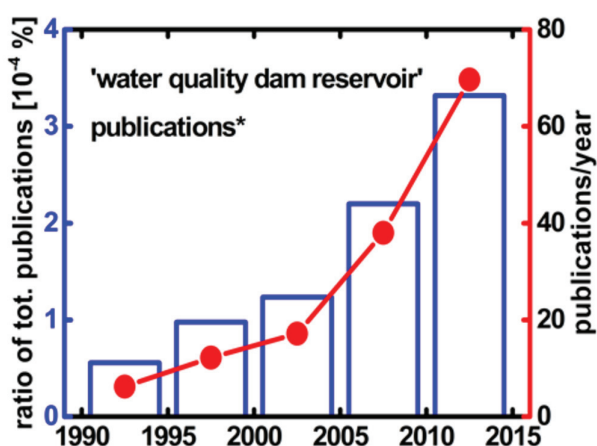


Figure 1: Statistics of scientific publications on the topic 'water quality dam reservoir'. Mean publications/year displayed as numbers; ratio of the total number of scientific publications displayed as bars. *Search results from Thomson Reuters 'Web of Science' (Thomson Reuters, 2014).

reservoirs. By now, there seems to be a general and qualitative understanding of consequences and processes caused by dams and the impoundment of reservoirs. However, any new dam and reservoir comes along with unique properties and it remains extremely difficult to predict their impacts on ecosystems exactly. There are indeed guidelines provided by the 'World Commission on Dams' meant for objective and integrated environmental impact assessments during dam planning (WCD, 2000). Such guidelines, however, imply that we are capable to estimate environmental impacts

of newly created dams and reservoirs, appropriately. A good example to disprove this hypothesis is the effect of greenhouse gas emissions from reservoirs which has only been considered by scientists, recently. The first publication on the topic ‘greenhouse gas dam reservoir’ listed in Thomson Reuters ‘Web of Science’ (Thomson Reuters, 2014) was only published in 1995 after anthropogenic greenhouse gas emissions and their effect on global warming became a scientific issue in 1970 (Landsberg, 1970). Further, we observe that modern computing, monitoring, and analytical technologies provide unprecedented insights into highly resolved processes that remained somehow invisible before. It is inevitable that any dam built, be it ever so well planned, will lead to unforeseen effects on the adjacent ecosystems. It is therefore likewise inevitable to establish extensive environmental monitoring programs after dam closure and reservoir impoundment in order to observe unforeseen effects at the earliest time and whenever possible develop effective mitigation measures.

1.3 Classification approaches for reservoirs

Lake classification approaches have often been similarly and adequately used for reservoirs as well. As such, reservoirs can be classified according to their geographical settings determining seasonal stratification and mixing characteristics. Globally, this results in the following reservoir mixing classes (Straškraba and Tundisi, 1999): oligomictic (tropics, low altitudes); deep polymictic (tropics, high altitudes); warm monomictic (sub-tropics); dimictic (warm temperate zone); cold monomictic (cold temperate zone); amictic (arctic); shallow polymictic (can occur in all geographical zones); and meromictic (can occur in all geographical zones). Another approach is the trophic classification system of lakes based on nutrient and chlorophyll contents as well as on turbidity induced by algae in the water. The following categories can be derived for lakes (Straškraba and Tundisi, 1999):

Table 1: Combined classification approach of reservoirs based on throughflow, mixing, and trophic classes. (modified from Straškraba and Tundisi, 1999)

	rapidly throughflowing (river-like)	intermediate retention times	long retention times (lake-like)
retention time R	$R \leq 15$ days	15 days $< R \leq 1$ year	1 year $< R$
mixing class	fully mixed	modified stratification and mixing characteristics	classical mixing classes and stratification properties
trophic class	flow prevents extensive phytoplankton growth	trophic characteristics modified by throughflow and modified stratification	classical trophic classes

oligotrophic, mesotrophic, eutrophic, hypertrophic, dystrophic (lakes with high contents of dissolved humic substances), and calcitrophic (lakes with calcium carbonate dominating dissolved solids). However, these approaches are only adequate for reservoirs with long lake-like hydraulic water retention times.

The limnologic properties of reservoirs further depend on their specific discharge characteristics leading to the following classification based on hydraulic water residence time R (Straškraba and Tundisi, 1999): Class A – rapidly throughflowing $R \leq 15$ days, Class B – intermediate retention times $15 \text{ days} < R \leq 1 \text{ year}$, and Class C – long retention times $R > 1 \text{ year}$. Straškraba and Tundisi (Straškraba and Tundisi, 1999) also provide a combined classification approach including all hydraulic water retention time, mixing classes, and trophic classes (Table 1).

This approach, however, is very unspecific for intermediate retention times. Further, it is still missing water level fluctuation as an important feature of reservoirs that can substantially affect limnologic characteristics. Particularly, fluctuating water levels in a reservoir main stream have impacts on dendritic tributary backwaters by pumping effects. In the following section characteristics of this dissertation's study area, the TGR, are set into a global context based on the above described classification approaches for reservoirs.

1.4 The Three Gorges Reservoir—history and characteristics of a unique study area

Although the decision-making to build the Three Gorges Dam (TGD) on the Yangtze River in China (Figure 2) took place long before international activities by the WCD, there was a long history of controversial discussion taking place among specialists within China. The idea to build a dam in the Three Gorges area dates back to 1919 and the person Sun Yat-sen who first of all developed the idea of a dam cascade along the Yangtze River (Ponseti and López-Pujol, 2006). It took another 73 years until the construction of the TGD was finally approved by the National People's Congress of China in April 1992 with only 67.8% of votes in favor of the TGD and a required two-thirds majority (Ponseti and López-Pujol, 2006). In 1994, the construction works for the TGD began.

Today, the TGR on the Yangtze River in China (Figure 2) is forming a deep and dendritic reservoir with a length of around 660 km, a water surface area of around $1.084 \cdot 10^9 \text{ m}^2$, and a maximum storage capacity of $39.3 \cdot 10^9 \text{ m}^3$. Around half of the inundated area is newly flooded and one third of water surface area is attributed to reservoir tributary backwaters (Ponseti and López-Pujol, 2006). The stepwise impoundment of the reservoir by the TGD was started in 2003 when the water level reached 139 m a.s.l., followed by a second step in 2006 up to a water level of 156 m a.s.l., and the

final step in 2010 reaching a water level height of 175 m a.s.l. (Ponseti and López-Pujol, 2006; CTGC, 2014; ICOLD, 2014; Becker et al., 2006). Even though the TGR gained a lot of controversial publicity,

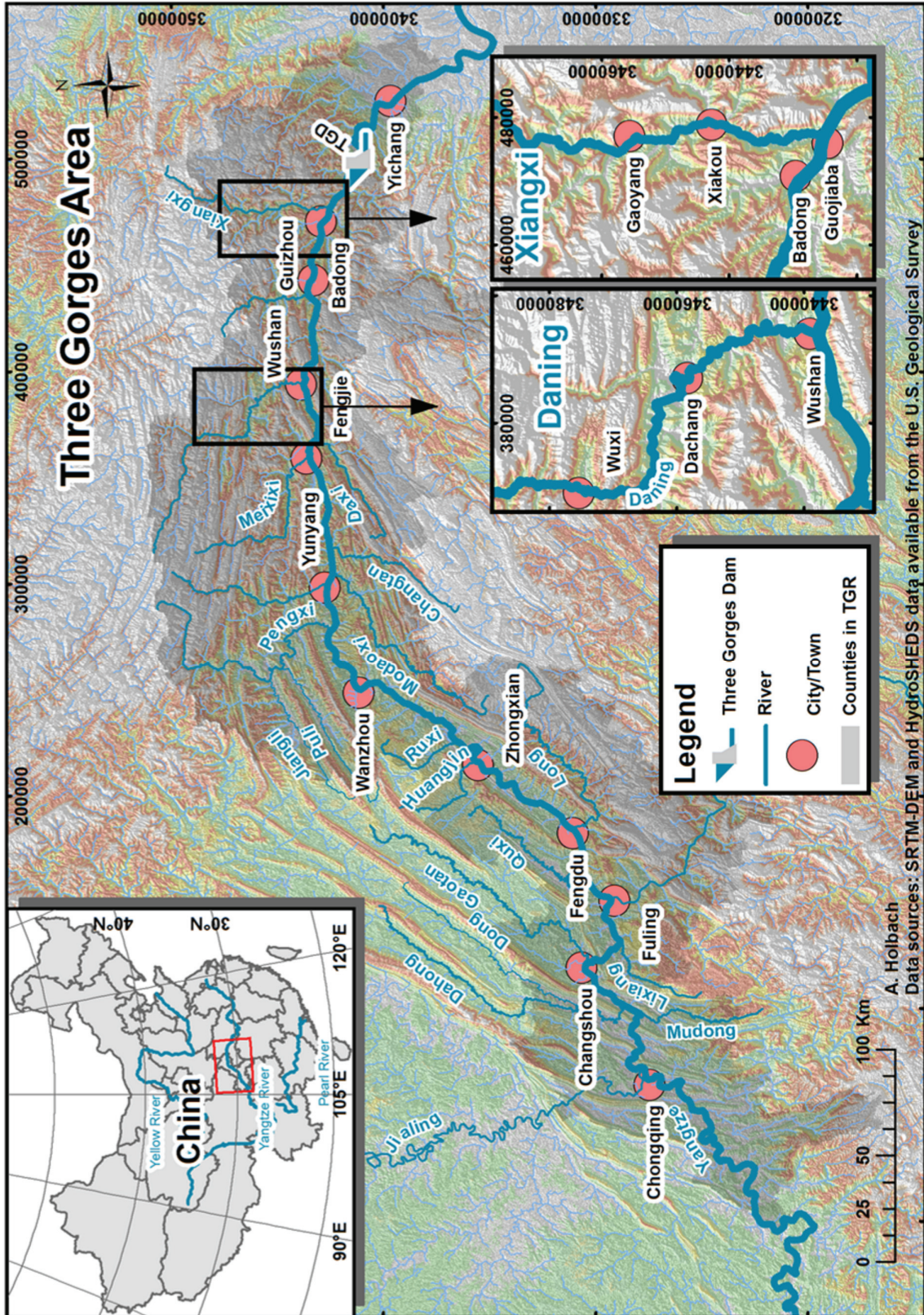


Figure 2: The Three Gorges Reservoir area within China and the specific study areas of the following publications in the Daning River and Xiangxi River backwaters.

there are 30 other large and deep reservoirs worldwide with comparable or larger magnitudes in terms of storage capacity ($\geq 20 \cdot 10^9 \text{ m}^3$) and dam height ($\geq 100 \text{ m}$) (Figure 3; ICOLD, 2014; Lehner et al., 2011).

The world's highest dams and largest reservoirs are homogeneously distributed across a wide range of latitudes (Figure 3). However, only the Itaipú Reservoir (25.4°S), impounded on the Paraná between Brazil and Paraguay in 1983, cannot only compete with the TGR (30.8°N) in terms of dimensions but also in terms of exceptionally low mean water residence times (Figure 3; Lehner et al., 2011; Berggren and Wallmann, 2012; CHINCOLD, 2014; Gong and Wan, 2006; World Bank, 1987). Despite their similarity, both reservoirs substantially differ in their trophic state and annual water level fluctuation (Table 2): The Itaipú is in a mainly oligotrophic state (Ribeiro et al., 2011) and its

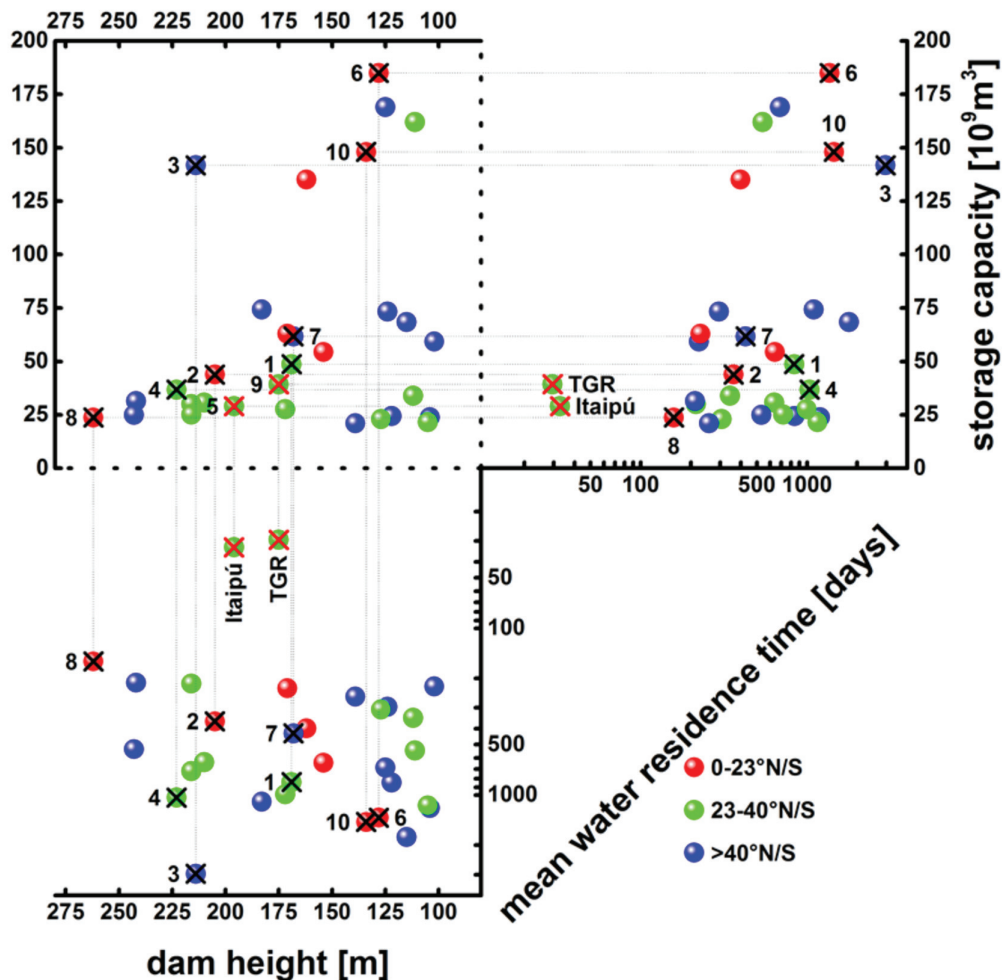


Figure 3: Properties of worldwide dams and reservoirs with dam heights $> 100 \text{ m}$ and storage capacities $> 20 \cdot 10^9 \text{ m}^3$. In comparison, the TGR and the Itaipú Reservoir have exceptionally low mean water residence times. Numbers refer to Table 2. (ICOLD, 2014; Lehner et al., 2011; Berggren and Wallmann, 2012; CHINCOLD, 2014; Gong and Wan, 2006; World Bank, 1987). Reproduced from Holbach et al., 2015 (section 2.3, Appendix A.3) with permission from The Royal Society of Chemistry.

Table 2: Properties of selected dams and reservoirs worldwide with dam heights > 100 m and storage capacities > 20*10⁹ m³. The TGR and the Itaipú Reservoir have exceptionally low mean water residence times (MWRT). The TGR has by far the largest water level fluctuation (WLF). Reproduced from Holbach et al., 2015 (section 2.3, Appendix A.3) with permission from The Royal Society of Chemistry.

No. Dam name	Country	Year	Dam and Reservoir dimensions			Reservoir Classification					WLF [m]	References
			Dam height [m]	Res. vol. [10 ⁹ m ³]	Res. area [km ²]	Ø depth [m]	MWRT [days]	Geographic	Trophic	Mixing		
1 Atatürk	Turkey	1992	169	49	817	60	838 long	37°N sub-tropical	eutrophic	n.a.	n.a.	2, 4, 11
2 Bakun	Malaysia	2011	205	44	695	63	362 intermediate	3°N tropical	n.a.	n.a.	n.a.	2, 6, 9
3 Hoover	USA	1935	223	37	635	58	1035 long	36°N sub-tropical	mesotrophic	monomictic	7	2, 4, 7
4 Itaipú	Brazil/Paraguay	1983	196	29	1350	21	33 intermediate	25°S sub-tropical	oligotrophic	polymictic	1	2, 3, 4, 5, 8
5 Kariba	Zimbabwe/Zambia	1959	128	185	5540	33	1367 long	17°N tropical	mesotrophic	monomictic	3	2, 3, 4
6 La Grande 2	Canada	1977	168	62	2835	22	428 long	54°N moderate	oligotrophic	dimictic	9	2, 3, 4
7 Manicouagan	Canada	1968	214	142	1940	73	2961 long	51°N moderate	oligotrophic	monomictic	6	2, 3, 4
8 Nuozhadu	China	2014	262	24	320	74	159 intermediate	23°N tropical	n.a.	n.a.	n.a.	1, 2
9 Three Gorges	China	2003	175	39	1084	36	30 intermediate	31°N sub-tropical	eutrophic	polymictic	30	2, 4, 10
10 Volta	Ghana	1965	134	148	8500	17	1452 long	6°N tropical	eutrophic	polymictic	3	2, 3, 4

¹CHINCOLD, 2014; ²ICOLD, 2014; ³ILEC, 2014; ⁴Lehner et al., 2011; ⁵Ribeiro et al., 2011; ⁶Sovacool and Bulan, 2011; ⁷Summit Technologies, 2014; ⁸Thomaz et al., 2006; ⁹World Bank, 1987; ¹⁰Xu et al., 2010; ¹¹Yazgan et al., 2001

water level normally varies by less than 1 m per year (Thomaz et al., 2006), whereas the TGR is mainly eutrophic and exhibits 30 m annual water level fluctuation (CTGC, 2014; Xu et al., 2010). These days, the TGR is the only large and deep eutrophic reservoir in the world with low mean water residence time and high annual water level fluctuation. Further, the Yangtze River and particularly the Three Gorges area are biodiversity hotspots and characterized by high rates of endemic flora and fauna (Zhang and Lou, 2011). Thus, there cannot be an object of comparison in terms of biodiversity and biocenoses due to the high rates of endemism in these areas (Zhang and Lou, 2011).

Climate in the catchment area of the TGR is associated with the East Asian summer monsoon (Becker et al., 2006). Thus, the Yangtze River exhibits strong runoff seasonality with maximum inflows into the TGR above 70000 m³/s in July and minimum inflows of 3500-7600 m³/s from December till March (CTGC, 2014; Figure 4). The TGD is operated to create a seasonal water level fluctuation within the TGR between 145 m a.s.l. and 175 m a.s.l. to compensate for this inflow and

outflow seasonality (Figure 4). Floods of the Yangtze River in summer need to be captured to avoid another devastating flood in the downstream reaches. Thus, the TGR water level is kept at a low level during the flood season from June till August. This ensures a large flood retention volume within the TGR but reduces the energy yield of the hydropower plant in the TGD. During September and October the reservoir is filled up to its peak water level of around 175 m a.s.l.. This, contrarily, reduces the flood retention volume but increases the energy yield of the hydropower plant. The high water level phase from November till December is then followed by a water level drawdown from January till June. As a whole, the TGR is already characterized by seasonally varying water residence times (Figure 4). Furthermore, the dendritic shape of the TGR water bodies strongly isolates its tributary backwaters from the hydrodynamics of the Yangtze River main stream. Mean water residence times can exceed 365 days in these areas and the slowly flowing waters are likely to exhibit thermal surface stratification in spring and summer (Xu et al., 2009).

The TGD was only recently closed in 2003 and it will take some more years or decades until kind of steady-state conditions will be reached. To sum it up, environmental monitoring and scientific evaluation of the processes related to the TGD and the impoundment of the TGR are of extraordinary

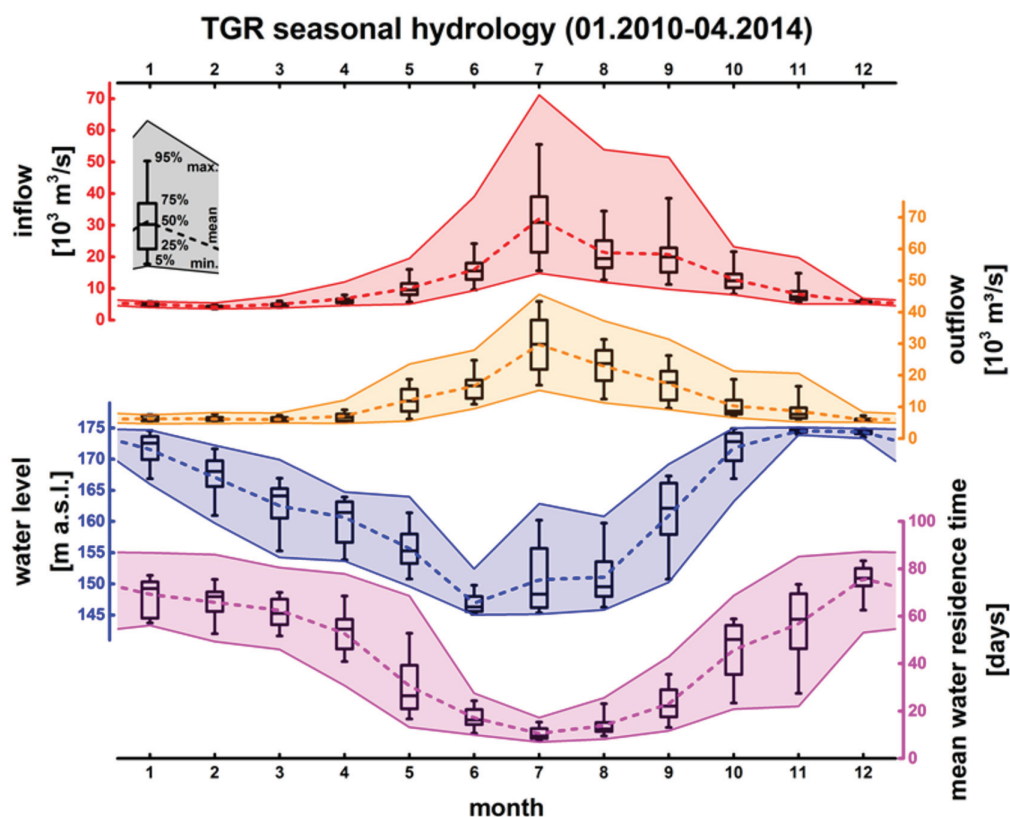


Figure 4: Seasonal hydrology of the TGR derived from daily inflow, outflow and water level data from 01.2010-04.2014. Data source: CTGC, 2014.

concern and international interest due to several reasons.

Immediate mitigation measures: The TGD impounds a globally unique reservoir. It is thus more than likely that effects on the adjacent ecosystems have been underestimated and/or even totally unexpected in the conducted feasibility studies and environmental impact assessments. Such effects urge for immediate scientifically based responses from decision makers and dam management to mitigate long-term negative impacts.

Biodiversity is a global concern: The worldwide decline of biodiversity is more and more caused by anthropogenic activities. Further, it becomes increasingly obvious that our human well-being is based on ecosystem processes and services provided by intact functional interactions of species. It still remains impossible to predict the spatial, temporal, and functional impact ranges on ecosystem services that are related to specific changes in species composition (Díaz et al., 2006). In time observation of biodiversity responses to the impoundment of the TGR as well as profound ecosystem management strategies are thus crucial to sustain functional properties and services provided for the regional, national, and global human population by the Yangtze River and the TGR area.

Colossal field experiment: Within and around the water bodies affected by the TGD, environmental scientists of manifold disciplines can follow large-scale responses to fundamental changes of aquatic ecosystem properties in unprecedented orders of magnitude. For example, environmental processes, mitigation measures, ecological engineering approaches, numerical models, as well as ecosystem reactions and adaptability can all be studied and tested in applied field experiments or pilot studies throughout the TGR area. The results of these studies will substantially contribute to the existing knowledge on (artificial) aquatic ecosystems and water body management.

Learning for the future: Detailed confrontation of the current environmental status with estimated consequences of the TGD and TGR by the conducted feasibility studies and environmental impact assessments needs to be done. This will reveal current gaps of understanding and specify those aspects for which it is necessary to revise the current guidelines. Especially, new results of the above mentioned field experiments and pilot studies need to find their way into the planning processes of future dams and reservoirs with comparable environmental aspects.

1.4.1 Intended benefits of the Three Gorges Dam

There were three main benefits intended by the construction of the TGD and the impoundment of the TGR (Ponseti and López-Pujol, 2006):

Flood Protection — The large storage capacity of the TGR is used to protect the downstream areas from devastating Yangtze River floods. In the 20th century alone, floods of the Yangtze River have

caused more than 300,000 deaths (Ponseti and López-Pujol, 2006). The TGR water level is thus kept at a low level of 145 m a.s.l. during the rainy season from June till August to provide sufficient flood retention volume. In July 2012, the TGR could successfully be used to mitigate serious flood peaks that exceeded those of former severe floods in 1954 and 1998 (Yang and Lu, 2013).

Hydropower — The TGD accommodates the world's largest hydropower plant now producing around 85,000 GWh/year. This amount accounted for around 1.8% of China's utilization of electrical energy in 2012 (IEA, 2014). During the dry season from October till February, the TGR water level is kept at a high level of around 175 m a.s.l. to enhance the energy yield of the installed hydropower plant.

Improved navigability — The navigability along the Yangtze River has been significantly improved by the impoundment of the TGR. Now it is possible for 10,000 t vessels (formerly 3,000 t) to cruise from Shanghai up to Chongqing. The amount of transported cargo increased considerably from around $10 \cdot 10^6$ t before the dam construction (Ponseti and López-Pujol, 2006) to $88 \cdot 10^6$ t in 2010 (MOEP, 2012).

1.4.2 Environmental threats related to the Three Gorges Dam

The construction of the TGD and the impoundment of the TGR have caused a series of environmental changes and threats in both upstream and downstream directions of the TGD. Qualitatively, most of these consequences have been expected within the conducted feasibility studies and environmental impact assessments (Fu et al., 2010). However, quantitative estimations have frequently mismatched the real scenarios after dam closure (Fu et al., 2010).

Immediately after its first impoundment, the frequency of geohazards such as earth quakes, landslides (Yang and Lu, 2013), and soil erosion (Seeber et al., 2010) has considerably increased and is attributed to water level related processes and land use changes within the TGR area. Furthermore, the unforeseen economic, social, and cultural progress within China during the dam building period is attributed for severe degradation of water quality in the Yangtze River and TGR. Despite intense efforts to enhance waste and sewage treatment in the TGR area, eutrophication of the TGR water bodies, particularly its tributary backwaters, was amongst the most serious and immediate impacts of TGR impoundment. Fu et al. (2010) mainly attribute this effect to a fairly underestimated increase of chemical fertilizers application in agriculture (Fu et al., 2010). Further, increased sedimentation intensity is likely to cause accumulation of pollutants in sediments (Lin et al., 2012; Ye et al., 2011). During low water level periods, the sediments of the water level fluctuation zone are extensively used as soils for agriculture. Increasing pollutant concentrations in different

compartments of the ecosystem can also lead to bioaccumulation within in specific organisms and, further, be subject to biomagnification across the current food web. Fish and freshwater shrimps from the TGR comprise a major part of the local residents' diet. Thus, both food derived from agriculture in the water level fluctuation zone and from fisheries in the TGR might be subject of increased pollution levels and possibly pose a health risk to the local people. There is no general trend of pollutant contents in fish related to the impoundment of the TGR, but there are first results of Mercury contents in fish that have exceeded the Chinese safety threshold values of 300 ng/g in 2011 (Wang and Zhang, 2013).

In the downstream reaches of the Yangtze River, the amount of erosion seriously exceeded the expected and design levels (Fu et al., 2010). After commissioning of the TGD, decreasing sediment loads in the downstream Yangtze River reaches caused a shift from sedimentary to erosive regimes. This has already affected the stability of river banks in the middle and lower reaches of the Yangtze River and even the Yangtze River delta near Shanghai now revealed erosive patterns (Dai and Lu, 2014). Considerable changes in the seasonal hydrologic regimes within the middle and lower reaches of the Yangtze River, including both Dongting Lake and Poyang Lake systems, have also been reported (Dai and Lu, 2014, Lai et al. 2014).

Changes in habitat structures and the obstruction of migratory routes have affected numerous aquatic animal species. After the likely extinction of the Yangtze River Dolphin (*Lipotes vexillifer*) (Turvey et al. 2007), now the persistence of many further endemic species of the Yangtze River, e.g. the Yangtze finless porpoise (*Neophocaena phocaenoides asiaorientalis*), the Chinese paddlefish (*Psephurus gladius*), and the Chinese sturgeon (*Acipenser sinensis*) are at stake (Zhang and Lou, 2011). Unreasonable harvesting, habitat loss/degradation, water pollution, and biological invasion are considered being the major threats to fish endangerment in the Yangtze River basin amongst which damming and hydraulic works are ranked third by affecting around 40% of all occurring fish species (Ye et al., 2014). Further, it has been estimated that the changing habitat conditions in the downstream reaches of the TGD could favor the spreading of amphibious snails of the genus *Oncomelania* that serve as intermediate hosts for the parasitic trematode worm *Schistosoma japonicum*. *S. japonicum* causes Schistosomiasis/Bilharzia in humans and poses a severe health risk to more than $50 \cdot 10^6$ people within China (Gray et al., 2012). Even though the transmission rate in the downstream reaches did decrease within recent years, this is mainly attributed to medical chemotherapeutic treatment of cattle and humans. This treatment is likely to overshadow an increasing transmission rate caused by effects of the TGD (McManus et al., 2010). In the long-term, lake-like areas within the TGR are further estimated to become suitable habitats for snails of the

genus *Oncomelania* and these areas could likewise become epidemic regions for *S. japonicum* (McManus et al., 2010).

From these numerous environmental threats related to the construction of the TGD, the cumulated scientific publications directly address the following aspects: eutrophication (sections 2.1 - 2.6), pollutant sources and transport (sections 2.1 - 2.6), bioaccumulation of heavy metals related to algae (section 2.2), and sedimentation of polluted suspended particulate matter (sections 2.2 and 2.3). Further, MINIBAT data, water and sediment samples, as well as corresponding analytical data were used in collaboration with other groups of the 'Yangtze-Hydro Project' to study aspects of bioaccumulation and biomagnification of pollutants in a conceptual modelling approach (section 3.1) and also microbial degradation of organic pollutants in TGR sediments (section 3.2).

1.4.3 The Daning River backwater

The Daning River (Figure 2) is one of 40 major tributaries of the TGR. It enters the Yangtze River main stream approximately 120 km upstream of the TGD through the Wushan Lake. This is a wide lake-like confluence zone which was formed next to the city Wushan after impoundment of the TGR. The Daning River has a total length of 162 km, its watershed covers around 4170 km², and its mean discharge amounts to 136 m³/s (CQWRB, 2010). The TGR backwater reaches about 60 km upstream into the former Daning River valley also including the famous scenic area of the 'Little Three Gorges' (Figure 5). The Daning River backwater is characterized by an alternating sequence of narrow gorges and wide lake-like structures. Since the impoundment of the TGR, frequent algal blooms and poor water quality have been observed within these water bodies. Here, algal blooms mainly are not limited by nutrients but by optimal hydrodynamic conditions in the Daning River backwater (Wang and Zheng, 2013). There are several discharge locations of different scales for treated and untreated



Figure 5: 'Little Three Gorges' in the Daning River backwater of the TGR. Photo: A. Holbach, 25.08.2011.

wastewater entering the Wushan Lake and water bodies further upstream in the Daning River backwater. Additionally, large urban areas of the original cities Wushan and Dachang as well as former agricultural areas are now inundated by the TGR. These areas could be subject to remobilization of various pollutants into the water bodies.

The detailed analysis of an algal bloom development in the Daning River backwater,

particularly the Wushan Lake, in August, 2011 is subject of the publication in section 2.1. Further, urban pollution impacts on water quality around Wushan city and Dachang city in the Daning River backwater could be delineated by MINIBAT and water chemistry data during a winter scenario in December, 2011 (section 2.4). Further, an integrated monitoring and numerical modelling study is presented in section 2.5 dealing with problematic effects of Wushan city's waste water treatment plant discharge location and a possible mitigation measure.

1.4.4 The Xiangxi River backwater

The Xiangxi River is another one of 40 major tributaries of the TGR with a total length of 94 km, a catchment area of 2994 km², and an average discharge of around 60 m³/s (Li et al., 2014). The closure of the TGD impounded a long channel-shaped backwater along the former Xiangxi River valley (Figure 2; Figure 6). This tributary is entering the Yangtze River main channel approximately 40 km upstream of the TGD near the town Guojiaba. At its maximum water level of 175 m a.s.l., the backwater reaches more than 35 km upstream into this valley. Similar to most TGR tributaries, the Xiangxi River backwater is seriously affected by frequent and severe algal blooms as well as land use and land cover changes. There is a research station of the Chinese Academy of Sciences-Institute of Hydrobiology (CAS-IHB) in the town Xiakou located around 20 km upstream of the confluence zone with the Yangtze River main stream. The CAS-IHB has become a major collaborating research partner supporting MINIBAT fieldwork from their station in Xiakou.

Two scientific publications of this cumulated dissertation have been derived from data recorded during four fieldtrips within the Xiangxi River backwater. One peer-reviewed journal publication includes the detailed analysis of spatio-temporal water quality and water content analysis in September 2012 along the whole Xiangxi River backwater (section 2.2). This study revealed that large density current cells can amplify pollutant transport into the Xiangxi River backwater during rising



Figure 6: Downstream view from Xiakou along the Xiangxi River backwater of the TGR. Photo: A. Holbach, 13.09.2012.

water level phase in the TGR. Another paper has been submitted for publication to 'Water Resources Research' on 09 January, 2015 and is currently under peer-review. This paper addresses the seasonality of water quality characteristics around the town Xiakou from compiled MINIBAT data analysis of four fieldtrips in the Xiangxi River backwater (section 2.3). The Yangtze River main stream turned out to be the major driving factor of

dissolved and particulate water contents in the Xiangxi River backwater whilst the formation of thermal stratification near the water surface is the major trigger for algal growth and water quality changes related to photosynthetic activity.

1.5 The MINIBAT multi-sensor system for in situ and online water quality measurements

The MINIBAT multi-sensor probe was the central monitoring and sampling device of this work. In the frame of the Yangtze-Project, I have contributed considerably to its technical enhancement and extension of its applicability to the conditions in the TGR. In particular, a remote-controlled sampling system was implemented and technically optimized. Further, I have contributed to minimize

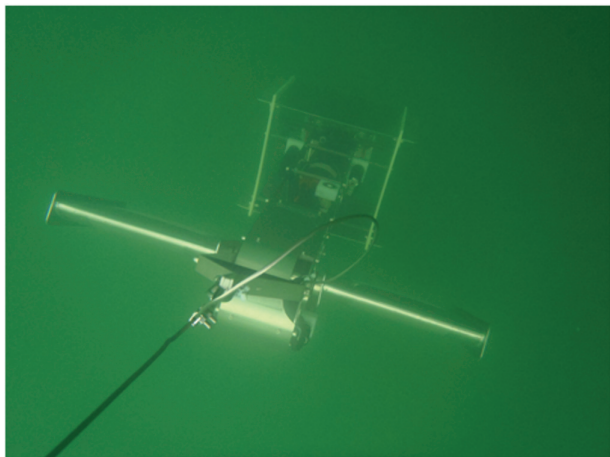


Figure 7: The MINIBAT in the water around Wushan in January 2013. Photo: A. Holbach, 15.01.2013.

disturbing sensor signals and malfunctions.

During application, the MINIBAT is connected to a boat with a data transmission cable for in situ and online measurements. A manual winch is used to adjust the length of the cable. The new and enhanced MINIBAT system is equipped with state of the art sensors to record nine water quality parameters as well as the developed remote-controlled water sampling system. Additionally, GPS and water depth data are simultaneously obtained from a Garmin GPSMAP 521s Chartplotter coupled with an echosounder on the boat. A pressure

sensor on the MINIBAT is used to determine its depth within the water body. At constant cable length, the MINIBAT can be dragged behind a boat at speeds of 5 to 10 km/h whilst it is diving at different depths up to around 30 m by use of its remote-controlled steerable wings. The MINIBAT can also be simply used as a depth-profiling probe in deeper waters when the boat does not move. A wide range of motorboat types can carry the MINIBAT as long as the winch can be properly fixed at a railing. 220 V AC electric power supply is obligatory and can either be provided from generators or from two car batteries in combination with 24V DC to 220 V AC power converters. All recorded data can be displayed in time on a computer connected to the data transmission cable. Thus, water samples can be taken at selected sites with water quality properties of specific interest to the current study. For example, different layers of stratified water bodies can be distinguished and sampled

directly by following the depth profile characteristics of different water quality parameters in an X/Y plot. Water samplers are released in sequence from the steering software on the computer.

1.6 Performed fieldwork and chemical analytics

In total, I attended nine fieldtrips for sampling and monitoring in China (Figure 8) as well as two MINIBAT test runs on Lake Constance in Germany. During eight out of nine fieldtrips a MINIBAT system could be applied; the newly developed MINIBAT of this project was available from June 2012 on for six remaining fieldtrips. The following scientific journal publications are based on data obtained from the fieldtrips in August 2011, December, 2011, June 2012, September 2012, November/December 2013, and March/April 2014. For all these fieldtrips, I was responsible for the prearrangements of sampling schedules, sampling equipment, as well as MINIBAT importation/exportation affairs on the German side. Our Chinese colleagues made the corresponding organizational and infrastructural arrangements within China. In the field, I was responsible for communication with our Chinese partners, MINIBAT setup on different boats, MINIBAT maintenance, selection of monitoring routes and sampling points in the water bodies, as well as for water sampling and sample preparation itself. At the KIT-IMG I got help in the labs for filter digestions from our technician Mrs. Cornelia Haug. Further, I performed IC analyses for dissolved anions assisted by our technician Mrs. Claudia Mößner, and I assisted Mrs. Claudia Mößner with the analyses of major, minor, and trace element contents using ICP-MS. Personally, I performed all the scientific data evaluation and interpretation of both MINIBAT and water chemistry datasets.

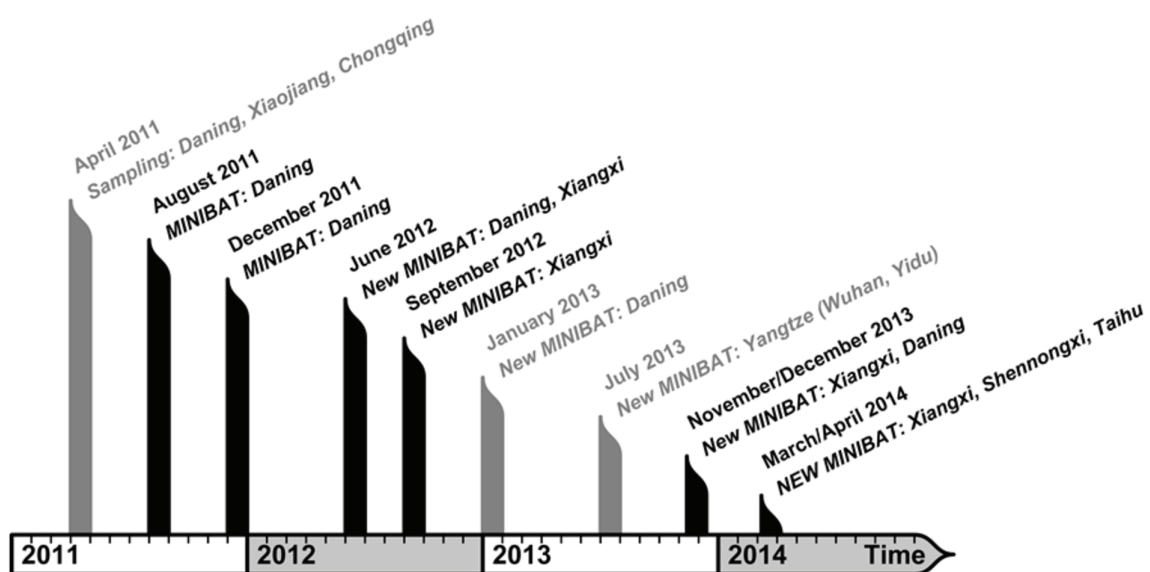
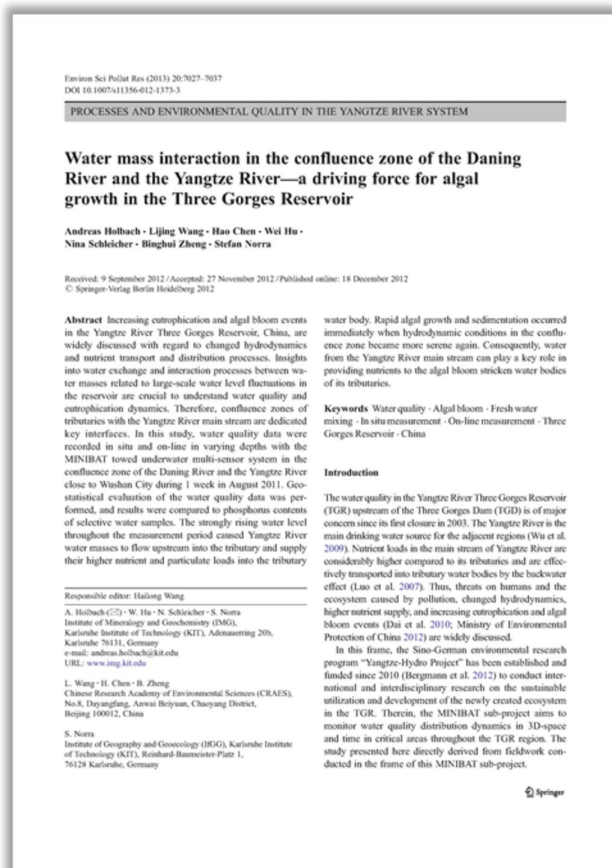


Figure 8: Timeline of the fieldwork conducted within the 'KIT-IMG' sub-project of the 'Yangtze-Hydro Project'. Note: in April 2011 the fieldwork was done without a MINIBAT. In August and December 2011 we could apply an old MINIBAT system. The newly developed MINIBAT system could be applied from June 2012 on. Data obtained from fieldtrips in black font are subject of the scientific publications cumulated in this dissertation.

2 First author scientific publications

2.1 Water mass interaction in the confluence zone of the Daning River and the Yangtze River—a driving force for algal growth in the Three Gorges Reservoir



Authors: *Andreas Holbach; Lijing Wang; Hao Chen; Wei Hu; Nina Schleicher; Binghui Zheng; Stefan Norra*

In: Environmental Science and Pollution Research, 2013, 20(10), 7027-7037, DOI: 10.1007/s11356-012-1373-320

Authorship statement

This peer-reviewed scientific journal article was written by me and is based on data obtained from a monitoring and sampling fieldtrip around Wushan in August, 2011. Personally, I was responsible for the preparation and accomplishment of the fieldwork including the first application of a MINIBAT system in the TGR as well as water sampling for analysis of dissolved and particulate water constituents. Further, I performed the corresponding analytics in the laboratories at KIT-IMG receiving

support from the technicians Claudia Mößner for ICP-MS analyses and Cornelia Haug for filter digestions. All scientific data evaluation including MINIBAT dataset analyses and corresponding geostatistical calculations were performed by me. Lijing Wang and Binghui Zheng were the responsible scientists and primary project partners from the Chinese Research Academy of Environmental Sciences (CRAES) who made the necessary arrangements for the fieldwork in China. Hao Chen from the CRAES was the responsible guide and attended our collaborated fieldwork. Wei Hu contributed hydrological and GIS data from sources in Chinese language. Nina Schleicher contributed to sample preparation and chemistry data evaluation. Stefan Norra designed and

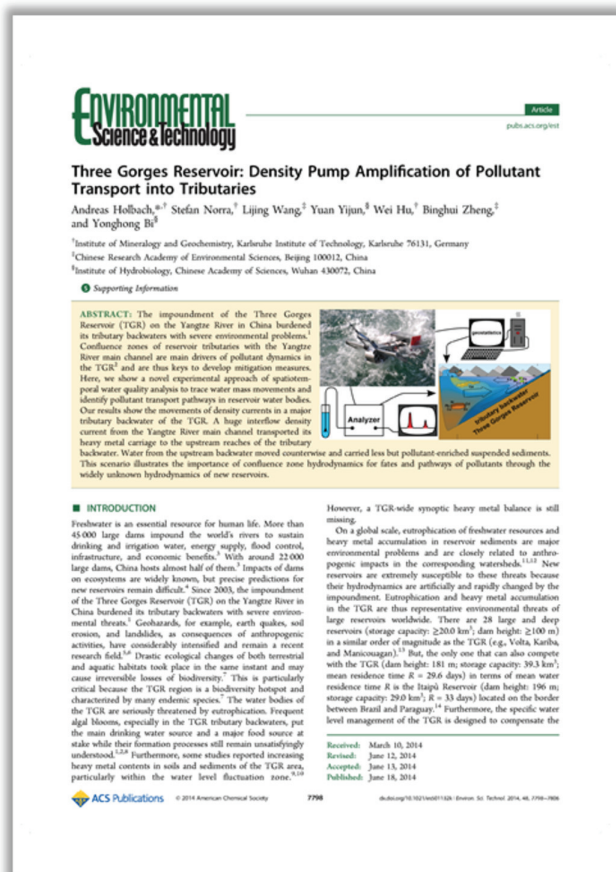
supervised the respective project and raised funds from the BMBF. All co-authors critically reviewed the manuscript and agreed to its publication.

Abstract

Increasing eutrophication and algal bloom events in the Yangtze River Three Gorges Reservoir, China, are widely discussed with regard to changed hydrodynamics and nutrient transport and distribution processes. Insights into water exchange and interaction processes between water masses related to large-scale water level fluctuations in the reservoir are crucial to understand water quality and eutrophication dynamics. Therefore, confluence zones of tributaries with the Yangtze River main stream are dedicated key interfaces. In this study, water quality data were recorded in situ and online in varying depths with the MINIBAT towed underwater multi-sensor system in the confluence zone of the Daning River and the Yangtze River close to Wushan City during 1 week in August 2011. Geostatistical evaluation of the water quality data was performed, and results were compared to phosphorus contents of selective water samples. The strongly rising water level throughout the measurement period caused Yangtze River water masses to flow upstream into the tributary and supply their higher nutrient and particulate loads into the tributary water body. Rapid algal growth and sedimentation occurred immediately when hydrodynamic conditions in the confluence zone became more serene again. Consequently, water from the Yangtze River main stream can play a key role in providing nutrients to the algal bloom stricken water bodies of its tributaries.

© The full article is reprinted with kind permission from Springer Science and Business Media and Environmental Science and Pollution Research in Appendix A.1.

2.2 Three Gorges Reservoir: Density Pump Amplification of Pollutant Transport into Tributaries



Authors: *Andreas Holbach; Stefan Norra; Lijing Wang; Yuan Yijun; Wei Hu; Binghui Zheng; Yonghong Bi*

In: Environmental Science & Technology, 2014, 48(14), 7798-7806, DOI: 10.1021/es501132k

Authorship statement

This peer-reviewed scientific journal article was written by me and is based on a MINIBAT fieldtrip in the Xiangxi River backwater of the TGR in September, 2012. Personally, I was responsible for the preparation and accomplishment of the fieldwork including application of the new MINIBAT system in the Xiangxi River backwater of the TGR as well as water sampling for analysis of dissolved and particulate water constituents. Further, I performed the corresponding analytics in

the laboratories at KIT-IMG receiving support from the technicians Claudia Mößner for ICP-MS analyses and Cornelia Haug for filter digestions. All scientific data evaluation including MINIBAT dataset analyses and corresponding geostatistical calculations were performed by me. Stefan Norra designed and supervised the respective project and raised funds from the BMBF. Lijing Wang and Binghui Zheng were the responsible scientists and primary project partners from the Chinese Research Academy of Environmental Sciences (CRAES) who made the necessary arrangements for the fieldwork in China. Yuan Yijun was the responsible guide in the field and attended and supported our collaborated fieldwork. Wei Hu attended and supported the fieldwork and contributed hydrological and GIS data from sources in Chinese language. Yonghong Bi was the responsible scientist from CAS-IHB who particularly facilitated the fieldwork in the Xiangxi River. All co-authors critically reviewed the manuscript and agreed to its publication

Abstract

The impoundment of the Three Gorges Reservoir (TGR) on the Yangtze River in China burdened its tributary backwaters with severe environmental problems. Confluence zones of reservoir tributaries with the Yangtze River main channel are main drivers of pollutant dynamics in the TGR and are thus keys to develop mitigation measures. Here, we show a novel experimental approach of spatiotemporal water quality analysis to trace water mass movements and identify pollutant transport pathways in reservoir water bodies. Our results show the movements of density currents in a major tributary backwater of the TGR. A huge interflow density current from the Yangtze River main channel transported its heavy metal carriage to the upstream reaches of the tributary backwater. Water from the upstream backwater moved counterwise and carried less but pollutant-enriched suspended sediments. This scenario illustrates the importance of confluence zone hydrodynamics for fates and pathways of pollutants through the widely unknown hydrodynamics of new reservoirs.

© The full article is reprinted with kind permission from ACS Publications and Environmental Science & Technology in Appendix A.2. Copyright © 2014 American Chemical Society.

2.3 Environmental water body characteristics in a major tributary backwater of the unique and strongly seasonal Three Gorges Reservoir, China

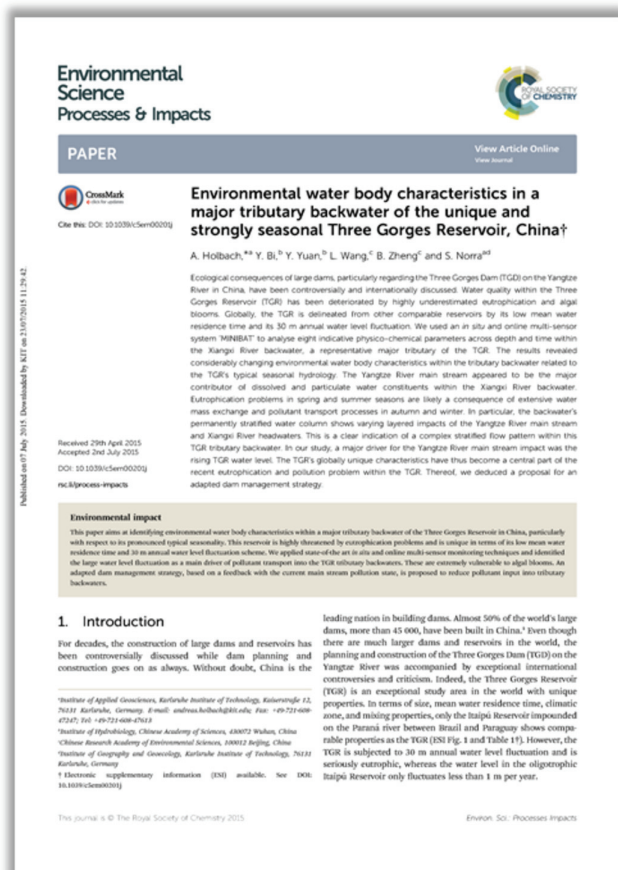
Authors: *Andreas Holbach; Yonghong Bi; Yijun Yuan; Lijing Wang; Binghui Zheng; Stefan Norra*

In: Environmental Science: Processes & Impacts, 2015, DOI: 10.1039/C5EM00201J.

Authorship statement

This peer-reviewed scientific journal article was written by me and is based on extensive MINIBAT fieldwork in the Xiangxi River backwater of the TGR during four fieldtrips in June 2012, September 2012, November/December 2013, and March 2014. Personally, I was responsible for the preparation and accomplishment of all the fieldwork including application of the new MINIBAT system in the Xiangxi River backwater of the TGR. All scientific data evaluation including MINIBAT dataset analyses and corresponding calculations

were performed by me. Yonghong Bi was the responsible scientist from the 'Chinese Academy of Sciences—Institute of Hydrobiology' who particularly facilitated the fieldwork in the Xiangxi River. Yuan Yijun was the responsible guide in the field and attended and supported our collaborated fieldwork. Lijing Wang and Binghui Zheng were the responsible scientists and primary project partners from the Chinese Research Academy of Environmental Sciences (CRAES) who made the necessary arrangements for the fieldwork in China. Stefan Norra designed and supervised the respective project and raised funds from the BMBF. All co-authors critically reviewed the manuscript and agreed to its publication

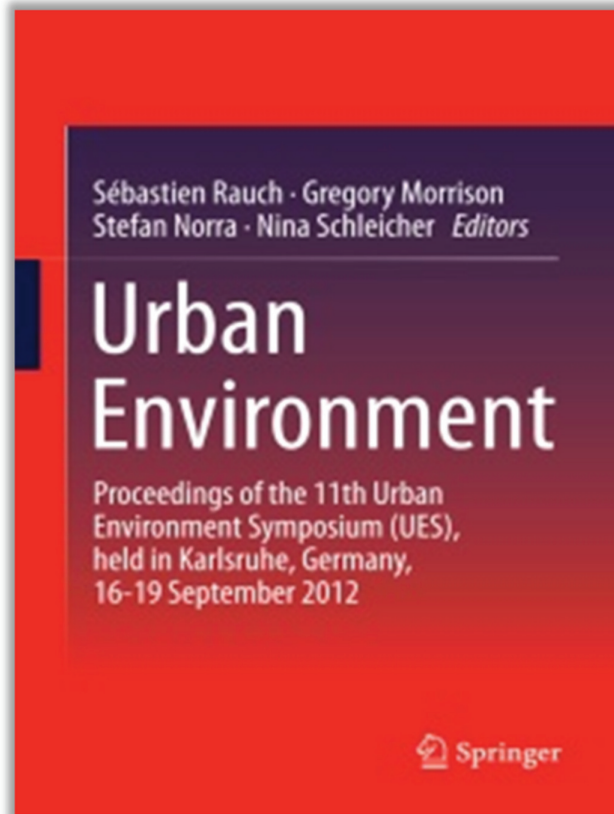


Abstract

Ecological consequences of large dams, particularly regarding the Three Gorges Dam (TGD) on the Yangtze River in China, have been controversially and internationally discussed. Water quality within the Three Gorges Reservoir (TGR) has been deteriorated by highly underestimated eutrophication and algal blooms. Globally, the TGR is delineated from other comparable reservoirs by its low mean water residence time and its 30 m annual water level fluctuation. We used the in situ and online multi-sensor system 'MINIBAT' to analyse eight indicative physico-chemical parameters across depth and time within the Xiangxi River backwater, a representative major tributary of the TGR. The results revealed considerably changing environmental water body characteristics within the tributary backwater related to the TGR's typical seasonal hydrology. The Yangtze River main stream appeared to be the major contributor of dissolved and particulate water constituents within the Xiangxi River backwater. Eutrophication problems in spring and summer seasons are likely a consequence of extensive water mass exchange and pollutant transport processes in autumn and winter. In particular, the stratified water column shows varying layered impacts of the Yangtze River main stream and the Xiangxi River headwaters. This is a clear indication of a complex stratified flow pattern within this TGR tributary backwater. In our study, a major driver for the Yangtze River main stream impact was the rising TGR water level. The TGR's globally unique characteristic has thus become a central part of the recent eutrophication and pollution problem within the TGR. Herefrom, we deduced a proposal for an adapted dam management strategy.

© The full article is reprinted with permission from The Royal Society of Chemistry in Appendix A.3.

2.4 Urban Pollutant Plumes around Wushan and Dachang City in the Three Gorges Reservoir



Authors: *Andreas Holbach; Lijing Wang; Hao Chen; Nina Schleicher; Wei Hu; Binghui Zheng; Stefan Norra*

In: Sébastien Rauch; Gregory Morrison; Stefan Norra; Nina Schleicher (eds.), *Urban Environment*, Springer, 2013, 437-447, DOI: 10.1007/978-94-007-7756-9_38

Authorship statement

This scientific article was written by me and is based on a dataset obtained from a monitoring and sampling fieldtrip around Wushan and Dachang in December, 2011. Personally, I was responsible for the preparation and accomplishment of the fieldwork including the application of a MINIBAT in the Daning River backwater of the TGR as well as water sampling for analysis of dissolved and particulate water

constituents. Further, I performed the corresponding analytics in the laboratories at KIT-IMG receiving support from the technicians Claudia Mößner for ICP-MS analyses and Cornelia Haug for filter digestions. All scientific data evaluation including MINIBAT dataset analyses and corresponding geostatistical calculations were performed by me. Lijing Wang and Binghui Zheng were the responsible scientists and primary project partners from the Chinese Research Academy of Environmental Sciences (CRAES) who made the necessary arrangements for the fieldwork in China. Hao Chen from the CRAES was the responsible guide and attended our collaborated fieldwork. Wei Hu contributed hydrological and GIS data from sources in Chinese language. Nina Schleicher contributed to sample preparation and chemistry data evaluation. Stefan Norra designed and supervised the respective project and raised funds from the BMBF. All co-authors critically reviewed the manuscript and agreed to its publication

Abstract

The Three Gorges Reservoir (TGR) in the Yangtze River was among other reasons meant to improve and strengthen socio-economic development of the involved regions. Considerable economic growth and urbanization now pose additional threat to the water quality of the TGR due to urban pollutant inflows. The changed hydrological conditions in the TGR have considerably altered pollutant transport dynamics now causing higher susceptibility of the backwater areas to eutrophication and algal blooms. The Yangtze River is also widely used as a source for drinking water production. The assessment of the urban impact on the water quality in the TGR is, thus, crucial for sustainable future development planning. Measurements with an underwater multi-sensor system (MINIBAT) were performed in the frame of the “Yangtze-Project” around the cities of Wushan and Dachang on the Daning River in the backwater reaches of the TGR in December 2011. Hydrological conditions were stable at constant water level between 174–175 m.a.s.l and low discharge conditions in the TGR during sampling period. 3D distribution patterns of the parameters temperature, conductivity, and turbidity in the water bodies were modeled using geostatistics. Selected water samples from different depths were analyzed for dissolved and particulate constituents using ICP-MS. Results show plumes of higher temperature, conductivity and turbidity in the epilimnion around the investigated urban areas. The range of influence was larger for temperature and conductivity plumes. Significant increase of turbidity was detected around Dachang City during few hours. Urban impacts on the water quality were significant at the encountered conditions and need to be further investigated for risk assessment, especially concerning drinking water production and eutrophication problems.

© The full article is reprinted with kind permission from Springer Science and Business Media in Appendix A.4.

2.5 Integrated water quality monitoring and modeling in the Three Gorges Reservoir, China



Authors: *Andreas Holbach; Wei Hu; Lijing Wang; Hao Chen; Nina Schleicher; Binghui Zheng; Bernhard Westrich; Stefan Norra*

In: Hartwig Steusloff (ed.), *Integrated Water Resources Management Karlsruhe 2012—Conference Proceedings*, Fraunhofer Verlag, 2012, 132-138, ISBN: 978-3-8396-0478-6

Authorship statement

This scientific article was written by me and represents an extended abstract of my talk at the Integrated Water Resources Management (IWRM) conference held in Karlsruhe on 21-22 November, 2012. The article was published in the corresponding proceedings book. Personally, I was responsible for the preparation and accomplishment of the fieldwork including the first application of a MINIBAT system in

the TGR as well as water sampling for analysis of dissolved and particulate water constituents. Further, I performed the corresponding analytics in the laboratories at KIT-IMG receiving support from the technicians Claudia Mößner for ICP-MS analyses and Cornelia Haug for filter digestions. All MINIBAT data evaluation and corresponding geostatistical calculations were performed by me. Wei Hu performed the complementary hydrodynamic numerical modelling calculations. Finally, both of us facilitated the integration of these datasets. Lijing Wang and Binghui Zheng were the responsible scientists and primary project partners from the Chinese Research Academy of Environmental Sciences (CRAES) who made the necessary arrangements for the fieldwork in China. Hao Chen from the CRAES was the responsible guide and attended our collaborated fieldwork. Nina Schleicher contributed to sample preparation and chemistry data evaluation. Bernhard Westrich and Stefan Norra designed and supervised the respective projects and raised funds from the BMBF. All co-authors critically reviewed the manuscript and agreed to its publication.

Abstract

Increasing eutrophication and algal bloom events in the Yangtze River Three Gorges Reservoir are widely discussed in relation to hydrodynamics and nutrient transport and distribution processes. Insights into water exchange and interaction dynamics between water masses related to large scale water level fluctuations in the reservoir are crucial to understand water quality and eutrophication dynamics. Therefore, confluence zones of tributaries with the Yangtze River main stream are dedicated key interfaces. In this study, water quality data recorded in situ and online with the MINIBAT towed underwater multi-sensor system is integrated with data obtained from simulations done with TELEMAC hydrodynamic 2D numerical modeling. Key scenario for the current study was a discharge peak and corresponding rising water level in the Yangtze River at its confluence zone with the Daning River following a heavy precipitation event in August 2011. Water quality data obtained from MINIBAT measurements during this specific period suggest that Yangtze River main stream water flowed upstream into the Daning River. Hydrodynamic 2D numerical modeling supports that hypothesis and enables to specify water and substance origins. Observed algal blooming can only be partly explained by the 2D modeling approach. 3D effects like the stabilization of thermal stratification at the water surface forming good conditions for algal blooming cannot be simulated but were measured with the MINIBAT. However, input of higher nutrient loads from Yangtze River water and from waste water discharges into the Wushan Lake are supported by the model and the field measurements and may have played a key role for the observed algal bloom formation.

© The full article is reprinted with kind permission from Fraunhofer Verlag and Fraunhofer-IOSB in Appendix A.5.

2.6 Dilution of pollution? Processes affecting water quality in the river-style Three Gorges Reservoir



Authors: *Andreas Holbach; Tilman Floehr; Irene Kranzioch; Anja Wolf*

In: Environmental Science and Pollution Research, 2013, 20(10), 7140-7141, DOI: 10.1007/s11356-012-1252-y

Authorship statement

This article is a concluding report about the ‘workshop on processes in the Yangtze River system’ held on the occasion of the 10th anniversary of joint Sino-German research cooperation in the Yangtze River basin at Tongji University in Shanghai on 22 and 23 September, 2012. In the first place, I had the idea to compile the generalized workshop results from presentations and discussions within this report. Therefore, I have received help from Tilman Floehr, Irene Kranzioch, and Anja Wolf. I wrote the resulting paper in the first place. All co-

authors critically reviewed the manuscript and agreed to its publication.

Abstract

The Three Gorges Reservoir (TGR) in the Yangtze River is a globally unique water body located in a rapidly developing area of China. Despite increasing efforts for pollution control, large amounts of various pollutants enter the TGR water bodies and cause severe eutrophication and increasing numbers of algal blooms. With respect to drinking water extraction, concentrations of anthropogenic pollutants, however, rarely reach critical levels. Dilution of these compounds by the large average discharge of 30,000 m³/s leads to low absolute concentrations, but tremendous total loads are transported further downstream and may remain a threat to connected ecosystems. At Tongji University in Shanghai, China, scientists and representatives from governmental institutions of China and Germany held the “Workshop on Processes in the Yangtze River System” to discuss recent

cutting edge environmental research in the Yangtze River with a focus on the TGR. Extensive exchange on the (1) “Yangtze River Water Ecosystem,” (2) “Pollutants in the Water/Soil/Sediment Interface,” (3) “Water Treatment and Management,” and (4) “Monitoring, Modeling and Management” lead to controversies about the ecological quality and environmental pollution status of the Yangtze River and the TGR. Indeed, this discussion impressively pointed out the necessity for further corresponding research. However, as a first step Priority pollutants could be identified. Looking ahead, the seriously polluted and eutrophic Taihu Lake was suggested for further Sino–German cooperative research for sustainability in the water sector.

© The full article is reprinted with kind permission from Springer Science and Business Media and Environmental Science and Pollution Research in Appendix A.6.

3 Co-authored related scientific publications

3.1 An integrated approach to model the biomagnification of organic pollutants in aquatic food webs of the Yangtze Three Gorges Reservoir ecosystem using adapted pollution scenarios



Authors: Björn Scholz-Starke; Richard Ottermanns; Ursula Rings; Tilman Floehr; Henner Hollert; Junli Hou; Bo Li; Lingling Wu; Xingzhong Yuan; Katrin Strauch; Wei Hu; Stefan Norra; **Andreas Holbach**; Bernhard Westrich; Andreas Schäffer; Martina Roß-Nickoll

In: Environmental Science and Pollution Research, 2013, 20(10), 7009-7026, DOI: 10.1007/s11356-013-1504-5

Authorship statement

This peer-reviewed scientific journal article is based on a modelling study that integrated field data, lab data, and data from literature sources into an integrated biomagnification model framework for the TGR. In particular, I have processed and contributed data on bathymetry, water quality, and water constituents from the

MINIBAT fieldwork as input data for the AQUATOX model. Further, I contributed to the revision and correction of the draft manuscript. In total my contribution to this article amounts to 15%.

Abstract

The impounding of the Three Gorges Reservoir (TGR) at the Yangtze River caused large flooding of urban, industrial, and agricultural areas, and profound land use changes took place. Consequently, substantial amounts of organic and inorganic pollutants were released into the reservoir. Additionally, contaminants and nutrients are entering the reservoir by drift, drainage, and runoff from adjacent agricultural areas as well as from sewage of industry, aquacultures, and households.

The main aim of the presented research project is a deeper understanding of the processes that determines the bioaccumulation and biomagnification of organic pollutants, i.e., mainly pesticides, in aquatic food webs under the newly developing conditions of the TGR. The project is part of the Yangtze-Hydro environmental program, financed by the German Ministry of Education and Science. In order to test combinations of environmental factors like nutrients and pollution, we use an integrated modeling approach to study the potential accumulation and biomagnification. We describe the integrative modeling approach and the consecutive adaption of the AQUATOX model, used as modeling framework for ecological risk assessment. As a starting point, pre-calibrated simulations were adapted to Yangtze specific conditions (regionalization). Two exemplary food webs were developed by a thorough review of the pertinent literature. The first typical for the flowing conditions of the original Yangtze River and the Daning River near the city of Wushan, and the second for the stagnant reservoir characteristics of the aforementioned region that is marked by an intermediate between lake and large river communities of aquatic organisms. In close cooperation with German and Chinese partners of the Yangtze-Hydro Research Association, other site-specific parameters were estimated. The MINIBAT project contributed to the calibration of physicochemical and bathymetric parameters, and the TRANSMIC project delivered hydrodynamic models for water volume and flow velocity conditions. The research questions were firstly focused on the definition of scenarios that could depict representative situations regarding food webs, pollution, and flow conditions in the TGR. The food webs and the abiotic site conditions in the main study area near the city of Wushan that determine the environmental preconditions for the organisms were defined. In our conceptual approach, we used the pesticide propanil as a model substance.

© The full article is reprinted with kind permission from Springer Science and Business Media and Environmental Science and Pollution Research in Appendix B.1.

3.2 Dechlorination and organohalide-respiring bacteria dynamics in sediment samples of the Yangtze Three Gorges Reservoir



Authors: Irene Kranzloch; Claudia Stoll; Andreas Holbach; Hao Chen; Lijing Wang, Binghui Zheng; Stefan Norra; Yonghong Bi; Karl-Werner Schramm; Andreas Tiehm

In: Environmental Science and Pollution Research, 2013, 20(10), 7046-7056, DOI: 10.1007/s11356-013-1545-9

Authorship statement

This peer-reviewed scientific journal article is based on degradation batch experiments performed on sediment samples from the TGR. In particular, I have provided sediment samples and corresponding water quality data from the MINIBAT fieldwork. I was responsible for GIS data handling and presentation. Further, I contributed to the revision and correction of the draft manuscript. In total my contribution to this article amounts to 15%.

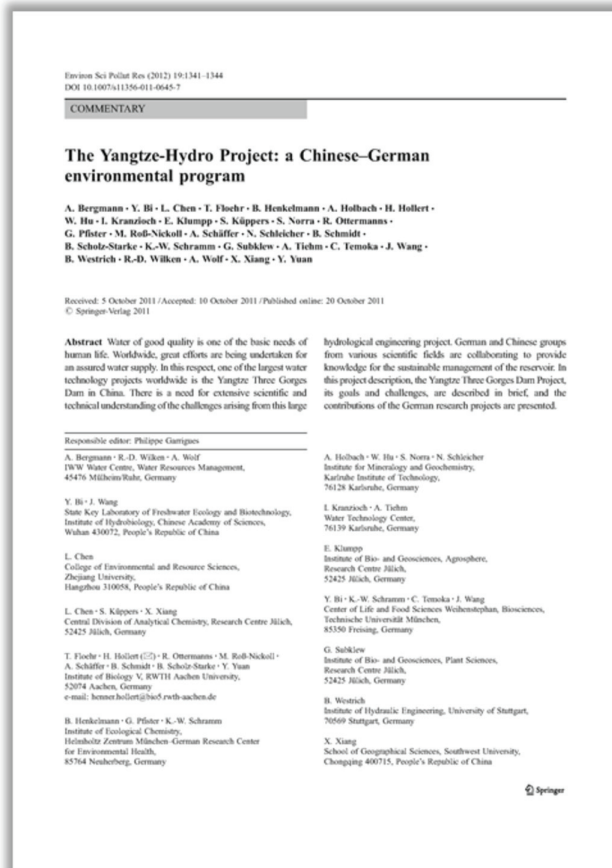
Abstract

Several groups of bacteria such as *Dehalococcoides* spp., *Dehalobacter* spp., *Desulfomonile* spp., *Desulfuromonas* spp., or *Desulfitobacterium* spp. are able to dehalogenate chlorinated pollutants such as chloroethenes, chlorobenzenes, or polychlorinated biphenyls under anaerobic conditions. In order to assess the dechlorination potential in Yangtze sediment samples, the presence and activity of the reductively dechlorinating bacteria were studied in anaerobic batch tests. Eighteen sediment samples were taken in the Three Gorges Reservoir catchment area of the Yangtze River, including the tributaries Jialing River, Daning River, and Xiangxi River. Polymerase chain reaction analysis indicated the presence of dechlorinating bacteria in most samples, with varying dechlorinating microbial community compositions at different sampling locations. Subsequently, anaerobic reductive dechlorination of tetrachloroethene (PCE) was tested after the addition of electron donors. Most

cultures dechlorinated PCE completely to ethene via cis-dichloroethene or trans-dichloroethene. Dehalogenating activity corresponded to increasing numbers of *Dehalobacter* spp., *Desulfomonile* spp., *Desulfitobacterium* spp., or *Dehalococcoides* spp. If no bacteria of the genus *Dehalococcoides* spp. were present in the sediment, reductive dechlorination stopped at cis-DCE. Our results demonstrate the presence of viable dechlorinating bacteria in Yangtze samples, indicating their relevance for pollutant turnover.

© The full article is reprinted with kind permission from Springer Science and Business Media and Environmental Science and Pollution Research in Appendix B.2.

3.3 The Yangtze-Hydro Project: a Chinese–German environmental program



Authors: Axel Bergmann; Yonghong Bi; Lei Chen; Tilman Floehr; Bernhard Henkelmann; **Andreas Holbach**; Henner Hollert; Wei Hu; Irene Kranzioch; Erwin Klumpp; Stephan Küppers; Stefan Norra; Richard Ottermanns; Gerd Pfister; Martina Roß-Nickoll; Andreas Schäffer; Nina Schleicher; Burkhard Schmidt; Björn Scholz-Starke; Karl-Werner Schramm; Günter Subklew; Andreas Tiehm; Cedrique Temoka; Jingxian Wang; Bernhard Westrich; Rolf-Dieter Wilken; Anja Wolf; X. Xiang; Ye Yuan

In: Environmental Science and Pollution Research, 2012, 19(4), 1341-1344, DOI: 10.1007/s11356-011-0645-7

Authorship statement

This peer-reviewed scientific journal article is based on the project applications as well as on experiences and ideas gathered

during first workshops and fieldwork within the Yangtze-Hydro Project. In particular, I have contributed to the MINIBAT sub-project description as well as to the revision and correction of the draft manuscript. In total my contribution to this article amounts to 5%.

Abstract

Water of good quality is one of the basic needs of human life. Worldwide, great efforts are being undertaken for an assured water supply. In this respect, one of the largest water technology projects worldwide is the Yangtze Three Gorges Dam in China. There is a need for extensive scientific and technical understanding of the challenges arising from this large hydrological engineering project. German and Chinese groups from various scientific fields are collaborating to provide knowledge for the sustainable management of the reservoir. In this project description, the Yangtze Three Gorges

Water quality and pollutant dynamics in the Three Gorges Reservoir

3 Co-authored related scientific publications

Dam Project, its goals and challenges, are described in brief, and the contributions of the German research projects are presented.

© The full article is reprinted with kind permission from Springer Science and Business Media and Environmental Science and Pollution Research in Appendix B.3.

4 Synoptic conclusion

From the scientific results collected in sections 2 and 3 of this dissertation, as well as information and data from scientific literature, I have derived a qualitative conceptual model of anthropogenic impacts on water body processes in the newly created ecosystem along the TGR (Figure 10). Distinct effects of anthropogenic point sources on water quality, pollutant contents, and water body processes could be identified (sections 2.1, 2.2, 2.4, and 2.5) within this work. However, the total pollutant loads in the TGR derive from a variety of point and non-point sources from urban areas,



Figure 9: Extensive agriculture on semi-terrestrial soils of the TGR water level fluctuation zone around Kaixian at the Xiaojiang River in April 2011. Photo: A.Holbach, 04.2011.

industrial plants, agriculture, and polluted inundated areas being not nearly and satisfyingly quantified and understood, yet (Fu et al., 2010). Further, there is a massive impact from the management of the TGD inducing an annual 30 m water level fluctuation which is opposed to the original seasonal water level cycle of the Yangtze River prior to construction of the TGD. Among others, this characteristic of the TGR is making it globally unique in terms of hydrodynamic processes, pollutant transport, and stratification characteristics (sections 2.1, 2.2, 2.3, 2.4, and 2.5).

These anthropogenic impacts interfere with a complex system connecting the TGR water bodies with their sediments and semi-terrestrial soils as well as with the biological food web of the TGR. Changes in this complex system can in turn have positive and/or negative consequences on utilized ecosystem services (Figure 10), which are mainly drinking water extraction (Liu et al., 2012), fisheries (Wang et al., 2013), and agriculture. It is noteworthy for the TGR that the semi-terrestrial soils of the reservoir water level fluctuation zone are widely used as agricultural soils throughout the TGR area (Figure 9; own field observations). Currently, local inhabitants of the TGR area rely on the production and consumption of local agricultural and fisheries products.

4.1 Utilized ecosystem services—water body processes and feedbacks from anthropogenic impacts

4.1.1 Drinking water

The quality of drinking water extracted from the TGR is mainly affected by the following processes in the water bodies (Figure 10):

- **Anthropogenic pollution, pollutant transport, resuspension, sedimentation, and pollutant release**

For drinking water extraction it is important that the pollution state of the extracted water does not pose a health risk to consumers. Anthropogenic pollution from point and non-point sources is ubiquitous in the TGR. In such dynamic water bodies, transport processes can either move pollutants towards or away from drinking water extraction points. This depends on the location of extraction points and on the current flow conditions. Especially, tributary backwaters of the TGR are highly affected by pollutants entering from the Yangtze River main stream through water exchange dynamics (sections 2.1 - 2.3, and 2.5). These are driven by water level changes (section 2.1) and density pump effects triggered by differences of thermal stratification between the Yangtze River main stream and its tributary backwaters (section 2.2). Urban pollution of TGR water bodies can also considerably affect water quality (sections 2.1, 2.2, 2.4, 2.5, and 2.6). Merely taking local flow paths into account when discharge locations are being established can alter pollutant distributions and mitigate corresponding effects. Overall, however, the pollutant concentrations of TGR waters measured within this work did not exceed current thresholds of drinking water guidelines. Sedimentation processes (sections 2.1 and 2.3) remove particles and attached pollutants from the upper water column, whereas resuspension processes would act inversely. Pollutant release from sediments often happens due to microbial redox and mineralization processes. Particularly, the agriculturally used semi-terrestrial soils of the TGR water level fluctuation zone are critical in this respect. Any fertilizers and/or pesticides applied there during low water level periods would instantly get in contact with the TGR water bodies during the next high water level period. Resuspension and Pollutant release processes could, however, not be identified within this work.

- **Eutrophication, algal growth, and toxin release**

The concentrations of NO_3^- (aq) that I have measured from the TGR water samples were all below 10 mg/L (unpublished data) and are thus not critical with respect to drinking water guidelines (WHO, 2011 and DVGW, 2011). However, due the additionally high phosphorus

concentrations, in most cases algal growth in the TGR is not limited by nutrients (sections 2.1 and 2.3). High contents of algae in the water can aggravate the drinking water treatment processes and cause bad odors, high photosynthetic activity can strongly modify pH and O₂ concentrations (sections 2.1, 2.2, and 2.3) so that pH could even exceed thresholds of drinking water guidelines. Further, I have found evidence for bioaccumulation of heavy metals in algae (section 2.2). The most serious threat in this respect, however, is the production and release of toxins released by cyanobacteria (blue-green algae). These are posing a severe health risk to consumers. It was found that Chlorophyll *a* correlates with concentrations of microcystins released by cyanobacteria in the TGR (Xu et al., 2011). Even though the concentrations measured by Xu et al. (2011) did not exceed WHO (WHO, 2011) guideline of 1 µg/L, the area around Wushan city with 0.57 µg/L showed the highest contamination with microcystins along the TGR indicating potential risk for drinking water safety related to algal bloom events.

- **Pollutant degradation**

Non-persistent substances in water bodies are degraded by various physico-bio-chemical processes, in particular by microbes. In this respect, one important example is the active dechlorination of chloroethenes by bacteria in TGR sediments (section 3.2) which was proven in a study to which my work did considerably contribute. Pollutant degradation is, of course, solely beneficial with respect to utilized ecosystem services including drinking water extraction.

4.1.2 Fisheries

The TGR is also a considerable fishing resource on which the local inhabitants rely. The yield and quality of this utilized ecosystem service is mainly affected by the following processes in the water bodies (Figure 10):

- **Biomass growth, food web dynamics, bioaccumulation, biomagnification, and ecotoxicity**

The overall fish density and catch yield in the TGR increased considerably after impoundment of the TGR (Wang et al., 2013). Increased primary production in the TGR is likely to result in higher fish biomass. This work has considerably contributed to the understanding of algal growth dynamics as an important contributor to primary production of biomass in the TGR (sections 2.1, 2.2, 2.3, and 2.5), as well as bioaccumulation (sections 2.2 and 3.1), food web dynamics (3.1), biomagnification (3.1), and ecotoxicity (3.1) in the TGR. Pollutants can be subject to biomagnification across aquatic food webs before fishes are consumed by humans. Bioaccumulation in algae (section 2.2) as primary producers is thus forming one

starting point, here. Sedimentation of polluted particulate matter (sections 2.2 and 2.3) could form another starting point by increased exposure of grazing organisms and bottom feeding fishes. Zheng et al. (2007) have shown that fishes from the TGR show slight contamination below food standard thresholds with the As, Cd, Cr, Cu, Hg, Pb, and Zn, whereas for Hg, occasionally more than 300 ng/g were found thus exceeding the safety level for human consumption (Wang and Zhang, 2013). Despite Zn, fishes occupying the bottom water layer showed higher contents than those in the middle and upper water layer thus indicating effects of contaminated sediments. Within food webs, ecotoxic effects can occur on any trophic level. From an anthropogenic perspective the worst case would be human health effects by consuming contaminated fisheries products. However, any ecotoxic effects on other food web levels could strongly alter the composition of aquatic biocenoses and cause drastic changes of fishery yields. So far, the results of this dissertation and of other studies are not universal and representative enough to give a conclusive statement on the magnitudes and possible health risks for local residents in the TGR area by these processes.

- **Pollutant release and pollutant degradation**

In particular, microbial redox and mineralization processes in sediments can cause both release of pollutants into the water column and degradation of non-persistent pollutants. I have contributed to prove the presence of active microbial communities capable of degrading chloroethenes in many TGR sediments (section 3.2). This is beneficial in terms of all utilized ecosystem services. Release of pollutants or toxic intermediate products of degradation processes from sediments can on the other hand also increase the exposure of aquatic organisms and form starting points of the accumulation and magnification processes described above. To my knowledge, however, respective and representative data are not available until now.

4.1.3 Agriculture

As mentioned above and illustrated in Figure 9, the semi-terrestrial soils of the TGR water level fluctuation zone are extensively used for agriculture during low water level periods. In this respect, also revegetation and phytoremediation with plants that accumulate pollutants and stabilize soils is currently discussed and investigated (e.g. Peng et al., 2014). Agricultural production in this ecosystem compartment is affected by the following water body related processes (Figure 10):

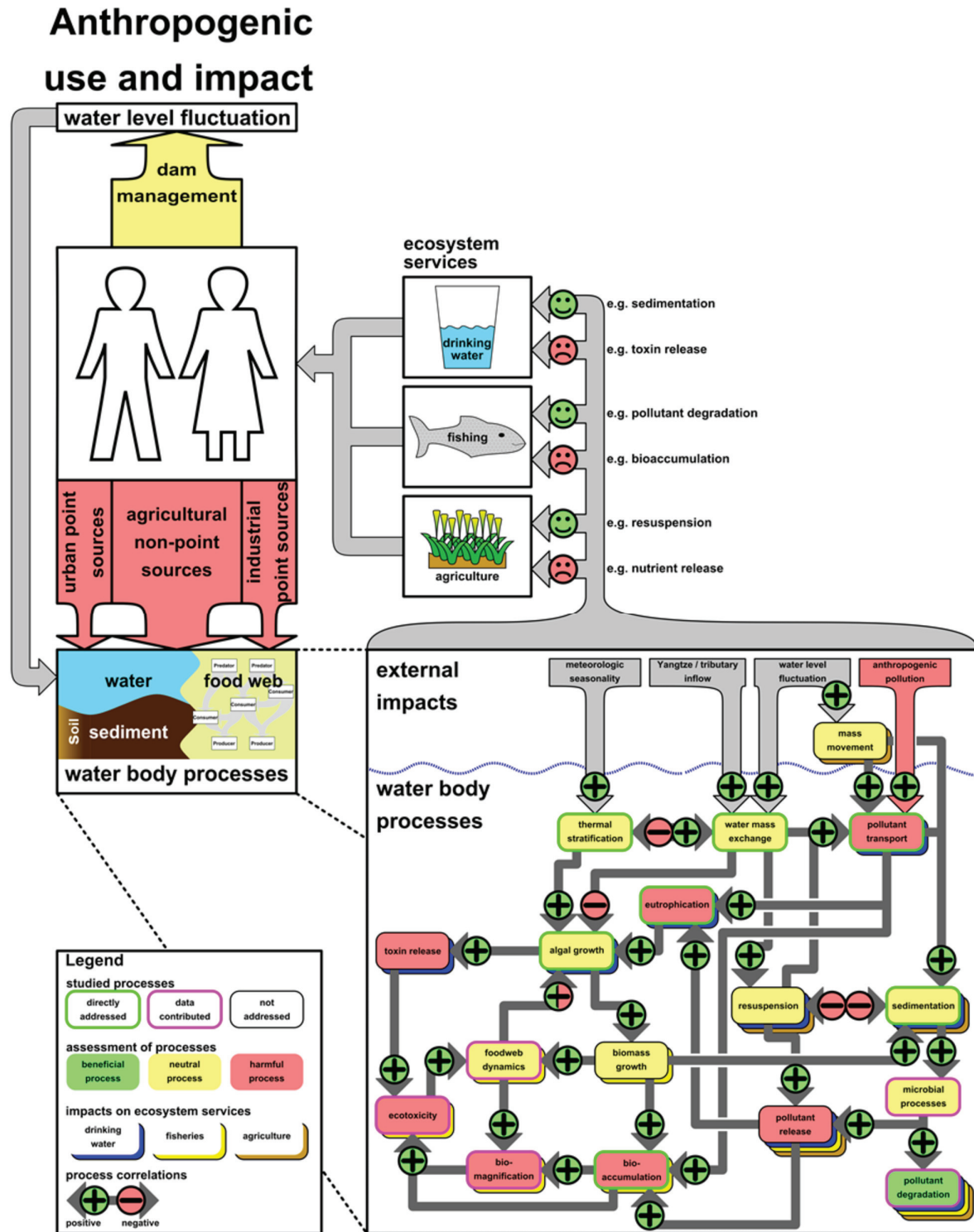


Figure 10: Qualitative conceptual model of anthropogenic impact on processes within the Three Gorges Reservoir ecosystem as well as corresponding consequences for utilized ecosystem services. Specific contributions of the cumulated scientific publication of this dissertation to the understanding of the complex system are marked according to the legend.

- **Mass movement, resuspension, sedimentation**

All these processes either cause loss or gain of material in the semi-terrestrial soils of the TGR water level fluctuation zone. The quality of the resulting material will then affect the quality and yields of produced agricultural crops and thus determine the benefits of this utilized ecosystem service. Landslides, soil erosion, and resuspension lead to gradual loss of soil material from the water level fluctuation zone. On the contrary, sedimentation (sections 2.1 and 2.3) can deliver new material to these areas during high water level periods. Thus, in the long term, the pollution state of sedimented material (section 2.2) could become a determining factor of the quality of semi-terrestrial soils in these areas.

- **Pollutant release and pollutant degradation**

Both processes improve the pollution state of semi-terrestrial soils in the water level fluctuation zone. At the same time, however, nutrients can transfer into the water column, decrease soil fertility, and as described above aggravate eutrophication of the water bodies. Pollutant degradation (section 3.2) in semi-terrestrial soils, however, decreases the exposure of agricultural crops and consequently contributes to their good quality for human consumption.

4.2 Relevance of tributary backwaters in the newly created ecosystem along the Three Gorges Reservoir

The newly created ecosystem along the TGR consists of the water bodies in the Yangtze River main stream and its tributary backwaters. These water bodies are inhabited by a certain biocenoses and are in direct contact with sediments at the reservoir bottom and semi-terrestrial soils of the water level fluctuation zone, as well as the vegetation of the water level fluctuation zone. Major inputs into this ecosystem derive from the Yangtze River inflow, tributary inflows, urban and industrial point sources as well as agricultural non-point sources. Major output of this system is the TGD outflow. On the basis of this dissertation's results, a scheme of the spatial distribution of the relevant water body processes and external impact factors can be drawn (Figure 11).

Within this system, the Yangtze River main stream is characterized by river-like hydrodynamic conditions. It is fully mixed and transport processes happen linearly from upstream to downstream. Along the Yangtze River main stream, there are numerous cities, industries, and loading bays for mining materials acting as point sources of pollutants (sections 2.1, 2.2, 2.4, and 2.5). Agricultural areas act as non-point sources of nutrients and e.g. pesticides.

The TGR tributary backwaters amount to one third of the total reservoir area (Ponseti and López-Pujol, 2006) and exhibit very different characteristics. Their water masses and dissolved solids mainly derive from the Yangtze River main stream (section 2.3). However, slower flow velocities and much larger water residence times induce the sedimentation of suspended particulate matter and decreasing turbidity there (sections 2.1 and 2.3). Further, there is a seasonally changing but permanently present stratification in the water column (section 2.3). This stratification leads to the formation of large-scale density current circulations between tributary backwaters and the Yangtze River main stream. Absolute water mass exchange is mainly driven by water level changes in the TGR. However, the additional density pump effect (section 2.2) amplifies lateral transport distances many times over. As such, dissolved and particulate pollutants (e.g. nutrients and heavy metals) can enter far into tributary backwaters. The frequent formation of algal blooms within TGR tributary backwaters is then an obvious consequence of excess nutrient loads and stable thermal surface stratification mainly occurring in spring and summer. Algal blooms strongly enlarge the primary production within the ecosystem and consequently affect the related food web. Especially bioaccumulation of heavy metals in algae (section 2.2) can form a starting point of biomagnification (section 3.1) across the food web. The contribution of urban, industrial, agricultural, and mining areas to pollutant inputs from the tributary watersheds themselves is of course dependent on the specific regional settings. For example, I have found significant impacts of urban pollution on water quality around Dachang city far within in the Daning River backwater in winter (section 2.4). With respect to nutrients, the contribution of tributary headwaters amounts to less than 3% of those found within TGR tributary backwaters (Huang et al., 2014).

Overall it is obvious, that the Yangtze River main stream is characterized by higher pollution levels and loads. Massive dilution of pollutants by the vast Yangtze River discharge, however, mainly keeps their concentrations below critical levels. In terms of water body relevant physico-bio-chemical processes and the corresponding utilization of ecosystem services, however, the tributary backwaters of the dendritic TGR are to a large extent more complex, relevant, and significant. They require much more attention from environmental scientists. Further, latest environmental research in the TGR was very much focused on algal blooms and specific ecological conditions leading to their formation. This work also contributed a lot to understand these processes in particular. The more, it revealed large-scale pollutant transportation processes from the Yangtze River main stream into its TGR tributary backwaters stoking further eutrophication, there. I also found evidence for processes possibly causing long-term environmental threats such as accumulation of pollutants in sediments, semi-terrestrial soils, and organisms. So far, these have only been unsatisfyingly and insufficiently addressed by scientific studies.

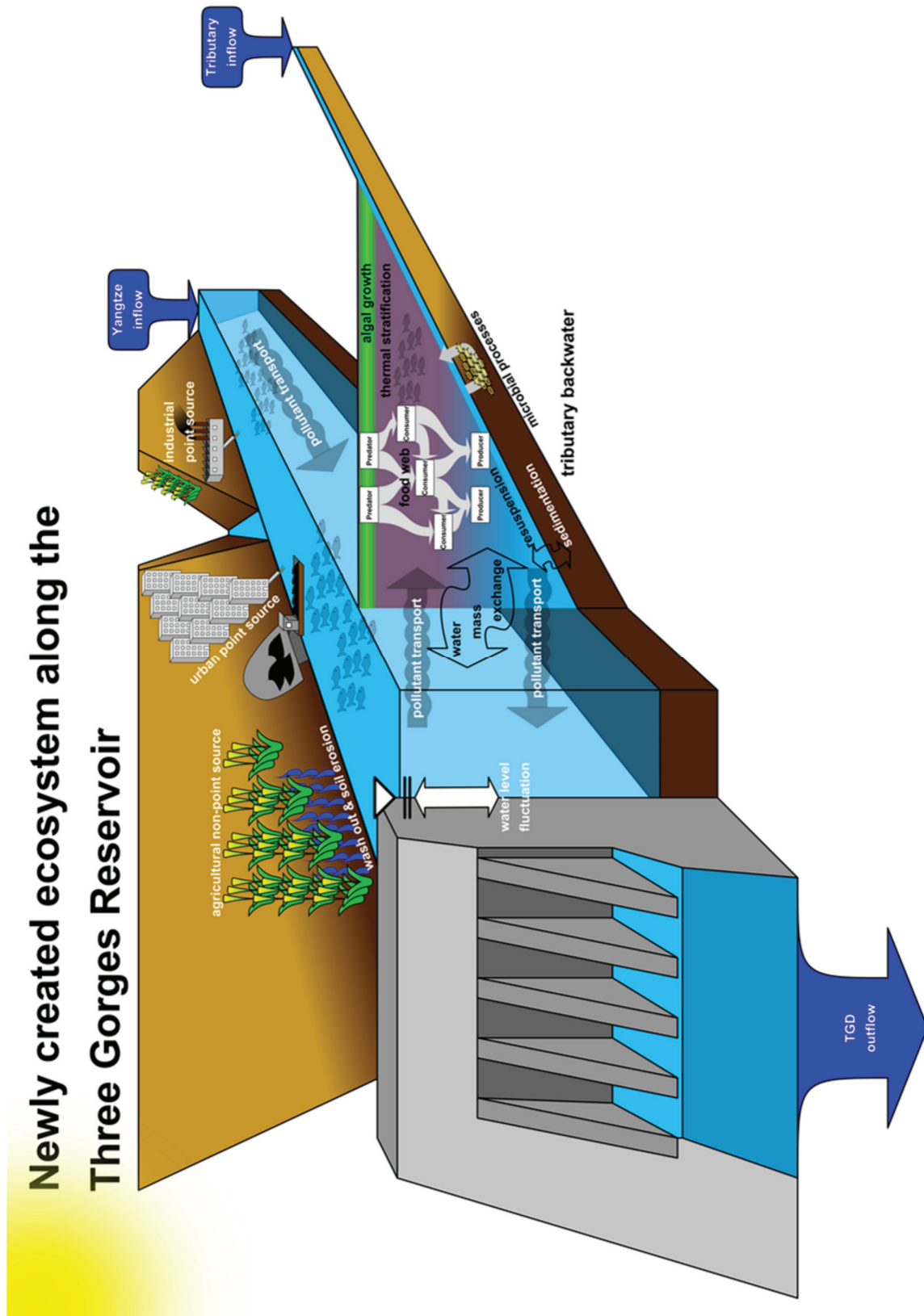


Figure 11: Spatial scheme of water body processes and external impact factors within the newly created ecosystem along the TGR.

4.3 Applicability and implications of the results

Revisiting the key points of section 1.4 that summarize reasons for environmental monitoring and scientific evaluation of water body processes related to the TGD and the impoundment of the TGR, the following conclusions can be drawn:

The results of this work can considerably contribute to the development of **immediate mitigation measures** of environmental threats in the TGR. Particularly, eutrophication and algal blooms have been highly underestimated in the environmental impact assessment reports for the TGD (Xu et al., 2013) and may pose real threats to drinking water safety in the near future. I have significantly contributed to understand algal bloom formation conditions in the TGR as well to identify and explain responsible nutrient transportation processes. Concepts considering adapted water level management strategies for algal bloom control are scientifically discussed (Yang et al., 2013) and also seem, from the perspective of this work, to be plausible. Evidence for the sedimentation of polluted suspended matter could also be derived from this work. With respect to long-term environmental threats, especially pollutant accumulation in semi-terrestrial soils and organisms need to be urgently and systematically studied to allow for conclusions and possibly develop mitigation measures.

Biodiversity is a global concern and humans rely on ecosystem processes and services provided by intact functional interactions of species. The integrated modelling approach of biomagnification across food webs (section 3.1) is a first step towards understanding pollutant behavior and corresponding toxic effects across the newly created aquatic ecosystem at the TGR. As such, the quality and quantity yield of utilized ecosystem services can also be estimated according to different future development scenarios as well as to the importance of intact functional interactions and biodiversity within the ecosystem.

For this work, the TGR served as study area for the development of **colossal field experimental** methods. The MINIBAT in situ and online multi-sensor system could be successfully used to establish 2D and 3D spatial water quality monitoring concepts (sections 2.1, 2.4, and 2.5) as well as a newly developed 4D spatio-temporal one (section 2.2). By these means, hydrological and physico-bio-chemical processes affecting water quality characteristics and pollutant dynamics could be successfully observed and evaluated with respect to the unique properties of the TGR. Consequently, this work significantly contributes to the existing knowledge on the TGR and on (artificial) aquatic ecosystems in general as well as on methodological water quality monitoring approaches.

Learning for the future: A recent review concluded that “the underestimated eutrophication in the reservoir area could be a major weakness of the Environmental Impact Assessment Report” (Xu et al., 2013) prepared by Chinese authorities prior to the TGD construction in 1993. Scientific results, including this work, should be systematically confronted with estimated environmental impacts of the TGD. This will specify aspects that require revision to improve environmental impact assessment guidelines for the planning procedures of future dam-projects.

Despite all gained new and important scientific-technical aspects about water quality characteristics and pollutant dynamics in the TGR, not only scientists agree that in the long-term a simple reduction of pollutant inputs is the best and most efficient way to mitigate the environmental challenges at the TGR.

Acknowledgement

This research was funded by the Federal Ministry of Education and Research of Germany (BMBF grant no. 02WT1131), the National Nature Science Foundation of China (31123001), the China Three Gorges Corporation (0711442), and the International Science and Technology Cooperation Program of China (MOST grant no. 2007DFA90510). Further, I have received funds from the KIT Graduate School for Climate and Environment to give a talk at the 10th annual meeting of the Asia-Oceania Geoscientific Society held in Brisbane, Australia, in July 2013.

The project preparation and execution of extensive fieldwork was only possible due to the inexhaustible efforts of our partners Lijing Wang, Binghui Zheng, and Yonghong Bi as well as the ‘Yangtze Project’ coordinators Günter Subklew and Rolf-Dieter Wilken.

Much of the data within this work would not exist without Peter Haushahn’s skillful emergency remote diagnostics for MINIBAT troubleshooting in the field. From him, I have learnt a lot about sensor technology, fixing electronics, and improvising. Further, he was a jolly good fellow in the field for two times.

I have received great support and help for my fieldwork in China and in the labs at KIT from Hao Chen, Gabriele Conrad, Defu Liu, Jasmin Fetzer, Cornelia Haug, Wei Hu, Pirimzhe Kelashvili, Sven Knoch, Simon Leib, Claudia Mößner, Beate Oetzel, Chengrong Peng, Gesine Preuß, Lucas Reid, Alexander Scheibelein, Zhengjian Yang, Yijun Yuan, Jialei Zhang, and Yongsheng Zhang.

Thanks to the nice colleagues from the Yangtze-Hydro Project for the great and friendly working atmosphere: Axel Bergmann, Katrin Bieger, Dominic Deyerling, Tilman Floehr, Henner Hollert, Irene Kranzioch, Stephan Küppers, Martina Roß-Nickoll, Andreas Schäffer, Björn Scholz-Starke, Andreas Tiehm, Bernhard Westrich, and Anja Wolf.

Thanks to my colleagues at KIT for exchanging ideas, giving assistance, and keeping the institute and working group in a good and motivating mood: Zsolt Berner, Denise Böhnke, Nicolas Börsig, Alexander Diener, Elisabeth Eiche, Arno Hartmann, Peter Illner, Utz Kramar, Fabienne Kürner, Harald Neidhardt, Thomas Neumann, Alexandra Nothstein, Sebastian Potsch, Nina Schleicher, Xiaohui Tang, and Chen Yuan.

Special thanks to Stefan Norra for being a demanding but always fair and understanding supervisor and supporting colleague. For me, he found the perfect balance between giving me scientific freedom and putting me back on track.

Acknowledgement

Words cannot express enough thanks to ...

... my sister Daniela and my brother Stefan for always being proud and believing in me.

... my parents Renate and Hans for their unconditional love and infinite support.

*... my wife Rachel and my daughter Amelie for being my safe haven and simply making me
happy.*

References

- (Becker et al., 2006) Becker, S.; Gemmer, M.; Jiang, T. Spatiotemporal analysis of precipitation trends in the Yangtze River catchment. *Stochastic Environmental Research and Risk Assessment* 2006, 20, 435-444.
- (Berggren and Wallmann, 2012) Berggren, L.; Wallmann, L. Longtan Dam—Dam safety and production losses under dynamic load. Department of Fire Safety Engineering and Systems Safety, Lund University, Sweden 2012, Report 5386.
- (CHINCOLD, 2014) Chinese National Committee on Large Dams. Dam information—Dam Projects—Nuozechu Hydropower Project. <http://www.chincold.org.cn> (accessed 07 November, 2014).
- (CTGC, 2014) China Three Gorges Corporation. <http://cwic.com.cn/inc/sqsk.php> (accessed 10 October, 2014).
- (CQWRB, 2010) Chongqing Water Resources Bureau, China. Chongqing water function zoning revision report. 2010. <http://www.cqwater.gov.cn/Pages/Home.aspx> (in Chinese).
- (Dai and Lu, 2014) Dai, S.; Lu, X. Sediment load change in the Yangtze River (Changjiang): A review. *Geomorphology* 2014, 215, 60-73.
- (Díaz et al., 2006) Díaz, S.; Fargione, J.; Chapin III, S.; Tilman, D. Biodiversity loss threatens human well-being. *PLoS Biology* 2006, 4(8), e277.
- (DVGW, 2011) Deutscher Verein des Gas- und Wasserfaches. Erste Verordnung zur Änderung der Trinkwasserverordnung vom 3. Mai 2011 – Nichtamtliche Vollversion. In: *Bundesgesetzblatt Jahrgang 2011 Teil Nr. 21.* (in German)
- (Fu et al., 2010) Fu, B.; Wu, B.; Lü, Y.; Xu, Z.; Cao, J.; Niu, D.; Yang, G.; Zhou, Y. Three Gorges Project: Efforts and challenges for the environment. *Progress in Physical Geography* 2010, 34(6), 741-754.
- (Gong and Wan, 2006) Gong, P.; Wan, J. Preliminary analysis of effects of comprehensive development of cascade hydropower project on river course. *Hydropower* 2006, 1465-1471.
- (Gray et al., 2012) Gray, D.; Thrift, A.; Williams, G.; Zheng, F.; Li, Y.; Guo, J.; Chen, H.; Wang, T.; Xu, X.; Zhu, R.; Zhu, H.; Cao, C.; Lin, D.; Zhao, Z.; Li, R.; Davis, G.; McManus, D. Five-Year Longitudinal Assessment of the Downstream Impact on Schistosomiasis Transmission following Closure of the Three Gorges Dam. *PLoS Neglected Tropical Diseases* 2012, 6(4), e1588.

- (Hertwich, 2013) Hertwich, E. Addressing Biogenic Greenhouse Gas Emissions from Hydropower in LCA. *Environmental Science & Technology* 2013, 47, 9604–9611.
- (Huang et al., 2014) Huang, Y.; Zhang, P.; Liu, D.; Yang, Z.; Ji, D. Nutrient spatial pattern of the upstream, mainstream and tributaries of the Three Gorges Reservoir in China. *Environmental Monitoring and Assessment* 2014, 186(10), 6833-6847.
- (ICOLD, 2014) International Commission on Large Dams. World Register of Dams. <http://www.icold-cigb.org> (accessed 05 March, 2014).
- (IEA, 2014) International Energy Agency. China, People's Republic of: Indicators for 2012. <http://www.iea.org> (accessed 22 September, 2014).
- (Jørgensen, 2005) Jørgensen, S; Löffler, H.; Rast, W.; Straškraba, M. (eds.) Evaluating lake and reservoir water quality. In: *Lake and Reservoir Management. Developments in Water Science* 2005, 54, 107-168.
- (ILEC, 2014) International Lake Environment Committee Foundation (ILEC). World Lake Database. <http://wldb.ilec.or.jp/> (accessed 13 November, 2014).
- (Lai et al. 2014) Lai, X.; Jiang, J.; Yang, G.; Lu, X. Should the Three Gorges Dam be blamed for the extremely low water levels in the middle-lower Yangtze River? *Hydrological Processes* 2014, 28, 150–160.
- (Landsberg, 1970) Landsberg, H.; Man-Made Climatic Changes. *Science* 1970, 170(3964), 1265-1274.
- (Lehner et al., 2011) Lehner, B.; Reidy Liermann, C.; Revenga, C.; Vörösmarty, C.; Balazs Fekete, B.; Crouzet, P.; Döll, P.; Endejan, M.; Frenken, K.; Magome, J.; Nilsson, C.; Robertson, J.; Rödel, R.; Sindorf, N.; Wisser, D. Global Reservoir and Dam (GRanD) database. Version 1.1, 2011.
- (Li et al., 2014) Li J.; Jin, Z.; Yang, W. Numerical modeling of the Xiangxi River algal bloom and sediment-related process in China, *Ecological Informatics* 2014, 22, 23-35.
- (Lin et al., 2012) Lin, J.; Fu, C.; Zhang, X.; Xie, K.; Yu, Z. Heavy metal contamination in the water-level fluctuating zone of the Yangtze River within Wanzhou section, China. *Biological Trace Element Research* 2012, 145, 268-272.
- (Liu et al., 2012) Liu, L.; Liu, D.; Johnson, D.; Yi, Z.; Huang, Y. Effects of vertical mixing on phytoplankton blooms in Xiangxi Bay of Three Gorges Reservoir: Implications for management. *Water Research* 2012, 46(7), 2121–2130.
- (McAllister et al., 2001) McAllister, D.; Craig, J.; Davidson, N.; Delany, S.; Seddon, M. Biodiversity Impacts of Large Dams. Background Paper Nr. 1 Prepared for IUCN / UNEP / WCD 2001.

- (McCartney et al., 2001) McCartney, M.; Sullivan, C.; Acreman, M. Ecosystem Impacts of Large Dams. Background Paper Nr. 2 Prepared for IUCN / UNEP / WCD 2001.
- (McManus et al., 2010) McManus, D.; Gray, D.; Li, Y.; Gail, Z. Schistosomiasis in the People's Republic of China: the Era of the Three Gorges Dam. *Clinical Microbiology Reviews* 2010, 23(2), 442-466.
- (MOEP, 2012) Ministry of environmental protection of the People's Republic of China. Three Gorges Bulletin in 2011. 2012. <http://english.mep.gov.cn>.
- (Nilsson et al., 2005) Nilsson, C.; Reidy, C.; Dynesius, M.; Revenga, C. Fragmentation and Flow Regulation of the World's Large River Systems. *Science* 2005, 308, 405-408.
- (Peng et al., 2014) Peng, C.; Zhang, L.; Qin, H.; Li, D. Revegetation in the water level fluctuation zone of a reservoir: An ideal measure to reduce the input of nutrients and sediment. *Ecological Engineering* 2014, 71, 574-577.
- (Ponseti and López-Pujol, 2006) Ponseti, M.; López-Pujol, J. The Three Gorges Dam project in China: History and consequences. *HMiC: Història Moderna I Contemporània* 2006, 151-188.
- (Ribeiro et al., 2011) Ribeiro Filho, R.; Petrere Junior, M.; Benassi, S.; Pereira, J. Itaipu Reservoir limnology: eutrophication degree and the horizontal distribution of its limnological variables. *Brazilian Journal of Biology* 2011, 71(4), 889-902.
- (Seeber et al., 2010) Seeber, C.; Hartmann, H.; Xiang, W.; King, L. Land use change and causes in the Xiangxi catchment, Three Gorges area derived from multispectral data. *Journal of Earth Science* 2010, 21(6), 846-855.
- (Sovacool and Bulan, 2011) Sovacool, B.; Bulan, L. Behind an ambitious megaproject in Asia: The history and implications of the Bakun hydroelectric dam in Borneo. *Energy Policy* 2011, 39, 4842-4859.
- (Straškraba and Tundisi, 1999) Straškraba, M.; Tundisi, J. Reservoir water quality management. In *Guidelines of Lake Management Vol.9*. International Lake Environment Committee Foundation, Shiga, Japan, 1999.
- (Stone, 2008) Stone, R. Three Gorges Dam: Into the Unknown. *Science* 2008, 321, 628-632.
- (Summit Technologies, 2014) Summit Technologies, Inc. Lake Mead Water Database. <http://lakemead.water-data.com/> (accessed 13 November, 2014).

References

- (Thomaz et al., 2006) Thomaz, M.; Pagioro, A.; Bini, M.; Murphy, J. Effect of reservoir drawdown on biomass of three species of aquatic macrophytes in a large sub-tropical reservoir (Itaipu, Brazil). *Hydrobiologia* 2006, 570, 53–59.
- (Thomson Reuters, 2014) Thomson Reuters Web of Science. <http://www.webofknowledge.com> (accessed 28 October, 2014).
- (Turvey et al. 2007) Turvey, S.; Pitman, R.; Taylor, B.; Barlow, J.; Akamatsu, T.; Barrett, L.; Zhao, X.; Reeves, R.; Stewart, B.; Wang, K.; Wei, Z.; Zhang, X.; Pusser, L.; Richlen, M.; Brandon, J.; Wang, D. First human-caused extinction of a cetacean species? *Biology Letters* 2007, 3(5), 537-540.
- (Wang et al., 2013) Wang, K.; Duan, X.; Liu, S.; Chen D.; Liu, M. Acoustic assessment of the fish spatio-temporal distribution during the initial filling of the Three Gorges Reservoir, Yangtze River (China), from 2006 to 2010. *Journal of Applied Ichthyology* 2013, 29, 1395-1401.
- (Wang and Zhang, 2013) Wang, F; Zhang, J. Mercury contamination in aquatic ecosystems under a changing environment: Implications for the Three Gorges Reservoir. *Chinese Science Bulletin* 2013, 58(2), 141-149.
- (Wang and Zheng, 2013) Wang, L.; Zheng, B. Prediction of chlorophyll-a in the Daning River of Three Gorges Reservoir by principal component scores in multiple linear regression models. *Water Science and Technology* 2013, 67(5), 1150-1158.
- (WCD, 2000) World Commission on Dams. Dams and development—a new framework for decision making. The Report of the World Commission on Dams. Earthscan Publications 2000, London.
- (WHO, 2011) World Health Organization. Guidelines for drinking-water quality. 2011, 4th ed. isbn: 978-92-4-154815-1.
- (World Bank, 1987) World Bank. Malaysia Power Sector Issues and Options. Report No.6466-MA 1987.
- (Wu et al., 2012) Wu, J.; Gao, X.; Giorgi, F.; Chen, Z.; Yu, D. Climate effects of the Three Gorges Reservoir as simulated by a high resolution double nested regional climate model. *Quaternary International* 2012, 282, 27-36.
- (Xu et al., 2009) Xu, Y.; Cai, Q.; Shao, M.; Han, X.; Cao, M. Seasonal dynamics of suspended solids in a giant subtropical reservoir (China) in relation to internal processes and hydrological features. *Quaternary International* 2009, 208, 138–144.

References

- (Xu et al., 2010) Xu, Y.; Cai, Q.; Han, X.; Shao, M.; Liu, R. Factors regulating trophic status in a large subtropical reservoir, China. *Environmental Monitoring and Assessment* 2010, 169(1-4), 237-248.
- (Xu et al., 2011) Xu, C.; Chen, J.; Huang, Y.; Qiu, Z.; Luo, J.; Zeng, H.; Zhao, Q.; Cao, J.; Shu, W. Identification of microcystins contamination in surface water samples from the Three Gorges Reservoir, China. *Environmental Monitoring and Assessment* 2011, 180(1-4), 77-86.
- (Xu et al., 2013) Xu, X.; Tan, Y.; Yang, G. Environmental impact assessments of the Three Gorges Project in China: Issues and interventions. *Earth-Science Reviews* 2013, 124, 115-125.
- (Yang et al., 2013) Yang, Z.; Liu, D.; Ji, D.; Xiao, S.; Huang, Y.; Ma, J. An eco-environmental friendly operation: An effective method to mitigate the harmful blooms in the tributary bays of Three Gorges Reservoir. *Science China Technological Sciences* 2013, 56(6), 1458-1470.
- (Yang and Lu, 2013) Yang, X.; Lu, X. Ten years of the Three Gorges Dam: a call for policy overhaul. *Environmental Research Letters* 2013, 8, 041006, 1-5.
- (Yazgan et al., 2001) Yazgan, M.; Armağan, B.; Yeşilnacar, M. Seasonal variations of the water quality of Atatürk Dam Lake. *International Symposium on water resources and environmental impact assessment* 2001.
- (Ye et al., 2011) Ye, C.; Li, S.; Zhang, Y.; Zhang, Q. Assessing soil heavy metal pollution in the water-level-fluctuation zone of the Three Gorges Reservoir, China. *Journal of Hazardous Materials* 2011, 191 (1-3), 366-372.
- (Ye et al., 2014) Ye, S.; Li, Z.; Zhang, T.; Liu, J.; Xie, S. Assessing fish distribution and threats to fish biodiversity in the Yangtze River Basin, China. *Ichthyological Research* 2014, 61(2), 183-188.
- (Zhang and Lou, 2011) Zhang, Q.; Lou, Z. The environmental changes and mitigation actions in the Three Gorges Reservoir region, China. *Environmental Science & Policy* 2011, 14(8), 1132-1138.
- (Zheng et al., 2007) Zheng, Z.; Li, H.; Jin, L.; Zhenbin, W. Analysis of Heavy Metals of Muscle and Intestine Tissue in Fish in Banan Section of Chongqing from Three Gorges Reservoir, China. *Polish Journal of Environmental Studies* 2007, 16(6), 949-958.

A Appendix—Full papers of first author scientific publications

A.1 Water mass interaction in the confluence zone of the Daning River and the Yangtze River—a driving force for algal growth in the Three Gorges Reservoir

Water mass interaction in the confluence zone of the Daning River and the Yangtze River—a driving force for algal growth in the Three Gorges Reservoir

Andreas Holbach · Lijing Wang · Hao Chen · Wei Hu ·
Nina Schleicher · Binghui Zheng · Stefan Norra

Received: 9 September 2012 / Accepted: 27 November 2012 / Published online: 18 December 2012
© Springer-Verlag Berlin Heidelberg 2012

Abstract Increasing eutrophication and algal bloom events in the Yangtze River Three Gorges Reservoir, China, are widely discussed with regard to changed hydrodynamics and nutrient transport and distribution processes. Insights into water exchange and interaction processes between water masses related to large-scale water level fluctuations in the reservoir are crucial to understand water quality and eutrophication dynamics. Therefore, confluence zones of tributaries with the Yangtze River main stream are dedicated key interfaces. In this study, water quality data were recorded in situ and on-line in varying depths with the MINIBAT towed underwater multi-sensor system in the confluence zone of the Daning River and the Yangtze River close to Wushan City during 1 week in August 2011. Geo-statistical evaluation of the water quality data was performed, and results were compared to phosphorus contents of selective water samples. The strongly rising water level throughout the measurement period caused Yangtze River water masses to flow upstream into the tributary and supply their higher nutrient and particulate loads into the tributary

water body. Rapid algal growth and sedimentation occurred immediately when hydrodynamic conditions in the confluence zone became more serene again. Consequently, water from the Yangtze River main stream can play a key role in providing nutrients to the algal bloom stricken water bodies of its tributaries.

Keywords Water quality · Algal bloom · Fresh water mixing · In situ measurement · On-line measurement · Three Gorges Reservoir · China

Introduction

The water quality in the Yangtze River Three Gorges Reservoir (TGR) upstream of the Three Gorges Dam (TGD) is of major concern since its first closure in 2003. The Yangtze River is the main drinking water source for the adjacent regions (Wu et al. 2009). Nutrient loads in the main stream of Yangtze River are considerably higher compared to its tributaries and are effectively transported into tributary water bodies by the backwater effect (Luo et al. 2007). Thus, threats on humans and the ecosystem caused by pollution, changed hydrodynamics, higher nutrient supply, and increasing eutrophication and algal bloom events (Dai et al. 2010; Ministry of Environmental Protection of China 2012) are widely discussed.

In this frame, the Sino-German environmental research program “Yangtze-Hydro Project” has been established and funded since 2010 (Bergmann et al. 2012) to conduct international and interdisciplinary research on the sustainable utilization and development of the newly created ecosystem in the TGR. Therein, the MINIBAT sub-project aims to monitor water quality distribution dynamics in 3D-space and time in critical areas throughout the TGR region. The study presented here directly derived from fieldwork conducted in the frame of this MINIBAT sub-project.

Responsible editor: Hailong Wang

A. Holbach (✉) · W. Hu · N. Schleicher · S. Norra
Institute of Mineralogy and Geochemistry (IMG),
Karlsruhe Institute of Technology (KIT), Adenauerring 20b,
Karlsruhe 76131, Germany
e-mail: andreas.holbach@kit.edu
URL: www.img.kit.edu

L. Wang · H. Chen · B. Zheng
Chinese Research Academy of Environmental Sciences (CRAES),
No.8, Dayangfang, Anwai Beiyuan, Chaoyang District,
Beijing 100012, China

S. Norra
Institute of Geography and Geoecology (IfGG), Karlsruhe Institute
of Technology (KIT), Reinhard-Baumeister-Platz 1,
76128 Karlsruhe, Germany

A profound understanding of the processes leading to the formation of algal blooms, especially harmful algal blooms, is necessary but is neither achieved internationally (Roelke and Pierce 2011) nor for the TGR (Zhang et al. 2010). Vertical Mixing dynamics (Liu et al. 2012), density current-driven nutrient inputs into tributary backwaters (Ji et al. 2010; Luo et al. 2007), temperature and thermal stratification (Zhang et al. 2010), as well as light attenuation by suspended particles (Xu et al. 2010) are all considered being regulatory factors for the formation of algal blooms in TGR. The importance of “Effects of inflow on harmful algal blooms” (Roelke and Pierce 2011) was highlighted by a same-titled special issue in the *Journal of Plankton Research*. Each algal bloom formation is an individual event, and its driving forces depend on the prevailing specific ecological conditions. It is, thus, important and necessary to study the processes leading to algal blooms in a very high spatial and temporal resolution to figure out the driving forces and ecological interactions leading to single algal bloom events. The synthesis of such datasets will then significantly contribute to a better generalized understanding of algal bloom formation. The dataset described in this paper was recorded from 23 to 29 August 2011 after heavy precipitation and a subsequent discharge peak and water level increase in TGR. This event triggered the inflow of huge water masses from the Yangtze River into the lower section of the Daning River, so-called Wushan Lake. The

observed results reveal very detailed insights into the related water mass interactions and water quality dynamics in the confluence zone of the Daning River and the Yangtze River. The corresponding developments and distributions of several water quality parameters are discussed in relation to observed algal blooming within the Wushan Lake water body.

Material and methods

Study area—confluence zone of the Daning River and the Yangtze River

The Daning River is a tributary of the TGR entering the Yangtze River main stream through the Wushan Lake, a confluence zone which formed next to Wushan City after the impounding by the TGD (Fig. 1). The Daning River has a length of 162 km, a watershed of 4,170 km², and a mean discharge of 136 m³/s (Chongqing Water Resources Bureau, China 2010). The backwater area reaches about 60 km upstream (Compilation Committee of Chongqing Atlas, China 2007) and comprises the “Little Three Gorges,” a famous National Park and scenic spot in China and several wide lake-like structures.

Frequent algal blooms and low water quality due to high total phosphorus (TP) loads threaten the Daning River since the impounding of the TGD (Ministry of Environmental

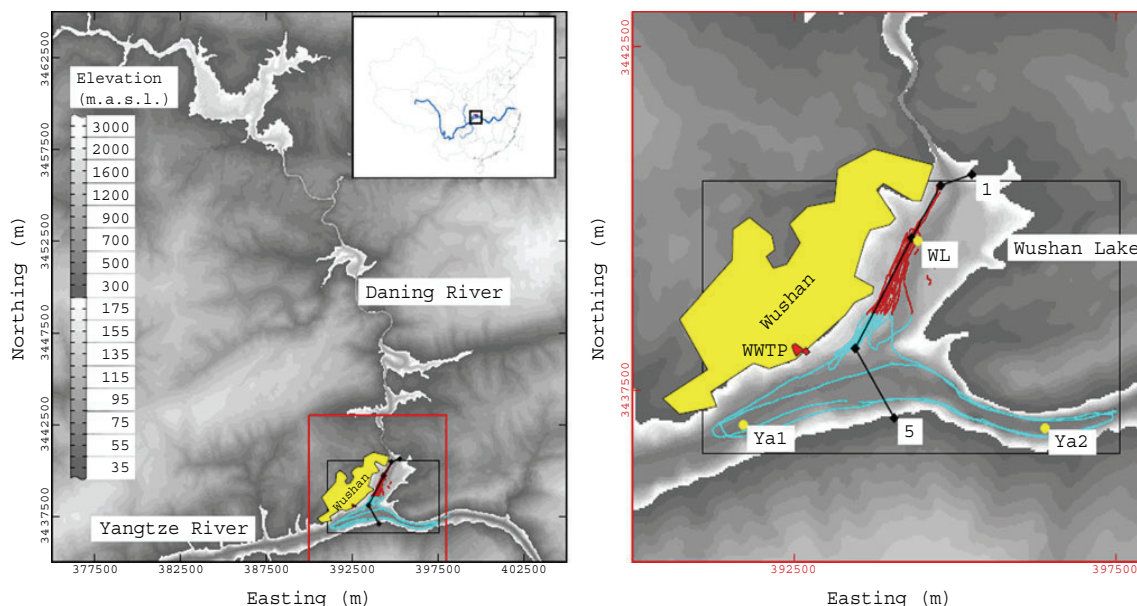


Fig. 1 Map of the study area at the confluence zone of the Daning River and the Yangtze River. Coordinates in UTM zone 49 easting and northing format. *Right side* shows the area zoomed to the *red square*. Wushan City—*yellow polygon*. WWTP—*red polygon*. Measurement cruises—*blue and red* (selected points for Fig. 3) dots. Water sampling

locations—*yellow points*. Cross-section path (Fig. 4)—*black line*. Elevation and bathymetry data derived from German Aerospace Center (2010), United States Geological Survey (2006), and MINIBAT ground depth measurements

Protection of China 2012; Zhang et al. 2010). However, significant parts of nutrients in the TGR also originate from non-point sources like fertilizer washout (Luo et al. 2007, Ministry of Environmental Protection of China 2012, Zheng et al. 2009). There are several discharge locations of different scales for treated and untreated wastewater entering the Wushan Lake and upstream water bodies. Additionally, large areas of former cities and agricultural areas are now inundated and may cause remobilization of various pollutants from the sediments.

In situ and on-line measurement of physicochemical water parameters with the MINIBAT

The MINIBAT towed underwater multi-sensor system (Stüben et al. 1994; Casagrande 1995) is connected to a boat with a data transmission cable. Sensors on the applied instrument (Table 1) measure six physicochemical water quality parameters. Chlorophyll *a* (Chl*a*) is measured in vivo by a calibrated fluorometer at 685 nm wavelength. Calibration was done by the producer (Dr. Haardt Optik Mikroelektronik) using crystalline Chl*a* standards dissolved in acetone. In vivo Chl*a* measurements can be affected by various factors and, thus, cause underestimation of real Chl*a* concentrations. However, the producer specifies a corresponding error of less than 10 %. Gregor and Maršálek (2004) also reported highly correlated in vivo Chl*a* fluorescence with Chl*a* quantified by the standard ISO method for reservoir water bodies. Positioning data is obtained from a Garmin GPSMAP 421s Chartplotter coupled with a transducer for ground depth sounding on the boat and a pressure sensor on the MINIBAT for its depth determination.

At constant cable length, the MINIBAT can be dragged behind a boat at speeds of approximately five knots and meanwhile be steered to different depths by use of remote controlled movable wings. Mostly, MINIBAT measurements are following a vertical sinusoidal dive course combined with either a straight or a zigzag horizontal course. When the boat stops, the MINIBAT can be lowered to depths just above the bottom of the water for depth profiling in deep waters. Easting and northing coordinates of the MINIBAT position are corrected for the cable length using

its depth *d* (in meters), direction of movement α ($0^\circ=N$, clockwise) of the boat and assuming a straight line of the dragging cable with length *l* (in meters).

$$\delta (\text{Easting}) = \sin(\alpha) \times \sqrt{l^2 - d^2} \quad (1)$$

$$\delta (\text{Northing}) = \cos(\alpha) \times \sqrt{l^2 - d^2} \quad (2)$$

Positioning and sensor data are recorded directly by a computer and saved as mean values every second. During the measurement campaign in August 2011, measurement cruises were densely performed in the surface waters between 0 and 13 m depth at 30 m cable length using approximately sinusoidal diving course. Depth profiling was done at selected sites.

Evaluation and geostatistical interpolation of physicochemical water quality parameters

2D and 3D geostatistical kriging estimation of water quality data was already used for various studies (e.g., Chehata et al. 2007; Murphy et al. 2010; Rathbun 1998). However, several studies carried out with a MINIBAT or similar instruments lack a detailed description about which method was used for spatial interpolation of the data (e.g., McBride et al. 2006; Woodson et al. 2009). Others apply inverse distance weighted (IDW) approaches without considering the unique properties and spatial dependency of each dataset and variable (e.g., Haas 2008). Standard 3D kriging methods as also used by Haas (2008) do not significantly improve interpolated data obtained from MINIBAT measurements compared to IDW technique. Here, the special spatial distribution structure of measurement points was taken into account for the directional variogram calculation to improve the quality of kriging results and to benefit from the uncertainty estimation received from the kriging procedure. The 3D geostatistical software package Isatis developed by Geovariances was used to evaluate and interpolate the measured datasets for the parameters temperature (*T*), electrical conductivity corrected for 25 °C (EC₂₅), turbidity (Turb), and Chl*a*.

Table 1 Specifications of sensors on the applied MINIBAT

Sensor	Principle	Measuring range/resolution	Accuracy	Response time
Pressure	Piezo-resistant	0–100/0.01 dbar	±0.35 %	50 ms
Temperature	PT 100	–2–40/0.01 °C	±0.01 °C	300 ms
Conductivity (EC ₂₅)	7 pole flow cell	0–60/0.001 mS/cm	±0.01 mS/cm	70 ms
Chlorophyll <i>a</i>	Fluorometry (685 nm)	0–250/0.03 µg/L	<10 %	100 ms
Turbidity	Mie-backscattering	0–10/0.001 BS%	0.001 %	100 ms
Oxygen saturation	Clark electrode	0–150/0.1 %	±2 %	3 s (63 %), 10 s (95 %)
pH	Potentiometry (Ag/AgCl)	0–14/0.01 pH	±0.1 pH	

For each parameter, directional variogram models (Table 2) were fit to experimental anisotropic variograms in both horizontal and vertical directions. To calculate the vertical experimental variogram, a migration procedure of the horizontally widely distributed data points into the nearest node in a regular gridfile ($500 \times 500 \times 0.25$ m) was performed in Isatis. The resulting gridfile reduces the distance between two sampling points to only its vertical component. The raw data points in their sinusoidal spatial structure would otherwise lead to variograms mainly derived from horizontal distances absolutely not representing variances related to the vertical distance component.

Table 2 Directional variogram model function combinations used for the kriging estimation of different water quality parameters on 3 days in the water bodies of the confluence zone

Parameter	Date	Function type	Range (m)	Sill	
Temperature	23 August 2011	Spherical	x, y, z 25.4	0.018	
		Spherical	x, y, z 600	0.035	
		Spherical	x, y 10^6 , z 10	0.185	
	27 August 2011	Spherical	x, y 36.42, z 1	0.022	
		Spherical	x, y 101, z 10	0.052	
		Linear	x, y 10^6 , z 11	0.25	
	29 August 2011	Exponential	x, y 125, z 5	0.011	
		Spherical	x, y 10^6 , z 5	0.006	
	EC ₂₅	23 August 2011	Nugget effect		0.25
Spherical			x, y, z 500	3.5	
Spherical			x, y 10^6 , z 0.01	0.6	
Gaussian			x, y 10^6 , z 10	10	
27 August 2011		Nugget effect		0.07	
		Linear	x, y 500, z 7	0.12	
		Linear	x, y 50, z 10^6	0.08	
29 August 2011		Nugget effect		0.008	
		Spherical	x, y : 162, z 10	0.035	
		Spherical	x, y 500, z 10	0.02	
Turbidity		23 August 2011	Nugget effect		0.02
	Spherical		x, y 25, z 0.01	0.03	
	Spherical		x, y 700, z 12	0.3	
	27 August 2011	Spherical	x, y 43, z 0.5	0.007	
		Linear	x, y 700, z 5	0.04	
	29 August 2011	Spherical	x, y 162, z 2.5	0.013	
		Spherical	x, y 500, z 3	0.007	
	Chlorophyll <i>a</i>	23 August 2011	Nugget effect		0.454
			Exponential	x, y 500, z 10	6.5
27 August 2011		Spherical	x, y 43.2, z 2	7	
		Spherical	x, y 500, z 5	20	
29 August 2011		Spherical	x, y 232, z 4	24.91	

Cross-validation was performed to test the applicability of the defined variogram models. These were then used for a 3D kriging procedure with a search neighborhood ($500 \times 500 \times 5$ m) into grid files ($30 \times 30 \times 0.5$ m) representing the volumes of the water bodies. Kriging estimation was only performed in between the data points. No extrapolation was intended. Referring to Journel and Rossi (1989) in this case, the ordinary kriging approach can be used to achieve reasonable kriging results, even in the presence of a global trend component. Only the experimental variogram tends to predict too high estimation errors in presence of a global trend (Armstrong 1998). This effect was minimized by manually excluding data points from high gradient areas from the experimental variogram calculation.

Water sampling and sample preparation

A Hydro-Bios FreeFlow Sampler was used for water sampling from below the water surface, the middle of the water column, and just above the bottom of the water body at selected sites (Fig. 1). On 23 August, samples were taken from the Wushan Lake (WL). Samples from the Yangtze River upstream (Ya1) and downstream (Ya2) of the confluence zone were taken on 27 August (Fig. 1). Additionally, samples from two wastewater treatment plant (WWTP) discharge channels were taken on 26 August (Fig. 1). The first channel contained unmixed water entering the Yangtze River over concrete cascades. Water from the second channel was already leveled and mixed with Yangtze water. Samples were filtered (Sartorius stedim CAMembran, 0.45 μ m, 25 mm) to separate dissolved from suspended particulate matter. Whenever possible, 100 mL was filtered; otherwise, the volumes were recorded. For cation analysis, samples of 20 mL were acidified with 50 μ L of 65 % HNO₃ (Merck, Suprapur) and stored at 5 °C in 20 mL PET bottles. Filters were air dried and sealed.

Analysis of phosphorus contents in the dissolved and particulate phases

Prior to analysis, filters were digested using 65 % HNO₃ as oxidation agent and 40 % HF and 70 % HClO₄ as digestion agents (all Merck, Suprapur) at 175–200 °C. HF and HClO₄ were fumed off, and the residues were dissolved in 10 mL 1 % HNO₃ for analysis. Dissolved phosphorus (DP) was analyzed from the acidified water samples and particulate phosphorus (PP) from the filter digestions using an X-Series 2 ICP-MS (Thermo Fisher Scientific Inc.) in collision cell mode to eliminate polyatomic clusters. ¹⁰³Rh and ¹¹⁵In were used as internal standards and phosphorus ICP Standard (Merck, CertiPUR) as calibration and cross-check standard throughout the analysis procedure. Four blank filters were tested and revealed blank phosphorus concentrations of

11.66±0.46 µg/L (“±” indicates standard deviation of the PP distribution) in the digestion solution which was subtracted from all analyzed digestion samples. USGS GXR-2 (Gladney and Roelandts 1990) and IAEA SL-1 (NOAA 1995) geochemical standards were also digested four times and revealed phosphorus recovery rates of 107±8 % for GXR-2 and 118±13 % for SL-1, respectively.

Hydrological and weather conditions during the sampling period

Hydrological data were obtained from the Chongqing Water Resources Bureau, China (2011). Heavy thunderstorms in the night before 23 August caused discharge peaks in the upper Daning River at Wuxi and the Yangtze River main stream (Fig. 2). Water level at Wushan was steadily rising with decreasing slope from 146.38 m on 22 August to 149.89 m on 30 August. Surface air temperature at the 2nd Jingtang Road Monitoring Station in the Wushan County at 09:00 AM (Environmental Protection Agency of Wushan County, China 2012) dropped considerably from 26.4 °C on 22nd to 19.6 °C on 23 August before it steadily increased to 24.2 °C on 30 August.

Results—development of water quality parameter distribution in the confluence zone

Water quality depth profile changes in the Wushan Lake during the measurement period

Measurement locations only within the Wushan Lake were selected (Fig. 1) to compare depth-dependent water quality properties between the three measurement days. Depth profiles of mean values per depth interval within the Wushan Lake show considerable changes from 23 to 29 August for all measured water quality parameters (Fig. 3).

T and EC_{25} steadily increased from deep waters (24.9 °C and 312 µS/cm at 110 m above sea level (a.s.l.)) to the surface (26.7 °C and 327 µS/cm at 147.5 m a.s.l.) on 23 August. The vertical T gradient got markedly stronger above 143 m a.s.l. To the contrary, T stayed fairly constant around

26 °C for major parts of the profiles on 27 August between 111 and 147 m a.s.l. Only the surface water up to 150 m a.s.l. revealed a layer with considerably increasing T up to 28.1 °C. The T pattern on 29 August was similarly constant around 26 °C between 103 and 144 m a.s.l. and revealed a significant surface warming up to 27.2 °C. Noteworthy is the increasing thickness of the warm surface layer from 3 m on 27 to 6 m on 29 August. Both profiles from 27 and 29 August exhibited pronounced thermoclines below 111 and 103 m a.s.l. reaching T low as 20.2 °C (93 m a.s.l.) and 22.8 °C (97 m a.s.l.), respectively. Apart from the constant EC_{25} values at the water surface, both EC_{25} profiles on 27 and 29 August appear very similar to the corresponding T profiles. Thermoclines go along with decreasing EC_{25} down to 285 µS/cm (93 m a.s.l.) on 27 August and 305.2 µS/cm (109 m a.s.l.) on 29 August, respectively. Above the thermoclines, EC_{25} ranged around 330 µS/cm.

At the water surface, all three parameters $Chla$, oxygen saturation, and pH increased from 23 to 29 August (Table 3). In the deeper parts of the water column, $Chla$ showed lower concentrations on 27 and 29 August compared to 23 August, whereas oxygen saturation and pH reveal a shift to higher values.

Turb generally increased from 23 to 27 August followed by a decrease to 29 August for the whole measured water column. Additionally, the elevation of maximum Turb in the water column decreased steadily from 145 m a.s.l. (5.65 BS%) on 23 to 139.4 m a.s.l. (5.96 BS%) on 27 to 138.9 m a.s.l. (5.36 BS%) on 29 August, even in the presence of a rising water level throughout the measurement time (Fig. 2).

Water quality distribution changes in a cross section through the Wushan Lake and across the Yangtze River

All cross sections for the parameters T , EC_{25} , Turb, and $Chla$ (Fig. 4) revealed major changes during the measurement campaign from 23 to 29 August. The presented cross section (Fig. 1) proceeds relatively close to the western shore of the Wushan Lake across areas with strongly varying depth. Measurements up to approximately 13 m depth were carried out very densely in this area on all three

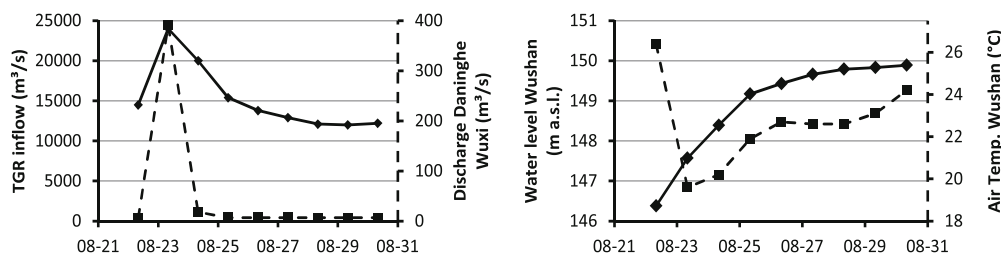
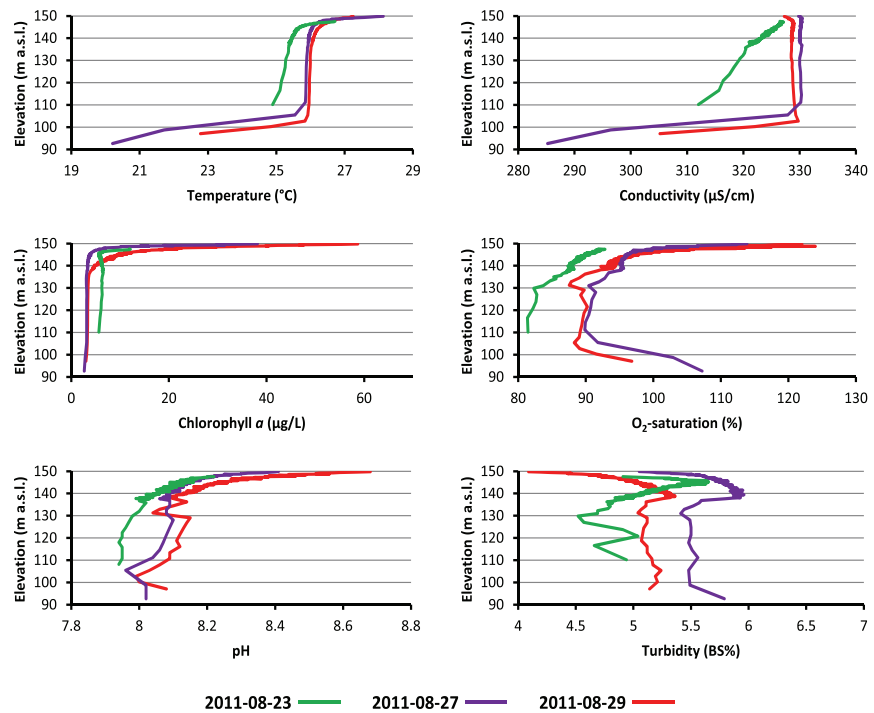


Fig. 2 Hydrological (Chongqing Water Resources Bureau 2011) and surface air temperature conditions (Environmental Protection Agency of Wushan County, China 2012) around the sampling period from 22

to 30 August. The solid/dashed data lines correspond to the solid/dashed ordinates

Fig. 3 Depth profiles of six water quality parameters in the Wushan Lake water body from 23 to 29 August. Selected points for depth profiles in Fig. 1



measurement days, and results of kriging estimation can, thus, be most reasonably compared there.

On 23 August, the left side of the cross section within the Wushan Lake was strongly stratified for *T* and *EC*₂₅ (Fig. 4) whereas the water close to the Yangtze River main channel revealed a much weaker stratification. *Chl**a* and *Turb* revealed an opposing distribution. *Turb* reached up to 8.3 BS% in the water close to the Yangtze River main channel where there were only 3 to 4 μg/L *Chl**a* in the measured water column. Contrarily, *Chl**a* was present between 5 and 7 μg/L in deeper

waters of the Wushan Lake and up to 21 μg/L in a thin surface layer whereas *Turb* only ranged between 4.5 and 5.5 BS% (see also Fig. 3).

On 27 August, all four parameters were distributed very equally in horizontal direction along the cross section. Besides the surface water, there were almost constant values for all four parameters. *T* and *Chl**a* concentration shifted to values similar to the Yangtze River main channel on 23 August, around 26 °C and 3 to 4 μg/L, respectively. *EC*₂₅ revealed a general slight increase up to 329–331 μS/cm in the whole measured cross section. *Turb* values ranged between 5.5 and 6.5 BS% being in between the minimum and maximum values of 23 August. The water surface exhibited a thin (2 to 3 m) layer with higher *T* (<28.5 °C), lower *Turb* (>4.8 BS%), and higher *Chl**a* concentration (<69 μg/L). Only *EC*₂₅ did not show a pronounced stratification at the water surface (see also Fig. 3).

On 29 August, the stratification at the water surface for *T*, *Turb*, and *Chl**a* became much stronger for the cross-section parts in the Wushan Lake (see also Fig. 3), whereas it was lost in the Yangtze River main channel. The main channel surface water was similar to the deeper water of the cross section on 27 August. *EC*₂₅ generally declined slightly compared to 27 August now ranging between 327 and 330 μS/cm.

Phosphorus contents in water samples from selected sites in the study area

TP concentration and its partition into DP and suspended PP differed considerably between sampling dates, water depths,

Table 3 Value distribution of parameters at the Wushan Lake water surface on 3 days

Parameter	Value	23 August 2011	27 August 2011	29 August 2011
Chlorophyll <i>a</i> (μg/L)	Min	5.0	13.5	35.7
	Max	29.6	79.9	118.9
	Mean	12.0	38.2	58.7
	SD	4.6	11.3	12.7
	Oxygen saturation (%)	Min	87.0	96.5
	Max	97.8	126.5	141.1
	Mean	91.9	113.9	122.0
	SD	2.3	5.7	4.4
pH	Min	8.1	8.2	8.5
	Max	8.4	8.7	8.8
	Mean	8.2	8.4	8.7
	SD	0.04	0.07	0.04

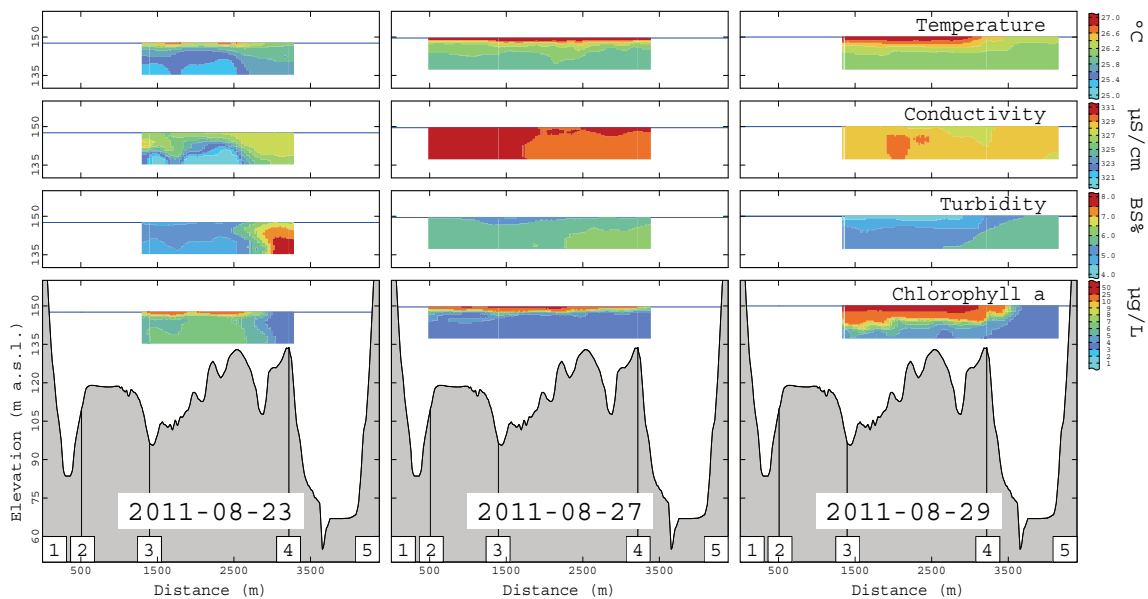


Fig. 4 Cross sections with kriging estimations for four water quality parameters across the Wushan Lake (1–4) and across the Yangtze River main channel (4–5) with corresponding bathymetry and elevation data from 23 to 29 August. Vertical lines—vertices (1–5) in Fig. 1

and the sampling sites (Fig. 5). On 23 August, DP behaved contradictory to PP in the WL water samples. DP increased significantly from the bottom to the water surface, whereas PP concentrations decreased from the bottom to the surface. Since DP concentrations are considerably higher than PP concentrations, TP is following the trend with depth of DP.

On 27 August, the bottom water samples from Ya1 and Ya2 contained significantly lower TP and DP compared to all other samples. The middle and surface water samples ranged between 82.2 and 88.3 µg/L TP and 67.4 and 78.3 µg/L DP, respectively. PP in the Yangtze River did not differ significantly between water depth and sampling sites and was 12.6±1.9 µg/L. Phosphorus contents in the two WWTP discharge channels were considerably higher (DP 405 and 140 µg/L; PP 26.1 and 124 µg/L; TP 431 and 265 µg/L).

Development of chlorophyll *a* distribution in the confluence zone

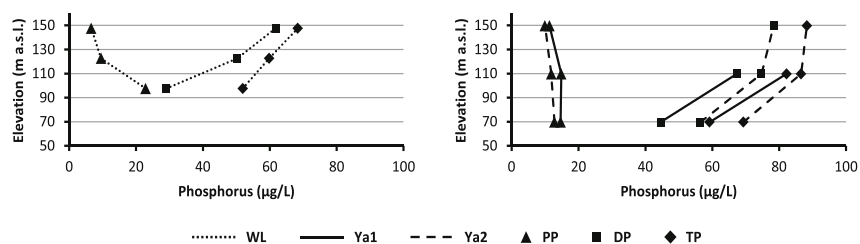
On 23 August, higher Chla concentrations at the water surface were limited to the western shore of the Wushan

Lake (Fig. 6a) reaching 21 µg/L there, but the concentration decreased to 4–6 µg/L close to the eastern shore. Approaching the Yangtze River main stream, Chla concentrations at the water surface decreased drastically down to 3 to 4 µg/L (see also Fig. 4).

On 27 August, surface Chla concentrations up to 69 µg/L were found in the Wushan Lake. On that day, the measurement cruises came close to the WWTP discharge location. Here, a plume of higher Chla concentrations (>10 µg/L) was monitored leading from the direction of the WWTP into the Wushan Lake. Furthermore, a plume of lowest Chla concentrations between 3 and 4 µg/L was entering the Wushan Lake close to the eastern shore of its entrance.

Chla in the surface water on 29 August reached even higher values up to 101 µg/L in the Wushan Lake. Also, the expansion of high concentrations did further increase toward the Yangtze River main stream, and there was no more significant plume of lower concentrations entering the Wushan Lake. Again, in the vicinity of the WWTP, there were higher concentrations of Chla. The extensively measured Yangtze

Fig. 5 DP, PP, and TP concentrations in water samples from different depths in the confluence zone of the Daning River and the Yangtze River. WL, Ya1, and Ya2 locations in Fig. 1



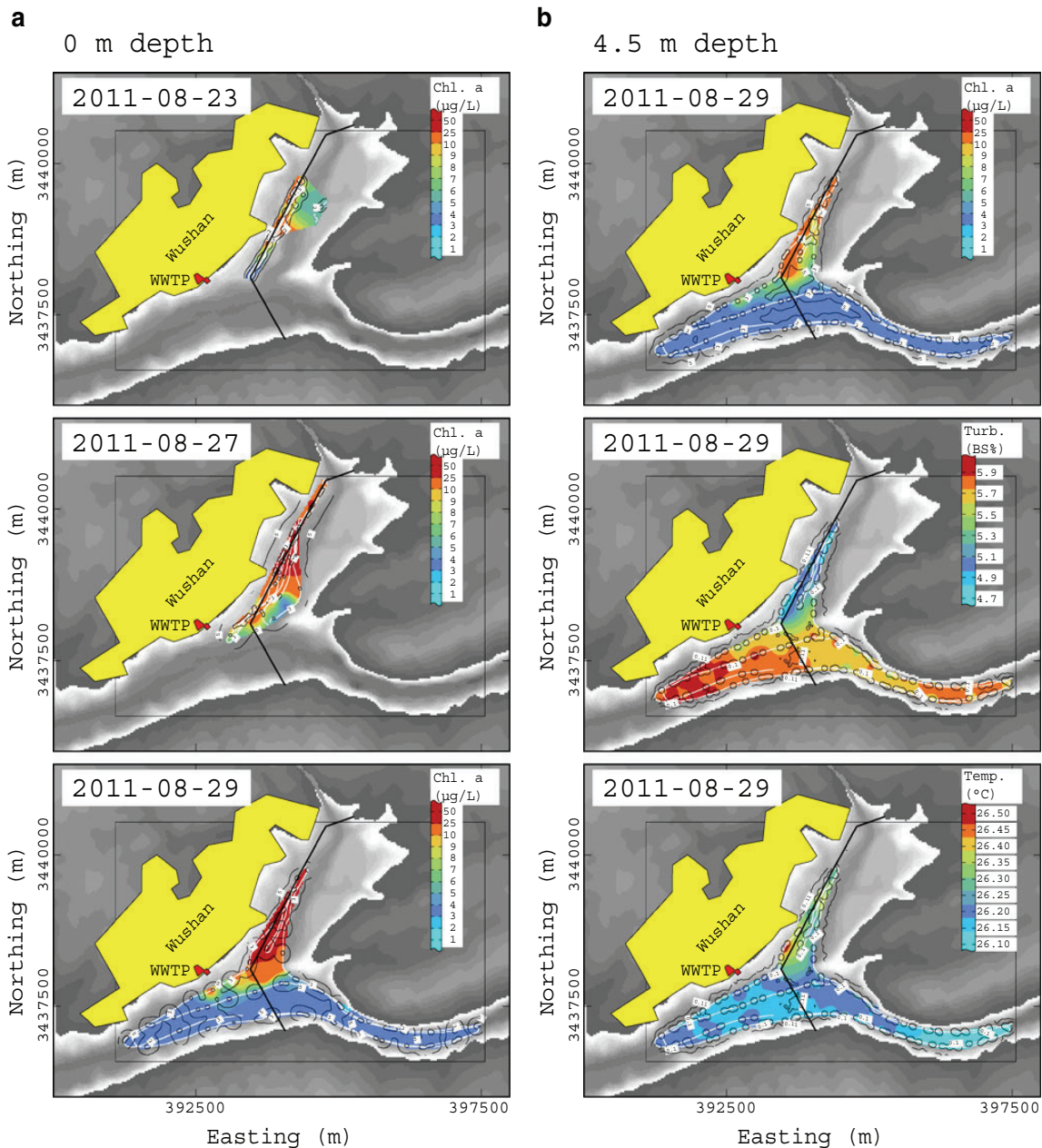


Fig. 6 Kriging estimations for: **a** Chla concentration from 23 to 29 August at the water surface. **b** Chla, Turb, and *T* at 4.5 m water depth on 29 August. Kriging standard deviations—*isolines*. Chla legend does

not have a linear scale to emphasize differences in lower concentration ranges. Cross section path (Fig. 4)—*black line*

River main stream homogeneously contained low Chla concentrations between 2 and 4 µg/L.

On 29 August, high Chla concentrations (>10 µg/L) in the Wushan Lake also expanded down vertically to around 5 m depth (Fig. 3). At 4.5 m depth, there were plumes of lower Chla concentrations and *T* but higher Turb values coming from the Yangtze River main stream and entering the Wushan Lake close to the eastern shore of its entrance (Fig. 6b).

Discussion—water mass interaction in the confluence zone and algal growth

Yangtze River water entered the Wushan Lake and reversed the tributary flow direction toward upstream

EC₂₅ as water mass indicator can be used to trace mixing processes (Gloss et al. 1980). *T* and EC₂₅ considerably

changed their depth profile properties in the Wushan Lake above ~110 m a.s.l. from 23 to 27/29 August (Fig. 3). The horizontal gradients present in the water bodies on 23 August were also erased in the same period (Fig. 4). The status of the Wushan Lake changed from horizontal and vertical insufficiently mixed water masses derived from its well-spaced inflowing tributaries (Talling 2009) to a well-mixed water body dominated by Yangtze River water quality. Substitution of the Wushan Lake T and EC_{25} profiles by values similar to the Yangtze River main stream on 23 August indicates that water originating from the Yangtze River main stream did mainly replace all the water formerly present above ~110 m a.s.l. in the measured Wushan Lake area. The changes in Chl_a and $Turb$ distribution also support that hypothesis. All water above ~110 m a.s.l. and below the surface thermal stratification shown in the depth profiles (Fig. 3) and the cross section (Fig. 4a) contained lower Chl_a concentrations and higher $Turb$ values on 27/29 August compared to 23 August. The higher surface T (Fig. 2) was surely due to warming from higher air T and sun irradiation.

The obvious replacement of huge amounts of water in the Wushan Lake by Yangtze River water is going along with a drastic increase in the reservoir water level at Wushan from 147.7 to 149.6 m a.s.l. following a discharge peak in the Yangtze River on 23 August (Fig. 2). The water flow direction in the Daning River was, thus, reversed and turned to upstream, forced by the water level and discharge boundary conditions in the Yangtze River main stream. Higher nutrient and suspended particle loads from Yangtze River waters were consequently transported into the less turbulent Wushan Lake.

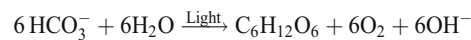
The deep waters below the thermocline at ~110 m a.s.l. remained unaffected by the Yangtze River water intrusion. Thermal stratification was stable enough to resist the impacting shear forces from water flow. The unexpected increasing oxygen content below the thermocline could even indicate another density current. Cold water rich in oxygen from the further upstream water bodies of the Daning River could have crawled downstream on the bottom of the former riverbed of the Daning River while much larger volumes of water pushed upstream driven by the Yangtze River flood.

Favorable conditions for algal growth formed in the Wushan Lake

Roelke and Pierce (2011) summarized the factors affecting algal growth: hydraulic flushing, stratification, salinity, sediment loading, and nutrient loading. In TGR, Liu et al. (2012) consider the ratio of mixing depth to euphotic depth as the main controlling factor for cyanobacteria blooms in tributaries. Mixing depth is mainly regulated by thermal stratification and its interaction with density current intrusions

determined by large-scale water level fluctuations and horizontal differences of water density. Nutrient supply into tributaries from the Yangtze River main stream is considered by Luo et al. (2007). Xu et al. (2010) point out that light attenuation by suspended particles is the limiting factor for algal growth in the Yangtze River main stream. Zhang et al. (2010) found T to be a key regulatory factor for algal blooms in the Daning River during flood and normal seasons when water temperature ranges between 17.7 and 35.3 °C. Considering all these limitations, the conditions at the water surface became very favorable for algal growth by 27 August. Mixing depth decreased by the stabilization of thermal stratification at the warming water surface. $Turb$ in the Wushan Lake, especially at the surface, dropped and the depth of maximum $Turb$ steadily increased indicating rapid sedimentation.

Still, the additional nutrient supply from the Yangtze River water and the WWTP discharge (Figs. 5 and 6) seemed to have had a significant positive impact on algal growth as indicated by higher Chl_a concentrations in the plumes from the WWTP on 27/29 August. Overall, the rapid increase of Chl_a concentration in the warm surface water plus increasing oxygen saturation and pH indicate a similarly growing photosynthetic activity. At $pH > 6.3$, the dominating carbonate species in water is HCO_3^- and the net photosynthesis equation is:



Produced O_2 and OH^- cause increasing oxygen saturation and pH.

Referring to Ellison and Brett (2006), DP can be considered as completely bioavailable while only certain parts of PP are. Especially during storm-water runoff, the amount of bioavailable PP can be considerably low. Yan and Zhang (2003) found only 8–23 % of PP in the Yangtze River to be bioavailable with lowest values during flood season in August.

In this study, the TP loads found in the upper Yangtze River mainly consisted of the dissolved fraction and were, thus, bioavailable when the Yangtze River water entered the Wushan Lake. Also the observed decrease in $Turb$ and related sedimentation would, consequently, not considerably affect the amount of bioavailable phosphorus.

Continuing upstream flow switched to middle layer density current under stabilized thermally stratified surface water

On 27 August, the water masses still continued pushing upstream into the Daning River. Water level in the TGR was continuously rising, and the upstream flow was indicated by the low Chl_a concentrations at the eastern shore of the entrance to the Wushan Lake and the plume of higher Chl_a concentrations ranging from the direction of the WWTP

discharge into the Wushan Lake (Fig. 6a). However, the surface water thermal stratification in the Wushan Lake seemed to have stabilized, and in the Wushan Lake, the upstream flow had changed to a middle layer density current underneath the stabilized surface layer and above the still present thermocline below ~110 m a.s.l.. Such middle layer density currents were already observed (Liu et al. 2012) and modeled (Jiang et al. 2011; Yu and Wang 2011) in tributaries of the TGR.

By 29 August, the stability of the thermal stratification did further establish and the warm surface layer now averaged to 6 m thickness compared to 3 m thickness on 27 August (Fig. 3). The water level still was rising slightly (Fig. 2), and in a depth of 4.5 m, there were plumes of Chla, Turb, and T obviously indicating water entering the Wushan Lake from the Yangtze River main stream (Fig. 6b). The thermal surface water stratification must have been stable enough to cause a complete decoupling of the surface water across the Wushan Lake from the lower middle layer density current still pushing water further upstream into the tributary.

Conclusions and implications for water quality management

As a short-term measure, the release of the treated and untreated wastewater further inside the main channel of the Yangtze River could considerably reduce the input of nutrient loads into the algal bloom sensitive Wushan Lake. Of course, the long-term goal must be a significant reduction of nutrient discharges into the TGR at all. Reduction of huge amounts of nutrients entering TGR via untreated sewage water and improvements of non-point source pollution control would considerably upgrade TGR water quality and reduce algal blooms.

The prevention of algal bloom formation by controlled releases from the reservoir, as proposed and discussed by Liu et al. (2012), would need further evaluation on the necessary daily water level fluctuation. They found a daily water level fluctuation of 3.8 m/day to be able to destabilize the thermal surface water stratification in the Xiangxi Bay and cause a crash in phytoplankton abundance. Attempts using flow management to control algal blooms already proved promising as exemplarily shown by Mitrovic et al. (2011) for weirs in the Australian Darling River. Our data suggest that a daily water level fluctuation <0.25 m/day (after 27 August 2011) and related flow velocities in the Wushan Lake were not capable to disrupt the development of a thermal stratification under the observed weather conditions. Rapid algal growth and expansion of the Chla surface coverage in the Wushan Lake were the consequences.

Acknowledgments The Yangtze-Project is funded by the Federal Ministry of Education and Research (BMBF grant no. 02WT1131) of Germany and the International Science and Technology Cooperation Program of China (MOST grant no. 2007DFA90510). Thanks to the Environmental Protection Agency and the Environmental Monitoring Station in Wushan, Chongqing, China for their great administrative and infrastructural support. Thanks to Claudia Mößner and Cornelia Haug for their great help in the labs. Thanks to both reviewers for their valuable and constructive comments that helped to substantially improve the manuscript.

References

- Armstrong M (1998) Basic linear geostatistics. Springer, Berlin
- Bergmann A, Bi Y, Chen L et al (2012) The Yangtze-Hydro Project: a Chinese–German environmental program. *Environ Sci Pollut Res* 19:1341–1344
- Casagrande CE (1995) The MiniBAT—a miniaturized towed sampling system. *Oceans '95* 3:638–641
- Chehata M, Jasinski D, Monteith MC, Samuals WB (2007) Mapping three-dimensional water-quality data in the Chesapeake Bay using geostatistics. *JAWRA* 43:813–828
- Chongqing Water Resources Bureau, China (2010) Chongqing water function zoning revision report. <http://www.cqwater.gov.cn/Pages/Home.aspx> (in Chinese)
- Chongqing Water Resources Bureau, China (2011) Hydrological information—rivers real-time water regime. <http://www.cqwater.gov.cn/swxx/jrbssq/Pages/Default.aspx>. Accessed 21–30 Aug 2011 (in Chinese)
- Compilation Committee of Chongqing Atlas, China (2007) Chongqing Atlas. Xi'an Cartographic, Xi'an. 92–93. ISBN: 978-7-80748-069-3 (in Chinese)
- Dai H, Zheng T, Liu D (2010) Effects of reservoir impounding on key ecological factors in the Three Gorges Region. *Procedia Environ Sci* 2:15–24
- Ellison ME, Brett MT (2006) Particulate phosphorus bioavailability as a function of stream flow and land cover. *Wat Res* 40:1258–1268
- Environmental Protection Agency of Wushan County, China (2012) 2nd Jingtian Road Monitoring Station, Wushan County, Chongqing Municipality
- German Aerospace Center (2010) Shuttle Radar Topography Mission, 1 Arc Second scenes E1090000N300000_SRTM_1_DEM – E1100000N310000_SRTM_1_DEM. <https://centaurus.caf.dlr.de:8443>. Accessed 27 July 2012
- Gladney ES, Roelands I (1990) 1988 Compilation of elemental concentration data for USGS geochemical exploration reference materials GXR-1 to GXR-6. *Geostandard Newslett* 14:21–118
- Gloss SP, Mayer LM, Kidd DE (1980) Advective control of nutrient dynamics in the epilimnion of a large reservoir. *Limnol Oceanogr* 25:219–228
- Gregor J, Maršálek B (2004) Freshwater phytoplankton quantification by chlorophyll *a*: a comparative study of in vitro, in vivo and in situ methods. *Water Res* 38:517–522
- Haas LW (2008) Improved performance capabilities for the Acrobat towed instrument platform: data collection, calibration and interpolation/graphic visualization. Virginia Institute of Marine Sciences—final report
- Ji DB, Liu D, Yang ZJ, Yu W (2010) Adverse slope density flow and its ecological effect on the algae bloom in Xiangxi Bay of TGR during the reservoir impounding at the end of flood season. *Shuili Xuebao (J Hydraul Eng)* 41:691–696 (in Chinese)
- Jiang D, Dai H, Liu W (2011) Influence of thermal density flow on hydrodynamics of Xiangxi Bay in Three Gorges Reservoir, China. *Procedia Environ Sci* 10:1637–1645

- Journel AG, Rossi ME (1989) When do we need a trend model in kriging? *Math Geol* 21:715–739
- Liu L, Liu D, Johnson DM, Yi Z, Huang Y (2012) Effects of vertical mixing on phytoplankton blooms in Xiangxi Bay of Three Gorges Reservoir: implications for management. *Wat Res* 46:2121–2130
- Luo ZX, Zhu B, Zheng BH, Zhang Y (2007) Nitrogen and phosphorus loadings in branch backwater reaches and the reverse effects in the main stream in Three Gorges Reservoir. *China Environ Sci* 27:208–212 (in Chinese)
- McBride C, Hamilton D, Gibbs M, White P, Stewart L (2006) BioFish survey of Lake Taupo. Centre for Biodiversity and Ecology Research, University of Waikato—report 68
- Ministry of Environmental Protection of China (2012) Three Gorges Bulletin 2005–2011. Ministry of Environmental Protection—The People's Republic of China. http://english.mep.gov.cn/standards_reports/threegorgesbulletin/. Accessed 31 Jul 2012
- Mitrovic SM, Lorraine H, Forugh D (2011) Use of flow management to mitigate cyanobacterial blooms in the Lower Darling River, Australia. *J Plankton Res* 33:229–241
- Murphy RR, Curriero FC, Ball WP (2010) Comparison of spatial interpolation methods for water quality evaluation in the Chesapeake Bay. *J Environ Eng* 136(2):160–171. doi:10.1061/(ASCE)EE.1943-7870.0000121
- NOAA (1995) Standard and reference materials for environmental science. Technical Memorandum NOS ORCA 94. http://docs.lib.noaa.gov/noaa_documents/NOS/ORCA/TM_NOS_ORCA/nos_orca_94_pt1.pdf. Accessed 27 Aug 2012
- Rathbun SL (1998) Spatial modelling in irregularly shaped regions: kriging estuaries. *Environmetrics* 9:109–129
- Roelke DL, Pierce RH (2011) Effects of inflow on harmful algal blooms: some considerations. *J Plankton Res* 33:205–209
- Stüben D, Stüben K, Haushahn P (1994) MINIBAT—a new, simple system for in-situ measurement, mapping and sampling of dissolved trace elements in aquatic systems. *Underwater Systems Design* 16:5–14
- Talling JF (2009) Electrical conductance—a versatile guide in freshwater science. *Freshw Rev* 2:65–78
- United States Geological Survey (2006) Shuttle Radar Topography Mission, 3 Arc Second scenes SRTM3N30E109–SRTM3N31E110. eros.usgs.gov. Accessed 27 Jul 2012
- Woodson CB, Washburn L, Barth JA, Hoover DJ, Kirincich AR, McManus MA, Ryan JP, Tyburczy J (2009) Northern Monterey Bay upwelling shadow front: observations of a coastally and surface-trapped buoyant plume. *J Geophys Res* 114: C12013
- Wu B, Zhang XX, Zhang XL, Yasun AJ, Zhang Y, Zhao DY, Ford T, Cheng SP (2009) Semi-volatile organic compounds and trace elements in the Yangtze River source of drinking water. *Ecotoxicology* 18:707–714
- Xu Y, Cai Q, Han X, Shao M, Liu R (2010) Factors regulating trophic status in a large subtropical reservoir, China. *Environ Monit Assess* 169:237–248
- Yan W, Zhang S (2003) The composition and bioavailability of phosphorus transport through the Changjiang (Yangtze) River during the 1998 flood. *Biogeochemistry* 65:179–194
- Yu ZZ, Wang LL (2011) Factors influencing thermal structure in a tributary bay of Three Gorges Reservoir. *J Hydrodyn* 23:407–415
- Zhang JL, Zheng BH, Liu LS, Wang LP, Huang MS, Wu GY (2010) Seasonal variation of phytoplankton in the DaNing River and its relationships with environmental factors after impounding of the Three Gorges Reservoir: a four-year study. *Procedia Environ Sci* 2:1479–1490
- Zheng BH, Wang LJ, Gong B (2009) Load of non-point source pollutants from upstream rivers into Three Gorges Reservoir. *Research of Environmental Sciences* 22:125–131 (in Chinese)

A.2 Three Gorges Reservoir: Density Pump Amplification of Pollutant Transport into Tributaries

Three Gorges Reservoir: Density Pump Amplification of Pollutant Transport into Tributaries

Andreas Holbach,^{*,†} Stefan Norra,[†] Lijing Wang,[‡] Yuan Yijun,[§] Wei Hu,[†] Binghui Zheng,[‡] and Yonghong Bi[§]

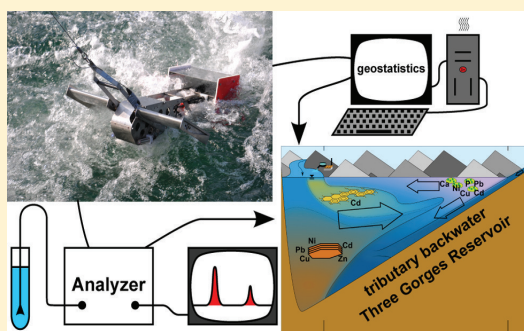
[†]Institute of Mineralogy and Geochemistry, Karlsruhe Institute of Technology, Karlsruhe 76131, Germany

[‡]Chinese Research Academy of Environmental Sciences, Beijing 100012, China

[§]Institute of Hydrobiology, Chinese Academy of Sciences, Wuhan 430072, China

Supporting Information

ABSTRACT: The impoundment of the Three Gorges Reservoir (TGR) on the Yangtze River in China burdened its tributary backwaters with severe environmental problems.¹ Confluence zones of reservoir tributaries with the Yangtze River main channel are main drivers of pollutant dynamics in the TGR² and are thus keys to develop mitigation measures. Here, we show a novel experimental approach of spatiotemporal water quality analysis to trace water mass movements and identify pollutant transport pathways in reservoir water bodies. Our results show the movements of density currents in a major tributary backwater of the TGR. A huge interflow density current from the Yangtze River main channel transported its heavy metal carriage to the upstream reaches of the tributary backwater. Water from the upstream backwater moved counterwise and carried less but pollutant-enriched suspended sediments. This scenario illustrates the importance of confluence zone hydrodynamics for fates and pathways of pollutants through the widely unknown hydrodynamics of new reservoirs.



INTRODUCTION

Freshwater is an essential resource for human life. More than 45 000 large dams impound the world's rivers to sustain drinking and irrigation water, energy supply, flood control, infrastructure, and economic benefits.³ With around 22 000 large dams, China hosts almost half of them.³ Impacts of dams on ecosystems are widely known, but precise predictions for new reservoirs remain difficult.⁴ Since 2003, the impoundment of the Three Gorges Reservoir (TGR) on the Yangtze River in China burdened its tributary backwaters with severe environmental threats.¹ Geohazards, for example, earth quakes, soil erosion, and landslides, as consequences of anthropogenic activities, have considerably intensified and remain a recent research field.^{5,6} Drastic ecological changes of both terrestrial and aquatic habitats took place in the same instant and may cause irreversible losses of biodiversity.⁷ This is particularly critical because the TGR region is a biodiversity hotspot and characterized by many endemic species.⁷ The water bodies of the TGR are seriously threatened by eutrophication. Frequent algal blooms, especially in the TGR tributary backwaters, put the main drinking water source and a major food source at stake while their formation processes still remain unsatisfyingly understood.^{1,2,8} Furthermore, some studies reported increasing heavy metal contents in soils and sediments of the TGR area, particularly within the water level fluctuation zone.^{9,10}

However, a TGR-wide synoptic heavy metal balance is still missing.

On a global scale, eutrophication of freshwater resources and heavy metal accumulation in reservoir sediments are major environmental problems and are closely related to anthropogenic impacts in the corresponding watersheds.^{11,12} New reservoirs are extremely susceptible to these threats because their hydrodynamics are artificially and rapidly changed by the impoundment. Eutrophication and heavy metal accumulation in the TGR are thus representative environmental threats of large reservoirs worldwide. There are 28 large and deep reservoirs (storage capacity: ≥ 20.0 km³; dam height: ≥ 100 m) in a similar order of magnitude as the TGR (e.g., Volta, Kariba, and Manicouagan).¹³ But, the only one that can also compete with the TGR (dam height: 181 m; storage capacity: 39.3 km³; mean residence time $R = 29.6$ days) in terms of mean water residence time R is the Itaipu Reservoir (dam height: 196 m; storage capacity: 29.0 km³; $R = 33$ days) located on the border between Brazil and Paraguay.¹⁴ Furthermore, the specific water level management of the TGR is designed to compensate the

Received: March 10, 2014

Revised: June 12, 2014

Accepted: June 13, 2014

Published: June 18, 2014

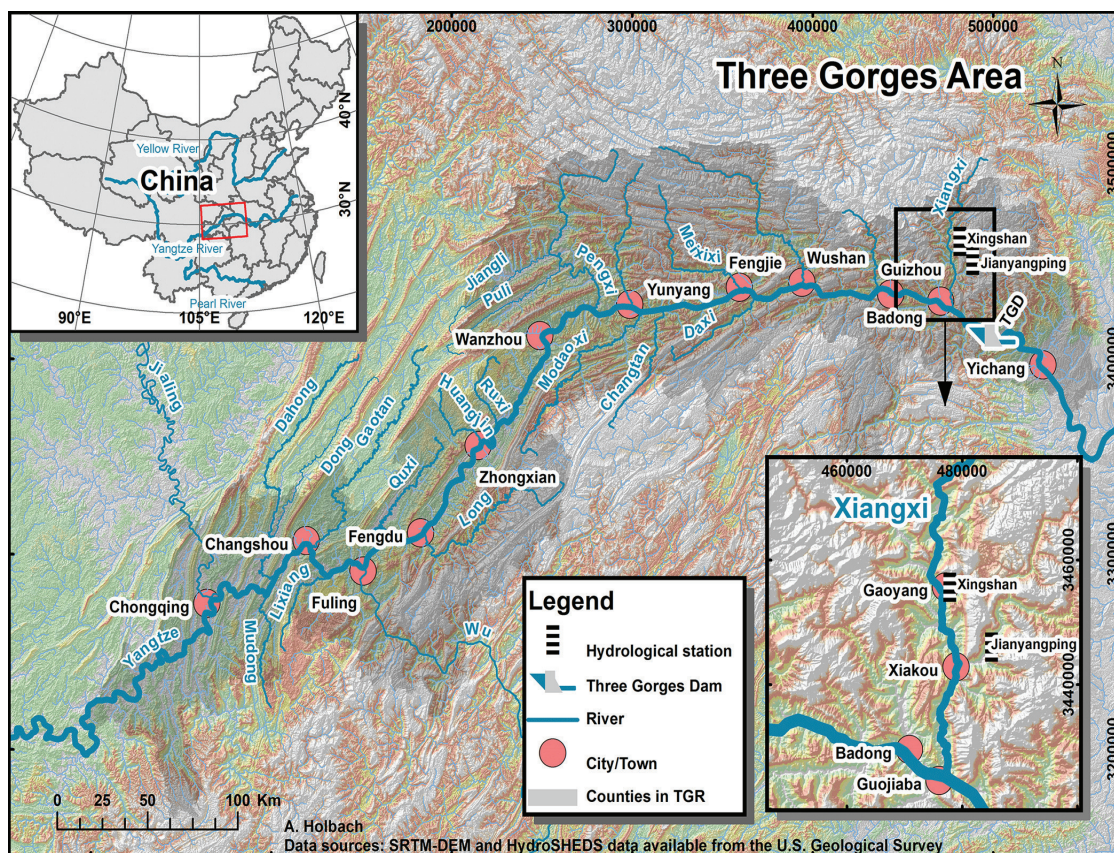


Figure 1. Outline of the Three Gorges Reservoir, its location within China, and our study area at the Xiangxi River. Coordinates of the upper left China overview map are in the WGS84 system; other coordinates are in the UTM zone 49 Easting and Northing format.

seasonal inflow changes between less than 5000 m³/s in winter and greater than 70 000 m³/s in summer (2010–2013).¹⁵ Its seasonal 30 m water level fluctuation (Itaipu Reservoir: <1 m)¹⁶ between 145 and 175 m above sea level (m a.s.l.) results in monthly R values within $8 \leq R \leq 81$ days for the whole TGR (Supporting Information, Figure 1). Reservoirs can be classified into three mixing classes: (A) fully mixed, $R \leq 20$ days; (B) intermediate, $20 < R \leq 300$ days; (C) well stratified, $300 \text{ days} < R$.¹⁷ The TGR as a whole consequently ranges seasonally between classes A and B. However, totally lakelike characteristics as in class C with $R > 365$ days can occur locally in its tributary backwaters during winter.¹⁸ Therefore, besides its global representativity, the TGR is also an outstanding and absolutely unique study area for effects of reservoir hydrodynamics, worldwide.

Confluence zones of reservoir tributaries with the Yangtze River main channel are main drivers of pollutant dynamics in the TGR² and are thus keys to develop mitigation measures. Dealing with large and dynamic reservoir water bodies, like the TGR, mixing of differing water masses is of peculiar importance. Similar to the striking role of estuarine biogeochemistry when rivers meet the sea,¹⁹ the associated confluence zones of different freshwater masses form key interfaces for physical, chemical, and biological interactions. These are responsible for the fate and pathways of numerous pollutants and the distribution of water quality across the mixing zones.²⁰ Such a confluence zone was formed within the

former Xiangxi River valley (Figure 1), one of 40 major tributaries of the TGR entering the Yangtze River main channel approximately 40 km upstream of the Three Gorges Dam (TGD).⁶ At its maximum water level of 175 m a.s.l., the TGR backwater reaches more than 35 km upstream into this narrow and channel-like valley (Figure 1). Similar to most TGR tributaries, the Xiangxi River backwater is seriously affected by algal blooms as well as land use and land cover changes.^{1,6}

In this study, we tried to capture the effects of hydrodynamic interactions between the Xiangxi River backwater and the Yangtze River main channel on the corresponding water quality distribution patterns. Therefore, we developed a method to integrate (1) in situ and online measurements with a MINIBAT multisensor probe²¹ with (2) a spatiotemporal geostatistical data evaluation and (3) element content analysis in the dissolved and particulate phases of selected water samples. The results of this novel experimental approach revealed the large-scale movement patterns of water masses and their corresponding pollutant loads throughout the Xiangxi River backwater. This method can be utilized for analyses of complex water body interactions even in very remote areas with reasonable amount of staff and material.

■ MATERIALS AND METHODS

In Situ and Online Water Quality Measurements with the MINIBAT. We performed in situ and online water quality measurements with the MINIBAT multisensor probe²¹

(Supporting Information, Figure 2) in the Xiangxi River backwater from 15 to 20 September 2012. This is the typical season for steep water level rise in the TGR initiated by the TGD management (Supporting Information, Figure 1). Thus, we expected high amounts of water exchange dynamics between the Yangtze River main channel and its tributary backwaters during this specific period. The MINIBAT is connected to a boat with a data transmission cable for in situ and online measurements. Our MINIBAT recorded nine water quality parameters (Supporting Information, Table 1) with 5 Hz frequency. For subsequent data evaluation, we used one data set per second. GPS data was obtained from a Garmin GPSMAP 521s Chartplotter and coupled with an echosounder on the boat and a pressure sensor on the MINIBAT for its positioning within the water body. At constant cable length, we mainly dragged the MINIBAT behind the boat along the center of the Xiangxi River backwater at speeds of 5–10 km/h. Meanwhile, we followed a sinusoidal dive course down to 30 m depth by use of the remote controlled steerable wings on the MINIBAT. Frequently, we stopped the boat and lowered the MINIBAT to depths just above the ground for complete depth profiling in deeper waters (Supporting Information, Figure 3). The MINIBAT is also equipped with a rack of five 50 mL remote controlled water samplers that we used to extract 27 water samples at selected profiles (Supporting Information, Figure 3).

Spatiotemporal Geostatistical Data Evaluation. Time can be mathematically considered as an additional dimension in a spatiotemporal coordinate system.²² The specific distribution of an environmental variable in space and time can then be treated as one realization of a spatiotemporal random function $Z(u, t)$ with $u \in \text{space}$ and $t \in \text{time}$. In our study, we consider the recorded MINIBAT values of each water quality parameter i as realizations of a spatiotemporal random variable $z_i(u, t)$ as a subset of $Z_i(u, t)$ with individual probability distributions.²² Kriging is a tool to optimally estimate the realization of the corresponding spatiotemporal random function $Z_i(u, t)$ based on a (semi)variogram model that is derived from experimental (semi)variograms of the measured data $z_i(u, t)$. Even in the presence of global trends in the environment (e.g., thermal stratification in lakes), ordinary kriging with a local neighborhood delivers reasonable estimation results with similar quality compared to the application of a trend model in the universal kriging approach, as long as no extrapolation beyond the sampling domain is intended.²³ We only used kriging to estimate data points within a convex hull around the acquired data points (Supporting Information, Figure 3). Consequently, we could neglect probable trend components within our data. Turbidity (turb) and chlorophyll a (chl_a) were interpolated by log-normal kriging.

We used the software *isatis* (Geovariances) to perform geostatistical data evaluation. Our recorded data points are characterized by three spatial coordinates: We projected the recorded GPS coordinates (WGS-84) to UTM zone 49 Easting and Northing values during import to *isatis*; Elevation above sea level e_s was calculated for each data point as $e_s = l_w - d_{bw}$ (l_w is the daily TGR water level;¹⁵ d_{bw} is the depth of each data point below l_w). The time of each data record t_i is thus a fourth component characterizing the data set in its spatiotemporal domain. Consequently, we could only perform spatiotemporal kriging after reasonably reducing the three-dimensional (3D) spatial coordinate system into a two-dimensional system. Because of the narrow and long channel-like shape of the

Xiangxi River backwater, we could replace the Easting and Northing values by a linear horizontal distance component d_h (Supporting Information, Figure 4). Therefore, we cumulated horizontal distance increments along the center of the water body starting at its confluence with the Yangtze River main channel. The resulting d_h values were projected onto our recorded MINIBAT data points. The final 3D spatiotemporal coordinate system consists of (d_h, e_s, t_i) as its three principle directions. From our recorded data sets, we drew experimental (semi)variograms along these three main directions and manually fit regional anisotropic variogram models (Supporting Information, Table 2). A moving local neighborhood (Supporting Information, Table 3) was used for the subsequent cross-validation (Supporting Information, Table 2 and Figure 5) and ordinary kriging calculations performed in *isatis*. We also checked the calculated kriging standard deviations against the absolute ranges of estimated water quality parameter values (Supporting Information, Table 4).

Water Sample Treatment and Analysis. We filtered the water samples through previously weighed filters (Sartorius Stedim cellulose acetate membrane; pore size, 0.45 μm ; diameter, 25 mm) to separate dissolved from suspended particulate matter (SPM). A 20 mL amount was acidified with 50 μL of 65% HNO_3 (Merck KGaA, Suprapur) and stored at 5 °C in PET bottles. Two 20 mL ultrapure water samples (Merck KGaA, Milli-Q) were acidified and also stored at 5 °C in PET bottles. Those were used as blank samples. Filters were air-dried and sealed. The loaded filters were weighed again and the SPM load was calculated as

$$\text{SPM} = (w_1 - w_0)/V_f$$

where w_0 is the raw filter weight, w_1 is the loaded filter weight, and V_f is the filtered water sample volume. We digested the filters with 65% HNO_3 as an oxidation agent and 40% HF and 70% HClO_4 as digestion agents (all Merck KGaA, Suprapur) at 175–200 °C. HF and HClO_4 were fumed off, and the residues were dissolved in 10 mL of 1% HNO_3 . We prepared seven blank digestions only applying the acids; we digested five blank filters as well as the two certified geochemical reference materials USGS GXR-2²⁴ and IAEA SL-1²⁵ for three times each. We analyzed the acidified water samples and the filter digestions with an X-Series 2 ICP-MS (Thermo Fisher Scientific Inc.). ¹⁰³Rh and ¹¹⁵In were used as internal standards; ICP multielement standard solution IV and phosphorus ICP standard (both Merck KGaA, CertiPUR) were used as calibration and cross-check standards. CRM-TMDW-A (High-Purity standards, Inc.) was used as the ISO 9001:2000 certified reference material during the analysis procedure. Blank concentrations and element recovery rates from the used reference materials can be found in Table 5 of the Supporting Information. We checked the analysis results of the filter digestions against background values in the source area of the Yangtze River²⁶ and against pollution grade thresholds of SPM in Germany.²⁷ Furthermore, we used Al as the normalizing element of the analyzed pollutant concentrations. Al serves as a proxy for the fine fraction of SPM, metal-to-Al ratios are relatively constantly distributed in the crust, and Al is not likely to be affected by anthropogenic sources.²⁸ Thus, we calculated element-to-Al ratios to compare pollutant enrichments in the SPM within our set of water samples:

$$\text{element}_{\text{Al}} = c(\text{element})/c(\text{Al})$$

where $c(\text{element})$ and $c(\text{Al})$ are mass concentrations in SPM.

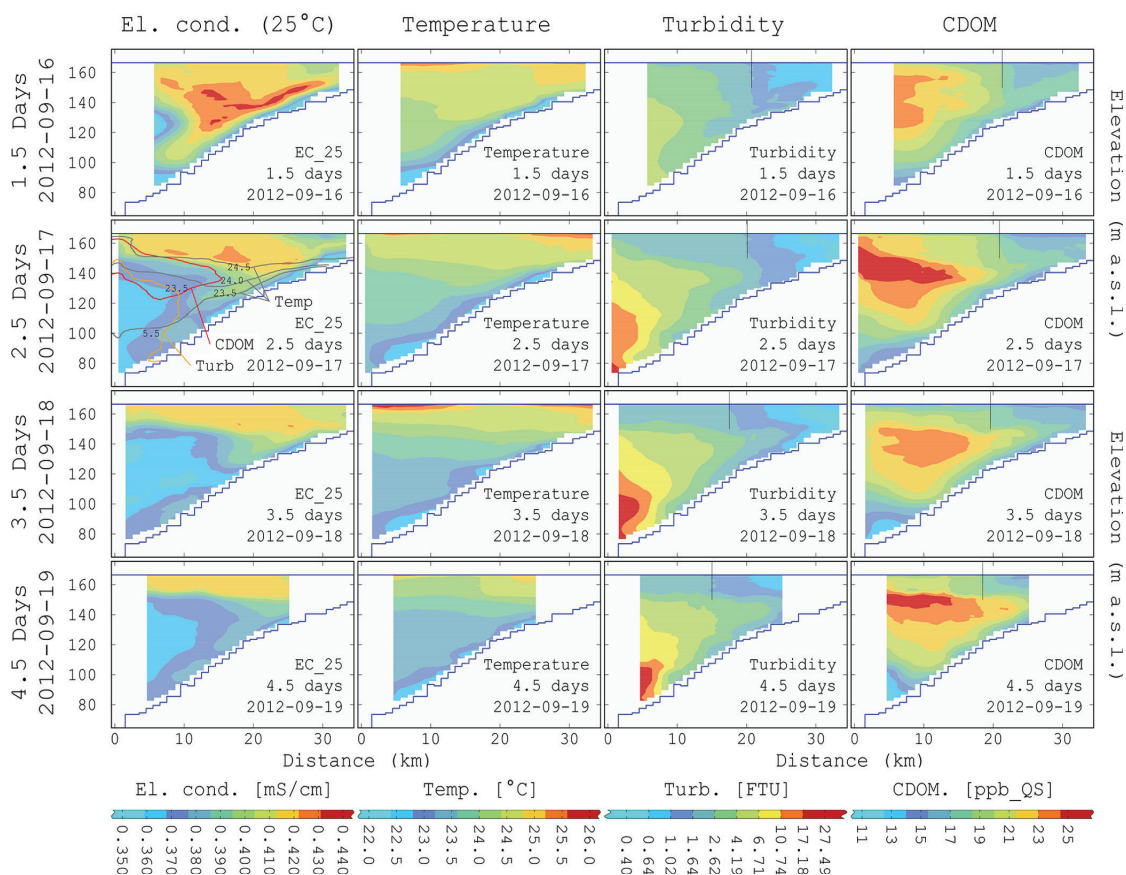


Figure 2. Dynamic water quality distribution along a longitudinal section of the Xiangxi River backwater. Four extracted time steps of the spatiotemporal interpolated water quality distribution for four out of seven analyzed water quality parameters. Selected isolines of T , CDOM, and turb are added to EC_{25} after 2.5 days. Vertical lines in the CDOM and turb columns indicate downstream moving water masses at the surface of the midstream Xiangxi River backwater. For spatial reference, see Figure 1; for the spatiotemporal interpolation domain, see Figure 3 of the Supporting Information.

Water Body Volume and Volume Flux Estimations. In ESRI ArcGIS 10, we used the publicly available SRTM digital elevation model (DEM)²⁹ with approximately $90 \text{ m} \times 90 \text{ m}$ resolution to derive elevation e_s contour lines in 5 m intervals between 50 and 200 m a.s.l. for the Xiangxi River valley only (Supporting Information, Table 6). From these contour isolines, we created a triangular irregular network (TIN) and calculated Xiangxi River backwater volumes V for different e_s using the “TIN Polygon Volume” tool in the “3D Analyst” extension of ArcGIS 10. We used the least-squares method to fit $V = f(e_s)$ as a second-order polynomial model function of the following form:

$$\delta V(e_s) = ae_s^2 + be_s + c$$

With the derived parameters $a = 142\,617$, $b = -32\,231\,772$, and $c = 1\,993\,651\,657$, we estimated daily volume changes in the Xiangxi River backwater (Supporting Information, Figure 6). Furthermore, we cumulated volume slices along the Xiangxi River backwater for $e_s = 166.3 \text{ m a.s.l.}$, which was the water level at the end of our measurement period, to estimate water mass exchanges on a purely volumetric basis (Supporting Information, Figure 7).

RESULTS AND DISCUSSION

Remarkable changes of water quality distribution in the Xiangxi River backwater took place during our fieldtrip (Figures 2 and 3). A huge tongue-like plume of lower electrical conductivity (EC_{25} ; normalized to 25°C), which we use as a conservative tracer of water masses,³⁰ intruded into the tributary backwater in the middle of the water column from 16 September on. Water masses with higher EC_{25} that formerly filled the middle of the tributary backwater were simultaneously pushed to the water surface. The temperature (T) behaved similarly when water with colder T values intruded from the Yangtze River main channel in the middle layer of the tributary backwater pushing water with higher T values to its surface. Meanwhile, we always found a layer of even lower EC_{25} and colder T values along the upstream bottom of the tributary backwater. Turb was also forming a tongue-like plume growing further and further from the Yangtze River main channel into the tributary backwater from 16 to 20 September. This plume was pronounced in the deeper parts of the corresponding EC_{25} plume. We found strong and significant ($p < 0.01$) positive Pearson correlations of turb with SPM load and total heavy metal concentrations in our water samples ($r(\text{SPM}) = 0.974$, $r(\text{Ni}) = 0.971$, $r(\text{Cu}) = 0.927$, $r(\text{Zn}) = 0.831$, $r(\text{Cd}) = 0.961$,

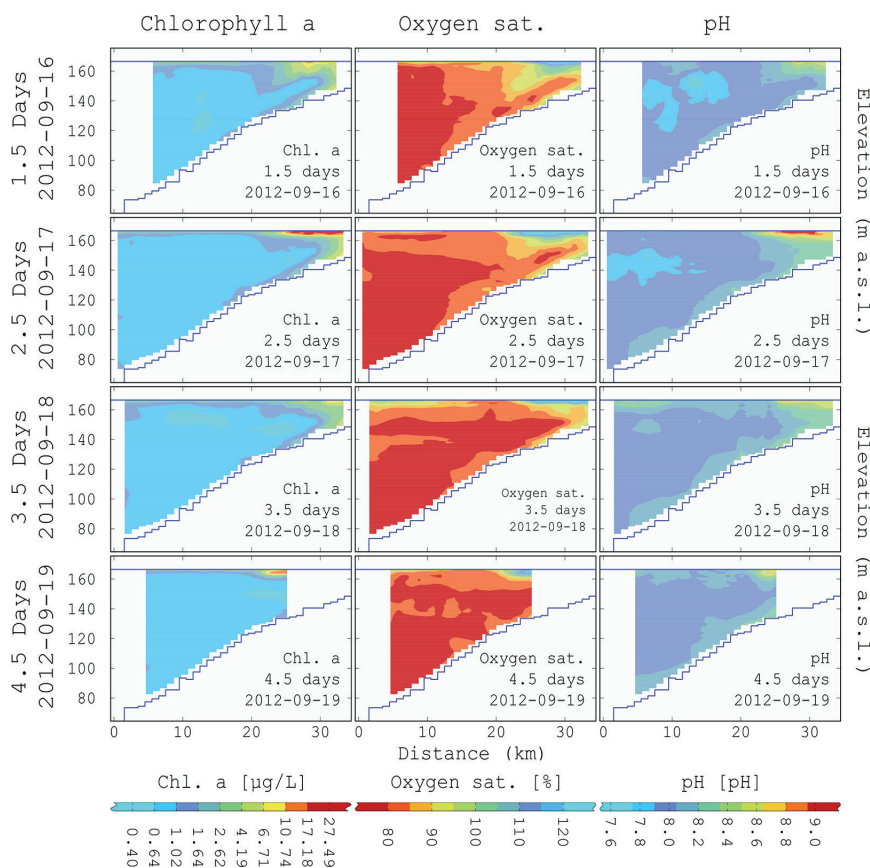


Figure 3. Dynamic water quality distribution along a longitudinal section of the Xiangxi River backwater (continued). Four extracted time steps of the spatiotemporal interpolated water quality distribution for three out of seven measured water quality parameters. For spatial reference, see Figure 1; for the spatiotemporal interpolation domain, see Figure 3 of the Supporting Information.

Heavy metal concentration ranges in SPM of the Xiangxi River backwater in September, 2012

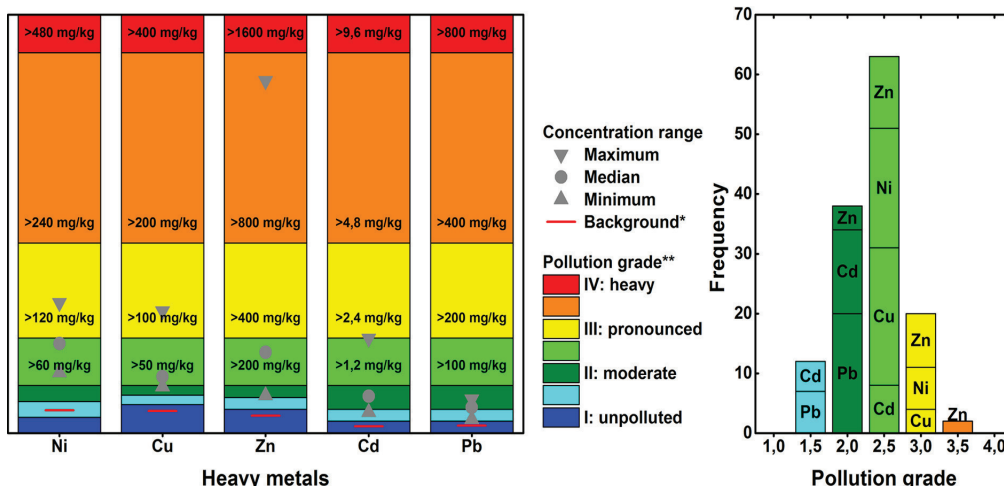


Figure 4. Heavy metal concentration ranges in SPM of the Xiangxi River backwater in September 2012 in comparison with *local background concentrations²⁶ and **pollution grade thresholds of SPM in Germany.²⁷ Note: heavy metal concentrations of all analyzed samples exceed local background values. Pollution grade mainly ranges between moderate (2.0) and pronounced (3.0) pollution.

$r(\text{Pb}) = 0.970$). Even though total and dissolved heavy metal contents were all below international drinking water guideline

values,^{31–33} heavy metal contents in SPM all exceeded local background values and mainly revealed moderate to

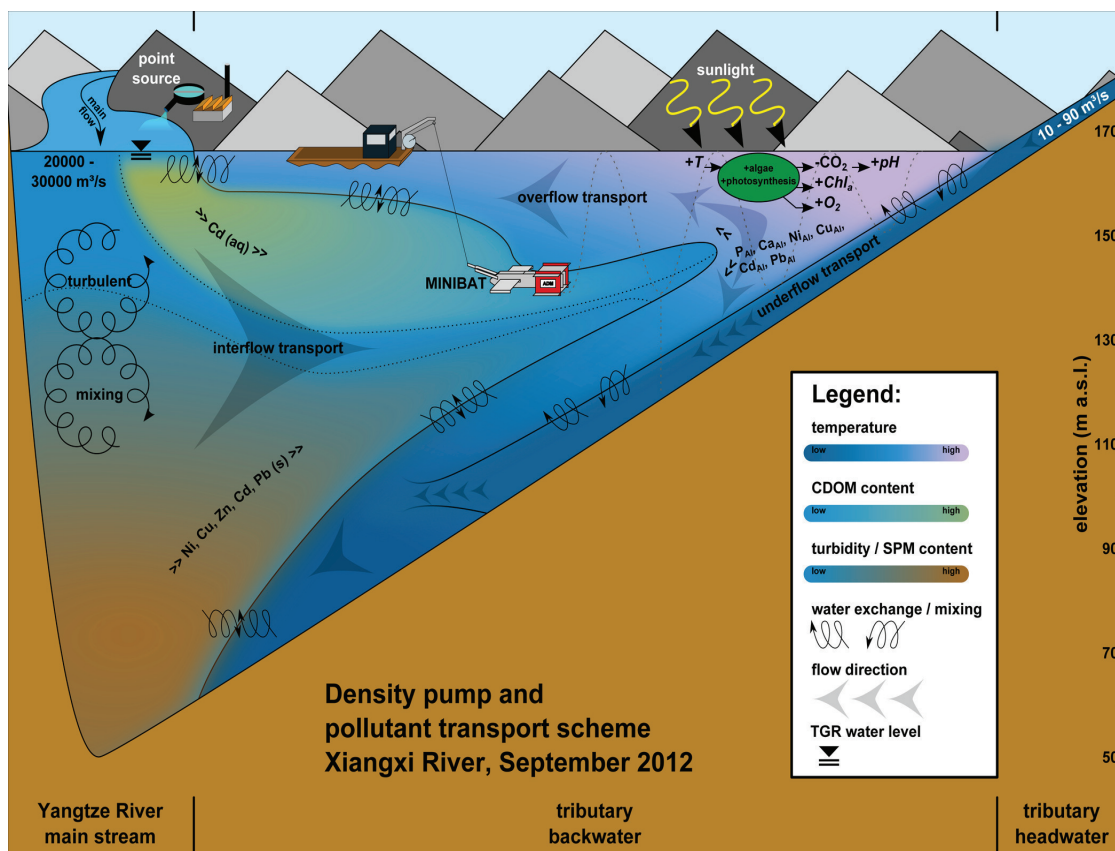
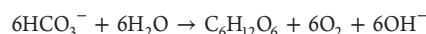


Figure 5. Simplified density pump and pollutant transport scheme of the Xiangxi River backwater in September 2012. Model flow pattern derived from a compilation of the dynamic distribution of all seven analyzed water quality parameters displayed in Figures 2 and 3. Note: turb plume has high total heavy metal concentrations; CDOM plume carries higher concentrations of dissolved Cd; enrichment of P_{Al} , Ca_{Al} , Ni_{Al} , Cu_{Al} , Cd_{Al} , and Pb_{Al} in SPM is related to algae and photosynthesis and distributed accordingly along the surface and the bottom of the upstream tributary backwater.

pronounced pollution grades²⁷ (Figure 4 and Supporting Information, Table 7). Consequently, we identified the observed turb plume and its upstream movement into the Xiangxi River backwater as an active transport pathway of total heavy metal loads. These were contained in polluted SPM from the Yangtze River main channel.³⁴ The fluorescence of colored dissolved organic matter (CDOM) formed a similar plume, but this one was pronounced in the upper parts of the EC_{25} plume. CDOM in surface waters can originate from (1) diffuse natural sources and (2) in situ creation by microbes but also from (3) anthropogenic sources like sewage water.³⁵ We regard urban sewage water from Guojiaba (Figures 1 and 5) located at the mouth of the Xiangxi River as the corresponding source of CDOM. Dissolved Cd shows a significant ($p < 0.05$) positive Pearson correlation with CDOM fluorescence ($r(Cd) = 0.421$), and the capability of dissolved organic matter to form complexes with heavy metals is widely known.³⁶ Both turb and CDOM distributions indicate downstream moving water masses at the surface of the midstream Xiangxi River backwater (Figure 2). This indicates a compensating overflow density current of water balancing the intruding water masses from the Yangtze River. chl_a fluorescence was highest at the surface of the upstream tributary backwater. Similarly, both O_2 -sat. and pH reached their highest values along the surface of the upstream tributary backwater. Algae use chl_a to

synthesize biomass according to the net equation of photosynthesis:



This process is favored in warm, stratified, stagnant, and enlightened water bodies and causes O_2 production and increasing pH as a result of OH^- production. Pearson correlations of chl_a fluorescence with element-to-Al ratios²⁸ of P, Ca, Ni, Cu, Cd, and Pb in the SPM (Supporting Information, Table 7) were positive and significant ($p < 0.01$) ($r(P_{Al}) = 0.938$, $r(Cd_{Al}) = 0.912$, $r(Ca_{Al}) = 0.872$, $r(Ni_{Al}) = 0.841$, $r(Cu_{Al}) = 0.832$, $r(Pb_{Al}) = 0.709$). Higher element-to-Al ratios indicate an enrichment of elements from nongeogenic sources,²⁸ for example, polluted anthropogenic particles and/or bioaccumulation. In Figure 8 of the Supporting Information, we exemplarily plotted the distribution of Cd_{Al} along the Xiangxi River backwater to show its strong relation to chl_a . Similar patterns are present for the other above-mentioned element-to-Al ratios. Planktonic algae in the TGR do not form $CaCO_3$ shells,³⁷ even though $CaCO_3$ often precipitates passively due to the shifted carbonic acid equilibrium by photosynthesis. This $CaCO_3$ can build up considerable proportions of the SPM load.³⁸ In fact, we see three options to explain the observed enrichment of pollutants in SPM: (1) bioaccumulation within planktonic algae, (2) coprecipitation/

adsorption with/to CaCO_3 , or (3) enhanced algal growth close to anthropogenic polluted SPM sources.

Surprisingly, we also found raised levels of chl_a , O_2 -sat., pH, and element-to-Al ratios (P_{Al} , Cd_{Al} , Ca_{Al} , Ni_{Al} , Cu_{Al} , Pb_{Al}) along the thalweg of the upstream tributary backwater (Figure 3 and Supporting Information, Figure 8). Remembering the lower EC_{25} and colder T values in the same region, we think that colder water from the mountainous Xiangxi River headwater formed an underflow density current along the thalweg channel of the tributary backwater (Figure 5). The momentum and kinetic energy of this current were continuously reduced by turbulent mixing across the boundary to the warmer surface of the stratified backwater. Thus, parts of the algae and pollutant-enriched SPM from the surface water could transfer into this underflow density current and move further downslope with it. However, we cannot draw conclusions about the further fate of these particles.

The huge water mass that entered from the Yangtze River main channel into the middle layer of the tributary backwater moved parallel to the T -isolines (Figure 2). Thus, the mechanism we observed was an interflow density current, determined by T -dependent density differences. During the week prior to our fieldtrip, the water level at the TGD rose considerably by more than 6 m up to 165.9 m a.s.l., and it slightly increased further to 166.3 m a.s.l. during our measurements (Supporting Information, Figure 6a).¹⁵ We compared the daily changes of water body volume within the Xiangxi River backwater from 8 to 21 September with cumulated inflow rates from the Xiangxi River catchment monitored by the hydrological stations “Xingshan” and “Jianyangping” (Figure 1 and Supporting Information, Figure 6c) in the upstream of our sampling area.³⁹ In total, the water body volume increased by $93.6 \times 10^6 \text{ m}^3$, from which about 44% was filled up with runoff from the Xiangxi River catchment itself, while the other 56% derived from the Yangtze River main channel (Supporting Information, Figure 6c). Thus, there was a net upstream flow from the Yangtze River main channel into the Xiangxi River backwater. When we purely consider the volumetric water body changes and neglect any stratification and hydrodynamic mixing effects, this water intrusion from the Yangtze River main channel would have reached a horizontal upstream shift of only around 1.35 km distance (Supporting Information, Figure 7). From our data (Figure 2), however, we can deduce an intruding turb plume that reached more than 20 km upstream into the tributary backwater. There are two major driving forces that appear responsible for this almost 15-fold amplification of water transport distance: (1) buoyancy force and (2) kinetic energy/momentum of the intruding water masses from the Yangtze River main channel. The steep water level rise in the TGR just before our monitoring period caused a net upstream flow of water masses into the Xiangxi River backwater (see above). After water level equilibrium was reached, there still remained the kinetic energy and momentum of the upstream moving water masses. The thermal stratification within the tributary backwater acted as a density pump and accumulated this upstream flow to a specific interflow depth determined by buoyancy forces. This further upstream flow caused the formation of a large circulation cell in the Xiangxi River backwater with an upstream interflow from the Yangtze River main channel and a downstream overflow from the midstream Xiangxi River backwater. Besides the steep water level rise, it was the coexistence of two linked water bodies with different hydrodynamic mixing characteristics

(riverlike in the Yangtze River main channel on the one hand, and more lakelike with pronounced stratification in the Xiangxi River backwater on the other hand) that caused the formation of this large circulation cell and thus the significant amplification of upstream pollutant transport distance. When compiling all the information from the data discussed above, we can derive a simplified density pump and pollutant transport flow model for the hydrological situation in September 2012 (Figure 5).

Generally, the Yangtze River main channel in the TGR carries much higher concentrations of nutrients and/or heavy metals than its tributaries.^{2,40} On the long-term and the reservoir scale, such a density pump effect could thus supply nutrients and polluted SPM to the upstream tributary backwaters. There, they could further aggravate eutrophication problems and support pollutant accumulation in sediments, food webs, and the agriculturally used flood plains of the TGR water level fluctuation zone. The seasonal and spatial representativity and significance of the density pump effect on the absolute water mass/pollutant exchanges between the Yangtze River main channel and its tributaries in the TGR need to be further evaluated in the future. Particularly, because the seasonal discharge pattern of the Yangtze River and the TGD water level management (Supporting Information, Figure 1) cause completely different but seasonally typical hydrodynamic conditions in the TGR. For the Xiangxi River backwater, it was already demonstrated that intruding density currents from the Yangtze River main channel occurred with a seasonal shift from underflows in winter and spring to interflows in summer and to overflows in autumn.⁴¹ Thus, an upstream transport into this tributary bay seems to be always present but is so far not quantified for pollutants. It is also crucial to evaluate the further fates and pathways of these pollutants in waters and sediments of the TGR and the Yangtze River with adequate techniques; they will move or accumulate either upstream or downstream, but they will stay somewhere. This we should know, not least because, throughout its catchment, the Yangtze River and its floodplains serve as a major source of water, food, and agricultural cropland for the whole of China⁴² as well as habitat for an invaluable biodiversity.⁶

Similar patterns with different impact and extent are very likely to occur in other reservoirs worldwide and should be addressed in further studies. Furthermore, the applied methods of combined spatiotemporal multisensor monitoring, analysis of water samples, and geostatistical modeling can be applied and are adaptable to numerous water quality related questions in lakes and reservoirs worldwide.

■ ASSOCIATED CONTENT

§ Supporting Information

Seasonal hydrodynamics in the TGR; the MINIBAT multi-sensor probe; how dense can we measure?—Challenges of water quality monitoring in remote areas; spatial dimension reduction for 3D spatiotemporal kriging; spatiotemporal kriging; analytical quality control of the applied water and SPM analyses; verification of the SRTM DEM for the Xiangxi River valley; element composition of water samples and SPM related to international thresholds and local background values; hydrological conditions in the TGR and the Xiangxi River backwater and water body volumetrics; cadmium-to-Al ratio distribution along the Xiangxi River backwater. This material is available free of charge via the Internet at <http://pubs.acs.org>.

AUTHOR INFORMATION

Corresponding Author

*Phone: 0049-721-608-47613; e-mail: andreas.holbach@kit.edu.

Notes

The authors declare no competing financial interest.

ACKNOWLEDGMENTS

Thank you to the three external reviewers whose critical and fair comments considerably contributed to improve the quality of this paper. This research was funded by the Federal Ministry of Education and Research of Germany (BMBF grant no. 02WT1131), the National Nature Science Foundation of China (31123001), the China Three Gorges Corporation (0711442), and the International Science and Technology Cooperation Program of China (MOST grant no. 2007DFA90510).

ABBREVIATIONS USED

TGR	Three Gorges Reservoir
TGD	Three Gorges Dam
a.s.l	above sea level
SPM	suspended particulate matter
turb	turbidity
chl _a	chlorophyll a
DEM	digital elevation model
EC ₂₅	electrical conductivity normalized to 25 °C
T	temperature
CDOM	colored-dissolved organic matter
O ₂ -sat.	O ₂ saturation

REFERENCES

- (1) Liu, L.; Liu, D.; Johnson, D.; Yi, Z.; Huang, Y. Effects of vertical mixing on phytoplankton blooms in Xiangxi Bay of Three Gorges Reservoir: Implications for management. *Water Res.* **2012**, *46* (7), 2121–2130.
- (2) Holbach, A.; Wang, L.; Chen, H.; Hu, W.; Schleicher, N.; Zheng, B.; Norra, S. Water mass interaction in the confluence zone of the Daning River and the Yangtze River—A driving force for algal growth in the Three Gorges Reservoir. *Environ. Sci. Pollut. Res.* **2013**, *20* (10), 7027–7037.
- (3) Nilsson, C.; Reidy, C. A.; Dynesius, M.; Revenga, C. Fragmentation and flow regulation of the world's large river systems. *Science* **2005**, *308*, 405–408.
- (4) McCartney, M. P.; Sullivan, C.; Acreman, M. C. *Ecosystem impacts of large dams*. Background Paper Nr. 2 Prepared for IUCN/UNEP/WCD, 2001.
- (5) Yang, X.; Lu, X. Ten years of the Three Gorges Dam: A call for policy overhaul. *Environ. Res. Lett.* **2013**, *8*, 1–5.
- (6) Seeber, C.; Hartmann, H.; Xiang, W.; King, L. Land use change and causes in the Xiangxi catchment, Three Gorges area derived from multispectral data. *J. Earth Sci.* **2010**, *21* (6), 846–855.
- (7) Zhang, Q.; Lou, Z. The environmental changes and mitigation actions in the Three Gorges Reservoir region, China. *Environ. Sci. Policy* **2011**, *14* (8), 1132–1138.
- (8) Zhang, J.; Zheng, B.; Liu, L.; Wang, L.; Hunag, M.; Wu, G. Seasonal variation of phytoplankton in the Daning River and its relationships with environmental factors after impounding of the Three Gorges Reservoir: A four-year study. *Procedia Environ. Sci.* **2010**, *2*, 1479–1490.
- (9) Lin, J.; Fu, C.; Zhang, X.; Xie, K.; Yu, Z. Heavy metal contamination in the water-level fluctuating zone of the Yangtze River within Wanzhou section, China. *Biol. Trace Elem. Res.* **2012**, *145*, 268–272.
- (10) Ye, C.; Li, S.; Zhang, Y.; Zhang, Q. Assessing soil heavy metal pollution in the water-level-fluctuation zone of the Three Gorges Reservoir. *China J. Hazard. Mater.* **2011**, *191* (1–3), 366–372.
- (11) Audry, S.; Schäfer, J.; Blanc, G.; Jouanneau, J.-M. Fifty-year sedimentary record of heavy metal pollution (Cd, Zn, Cu, Pb) in the Lot River reservoirs (France). *Environ. Pollut.* **2004**, *132*, 413–426.
- (12) Smith, V. H. Eutrophication of freshwater and coastal marine ecosystems a global problem. *Environ. Sci. Pollut. Res.* **2004**, *10* (2), 126–139.
- (13) International Commission on Large Dams. *World Register of Dams*. <http://www.icold-cigb.org> (accessed March 5, 2014).
- (14) Lehner, B.; Reidy Liermann, C.; Revenga, C.; Vörösmarty, C.; Fekete, B.; Crouzet, P.; Döll, P.; Endejan, M.; Frenken, K.; Magome, J.; Nilsson, C.; Robertson, J. C.; Rödel, R.; Sindorf, N.; Wisser, D. High resolution mapping of the world's reservoirs and dams for sustainable river flow management. *Front. Ecol. Environ.* **2011**, *9* (9), 494–502.
- (15) China Three Gorges Corporation. <http://cwic.com.cn/inc/sqsk.php> (accessed October 16, 2013).
- (16) Thomaz, S. M.; Pagioro, T. A.; Bini, L. M.; Murphy, K. J. Effect of reservoir drawdown on biomass of three species of aquatic macrophytes in a large sub-tropical reservoir (Itaipu, Brazil). *Hydrobiologia* **2006**, *570*, 53–59.
- (17) Straškraba, M.; Tundisi, J. G. Reservoir water quality management. In *Guidelines of Lake Management*; International Lake Environment Committee: Shiga, Japan, 1999; Vol. 9.
- (18) Xu, Y.; Cai, Q.; Shao, M.; Han, X.; Cao, M. Seasonal dynamics of suspended solids in a giant subtropical reservoir (China) in relation to internal processes and hydrological features. *Quat. Int.* **2009**, *208*, 138–144.
- (19) Bianchi, T. S. Estuarine chemistry. In *Estuarine Ecology*, 2nd ed.; Day, J. W., Crump, B. C., Kemp, W. M., Yáñez-Arancibia, A., Eds.; Wiley: Hoboken, NJ, 2012; pp 39–85.
- (20) Turner, A.; Millward, G. E. Suspended particles: Their role in estuarine biogeochemical cycles. *Estuarine, Coastal Shelf Sci.* **2002**, *55* (6), 857–883.
- (21) Stüben, D.; Stüben, K.; Haushahn, P. MINIBAT—A new, simple system for in-situ measurement, mapping and sampling of dissolved trace elements in aquatic systems. *Underwater Syst. Des.* **1994**, *16*, 5–14.
- (22) Kyriakidis, P. C.; Journel, A. G. Geostatistical space-time models: A review. *Math. Geol.* **1999**, *31* (6), 651–684.
- (23) Journel, A. G.; Rossi, M. E. When do we need a trend model in kriging? *Math. Geol.* **1989**, *21* (7), 715–739.
- (24) Gladney, E. S.; Roelandts, I. 1988 compilation of elemental concentration data for USGS geochemical exploration reference materials GXR-1 to GXR-6. *Geostand. Newsl.* **1990**, *14* (1), 21–118.
- (25) Cantillo, A. Y. *Standard and Reference Materials for Environmental Science*, Technical memorandum NOS ORCA 94, Pt.2; NOAA: Silver Spring, MD, November, 1995; pp 519–520.
- (26) Zhang, L.; Zhou, K. Background values of trace elements in the source area of the Yangtze River. *Sci. Total Environ.* **1992**, *25*, 391–404.
- (27) Federal ministry for the environment, nature conservation, and nuclear safety of Germany (BMUB). *Chemische Gewässergüteklassifizierung*, 2012. BMUB Website. <http://www.bmub.bund.de/themen/wasser-abfall-boden/binnengewasser/fluesse-und-seen/schutzziele-und-bewertungsparameter/chemische-gewaessergueteklassifizierung> (accessed March 6, 2014), in German.
- (28) Devesa-Rey, R.; Diaz-Fierros, F.; Barral, M. T. Normalization strategies for river bed sediments: A graphical approach. *Microchem. J.* **2009**, *91*, 253–265.
- (29) *Shuttle Radar Topography Mission*. USGS EROS Center: Sioux Falls, SD. <http://eros.usgs.gov> (accessed July 27, 2012).
- (30) Gloss, S. P.; Mayer, L. M.; Kidd, D. E. Advective control of nutrient dynamics in the epilimnion of a large reservoir. *Limnol. Oceanogr.* **1980**, *25*, 219–228.

- (31) The council of the European Union. On the quality of water intended for human consumption. In *Off. J. Eur. Communities* **1998**, *41*, 32–54.
- (32) World Health Organization. *Guidelines for Drinking-Water Quality*, 4th ed.; WHO: Geneva, Switzerland, 2011; pp 472–475.
- (33) Ministry of Health of China. Standards for drinking water quality. In *National Standards; GB 5749-2006*; 2006; in Chinese.
- (34) Rügner, H.; Schwientek, M.; Beckingham, B.; Kuch, B.; Grathwohl, P. Turbidity as a proxy for total suspended solids (TSS) and particle facilitated pollutant transport in catchments. *Environ. Earth Sci.* **2013**, *69*, 373–380.
- (35) Hudson, N.; Baker, A.; Reynolds, D. Fluorescence analysis of dissolved organic matter in natural, waste and polluted waters—A review. *River Res. Appl.* **2007**, *23*, 631–649.
- (36) Aiken, G. R.; Hsu-Kim, H.; Ryan, J. N. Influence of dissolved organic matter on the environmental fate of metals, nanoparticles, and colloids. *Environ. Sci. Technol.* **2011**, *45*, 3196–3201.
- (37) Zheng, H.; Song, L. R.; Yu, Z. G.; Chen, H. T. Post-impoundment biomass and composition of phytoplankton in the Yangtze River. *Int. Rev. Hydrobiol.* **2007**, *92* (3), 267–280.
- (38) Stabel, H.-H. The role of plankton biomass in controlling fluctuations of suspended matter in Lake Constance. *Hydrobiologia* **1986**, *140* (2), 173–181.
- (39) *Xingshan and Jianyang Ping Hydrological Stations Discharge Data*; Yichang Survey Bureau of Hydrology Resources: Yichang, China, September, 2012.
- (40) Luo, Z.; Zhu, B.; Zheng, B.; Zhang, Y. Nitrogen and phosphorus loadings in branch backwater reaches and the reverse effects in the main stream in Three Gorges Reservoir. *China Environ. Sci.* **2007**, *27*, 208–212 (in Chinese).
- (41) Yang, Z.; Liu, D.; Ji, D.; Xiao, S.; Huang, Y.; Ma, J. An eco-environmental friendly operation: An effective method to mitigate the harmful blooms in the tributary bays of Three Gorges Reservoir. *Sci. China Technol. Sci.* **2013**, *56*, 1458–1470.
- (42) Ponseti, M.; López-Pujol, J. The Three Gorges Dam project in China: History and consequences. *HMiC: Història Moderna i Contemporània* **2006**, 151–188.

Three Gorges Reservoir: density pump amplification of pollutant transport into tributaries

Andreas Holbach,[†] Stefan Norra,[†] Lijing Wang,[‡] Yuan Yijun,[§] Wei Hu,[†] Binghui Zheng,[‡]*

Yonghong Bi[§]

[†]Institute of Mineralogy and Geochemistry, Karlsruhe Institute of Technology, Karlsruhe 76131,
Germany (*e-mail: andreas.holbach@kit.edu)

[‡]Chinese Research Academy of Environmental Sciences, Beijing 100012, China

[§]Institute of Hydrobiology, Chinese Academy of Sciences, Wuhan 430072, China

Corresponding Author

*Phone: 0049-721-608-47613; e-mail: andreas.holbach@kit.edu.

SUPPORTING INFORMATION

Contents

Seasonal Hydrodynamics in the TGR (p. 3)

Figure 1, p. 3

The MINIBAT Multi-Sensor Probe (pp. 4-5)

Figure 2, p. 4

How Dense Can We Measure? – Challenges of Water Quality Monitoring in Remote Areas (pp. 6-7)

Figure 3, p. 7

Spatial Dimension Reduction for 3D Spatiotemporal Kriging (pp. 8-9)

Figure 4, p. 9

Spatiotemporal Kriging (pp. 10-14)

Figure 5, p.13; Table 2, p. 11; Table 3, p. 12; Table 4, p. 14

Analytical Quality Control of the Applied Water and SPM Analyses (p. 15)

Table 5, p. 15

Verification of the SRTM DEM for the Xiangxi River Valley (pp. 16-17)

Table 6, p.17

Element Composition of Water Samples and SPM Related to International Thresholds and Local Background Values (pp. 18-19)

Table 7, pp. 18-19

Hydrological Conditions in the TGR and the Xiangxi River Backwater and Water Body Volumetrics (pp. 20-22)

Figure 6, p. 21; Figure 7, p. 22

Cadmium-to-Al Ratio Distribution Along the Xiangxi River Backwater (p. 23)

Figure 8, p. 23

Seasonal Hydrodynamics in the Three Gorges Reservoir

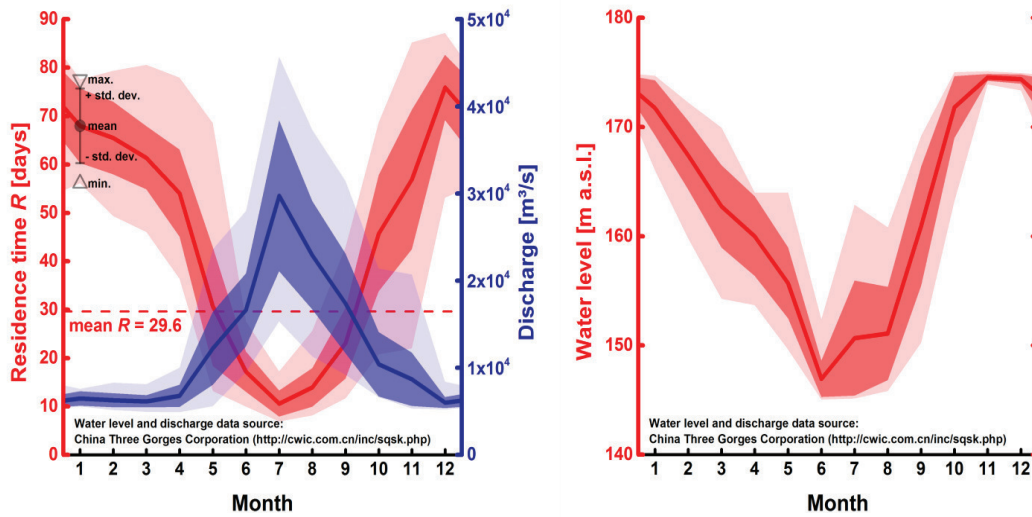


Figure 1. Monthly mean residence time, discharge (left), and water level (right) in TGR. Means, standard deviations and min./max. values derived from daily data for the years 2010-2013.^{(13),(15)}

The MINIBAT Multisensor Probe



Figure 2. Field application of the MINIBAT multisensor probe⁽²¹⁾ in the Xiangxi River. (l.) Underwater photo of the MINIBAT with its steerable wings in the front and some sensors visible in the back. (r.) MINIBAT measurement installation on a fishing boat in the Xiangxi River backwater. The MINIBAT is connected to the winch in the back and dragged through the water along the river. (photos: A. Holbach).

Table 1. Sensors installed on the MINIBAT and their specifications.

Parameter	Producer	Principle	Measuring range	Accuracy	Resolution	Response time
Pressure	ADM Elektronik	piezo-resistive	0 - 200 dbar	±0.1 dBar	0.005 dbar	0.04 s
O ₂	ADM Elektronik	Potentiometric (Clark electrode)	0 - 150% sat	±2% sat	0.02% sat.	3 s (63%)
Temperature	ADM Elektronik	Pt 100	-2 - 38°C	±0.01°C	0.001°C	0.12 s
El. conductivity	ADM Elektronik	7-pole-cell	0 - 6 mS/cm	±2 µS/cm	0.1 µS/cm	0.05 s
pH	AMT GmbH	Potentiometric (Ag/AgCl)	0 - 14 pH	0.02 pH	0.02 pH	1 s (63%)
H ₂ S*	AMT GmbH	Amperometric	0 - 10 mg/L	±3%	0.03 mg/L	<3 s
Chlorophyll <i>a</i> **	Turner designs	Fluorescence exc. 465 nm / fl. 696 nm	0.03 - 500 µg/L		0.01 µg/L	1 s
CDOM***	Turner designs	Fluorescence exc. 325 nm / fl. 470 nm	0.15 - 1250 ppb _{QS}	±5%	0.01 ppb _{QS}	1 s
Turbidity	Seapoint sensors, Inc.	Mie backscattering	0 - 750 FTU	±2%	< 0.001%	0.1 s
PAR (400-700 nm)****	LI-COR®	Photon flux density	0 - 10 mmol/(s*m ²)	±5%	0.01 µmol/(s*m ²)	10 µs

*The H₂S sensor did not operate stable and was not used during data evaluation. **Calibrated against algal monoculture of *Skeletonema costatum*. ***Calibrated against Quinine Sulfate in 0.05 M H₂SO₄. ****PAR data was not used for the current study.

How Dense Can We Measure? – Challenges of Water Quality Monitoring in Remote Areas

Ideally of course, we would know every single water quality parameter at any place and any time step across a certain study area and period. However, staff, time, equipment, money, and accessibility of some areas are often very limited and consequently, we have to rely on an equally limited number of measurements in space and time to draw our conclusions. Especially in remote areas, where there are no sophisticated networks to monitor water quality, we need to develop individual sampling strategies to meet demands of the intended research questions with our limited resources.

In our case, we were facing the challenge to monitor one week of water quality development in the more than 35 km long Xiangxi River backwater with only one MINIBAT. We had access to a fisherman's boat (**Figure 2**) in the town Xiakou located 20 km upstream of the confluence zone with the Yangtze River main channel. This boat could carry our MINIBAT equipment, but it could only reach speeds between 5-10 km/h. Including the time for frequent stationary depth profiling in deep waters, water sampling, and sample treatment, it was just possible to make the monitoring cruise from Xiakou to the confluence with the Yangtze River main channel within one workday. To cover the remaining Xiangxi River backwater areas and to detect temporal changes of water quality, we conducted repeated monitoring cruises to the upstream and to the downstream parts of the backwater stretch of the Xiangxi River during the remaining days of our monitoring period (**Figure 3**).

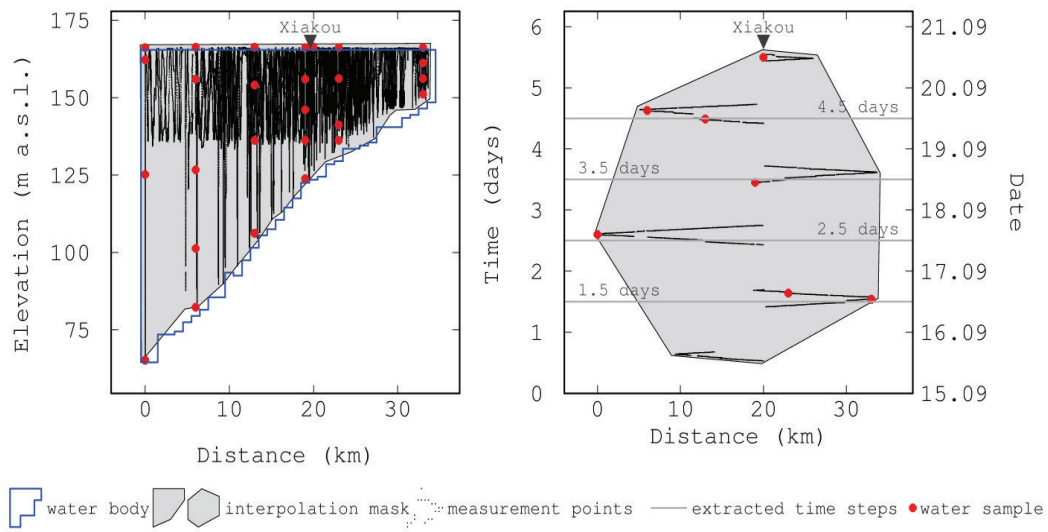


Figure 3. Scheme of our MINIBAT water quality measurement points within the applied spatiotemporal kriging interpolation domain. (l.) Longitudinal section along the center of the Xiangxi River backwater. Water depth is continuously decreasing from the confluence zone (0 km) towards the upstream of the backwater. (r.) measurement cruises along the Xiangxi River backwater versus time.

Spatial Dimension Reduction for 3D Spatiotemporal Kriging

For the spatiotemporal kriging calculations we reduced both UTM zone 49 Easting and Northing values to one linear horizontal distance component along the center of the narrow and long channel-like Xiangxi River valley. We assumed that the linear distance along the Xiangxi River backwater is much more relevant for water quality distribution than the actual geographical coordinates. However, there could still be significant differences of water quality across the river, e.g. due to effects from the banks and/or hydrodynamics. It is likely, that water flow and mixing processes will be enhanced along the center of the backwater, and delayed in bays and shallow areas close to the shoreline. We recorded two consecutive water quality depth profiles nearby Xiakou on 18 September 2012 (**Figure 4**). The first profile (blue) was recorded within a more shallow bay area than the second profile (red), approximately 150 m besides the center of the Xiangxi River. Even though, water quality distributions of both depth profiles appear to be very similar. Only EC₂₅, turb, and CDOM exhibit slightly stronger peak characteristics in the middle layer at the center of the river. This indicates that along the center of the Xiangxi River backwater flows and corresponding intrusion plumes would appear more pronounced close to its banks.

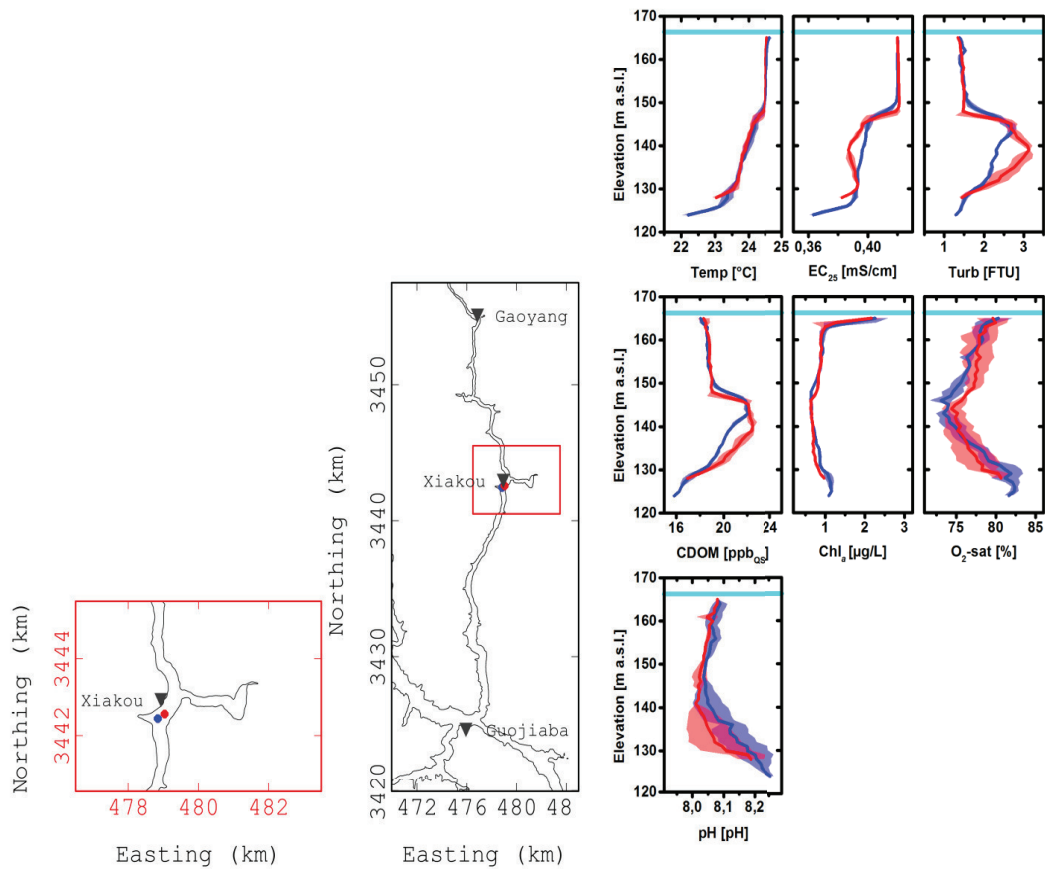


Figure 4. Similarity of two neighboring water quality depth profiles near Xiakou. First profile (blue) recorded from 10:38-10:44 AM, second profile (red) recorded from 10:48-10:53 AM on 18 September 2012. (left) Geographical reference. (right) depth profiles of the seven analyzed water quality parameters. We calculated mean values by the meter and plotted corresponding standard deviations around as filled areas.

Spatiotemporal Kriging

Geostatistical kriging estimation of regionalized variables is a well-known method. The estimations are based on the variogram statistics of the considered variable across its respective coordinate system. In isatis, we fit variogram models to the experimental data (**Table 2**), defined a moving local neighborhood for the calculations (**Table 3**), and tested the validity of the corresponding kriging procedures with a leave-one-out cross validation (**Table 2, Figure 5**). The kriging procedure is used for both estimation of the variable value itself and the corresponding estimation uncertainty as a measure for the estimation quality. This estimation uncertainty is called kriging standard deviation.^{(22),(23)} Within our data set there are areas with lower sampling density, especially in greater depths close to the confluence zone of the Xiangxi River backwater with the Yangtze River main channel (**Figure 3**). Still, the estimation uncertainties of our applied spatiotemporal kriging estimation (**Table 4**) happen to be very small compared to the absolute ranges of the analyzed water quality parameters (see article, **Figures 2 and 3**). Due to both the valid cross validation calculations and the small kriging standard deviations, we consider the spatiotemporal distribution of our sampling points to be sufficient for the applied geostatistical data evaluation and to derive spatiotemporal water quality dynamics throughout our spatiotemporal sampling domain.

Table 2. Variogram models and cross-validation statistics for spatiotemporal kriging estimations calculated in isatis.

Parameter	Model type	Sill	Ranges			Cross validation statistics		
			d_h	e_s	t_d	point no.	$ Std. err. \leq 2$	%
CDOM	Nugget	0.1						
	Cubic	2	19000	3000	80000	12869	12398	96.3
	Spherical	3.5	19000	3000	80000			
chl_a	Nugget	0.03						
	Cubic	0.12	9000	2000	60000	12992	12614	97.1
	Spherical	0.15	9000	2000	60000			
EC₂₅	Nugget	5.E-06						
	Cubic	3.E-04	28000	3500	70000	12035	11584	96.3
	Spherical	2.E-04	28000	3500	100000			
O₂-sat	Nugget	4						
	Cubic	25	9000	2000	70000	12914	12477	96.6
	Spherical	25	9000	2000	70000			
T	Nugget	0.01						
	Cubic	0.1	50000	4000	80000	13026	12736	97.8
	Spherical	0.3	50000	4000	80000			
turb	Nugget	0.005						
	Cubic	0.15	18000	3500	80000	12732	12301	96.6
	Spherical	0.1	18000	3500	80000			
pH	Nugget	0.001						
	Cubic	0.01	9000	2800	70000	13031	12428	95.4
	Spherical	0.01	9000	2800	70000			

Table 3. Parameters of the moving local neighborhood used for spatiotemporal kriging estimations in isatis.

<i>Space-time extent</i>			
Direction	Range	Unit	Scale factor
d_h	30000	m	1
e_s	3000	cm	100
t_d	30000	1.E-04 days	10000
Rotation	no		
Sub-divisions and limitations			
Angular sectors in d_h - t_d plane			4
Minimum no. of samples/sector			10
Optimum no. of samples/sector			100

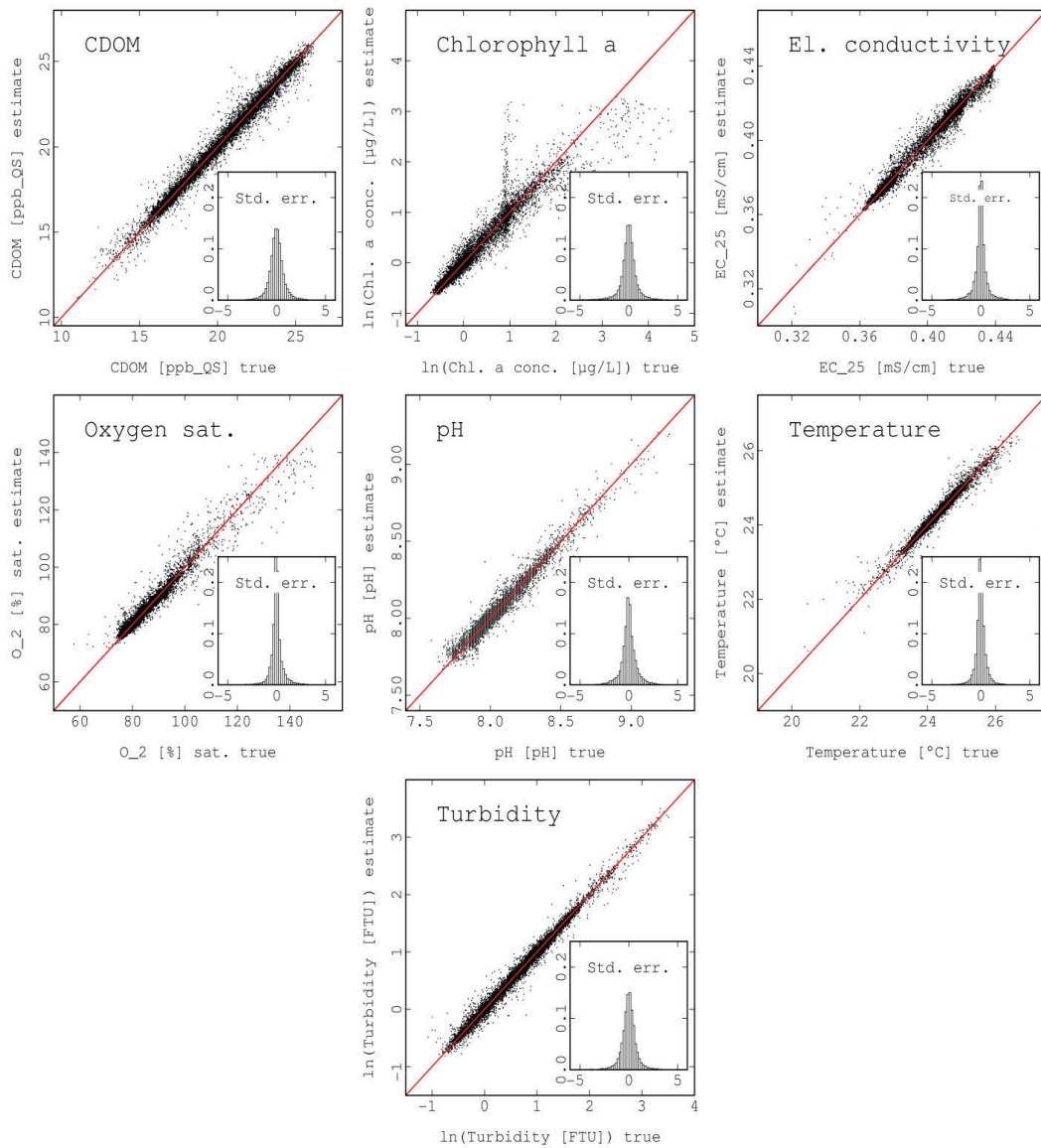


Figure 5. Cross-validation results. Scatter diagrams of space-time kriging estimations vs. true values for the seven analyzed water quality parameters. The corresponding histograms display the frequency distribution of corresponding standardized kriging errors. Note: chl_a and turb were estimated by log-normal kriging.

Table 4. Ranges of kriging standard deviations of the estimated water quality parameters within the applied spatiotemporal kriging interpolation domain.

Parameter	Min.	Max.
CDOM	0.07	1.63
chl_a	0.23	0.54
EC₂₅	0.00	0.01
O₂%	2.18	5.82
T	0.02	0.74
turb	0.02	0.45
pH	0.00	0.13

Analytical Quality Control of the Applied Water and SPM Analyses

Table 5. Analytical blank values and recovery rates of the applied digestions and chemical analyses.

	P	Ca	Ni	Cu	Zn	Cd	Pb
<i>Analytical blanks</i>							
Water	<DL	<0.01	<0.04	<0.4	<0.5	<0.001	<0.01
Digestion	5.52	0.25	0.52	0.36	9.17	0.009	0.24
	±1.05	±0.16	±0.46	±0.18	±4.92	±0.005	±0.06
Filter	5.33	0.24	0.59	0.96	7.74	0.12	0.26
	±0.51	±0.10	±0.23	±0.35	±4.14	±0.12	±0.04
<i>Recovery rates</i>							
TMDW	±5%						
	±10%						
SL-1⁽²⁵⁾	±10%						3/3
	±20%			3/3		0/3	3/3
	±30%				2/3		
GXR-2⁽²⁴⁾	±10%	3/3				3/3	3/3
	±20%		1/3		2/3		
	±30%			3/3			
		<i>certified</i>			<i>uncertified</i>		
		<i>X/Y within certified confidence interval</i>					

Verification of the SRTM DEM for the Xiangxi River Valley

The Shuttle Radar Topography Mission (SRTM) took place in February 2000. This was before the first inundation activities at the TGD. Therefore, the SRTM DEM is likely to represent the former morphology of the Xiangxi River valley which we assume to equal the recent bathymetry of the Xiangxi River backwater after the impoundment of TGR. However, the SRTM DEM could be subject to local errors and/or the impoundment of TGR could have considerably altered the bathymetry of the Xiangxi River valley already. To verify the accuracy, precision and utilization of the SRTM DEM in our study area we used the water depth data recorded with our echosounder of the Garmin GPSMAP® 521s Chartplotter. We crossed 1046 SRTM DEM grid cells with our MINIBAT measurements. For all these cells we calculated the corresponding mean values of $e_s(\text{MINIBAT}) = l_w - d_{bw}$ (where l_w is the daily TGR water level,⁽¹⁵⁾ d_{bw} is the water depth of each data point). The frequency distribution of elevation errors

$$err_{es} = e_s(\text{MINIBAT}) - e_s(\text{SRTM DEM})$$

has its clear maximum at 0 m and 92.3% of all 1046 calculated errors range between 4.9 m and 2.9 m (**Table 6**). The error distribution skewness towards negative values is apparently attributed to the spatial distribution of MINIBAT measurements and not to real errors of the SRTM DEM. We could exclusively perform MINIBAT measurements from the water surface. $e_s(\text{MINIBAT})$ values of SRTM DEM grids close to the banks are, thus, systematically biased towards too low elevations. Considering the error distribution maximum at 0 m and the small error range mentioned above, we decided that the SRTM DEM can be utilized to estimate the water body volumes in the Xiangxi River backwater.

**Element Composition of Water Samples and SPM Related to International Thresholds
and Local Background Values**

Table 7. Element compositions of water samples and SPM related to international thresholds and local background values.

Element		P	Ca	Ni	Cu	Zn	Cd	Pb
<i>Concentrations</i>								
	Unit	µg/L	mg/L	µg/L	µg/L	µg/L	µg/L	µg/L
	Min.	81.2	34.8	0.804	1.98	3.01	0.015	0.23
Total	Med.	106	38.1	1.49	4.27	8.5	0.029	0.78
	Max.	221	41.1	12.0	15.8	31.6	0.112	8.97
	Min.	41	34.5	0.33	1.32	0.62	0.007	0.031
Dissolved (<0.45 µm)	Med.	83	37.5	0.50	2.88	2.34	0.016	0.046
	Max.	199	39.9	1.01	5.67	8.89	0.021	0.271
<i>Drinking water directive threshold values</i>								
	EU⁽³¹⁾	n.a.	n.a.	20	2000	n.a.	5	10
	WHO⁽³²⁾	n.a.	n.a.	70	2000	n.a.	3	10
	China⁽³³⁾	n.a.	n.a.	n.a.	1000	1000	5	10

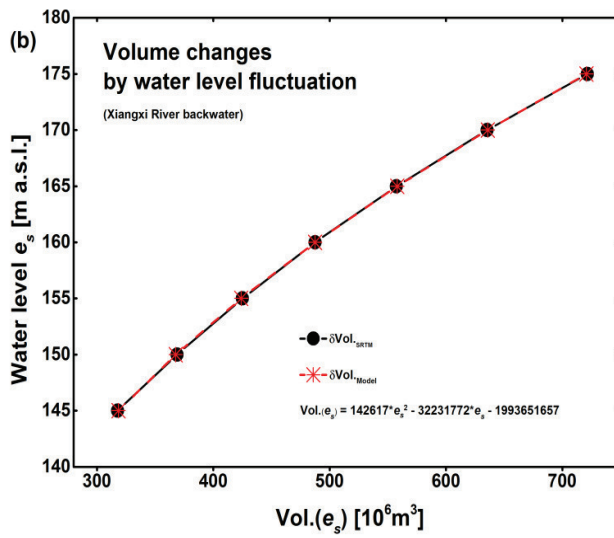
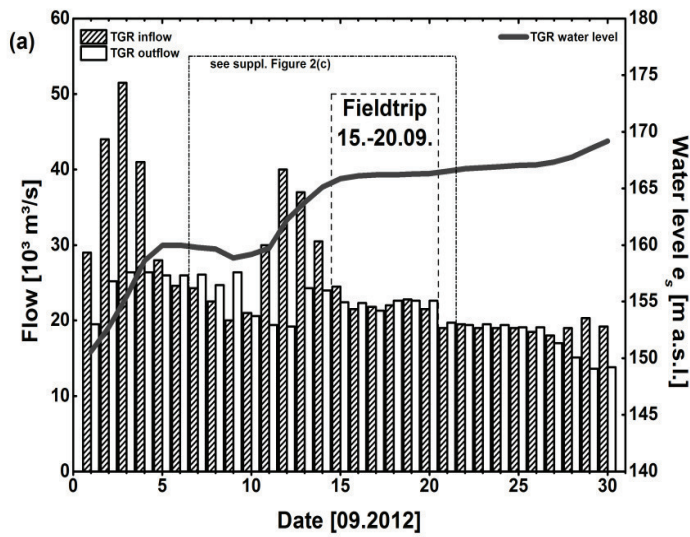
Table 7 (continued). Element compositions of water samples and SPM related to international thresholds and local background values.

Element		P	Ca	Ni	Cu	Zn	Cd	Pb
	Unit	g/kg	g/kg	mg/kg	mg/kg	mg/kg	mg/kg	mg/kg
SPM (>0.45 μm)	Min.	0.71	19.8	58.4	63.6	159	0.53	28.8
	Med.	1.26	34.4	71.4	94.2	340	0.93	54.5
	Max.	6.03	55.3	154	137	1482	2.39	71.2
<i>Background value Yangtze River sediment (<63 μm)⁽²⁶⁾</i>								
		n.a.	n.a.	28.7	23.2	74	0.17	15.6
	Factor	1.E+03	1.E+03	1.E+03	1.E+03	1.E+03	1.E+06	1.E+03
El_{Al}	Min.	7	0.20	0.65	0.63	1.6	5.6	0.47
	Med.	14	0.41	0.84	1.07	3.7	10.7	0.62
	Max.	217	1.16	4.01	2.83	17.3	85.8	1.03

Bold numbers indicate exceeding of threshold or local background values.

Hydrological Conditions in the TGR and the Xiangxi River Backwater and Water Body

Volumetrics



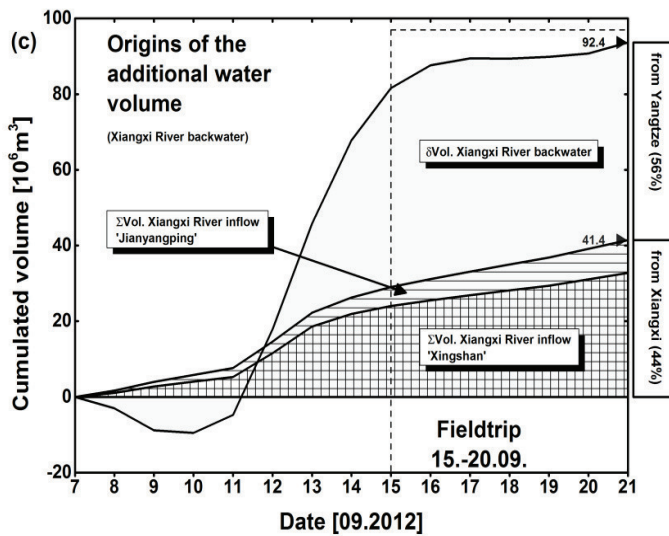


Figure 6. Hydrological conditions in TGR in September 2012 enclosing our fieldtrip. (a) Cumulated inflow into TGR is considerably higher than outflow during times of steep water level rise (01.-04.09 and 11.-14.09).⁽¹⁵⁾ (b) Water level to volume relationship in the Xiangxi River backwater derived from the SRTM-DEM⁽²⁹⁾ in ArcGIS 10. (c) Water volume changes and origins in the Xiangxi River backwater one week before and during our measurements.^{(15),(39)}

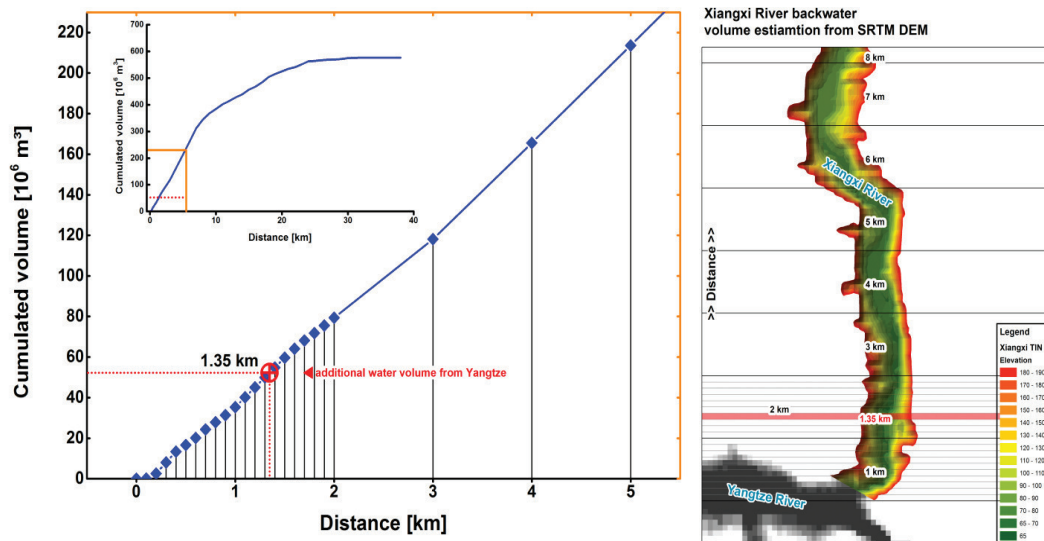


Figure 7. Volume estimation for the Xiangxi River backwater based on the SRTM-DEM and a water level of 163.3 m a.s.l.. Cumulating of volume slices along the Xiangxi River backwater calculated from the SRTM-DEM⁽²⁹⁾ in ArcGIS 10. The additional volume coming from the Yangtze River (see article, **Figure 4**) would only reach around 1.35 km upstream into the Xiangxi River backwater without any turbulence and density effects.

Cadmium-to-Al Ratio Distribution Along the Xiangxi River Backwater

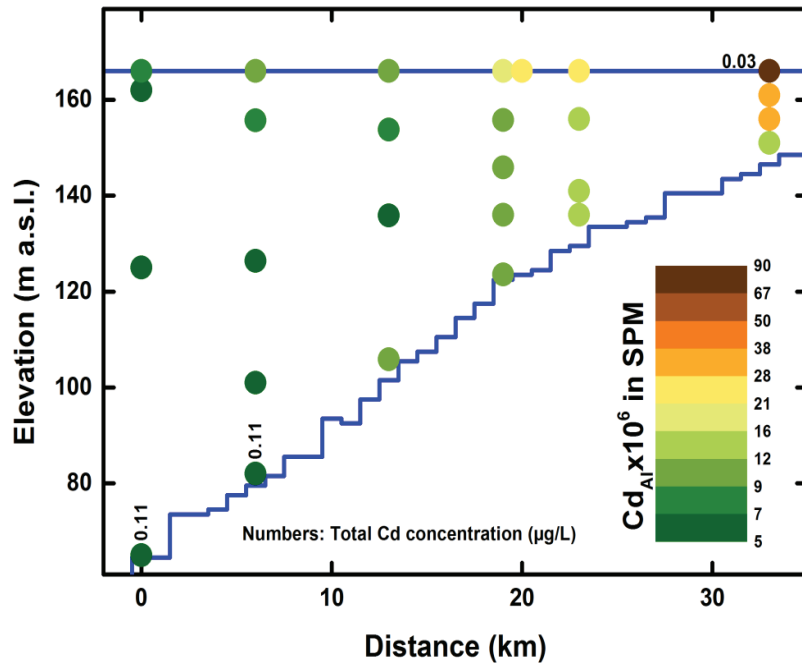


Figure 8. Distribution of $Cd_{Al} \times 10^6$ along the Xiangxi River backwater. Selected samples are also labelled with their total Cd concentrations. Note: Highest enrichment of Cd in appears in the surface water of the upstream Xiangxi River backwater, where there are also highest chl_a concentrations (see article, **Figure 3**). Patterns look similar for P_{Al} , Ca_{Al} , Ni_{Al} , Cu_{Al} , and Pb_{Al} .

A.3 Environmental water body characteristics in a major tributary backwater of the unique and strongly seasonal Three Gorges Reservoir, China



PAPER

View Article Online

View Journal



Cite this: DOI: 10.1039/c5em00201j

Environmental water body characteristics in a major tributary backwater of the unique and strongly seasonal Three Gorges Reservoir, China†

A. Holbach,^{*a} Y. Bi,^b Y. Yuan,^b L. Wang,^c B. Zheng^c and S. Norra^{ad}

Ecological consequences of large dams, particularly regarding the Three Gorges Dam (TGD) on the Yangtze River in China, have been controversially and internationally discussed. Water quality within the Three Gorges Reservoir (TGR) has been deteriorated by highly underestimated eutrophication and algal blooms. Globally, the TGR is delineated from other comparable reservoirs by its low mean water residence time and its 30 m annual water level fluctuation. We used an *in situ* and online multi-sensor system 'MINIBAT' to analyse eight indicative physico-chemical parameters across depth and time within the Xiangxi River backwater, a representative major tributary of the TGR. The results revealed considerably changing environmental water body characteristics within the tributary backwater related to the TGR's typical seasonal hydrology. The Yangtze River main stream appeared to be the major contributor of dissolved and particulate water constituents within the Xiangxi River backwater. Eutrophication problems in spring and summer seasons are likely a consequence of extensive water mass exchange and pollutant transport processes in autumn and winter. In particular, the backwater's permanently stratified water column shows varying layered impacts of the Yangtze River main stream and Xiangxi River headwaters. This is a clear indication of a complex stratified flow pattern within this TGR tributary backwater. In our study, a major driver for the Yangtze River main stream impact was the rising TGR water level. The TGR's globally unique characteristics have thus become a central part of the recent eutrophication and pollution problem within the TGR. Thereof, we deduced a proposal for an adapted dam management strategy.

Received 29th April 2015
Accepted 2nd July 2015

DOI: 10.1039/c5em00201j

rsc.li/process-impacts

Environmental impact

This paper aims at identifying environmental water body characteristics within a major tributary backwater of the Three Gorges Reservoir in China, particularly with respect to its pronounced typical seasonality. This reservoir is highly threatened by eutrophication problems and is unique in terms of its low mean water residence time and 30 m annual water level fluctuation scheme. We applied state-of-the art *in situ* and online multi-sensor monitoring techniques and identified the large water level fluctuation as a main driver of pollutant transport into the TGR tributary backwaters. These are extremely vulnerable to algal blooms. An adapted dam management strategy, based on a feedback with the current main stream pollution state, is proposed to reduce pollutant input into tributary backwaters.

1. Introduction

For decades, the construction of large dams and reservoirs has been controversially discussed while dam planning and construction goes on as always. Without doubt, China is the

leading nation in building dams. Almost 50% of the world's large dams, more than 45 000, have been built in China.¹ Even though there are much larger dams and reservoirs in the world, the planning and construction of the Three Gorges Dam (TGD) on the Yangtze River was accompanied by exceptional international controversies and criticism. Indeed, the Three Gorges Reservoir (TGR) is an exceptional study area in the world with unique properties. In terms of size, mean water residence time, climatic zone, and mixing properties, only the Itaipú Reservoir impounded on the Paraná river between Brazil and Paraguay shows comparable properties as the TGR (ESI Fig. 1 and Table 1†). However, the TGR is subjected to 30 m annual water level fluctuation and is seriously eutrophic, whereas the water level in the oligotrophic Itaipú Reservoir only fluctuates less than 1 m per year.

^aInstitute of Applied Geosciences, Karlsruhe Institute of Technology, Kaiserstraße 12, 76131 Karlsruhe, Germany. E-mail: andreas.holbach@kit.edu; Fax: +49-721-608-47247; Tel: +49-721-608-47613

^bInstitute of Hydrobiology, Chinese Academy of Sciences, 430072 Wuhan, China

^cChinese Research Academy of Environmental Sciences, 100012 Beijing, China

^dInstitute of Geography and Geoecology, Karlsruhe Institute of Technology, 76131 Karlsruhe, Germany

† Electronic supplementary information (ESI) available. See DOI: 10.1039/c5em00201j

The final stage of the TGR's impoundment with water levels ranging between 145 and 175 m above sea level (a.s.l.), has been reached since 2010. The huge impounded area now forms the more than 600 km long, partly more than 120 m deep, and markedly dendritic TGR (Fig. 1). So far, the main intentions of the TGD have been achieved: (1) the TGD is protecting the downstream regions from devastating Yangtze River floods that have caused more than 300 000 deaths in the 20th century alone;² (2) the world's largest hydropower plant is now generating around 85 000 GWh per year (ref. 5) accounting for around 1.8% of China's electricity consumption in 2012;⁶ (3) the navigation along the Yangtze River is now possible for 10 000 t vessels from Shanghai up to Chongqing and the transported cargo across the TGD river section has increased from around 10×10^6 t before the dam construction² to 88×10^6 t in 2010.³ However, the reservoir impoundment has fundamentally changed the ecological conditions and has also caused severe environmental hazards.⁷ Particularly, eutrophication was highly underestimated by conducted environmental impact assessments and now becomes visible by frequent algal blooms. These pose a serious threat to the utilization of the TGR as drinking water and fishery resources and have already been directly addressed by numerous scientific studies.^{4,8,9} Further, there are creeping environmental hazards with long-term effects caused by pollutant transport, accumulation, and/or mobilization in/from reservoir sediments. These have been less frequently studied so far⁹⁻¹¹ and synoptic conclusions on a reservoir scale are still missing for the TGR. In the long-term, however, these can be equally serious as algal blooms as the massive capture of sediments in the Yangtze River reservoirs has already been proven.^{12,13}

The presence of thermal density stratification in the TGR tributary backwaters was shown in several experimental field studies^{4,9,14} as well as predicted by various modelling approaches.^{15,16} One numerical modelling study even predicts the temporal occurrence of thermal stratification within the

Yangtze River main stream of the TGR.¹⁷ However, water body stratification alone does not represent any environmental threat at all but correlated physico-bio-chemical processes take place, such as the formation of algal blooms and pollutant transport processes. These can lead to problematic changes of water properties. In this field, several studies have pointed out the importance of processes in between the TGR tributary backwaters and the Yangtze River main stream. It was shown that the Yangtze River main stream in the TGR is characterized by higher concentrations of nutrients (N and P) and that import processes from the main stream into tributary backwaters are major drivers for eutrophication problems, there.^{18,19} In particular, extensive field studies have identified density currents and related three-dimensional hydrodynamics as major nutrient and pollutant pathways as well as a regulating factor for the formation of thermal stratification suitable for algal blooms.^{4,9,13,14} The corresponding nutrient transport, stratification and algal growth phenomena have also been numerically modelled with three-dimensional hydrodynamic approaches.^{20,21} However, nutrients, eutrophication and algal blooms are only part of the story and a more generalized approach is necessary to capture other problematic processes, such as heavy metal transport and accumulation as well. For the TGR, balances of fates and pathways of heavy metals have been so far missing in both field and modelling studies.

Throughout the year, the TGR water bodies are subjected to four distinctive typical hydrological periods. In this study, we applied state-of-the-art multi-sensor monitoring techniques to identify temporal distributions of physico-chemical water body characteristics within the impounded valley of the Xiangxi River, a major TGR tributary backwater (Fig. 1), throughout those typical hydrological periods. Therefore, we used a MINIBAT multi-sensor probe^{9,22} to assess depth profiles of eight indicative physico-chemical parameters in this water body. Further information from this basic dataset was derived mathematically. With particular respect to the above mentioned environmental threats (eutrophication, nutrients, and heavy metals), the dataset was analysed to outline stratification patterns in the water body, as well as impact ranges on the chemical composition of the water of both the Yangtze River mainstream and the Xiangxi River headwater on environmental characteristics of different layers. Further, changes of water body characteristics within the backwater itself were also of major interest. Getting back to a global perspective and the TGR's hydrological uniqueness, we further extracted corresponding unique characteristics to be found within its water bodies. Conclusions will be drawn regarding challenges for water quality control within the TGR itself but also for possible dam management strategies, in general.

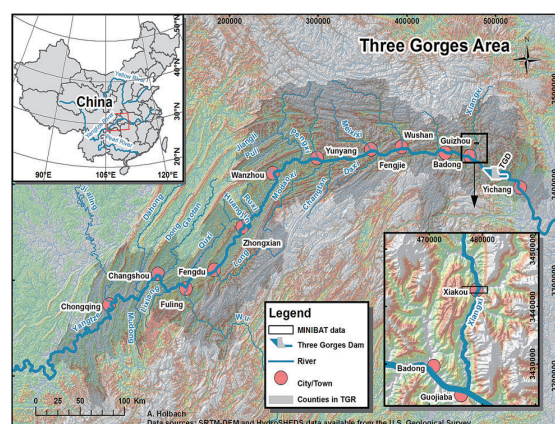


Fig. 1 Outline of the Three Gorges Reservoir, its location within China and the Xiangxi River backwater study area. Coordinates of the upper left overview map of China are in the WGS84 system; other coordinates are in the UTM zone 49 easting and northing format.

2. Materials and methods

2.1. Typical and distinctive annual hydrological periods in the TGR

The water level in the TGR is subjected to the specific management of the TGD and is meant to seasonally fluctuate between 145 and 175 m a.s.l. Climate in the catchment of the

TGR is associated with the East Asian summer monsoon.²³ Hence, the Yangtze River exhibits strong runoff seasonality with maximum inflows into the TGR ($>70\,000\text{ m}^3\text{ s}^{-1}$) in July and minimum values ($3500\text{--}7600\text{ m}^3\text{ s}^{-1}$) from December till March.²⁴ In this context, the TGD is operated to maximise its benefits for flood protection and electrical energy generation:

To ease summer discharge peaks and to avoid another devastating Yangtze River flood, the TGR water level is maintained at a low level during the flood season from June till August. This ensures a large flood retention volume within the TGR but reduces the energy yield of the hydropower plant in the TGD. The maximum outflow can be buffered by the reservoir and the TGD management resulting in maximum outflows of less than $50\,000\text{ m}^3\text{ s}^{-1}$.

During September and October, the reservoir is filled up to its peak water level of around 175 m a.s.l. This reduces the flood retention volume but increases the energy yield of the hydropower plant. The high water level phase from November till December is then followed by a water level drawdown from January till June. Consequently, four distinctive and typical hydrological scenarios are induced by the TGD management: low water level, rising water level, high water level, and falling water level (Fig. 2).

The monthly TGR water residence time (T_R) was calculated based on arithmetic mean values of daily TGD outflows (Q_{TGD}),²⁴ as well as water levels at the TGD (WL_{TGD}). Therefore, mean monthly volumes of the TGR water body (V_{TGR}) were linearly estimated from its minimum and maximum volumes (V_{min} : $22.15 \times 10^9\text{ m}^3$; V_{max} : $39.3 \times 10^9\text{ m}^3$),⁵ respectively, at water levels (WL_{min} : 145 m a.s.l.; WL_{max} : 175 m a.s.l.).²⁴

$$T_R = V_{\text{TGR}}/Q_{\text{TGD}}$$

$$V_{\text{TGR}} = V_{\text{max}} - (WL_{\text{max}} - WL_{\text{TGD}}) \times (V_{\text{max}} - V_{\text{min}}) / (WL_{\text{max}} - WL_{\text{min}}).$$

Hydrological scenarios in the TGR are systematically repeated on a yearly basis and thus represent the 'normal' hydrological conditions within the TGR. The conditions within

Table 1 Hydrological scenarios during the four MINIBAT fieldtrips^{5,24}

		Mar	Jun	Sep	Nov
TGR inflow [$\text{m}^3\text{ s}^{-1}$]	Min.	5300	11 600	21 500	5800
	Max.	5450	13 000	30 500	6200
TGD water level [m a.s.l.]	Min.	160.7	145.5	165.1	174.6
	Max.	160.9	145.7	166.3	174.7
Water residence time [days]	Min.	67.0	21.7	16.2	61.3
	Max.	67.2	22.8	18.6	85.2

the four fieldtrips of this study were well within this normal range (monthly means $\pm \sigma$ for the timeframe 01.2010–04.2014 in Fig. 2) of seasonally changing conditions. In turn, our acquired dataset can provide knowledge on the environmental water body characteristics during 'normal' conditions, but it can definitely not represent all kinds of possible conditions that may also occur, in particular not exceptional extreme events. These needed to be addressed from permanent long-term monitoring data.

The Xiangxi River, a typical one of the 40 major tributaries of the TGR, enters the Yangtze River approximately 40 km upstream of the TGD.²⁵ Periodic water level fluctuations of the TGR form an impounded backwater that reaches 30–40 km upstream into its dendritic long channel-like former valley.

We performed measurements with a MINIBAT multisensor probe (2.2) within this backwater during four fieldtrips in the years 2012–2014. We have covered four very typical and very different hydrological scenarios by each one of these fieldtrips (Fig. 2 and Table 1). During all fieldtrips, our base was always in the town Xiakou located approximately 20 km upstream of the Xiangxi River confluence with the Yangtze River main stream (Fig. 1). Hence, this section of the Xiangxi River was covered almost daily by MINIBAT measurements during the four fieldtrips. Furthermore, it is permanently located in the midst of the TGR backwater (Fig. 3) and reveals water depths of around 20 m in summer and 50 m in winter. This area turned out to be ideal to study patterns of environmental water body characteristics in the Xiangxi River backwater under typical and different hydrologic conditions.

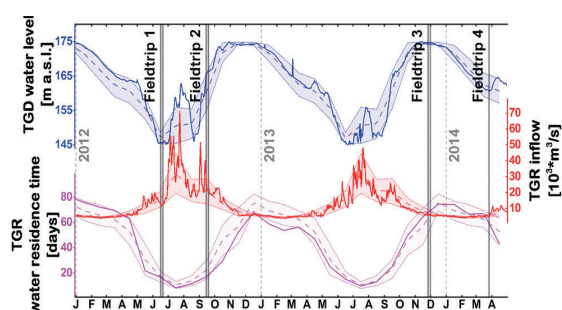


Fig. 2 Hydrological conditions in the TGR around our four conducted fieldtrips in the Xiangxi River backwater. Daily TGD water levels,²⁴ TGR inflows,²⁴ and corresponding calculated monthly TGR water residence times^{5,24} are plotted above monthly (01.2010–04.2014) means $\pm \sigma$ (dashed lines \pm shaded areas).

2.2. The MINIBAT underwater multisensor probe and recorded data

The MINIBAT is a multisensor probe for *in situ* and online measurements of relevant physico-chemical parameters in water bodies.²² The MINIBAT has already been successfully applied within the TGR.^{9,14} It is directly connected to a computer on a boat by a data transmission cable. The advanced MINIBAT system is equipped with sensors for eight physico-chemical indicative parameters of environmental conditions in the water (ESI Table 2†) as well as with a rack of five remote-control 50 mL water samplers. Physico-chemical parameters are highlighted individually in the following section. The parameters are recorded with 5 Hz frequency; for subsequent data evaluation, we used one dataset per second. We obtained the corresponding GPS and bathymetry data from a Garmin GPSMAP 521s

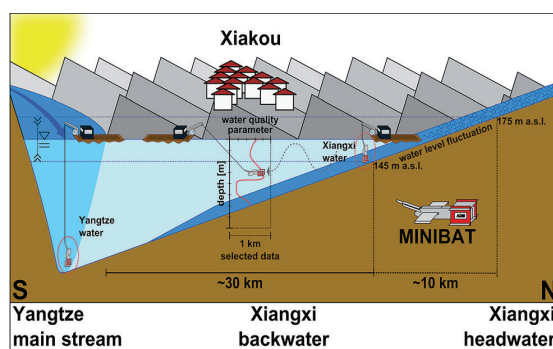


Fig. 3 Schematic illustration of *in situ* and online MINIBAT measurements in the Xiangxi River backwater used in this study. Note: the seasonal water level fluctuation between 145 and 175 m a.s.l. determines upstream monitoring boundaries for the MINIBAT. For geographic reference see Fig. 1.

Chartplotter that was coupled with a depth sounder on the boat. A pressure sensor on the MINIBAT was used to determine its depth under water. The MINIBAT can be applied from a boat in two ways: (1) it can be dragged through the water by the boat with $5\text{--}10\text{ km h}^{-1}$ and steered to different depths up to approximately 30 m by the use of its remote controlled wings; (2) it can also be used as a vertical profiling probe to reach larger depths when the boat does not move.

The MINIBAT raw data were recorded during four fieldtrips along the whole Xiangxi River backwater. From this vast dataset, a subset was selected from a very small horizontal area ($31.12 \pm 0.05^\circ\text{N}$) that equals around 1 km of the Xiangxi River backwater around Xiakou (Fig. 1 and 3). Remaining horizontal distances between measurement points were thus neglected during further data evaluation. Instead, we considered all analysed physico-chemical parameters i as functions $i(d, t)$ of both depth below water surface d and time t . Additionally, we selected the deepest measurements of the MINIBAT depth profile recorded at the most upstream location of the Xiangxi River backwater of each fieldtrip to approximate water quality conditions of the Xiangxi River headwater (Fig. 3). The deepest points from the MINIBAT depth profile in the Yangtze River main stream were selected similarly to approximate water quality conditions of the Yangtze River main stream. In March 2014, however, we could not perform MINIBAT measurements in the upstream Xiangxi River backwater.

2.2.1. Indicative physico-chemical parameters directly measured with the MINIBAT. Technical specifications of all sensors applied in this study can be found in ESI Table 2.†

Temperature (T). T is a fundamental physical property of water. It controls the aggregate state of water as well as density of water and is thus, particularly in freshwater, the driving force of water body stratification. Further, kinetics of bio-chemical processes generally depend on T .

Electrical conductivity (EC). The electrical conductivity of water is mainly related to its salinity and T . After standardization to 25°C , $EC_{25} \text{ } ^\circ\text{C}$ [$\mu\text{S cm}^{-1}$] is consequently often used as a proxy for salinity (Sal) [ppm]:

$$Sal = EC_{25} \text{ } ^\circ\text{C} \times f, \text{ where } 0.5 < f < 0.7.$$

Here, we used $f = 0.64$.²⁶ Further, $EC_{25} \text{ } ^\circ\text{C}$ is often a good conservative tracer through water mass mixing processes.²⁷

Coloured dissolved organic matter (CDOM). The sensor used here measures the fluorescence signal of water at 470 nm wavelength after excitation with 325 nm. Under these conditions, mainly humic-like substances are detected which are “derived from break-down of plant materials by biological and chemical processes in the terrestrial and aquatic environments”.²⁸ These can be of both natural and anthropogenic origin. In particular, organic compounds of urban sewage water exhibit corresponding fluorescence signals.²⁸ CDOM can therefore be a tracer of water masses and indicate water sources, e.g. sewage water. Light attenuation by CDOM can also have major impacts on the light environment in water bodies.

Turbidity ($Turb$). Turb of water is caused by colloids and suspended particles. Light attenuation caused by Turb can have major impacts on the light environment in water bodies. After verification, Turb can further serve as a proxy for the content of suspended particulate matter (SPM).

Chlorophyll a (Chl_a). Here, *in vivo* Chl_a concentrations were estimated from the fluorescence signal at 696 nm wavelength after excitation with 465 nm. Chl_a is the primary pigment of all photosynthetic organisms including all types of planktonic algae. The analysed Chl_a concentrations are thus a good proxy for algae abundance in general. Algal blooms, particularly excessive growth of toxin producing cyanobacteria, are a widely present serious risk for drinking water supply.

Oxygen saturation ($O_2\%$). In water, O_2 is produced by algal photosynthesis and consumed by aerobic respiration of organisms. An equilibrated water/air interface would always form 100% $O_2\%$. Corresponding over- or undersaturation is caused by the above mentioned bio-chemical processes. Anoxic conditions can occur due to little vertical turbulence. This is problematic for aerobic organisms and can further lead to microbial production of CH_4 , toxic H_2S , and the release of pollutants from sediments.

pH (pH). In natural water, pH depends on geogenic environmental settings of watershed and anthropogenic impacts. Within natural open water bodies, mainly photosynthesis, respiration, and assimilation of nitrogen cause vertical gradients and temporal changes of pH.²⁹ pH is further critical for the mobility and bioavailability of numerous pollutants.

Photosynthetically active radiation (PAR). This parameter covers a range of visible light between 400 and 700 nm wavelengths and was measured as photon flux density. From two simultaneously measured PAR values, we derived the euphotic depth (d_{eu}) where underwater PAR dropped to only 1% of the above water PAR.²⁹

2.2.2. Parameters derived from MINIBAT data and water samples

Suspended particulate matter (SPM). Additionally to the monitored MINIBAT parameters, numerous water samples were also taken at selected sites throughout the study area and during all four fieldtrip times. Here, analyses of SPM concentrations are used to study the Turb/SPM relationship. Specific

Paper

Environmental Science: Processes & Impacts

results of other water constituent analyses will be dealt with in another coming paper. From water samples ($V \approx 50$ mL), SPM was separated with previously weighed filters (Sartorius Stedim cellulose acetate membrane; pore size: $0.45 \mu\text{m}$; diameter: 25 mm). These filters were air dried and sealed before being weighed again. The SPM concentration was calculated as follows:

$$\text{SPM} = (w_L - w_0)/V_f$$

Here, w_0 is the raw filter weight, w_L is the loaded filter weight, and V_f is the filtered water sample volume. With respect to water density, the density of quartz (2.56 g cm^{-3}) is commonly used to estimate SPM related increase of water density $\Delta\rho_{\text{SPM}}$ with the following relationship:³⁰

$$\Delta\rho_{\text{SPM}} = \text{SPM} \times (1 - 1/2.56).$$

Water density (ρ). Density is a basic physical property of matter. In water bodies, vertical density gradients are responsible for stable stratification. The density of water depends on its T , as well as salinity and SPM. Hence, T and $\text{EC}_{25} \text{ } ^\circ\text{C}$ values as well as a Turb/SPM relationship can be used to estimate water density by applying the empirical equation of state.³⁰

Depth profiles of physico-chemical parameters (i). Depth profiles $i(d, t)$ were derived in 1 m depth intervals on a daily basis for all physico-chemical parameters i but PAR. Therefore, mean values and corresponding standard deviations were calculated from the selected MINIBAT data around Xiakou.

Vertical gradients ($\delta_z i$). Vertical gradients $\delta_z i = i_d/i_{d+1 \text{ m}}$ were derived from the daily depth profiles of physico-chemical parameters i . From water density estimates based on T , $\text{EC}_{25} \text{ } ^\circ\text{C}$, and Turb, we further calculated the vertical density gradients $\delta_z \rho$ as a measure of stratification intensity. Relationships of $\text{abs}(\delta_z i)$ with $\delta_z \rho$ were determined with both Pearson and Spearman correlation coefficients.

Temporal variability (var_i). We applied the commonly used squared difference approach to calculate temporal variability of physico-chemical parameters (not for PAR). For each depth d , the squared differences of i from day n to day $n + 1$ were therefore calculated:

$$\text{var}_i = [i_n(d) - i_{n+1}(d)]^2.$$

We intended to define a comprehensive general measure of temporal variability of physico-chemical properties in the water body around Xiakou. Therefore, var_c was introduced as a dimensionless comprehensive variable incorporating var_i of the different parameters i . To achieve similar comparable value distributions of var_i across different parameters i and across all four analysed hydrological scenarios, these var_i datasets required standardization. As a standardization method, we applied an adapted z -transformation³¹ by using the robust distribution which measures Median (med) as well as inter-quartile range r_{iq} for each individual parameter i :

$$\text{var}_{i\text{-std.}} = [\text{var}_i - \text{med}(\text{var}_i)]/r_{\text{iq}}(\text{var}_i).$$

The squared differences var_i are non-negative. Therefore, it is reasonable to simply sum up their standardized values $\text{var}_{i\text{-std.}}$ for each depth d and day interval $n/n + 1$ to receive var_c as a comprehensive variable of temporal physico-chemical variability in the water:

$$\text{var}_c = \sum_i \text{var}_{i\text{-std.}}$$

Further, we calculated Pearson and Spearman correlation coefficients of all var_i with var_c for each fieldtrip individually to extract contributions of single physico-chemical parameters i to var_c .

3. Results

3.1. Water density

From 107 water samples derived from all four fieldtrips, we found a strong linear relationship between $\log(\text{Turb})$ and $\log(\text{SPM})$ (Fig. 4). Therefore, we could estimate water density based on T , Sal (estimated from $\text{EC}_{25} \text{ } ^\circ\text{C}$), and SPM (estimated from Turb) using the empirical equation of state.³⁰ Water density differences in the study are ranged between 997.1 and 999.7 mg cm^{-3} . According to these results, 97.7% of water density variations in the water body around Xiakou depended on T , whereas only 1.8% and 0.5% were related to Sal and SPM, respectively. This is in accordance with prior findings for the same area.³²

3.2. Physico-chemical parameter distributions under the four different but typical hydrological scenarios

All distributions of the analysed parameters i characterising the water body around Xiakou are displayed in Fig. 5 in their seasonal order. Around Xiakou, parameter distributions exhibited three general seasonal patterns: (1) T , $\text{EC}_{25} \text{ } ^\circ\text{C}$, Turb, and CDOM have a peak in June/September and lower values in March/November. ρ and d_{eu} have an opposed

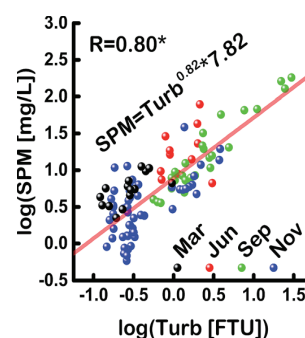


Fig. 4 Scatter plot of $\log(\text{SPM})$ versus $\log(\text{Turb})$ with least squares linear fit function. Pearson correlation coefficient (significant at a 0.05 level) and the fit function formula are plotted explicitly.

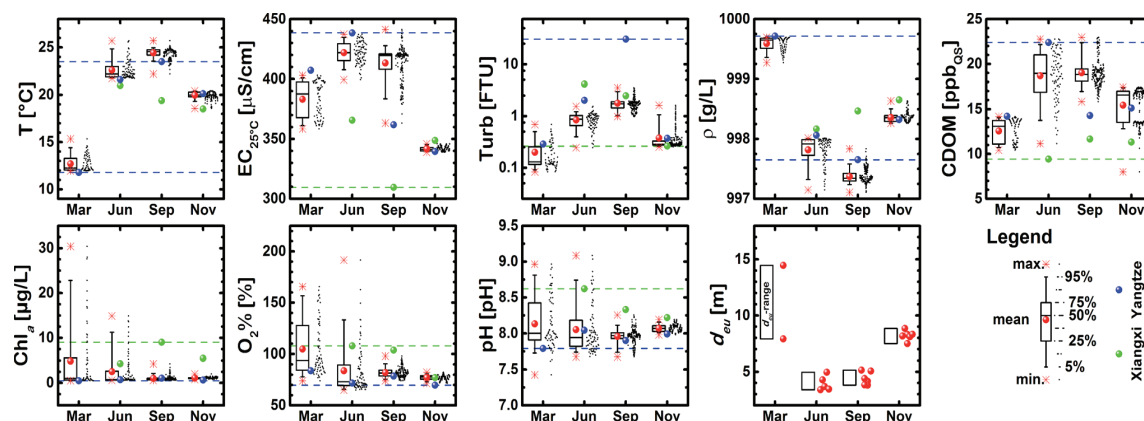


Fig. 5 Seasonal distribution plots of nine analysed characteristic parameters of the water body around Xiakou in the Xiangxi River backwater of the TGR. The corresponding source water conditions (not d_{400}) are given for the Xiangxi River and the Yangtze River main stream. Corresponding minimum and maximum source water conditions are marked with dashed lines. Note: there is a logarithmic scale for Turb and the d_{400} boxes represent the full value range.

pattern. Chl_a , $\text{O}_2\%$, and pH reached highest values in March/June and lower values in September/November. Median pH values ranged around 8.0 and it is noteworthy, that $\text{O}_2\%$ never dropped below 69% staying far away from anoxic conditions.

The Yangtze River main stream exhibited a strong seasonality for the parameters T , $\text{EC}_{25\text{ }^\circ\text{C}}$, Turb, ρ , and CDOM (Fig. 5). In general, the conditions around Xiakou in the Xiangxi River backwater followed these seasonal trends. Seasonality of the same parameters in the Xiangxi River source water was different but less pronounced and the patterns are not clearly mirrored within the Xiangxi River backwater conditions. The maximum range of source water conditions did border the conditions around Xiakou for $\text{EC}_{25\text{ }^\circ\text{C}}$ and CDOM. Only some scattered extreme values slightly exceeded these borders. T and ρ considerably exceeded the range of source water conditions in June and in September. The majority of Turb values around Xiakou were below the source water conditions. In March and June, Chl_a , $\text{O}_2\%$, and pH in the water body around Xiakou by far exceeded the source water conditions in positive direction.

3.3. Depth profile characteristics of physico-chemical parameters

Depth profiles of physico-chemical parameters in the water body around Xiakou considerably differ across the four hydrological periods covered by MINIBAT measurements (Fig. 6 and 7). First of all, thermal density stratification (T and ρ) was present under all four hydrological scenarios. The main stratification in March and June was attributed to the upper water body, whereas it appeared near the thalweg in September and November.

In March and June, the depth profiles of T , $\text{EC}_{25\text{ }^\circ\text{C}}$, Turb, ρ , and CDOM showed little daily variation across the corresponding fieldtrip periods. In September, however, all these four parameters revealed considerable shifts, particularly in the

middle of the water column. Within the November scenario, there were considerable shifts to lower T and CDOM that affected the whole water column.

The bottom water conditions around Xiakou in March were very similar to those of the Yangtze River main stream (T , $\text{EC}_{25\text{ }^\circ\text{C}}$, ρ , CDOM, Chl_a , $\text{O}_2\%$, and pH). In June, it was the middle water layer that represented the Yangtze River main stream conditions (T , $\text{EC}_{25\text{ }^\circ\text{C}}$, ρ , CDOM, Chl_a , and $\text{O}_2\%$), whilst we observed significant shifts of physico-chemical conditions (T , $\text{EC}_{25\text{ }^\circ\text{C}}$, Turb, $\text{O}_2\%$, and pH) in the middle water layer towards the Yangtze River main stream conditions in September. Interestingly, CDOM concentrations in the middle water layer increased at the same time and moved away from both Yangtze River main stream and Xiangxi River headwater water conditions.

In March, June and November, we found highest Turb values near the thalweg, only in September Turb reached its highest values in the middle water layer. In November, we observed increasing Turb and decreasing CDOM values near the thalweg below the thermocline. There was a shift of T and CDOM towards values similar to the Xiangxi River source water after 29 November, the fourth fieldtrip day. Furthermore, T and CDOM shifted towards lower values across the whole 50 m water column from 29–30 November, the fourth and fifth fieldtrip days.

The depth profiles of Chl_a , $\text{O}_2\%$, and pH were closely related to each other during both March and June scenarios (Fig. 7). Distinct peaks of all three parameters appeared near the water surface within the euphotic zones when there were also strong thermal density stratifications present.

It is remarkable that the strongest stratification was present in June when there were the lowest water levels and second highest discharge conditions (Table 1). Furthermore, the weakest stratification occurred in November, when water levels were highest and discharge conditions were lowest (Table 1).

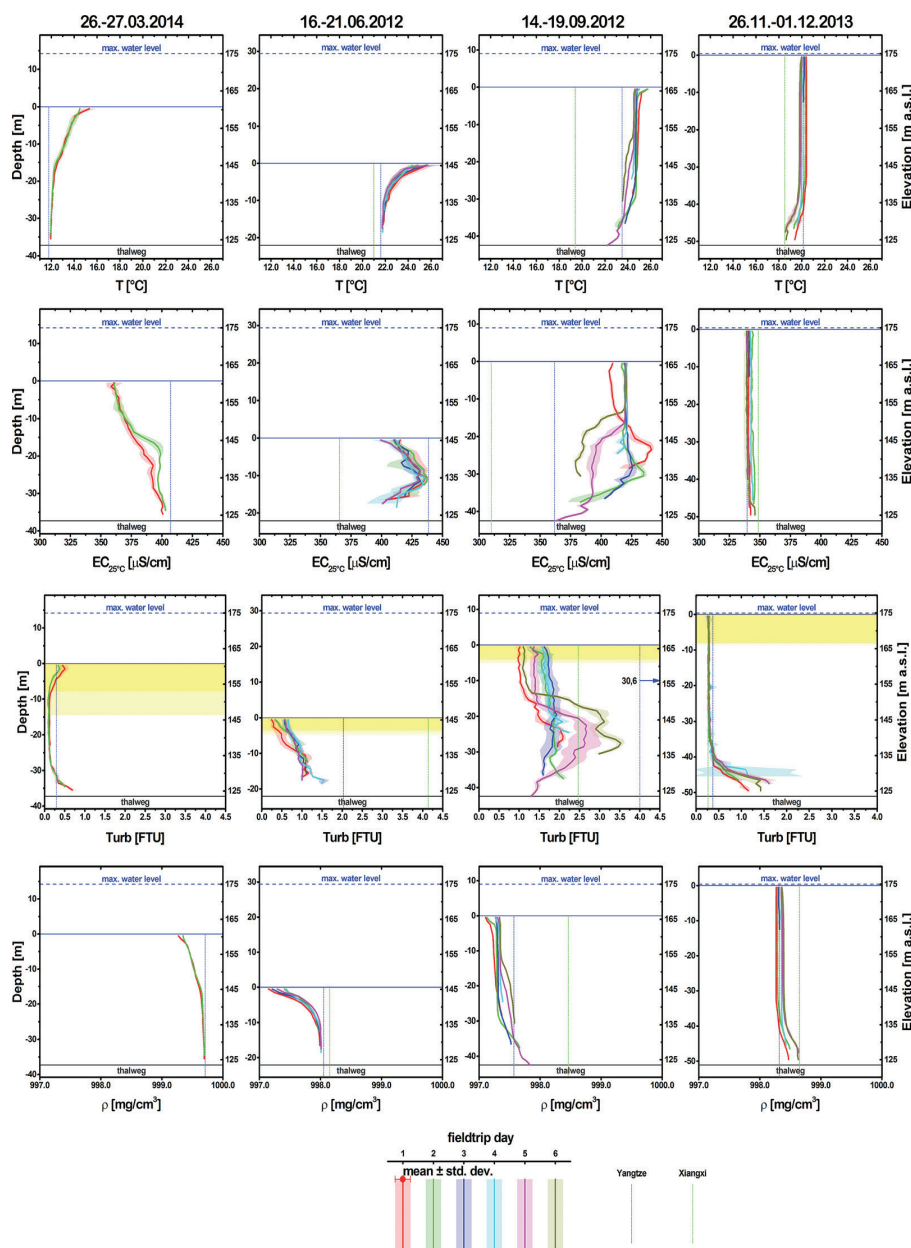


Fig. 6 Daily depth profiles of four out of eight analysed physico-chemical parameters $i \pm \sigma_i$ around Xiakou in the Xiangxi River backwater of the TGR during our four fieldtrip times. d_{eu} is marked yellow in the Turb graphs, because Turb affects light attenuation (Fig. 8). Source water conditions are marked by vertical dashed lines.

3.4. Dependencies of euphotic depth

Algal growth depends to a large extent on the light environment near the water surface. Turb, CDOM, and algae themselves in the surface water can cause significant light attenuation and thus reduce d_{eu} . Here, we found significant negative relationships of both Turb and CDOM in the euphotic zone with d_{eu} ($d_{eu} \sim -\text{CDOM}$; $d_{eu} \sim \text{Turb}^{-1}$) (Fig. 8). For Chl_a , this was not the case.

3.5. Density stratification and vertical physico-chemical gradients

As already stated in Section 3.1, T was the main driving factor of water density variations in the studied water body. Therefore, $\text{abs}(\delta_z T)$ exhibited very strong correlations with $\delta_z \rho$ during all analysed scenarios (Table 2). By far, the strongest vertical density gradients in the water body around Xiakou were present near the water surface in June (Fig. 9). In March and June, maximum gradients of $\delta_z \rho$ were attributed to the water

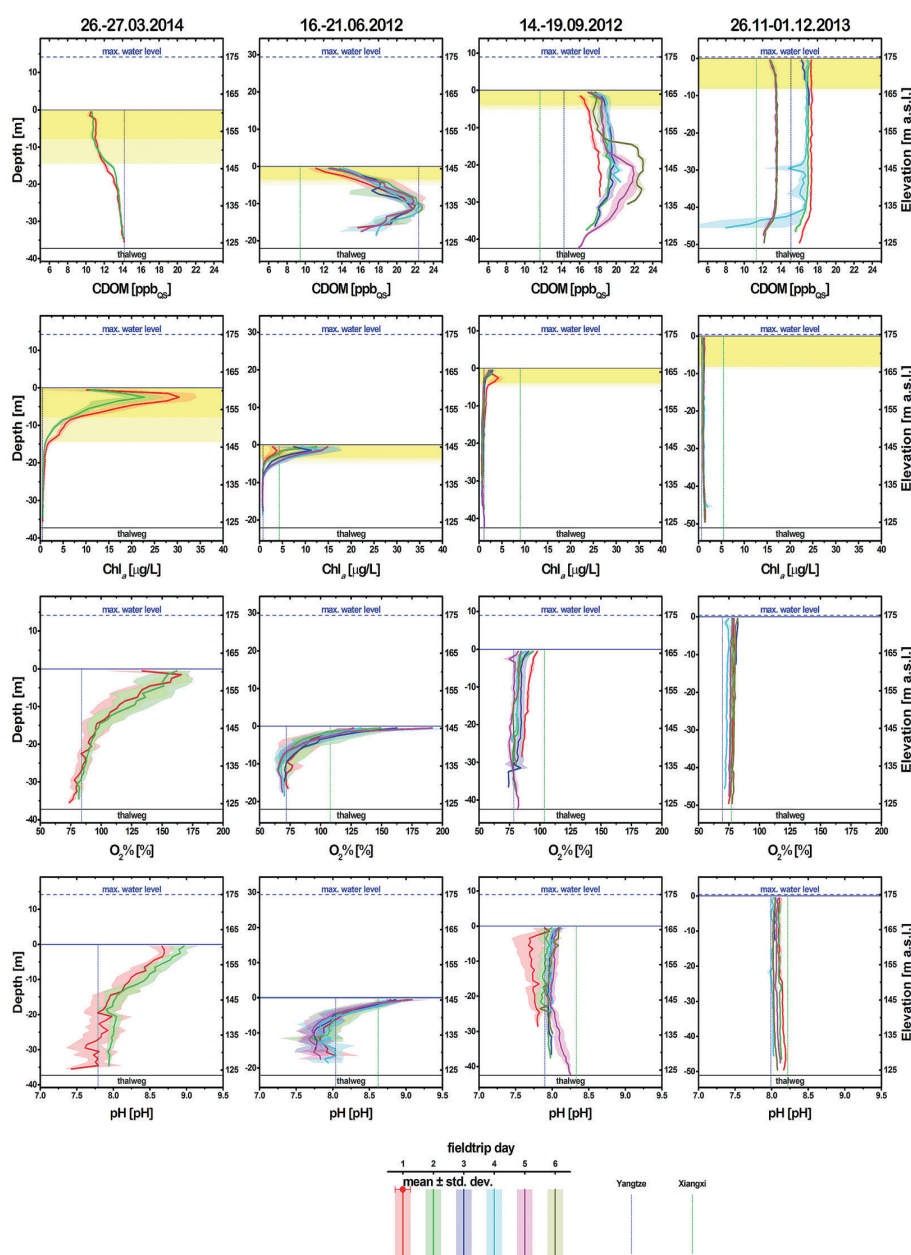


Fig. 7 Daily depth profiles of four out of eight analysed physico-chemical parameters $i \pm \sigma_i$ around Xiakou in the Xiangxi River backwater of the TGR during our four fieldtrip times. d_{eu} is marked yellow in the CDOM and Chl_a graphs, because CDOM affects light attenuation (Fig. 8) and algal growth depends on light conditions. Source water conditions are marked by vertical dashed lines (continued).

surface and correlated with $abs(\delta_z Chl_a)$, $abs(\delta_z O_2\%)$, and $abs(\delta_z pH)$ (Table 2). In September, there are three peaks of $\delta_z \rho$ along the depth profile at the water surface, in the middle water layer, and near the thalweg. These were mainly related to $abs(\delta_z EC_{25^\circ C})$, $abs(\delta_z Turb)$, and $abs(\delta_z CDOM)$ (Table 2). In November, we found highest $\delta_z \rho$ values near the bottom being correlated with $abs(\delta_z Turb)$ (Fig. 9 and Table 2).

3.6. Temporal variability of physico-chemical conditions in the water body around Xiakou

By far, the highest var_c values were present near the water surface in March and June (Fig. 9). In these seasons, var_{Turb} , var_{Chl_a} , and $var_{O_2\%}$ contributed most to var_c (Table 3). In September, the maximum var_c values appeared in the middle water layer and correlation was strongest with var_{Turb} , $var_{EC_{25^\circ C}}$, var_{Turb} , and var_{CDOM} . During the November scenario, var_c showed a relatively uniform distribution across the whole depth

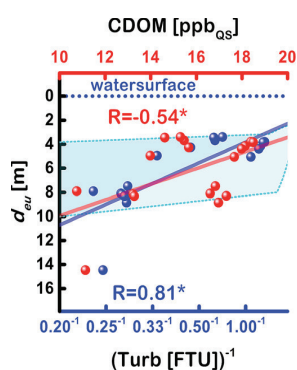


Fig. 8 Scatterplots of mean(CDOM) and mean(Turb)⁻¹ within the euphotic zone versus euphotic depth (d_{eu}). Lines represent least squares linear fit curves. Both Pearson and Spearman correlation coefficients (R) are significant at a 0.05 level. The blue shaded area represents the range of Turb $\sim d_{eu}$ relation from a study for the same area in 2009/2010.⁴

Table 2 Seasonally distributed Pearson and Spearman correlation coefficients of absolute physico-chemical vertical gradients $abs(\delta_z i)$ with vertical water density gradients $\delta_z \rho$ of the water body around Xiakou. Coefficients >0.5 and >0.7 are marked yellow and green, respectively

$abs(\delta_z i)$	Mar		Jun		Sep		Nov	
	Pears.	Spear.	Pears.	Spear.	Pears.	Spear.	Pears.	Spear.
$\delta_z T$	1.00	1.00	1.00	1.00	1.00	0.99	1.00	0.85
$\delta_z EC_{25^\circ C}$	0.22	0.48	0.01	-0.11	0.68	0.66	0.25	0.44
$\delta_z Turb$	0.01	-0.10	0.00	0.12	0.33	0.50	0.83	0.61
$\delta_z CDOM$	0.44	0.39	0.56	0.46	0.42	0.60	0.28	0.46
$\delta_z Chl_a$	0.76	0.88	0.71	0.84	0.26	0.35	0.31	0.34
$\delta_z O_2\%$	0.72	0.83	0.92	0.90	0.39	0.40	0.08	0.22
$\delta_z pH$	0.26	0.52	0.89	0.80	0.19	0.17	0.05	-0.12

Table 3 Seasonally distributed Pearson and Spearman correlation coefficients of temporal variability var_c with individual squared differences var_i of physico-chemical parameters i in the water body around Xiakou. Coefficients >0.5 and >0.7 are marked in yellow and green, respectively

var_i	Mar		Jun		Sep		Nov	
	Pears.	Spear.	Pears.	Spear.	Pears.	Spear.	Pears.	Spear.
var_T	0.42	0.21	0.95	0.32	0.84	0.55	0.49	0.33
$var_{EC_{25^\circ C}}$	-0.26	0.15	0.27	0.02	0.88	0.76	0.32	0.48
var_{Turb}	0.94	0.61	0.08	0.16	0.94	0.85	0.34	0.34
var_{CDOM}	0.01	0.08	0.05	0.15	0.84	0.79	0.87	0.72
var_{Chl_a}	0.88	0.37	0.78	0.71	0.22	0.07	0.29	0.34
$var_{O_2\%}$	0.52	0.48	0.97	0.59	0.25	0.36	0.07	0.21
var_{pH}	0.25	0.20	0.42	0.13	0.35	0.43	0.67	0.68

profile with only a slight peak near the thalweg. Correlation was the strongest with var_{CDOM} and var_{pH} .

4. Discussion

The synopsis of our broad resulting dataset reveals fundamental environmental characteristics of the water body around Xiakou, in particular to those that are related to the distinct and unique typical seasonal hydrology of the TGR.

4.1. Environmental conditions for algae in the Xiangxi River backwater

Basically, algae rely on a suitable range of T as well as sufficient supply with nutrients and light. Algal blooms have turned out to be the most obvious and primarily the most disturbing water quality issue in the TGR. By now, it is obvious that algal blooms in the TGR are mainly not limited by nutrient availability^{4,20,25}

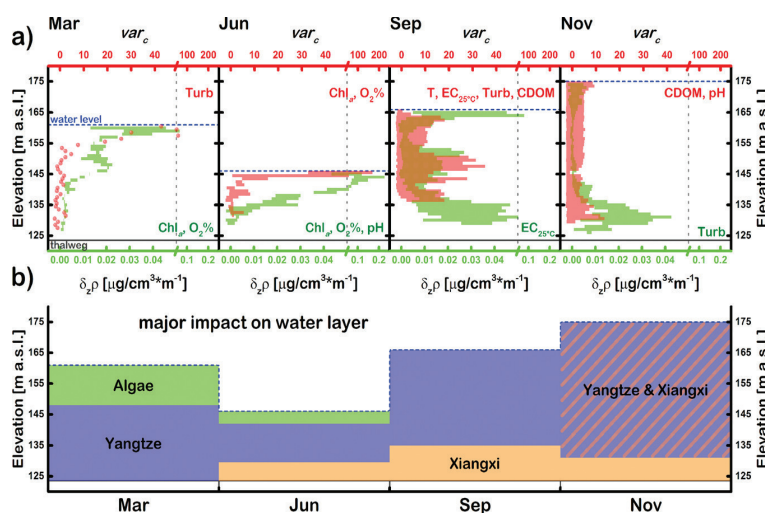


Fig. 9 (a) Seasonal ranges of temporal variability var_c and vertical water density gradients $\delta_z \rho$ along depth profiles in the water body around Xiakou. The corresponding correlating physico-chemical parameters are plotted explicitly when both Spearman and Pearson correlation coefficients were >0.5 (Tables 2 and 3). Note: both horizontal axes have a scale break indicated by vertical dashed lines. (b) Derived major impacts on physico-chemical conditions in distinguishable water layers across seasons.

but by temporally occurring optimal stratification^{4,16,21,33} and light environment conditions⁴ near the water surface.

We have found the highest Chl_a, O₂%, and pH values of our study within the surface water in March and June (Fig. 5 and 7). Furthermore, their vertical gradients also correlate with density stratification during both these scenarios (Table 2), while Chl_a, and O₂% were also amongst the parameters contributing most to temporal variability of physico-chemical conditions (Table 3). These parameters are all closely related to the algae content as well as photosynthetic activity and consequently indicate a strong impact of algae on the physico-chemical conditions and dynamics within the surface water layers in March and June (Fig. 9b). What are the specific reasons for that?

First of all, water being warmer and having much lower density than the source water (Fig. 5) was present at the water surface (Fig. 6) in March and June. This was forming a water package being stably isolated from the flow and mixing processes possibly taking place below. Further, we found negative correlation of d_{eu} with Turb (Fig. 8). This indicates that Turb affects light availability for algae. A similar range for this relationship was found in the same area around Xiakou for the years 2009/2010.⁴ Additionally, our results provide evidence that CDOM is also limiting the light availability in the studied water body (Fig. 8). Highest CDOM and Turb values occurred in June and September and were particularly enhanced within those water layers dominated by the Yangtze River main stream conditions (Fig. 7 and 9b). The high Turb values are related to excessive SPM loads of the Yangtze River main stream during the rainy season, whereas high CDOM contents are very likely to originate from urban sewage of the town Guojiaba near the confluence zone of the Xiangxi River with the Yangtze River. Corresponding evidence was provided in a former study analysing pollutant transport phenomena in the Xiangxi River backwater during the September scenario in detail.⁹

Based on our results, the conditions in March were most favourable for algal growth because the surface water was stably stratified and lowest Turb values and CDOM concentrations allowed for deep and sufficient light infiltration. This is in very good accordance with the fact that Chl_a concentrations also showed their maximum in March.

4.2. Contributions to dissolved and particulate water constituents

4.2.1. The main actor: Yangtze River main stream. From Fig. 5, it becomes apparent that under the observed normal hydrological scenarios, the Yangtze River was the main driving factor for the seasonality of a number of physico-chemical parameters (T , EC_{25 °C}, Turb, ρ , CDOM) in the water body around Xiakou. The distributions of these parameters generally follow the Yangtze River main stream conditions. In particular, dissolved (indicated by EC_{25 °C} and CDOM) and particulate (indicated by Turb) water constituents are mainly derived from the Yangtze River main stream. Furthermore, our results imply that September was the scenario most relevant for water mass exchange between the Yangtze River main stream and the Xiangxi River backwater. This becomes obvious from the

changing depth profile characteristics of EC_{25 °C}, Turb, and CDOM as well as from the large contributions of $\text{var}_{\text{EC}_{25\text{ °C}}}$, var_{Turb} , and var_{CDOM} to the total temporal variability of physico-chemical properties var_c in September (Table 3). Maximum var_c values in this season appeared in the middle water layer (Fig. 8). As we have seen in a former study,⁹ this layer was affected by a massive interflow density current intrusion from the Yangtze River main stream after a considerable water level rise in the TGR. Even 20 km upstream within the Xiangxi River backwater, we were subsequently able to observe corresponding radical changes of physico-chemical properties within only some days. Amongst large reservoirs worldwide, the TGR is unique in terms of its immense water level fluctuation (Section 1). Indeed, this unique property forms an enormous tidal pump between the Xiangxi River backwater and the Yangtze River main stream. Rising water levels in the TGR Yangtze River main stream induce a net upstream flow into tributary backwaters as long as inflows from the tributary headwaters are not extremely high. *E.g.*, around the September scenario, when TGR water level was rising by 6 m, the additional water volume of the Xiangxi River backwater was contributed almost equally by both headwater inflows and water from the Yangtze River main stream.⁹ This tidal pump is further amplified by the formation of density current circulation cells.^{4,9} Pollutant fluxes, explicitly including nutrients and heavy metals, from the Yangtze River main stream into the Xiangxi River backwater thus appear to be mainly attributed to the rising water level period in autumn. A recent study has shown that phosphorus and nitrogen input from the Yangtze River main stream into the Xiangxi River backwater amount to 80% respectively 60% of the backwater's nutrient balance.¹⁸ In this study, total phosphorus concentrations from April till August ranged between 0.17 $\mu\text{g L}^{-1}$ and 0.3 $\mu\text{g L}^{-1}$ whereas from September till December these were below 0.13 $\mu\text{g L}^{-1}$. Furthermore, high loads of particle bound heavy metals have been transported into the Xiangxi River backwater during the September scenario.⁹ Generally, large amounts of nutrients and heavy metals in the TGR occur being bound to particles.^{9,14,18} Hence, turbidity signals from the Yangtze River main stream within the Xiangxi River backwater are an obvious indication of the corresponding particle related pollutant transport.

4.2.2. The Xiangxi River headwater: taking its chance in winter. The comparison of physico-chemical conditions in the Xiangxi River headwater with depth profiles in the water body around Xiakou reveals obvious impacts of the Xiangxi River headwater conditions to the bottom water layer in June (EC_{25 °C}, CDOM) September (T , ρ , pH), and November (T , ρ , CDOM) (Fig. 6, 7 and 9). In June and September, these obvious impacts remain strongly limited to the bottom water and do not seem to significantly interfere with overlaying water. In November, however, water masses with low concentrations of CDOM appeared near the thalweg on 29 November and were rapidly mixed with the above water column causing marked reduction of the CDOM concentration there as well (Fig. 7). This fact is also expressed in the large contribution of var_{CDOM} to var_c in November (Table 3). The rapid distribution of changing CDOM across the whole water column that originated from the bottom

layer can be regarded as a tracer for any dissolved substances. During the high water level period, changes of water characteristics in the bottom water layer can rapidly alter the physico-chemical properties of the whole water column around Xiakou as there is nearly no thermal density stratification present in the upper water layers. Even though the contribution of the Xiangxi River headwater to the total nutrient balances of the backwater is comparably low, concentrations in the tributary headwater can be temporally very high.^{18,20,21} As such, introduced pollutants from the upstream water bodies can seriously contribute to nutrient concentrations in the Xiangxi River backwater during the high water level period in winter.

4.3. The backwater of the Xiangxi River as temporal buffer of physico-chemical properties

The range of $EC_{25} \text{ } ^\circ\text{C}$ values in the water body around Xiakou is bordered by the source water conditions (Fig. 5). This is evidence for conservative water mass mixing processes between the Yangtze River main stream and the Xiangxi River headwater. Furthermore, from $EC_{25} \text{ } ^\circ\text{C}$ as shown in Fig. 5, a strong temporal water quality buffer capacity of the Xiangxi River backwater can be derived. The seasonal sequence of $EC_{25} \text{ } ^\circ\text{C}$ in the Yangtze River main stream appears to spearhead $EC_{25} \text{ } ^\circ\text{C}$ parameters in the Xiangxi River backwater (Fig. 5). In September, the majority of $EC_{25} \text{ } ^\circ\text{C}$ values fit well into the range of the preceding June event. Both source waters in September, however, revealed much lower $EC_{25} \text{ } ^\circ\text{C}$. Obviously, the water around Xiakou still contained the dissolved solids from the preceding summer season. Water residence time in the tributary backwaters of the TGR can be greater than 365 days³⁴ and by far exceed the maximum of 81 days that we calculated for the whole TGR. Thus, water that once enters a TGR tributary backwater can stay there for a long time retaining some stable physico-chemical characteristics whilst the conditions in its source water might change considerably. This finding is of particular interest regarding pollutants (*e.g.* nutrients) that enter the Xiangxi River backwater during the rising and high water level periods. Nutrients as an example can derive from both the Yangtze River main stream (Section 4.2) and the Xiangxi River headwater (Section 4.2.2) and will be retained within the backwater. As such, eutrophication problems in the spring and summer periods are seriously driven by nutrient transport dynamics in the preceding autumn and winter seasons. Due to the fact that algal blooms in the TGR are mainly not limited by nutrients,^{4,20,25} we propose that the effective nutrient transportation processes from the Yangtze River main stream into its tributary backwaters are the most prominent reason for algal blooms in the TGR. According to our results, this transport is mainly taking place within the autumn season which has attracted little attention by environmental scientists, so far. Furthermore, regarding the seasonality of Turb distributions (Fig. 5) provides evidence for sedimentation processes taking place within the Xiangxi River backwater. The majority of Turb values fall below the simultaneously prevailing Turb conditions of both source waters with minimum values being reached in March. Hence, SPM concentrations in the water column must be decreasing

due to sedimentation. As a consequence, contaminated particles entering into the backwater during the rising water level phase, as it was the case during the September scenario,⁹ are very likely to settle down and accumulate within the sediments and semi-terrestrial soils of the water level fluctuation zone. This possible creeping environmental threat to sediment and semi-terrestrial soil quality is, however, only insufficiently studied, yet.

4.4. The observed effects put into a general context

Indeed, the observed effects of water mass interactions and their environmental impacts for the TGR and its major tributary backwater of the Xiangxi River are not totally new in themselves. The distribution of pollutants from inflowing waters into stratified water bodies is closely linked to the formation of corresponding density currents and vertical mixing processes.³⁵ In particular, the availability of nutrients to algae near the water surface requires appropriate water body conditions. Furthermore, pollutants within the particulate phase are also likely to be withdrawn from the water column by sedimentation.³⁵

The investigated area of this study revealed a complex interacting system of two separate inflows. Pathways of multiple gravitational inflows into a stratified reservoir in Australia have already been studied.³⁶ Each inflow influenced the physico-chemical structure of the stratified water body according to its density and volume flux in downstream direction. In this respect, we are dealing with an exceptional case here. The flow directions are not solely linear from upstream to downstream. On the one hand, inflows from the Xiangxi River headwater form an ordinary underflow constantly moving downstream (Fig. 6, 7 and 9). On the other hand, water from the Yangtze River main stream is forming intrusions moving upstream as an underflow (June) or interflow (September) into the dendritic tributary backwater. Further, the intensity of this intrusion is driven by both gravitational forces and the tidal pump caused by TGR water level fluctuations (Section 4.2.1). It is obvious from the physico-chemical characteristics (Fig. 6 and 7) that the intruding waters of both inflows also reach the surface of the tributary backwater in autumn and winter (Fig. 6, 7 and 9). As tracer experiments in a Spanish stratified reservoir have shown, this can happen very rapidly by partial mixing at the interface between the density current and the overlying water.³⁷ Particularly, when a density current intrusion enters right below the surface mixed layer, corresponding tracers could quickly reach the water surface as well.³⁷ This was the case here in both September and November scenarios. As such, dissolved nutrients originating from either the Xiangxi River headwater or the Yangtze River main stream are very likely to reach the surface water layer and aggravate eutrophication problems, there.

Under normal hydrological conditions, the Yangtze River's major role in providing dissolved and particulate water constituents to the Xiangxi River backwater becomes obvious from our data. The same fact is also known for nutrients.¹⁸ Furthermore, the TGR exhibits an exceptional flow and mixing pattern with its tributary backwaters which happens to be strongly linked to the enormous annual TGR water level

fluctuation. Consequently, major parts of the current pollution within its tributary backwaters can be attributed to the TGR water level fluctuation, being its outstanding and unique feature in a global context.

5. Conclusions and recommendations for water quality control

Under the observed normal hydrological conditions in the TGR, we found seasonally very different environmental water body characteristics around Xiakou in the Xiangxi River backwater. The falling and low water level phases were characterized by pronounced thermal density stratification near the water surface and went along with high algal abundance that dominated major physico-chemical conditions and dynamics. The rising water level season in September was characterized by radical changes of physico-chemical properties within only some days driven by inflowing water from the Yangtze River main stream. During the high water level period in November, underflowing water from the Xiangxi River headwater was able to rapidly alter the physico-chemical conditions of the whole upper water column as there was nearly no thermal density stratification present.

The Yangtze River main stream appeared to be the main driver of dissolved and particulate water constituents within the Xiangxi River backwater. As such, it is also the main contributor of pollutants to this water body. This is particularly serious as we also identified an enormous physico-chemical buffer capacity of this tributary backwater. Hence, nutrients entering from the Yangtze River main stream into the Xiangxi River backwater during the rising water level period can still be available to algae in the following spring and summer seasons.

As highlighted in 'Introduction', the TGR is globally unique due to its enormous annual water level fluctuation scheme. The results of this study have provided evidence that this water level fluctuation itself has become a central part of the recent eutrophication and pollution problems in the TGR, particularly within its tributary backwaters. Surely this phenomenon is not limited to the Xiangxi River backwater because it is symptomatic for the TGR that the Yangtze River main stream is characterized by higher pollution levels than its tributaries.^{19,38} It is also obvious that similar processes of varying magnitudes do and/or will occur in reservoirs worldwide. Therefore, this study provides adequate monitoring strategies and a database to be built on. Again, it is noteworthy that our study did only cover 'normal' hydrological scenarios related to the typical and systematic water level changes induced by the TGD management. Exceptional extreme events may rapidly alter this described interacting system between the Yangtze River main stream and its tributary backwaters very seriously.

Are there now any ways to mitigate the current 'normal' situation?

Controlled water level fluctuations in the TGR are seriously considered as an effective way to mitigate algal blooms in TGR tributary backwaters.^{4,25} Therefore, strong turbulences near the

water surface should be induced by artificial water level fluctuations in the TGR (TGD management) and cause the collapse of stable thermal density stratification at the water surface. From the perspective of our study, such an approach seems plausible to mitigate threats by algal blooms alone. But, it is not capable to reduce the pollutant inputs from the Yangtze River main stream into its tributary backwaters. To account for this as well, the rising water level phase of the TGR would require a feedback with pollutant concentrations in the Yangtze River main stream. Within the frame of guaranteed flood protection, we therefore propose that the TGR should only be filled up when pollutant/SPM concentrations in the Yangtze River main stream have dropped below some thresholds after the summer rainy season. How to specify this suggestion? Major nutrient⁴⁴ and heavy metal⁹ fractions are to be found within the SPM. Contents of SPM in the Yangtze River main stream generally drop very rapidly after the flood season in summer. For instance, in their study, Yang *et al.* (2015)¹⁸ identified highest total phosphorus concentrations around $0.3 \mu\text{g L}^{-1}$ in the Yangtze River main stream in late August 2013 when water levels in the TGR have already started to rise (Fig. 2). Just one month later, they measured lowest total phosphorus concentrations of $0.1 \mu\text{g L}^{-1}$. In this case, a slight delay of the rising water level period would have drastically reduced phosphorus input into the Xiangxi River backwater by intruding water masses from the Yangtze River main stream.

Furthermore, a gentler rise of the water level in autumn could also reduce particle transport distances upstream into tributary backwaters due to their earlier sedimentation. As discussed above, transport processes from the Yangtze River main stream appear to be mainly linked to water level fluctuations and to the formation of corresponding density current cells. Our proposal is thus only capable to reduce the pollutant transport directly linked to water level fluctuations. Other processes will remain active and a general reduction of the current pollution state still needs to be the primary long-term goal. We are aware that the TGR water level fluctuation scheme was optimised for two of its primary goals, flood protection and power generation. Our proposed approach would obviously require increasing monitoring efforts, flexibility of the TGD management, and would lead to some deficiencies in power generation. Still, it might help to mitigate the spatial range of pollution and eutrophication within the precious and most vulnerable TGR tributary backwaters. It is similarly applicable to dendritic reservoirs worldwide, where comparable effects of varying magnitudes can occur.

Acknowledgements

This research was funded by the Federal Ministry of Education and Research of Germany (BMBF grant no. 02WT1131), the National Natural Science Foundation of China (31123001), the China Three Gorges Corporation (0711442), and the International Science and Technology Cooperation Program of China (MOST grant no. 2007DFA90510).

Notes and references

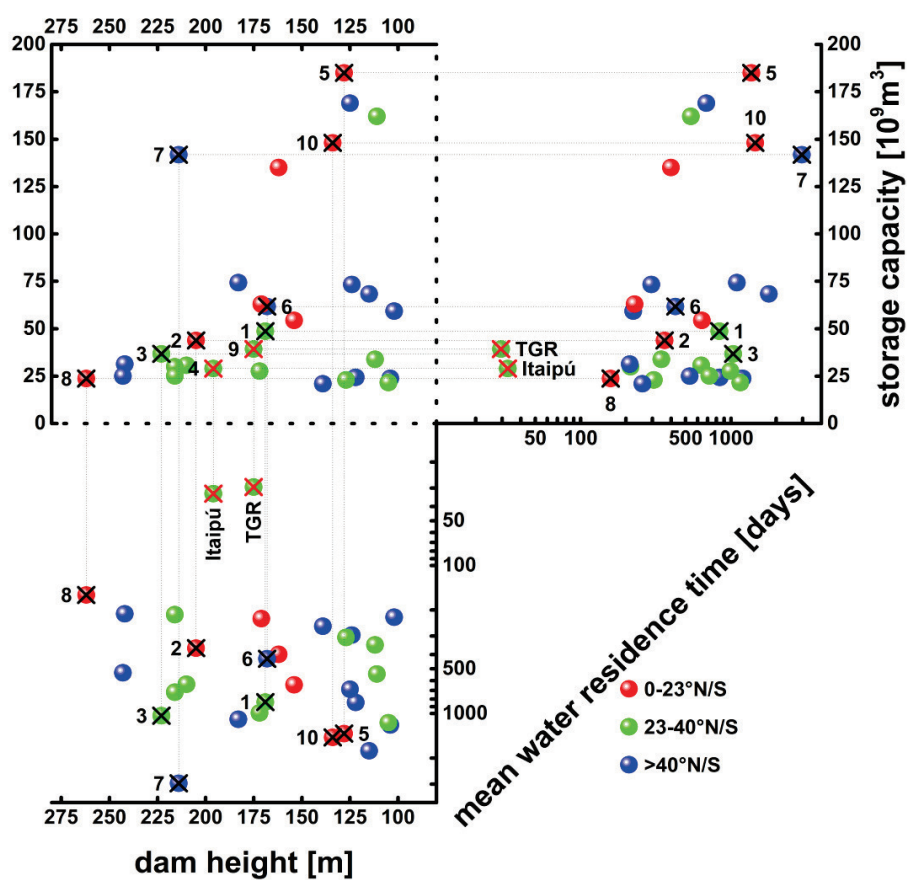
- 1 C. Nilsson, C. A. Reidy, M. Dynesius and C. Revenga, *Science*, 2005, **308**, 405–408.
- 2 M. Ponseti and J. López-Pujol, *HMiC: Història Moderna i Contemporània*, 2006, 151–188.
- 3 Ministry of Environmental Protection of the People's Republic of China, *Three Gorges Bulletin in 2011, 2012*, <http://english.mep.gov.cn>.
- 4 L. Liu, D. Liu, D. Johnson, Z. Yi and Y. Huang, *Water Res.*, 2012, **46**(7), 2121–2130.
- 5 International Commission on Large Dams, *World Register of Dams*, 2014, <http://www.icold-cigb.org>, accessed September 22, 2014.
- 6 International Energy Agency, *China, People's Republic of: Indicators for 2012, Statistics*, 2014, <http://www.iea.org>, accessed September 22, 2014.
- 7 B. Fu, B. Wu, Y. Lü, Z. Xu, J. Cao, D. Niu, G. Yang and Y. Zhou, *Progr. Phys. Geogr.*, 2010, **34**(6), 741–754.
- 8 X. Yang and X. Lu, *Environ. Res. Lett.*, 2013, **8**, 1–5.
- 9 A. Holbach, S. Norra, L. Wang, Y. Yuan, W. Hu, B. Zheng and Y. Bi, *Environ. Sci. Technol.*, 2014, **48**(14), 7798–7806.
- 10 J. Lin, C. Fu, X. Zhang, K. Xie and Z. Yu, *Biol. Trace Elem. Res.*, 2012, **145**, 268–272.
- 11 C. Ye, S. Li, Y. Zhang and Q. Zhang, *J. Hazard. Mater.*, 2011, **191**(1–3), 366–372.
- 12 Z.-Y. Wang, Y. Li and Y. He, *Water Resour. Res.*, 2007, **43**, W04401.
- 13 Z. Yang, H. Wang, Y. Saito, J. D. Milliman, K. Xu, S. Qiao and G. Shi, *Water Resour. Res.*, 2006, **42**, W04407.
- 14 A. Holbach, L. Wang, H. Chen, N. Schleicher, W. Hu, B. Zheng and S. Norra, *Environ. Sci. Pollut. Res.*, 2013, **20**(10), 7027–7037.
- 15 Y. Xu, M. Zhang, L. Wang, L. Kong and Q. Cai, *Quaternary Int.*, 2011, **244**, 272–279.
- 16 Z. Yu and L. Wang, *J. Hydrodyn. Ser. B (English Ed.)*, 2011, **23**(4), 407–415.
- 17 L. Dai, H. Dai and D. Jiang, *J. Food, Agric. Environ.*, 2012, **10**(2), 1174–1178.
- 18 L. Yang, D. Liu, Y. Huang, Z. Yang, D. Ji and L. Song, *Ecol. Eng.*, 2015, **77**, 65–73.
- 19 Y. Huang, P. Zhang, D. Liu, Z. Yang and D. Ji, *Environ. Monit. Assess.*, 2014, **186**(10), 6833–6847.
- 20 H. Dai, J. Mao, D. Jiang and L. Wang, *PLoS One*, 2013, **8**(7), e68186.
- 21 J. Li, Z. Jin and W. Yang, *Ecol. Informat.*, 2014, **22**, 23–35.
- 22 D. Stüben, K. Stüben and P. Haushahn, *Underwat. Syst. Des.*, 1994, **16**, 5–14.
- 23 S. Becker, M. Gemmer and T. Jiang, *Stoch. Environ. Res. Risk Assess.*, 2006, **20**, 435–444.
- 24 China Three Gorges Corporation, 2014, <http://cwic.com.cn/inc/sqsk.php>, accessed October 10, 2014.
- 25 Z. Yang, D. Liu, D. Ji, S. Xiao, Y. Huang and J. Ma, *Sci. China: Technol. Sci.*, 2013, **56**(6), 1458–1470.
- 26 United States Department of the Interior, *National Irrigation Water Quality Program Information Report No. 3*, 1998.
- 27 S. P. Gloss, L. M. Mayer and D. E. Kidd, *Limnol. Oceanogr.*, 1980, **25**, 219–228.
- 28 N. Hudson, A. Baker and D. Reynolds, *River Res. Appl.*, 2007, **23**, 631–649.
- 29 W. Lampert and U. Sommer, *Limnoolökölogie*, 1999.
- 30 Z.-G. Ji, *Hydrodynamics and Water Quality: Modeling Rivers, Lakes, and Estuaries*, 2007.
- 31 J. Bortz, *Statistik für Sozialwissenschaftler*, Springer, Berlin, 5th edn, 1999.
- 32 Z. Yang, D. Liu, D. Ji and S. Xiao, *Sci. China: Technol. Sci.*, 2010, **53**(4), 1114–1125.
- 33 K. Zhu, Y. Bi and Z. Hu, *Sci. Total Environ.*, 2013, **450–451**, 169–177.
- 34 Y. Xu, Q. Cai, M. Shao, X. Han and M. Cao, *Quaternary Int.*, 2009, **208**, 138–144.
- 35 G. Friedl and A. Wüest, *Aquat. Sci.*, 2002, **64**, 55–65.
- 36 C. L. Marti, R. Mills and J. Imberger, *Adv. Water Resour.*, 2011, **34**, 551–561.
- 37 A. Cortés, W. E. Fleenor, M. G. Wells, I. de Vicente and F. J. Rueda, *Limnol. Oceanogr.*, 2014, **59**(1), 233–250.
- 38 Z. Luo, B. Zhu, B. Zheng and Y. Zhang, *China Environ. Sci.*, 2007, **27**, 208–212.



Environmental Science: Processes & Impacts

ARTICLE

Electronic Supplementary Information



ESI Fig. 1 Properties of dams and reservoirs worldwide with dam heights > 100 m and storage capacities > $20 \cdot 10^9 \text{ m}^3$. The TGR and the Itaipú Reservoir have comparable magnitudes, are located in the sub-tropics, and have exceptionally low mean water residence times.^{1,42,43,44,45,46} Crossed and numbered points refer to ESI Table 1.



Environmental Science: Processes & Impacts

ARTICLE

ESI Table 1 Properties of selected dams and reservoirs worldwide with dam heights > 100 m and storage capacities > $20 \times 10^9 \text{ m}^3$. The TGR and the Itaipu Reservoir have comparable magnitudes, are located in the sub-tropics, have exceptionally low mean water residence times (MWRT), and are polymictic. The TGR, however, is eutrophic and has by far the largest water level fluctuation. Numbers (No.) refer to ESI Fig. 1.

No. Dam name	Country	Year	Dam and Reservoir dimensions			Reservoir Classification					References	
			Dam height [m]	Res. vol. [10^9 m^3]	Res. area [km ²]	Ø depth [m]	MWRT [days]	Geographic	Trophic	Mixing		WLF [m]
1 Atatürk	Turkey	1992	169	49	817	60	838 long	37°N sub-tropical	eutrophic	n.a.	n.a.	41,43,50
2 Bakun	Malaysia	2011	205	44	695	63	362 intermediate	3°N tropical	n.a.	n.a.	n.a.	41,44,46
3 Hoover	USA	1935	223	37	635	58	1035 long	36°N sub-tropical	mesotrophic	monomictic	7	41,43,47
4 Itaipu	Brazil/Paraguay	1983	196	29	1350	21	33 intermediate	25°S sub-tropical	oligotrophic	polymictic	1	41,43,44,45,48
5 Kariba	Zimbabwe/Zambia	1959	128	185	5540	33	1367 long	17°N tropical	mesotrophic	monomictic	3	41,43,44
6 La Grande 2	Canada	1977	168	62	2835	22	428 long	54°N moderate	oligotrophic	dimictic	9	41,43,44
7 Manicouagan	Canada	1968	214	142	1940	73	2961 long	51°N moderate	oligotrophic	monomictic	6	41,43,44
8 Nuozhadu	China	2014	262	24	320	74	159 intermediate	23°N tropical	n.a.	n.a.	39,41	
9 Three Gorges	China	2003	175	39	1084	36	30 intermediate	31°N sub-tropical	eutrophic	polymictic	30	41,43,49
10 Volta	Ghana	1965	134	148	8500	17	1452 long	6°N tropical	eutrophic	polymictic	3	41,43,44



Environmental Science: Processes & Impacts

ARTICLE

ESI Table 2 Sensors installed on the MINIBAT and their specifications.

Parameter	Producer	Principle	Measuring range	Accuracy	Resolution	Response time
Pressure	ADM Elektronik	piezo-resistive	0 - 200 dbar	±0.1 dBar	0.005 dbar	0.04 s
O ₂	ADM Elektronik	Potentiometric (Clark electrode)	0 - 150% sat	±2% sat	0.02% sat.	3 s (63%)
Temperature	ADM Elektronik	Pt 100	-2 - 38°C	±0.01°C	0.001°C	0.12 s
EL. conductivity	ADM Elektronik	7-pole-cell	0 - 6 mS/cm	±2 µS/cm	0.1 µS/cm	0.05 s
pH	AMT GmbH	Potentiometric (Ag/AgCl)	0 - 14 pH	0.02 pH	0.02 pH	1 s (63%)
H ₂ S*	AMT GmbH	Amperometric	0 - 10 mg/L	±3%	0.03 mg/L	<3 s
Chlorophyll <i>a</i> **	Turner designs	Fluorescence (exc. 465 nm / fl. 696 nm)	0.03 - 500 µg/L		0.01 µg/L	1 s
CDOM***	Turner designs	Fluorescence (exc. 325 nm / fl. 470 nm)	0.15 - 1250 ppbqs	±5%	0.01 ppbqs	1 s
Turbidity	Seapoint sensors, Inc.	Mie backscattering	0 - 750 FTU	±2%	<0.001%	0.1 s
PAR (400-700 nm)	LI-COR®	Photon flux density	0 - 10 mmol/(s*m ²)	±5%	0.01 µmol/(s*m ²)	10 µs

*The H₂S sensor did not operate stable and was not used during data evaluation. **Calibrated against algal monoculture of *Skeletonema costatum*. ***Calibrated against Quinine Sulfate in 0.05 M H₂SO₄.



Environmental Science: Processes & Impacts

ARTICLE

ESI - Notes and references

- 41 L. Berggren and L. Wallmann, MSc. Thesis, Lund University, 2012.
- 42 Chinese National Committee on Large Dams, *Dam information—Dam Projects—Nuozhadu Hydropower Project*, <http://www.chincold.org.cn>, (accessed 07 November, 2014).
- 43 P. Gong and J. Wan, *Hydropower*, 2006, 1465-1471.
- 44 International Commission on Large Dams, *World Register of Dams*, <http://www.icold-cigb.org>, (accessed 05 March, 2014).
- 45 World Bank, *Malaysia Power Sector Issues and Options*, Report No.6466-MA, 1987.
- 46 B. Lehner, C. Reidy Liermann, C. Revenga, C. Vörösmarty, B. Balazs Fekete, P. Crouzet, P. Döll, M. Endejan, K. Frenken, J. Magome, C. Nilsson, J. Robertson, R. Rödel, N. Sindorf and D. Wisser, *Global Reservoir and Dam database*. Version 1.1, 2011.
- 47 International Lake Environment Committee Foundation, *World Lake Database*, url: <http://wldb.ilec.or.jp/>, (accessed 13 November, 2014).
- 48 R. Ribeiro Filho, M. Petrere Junior, S. Benassi and J. Pereira, *Braz. J. Biol.*, 2011, **71(4)**, 889-902.
- 49 B. Sovacool and L. Bulan, *Energy Policy*, 2011, **39**, 4842-4859.
- 50 Summit Technologies, Inc., *Lake Mead Water Database*, <http://lakemead.water-data.com/>, (accessed 13 November, 2014).
- 51 M. Thomaz, A. Pagioro, M. Bini and J. Murphy, *Hydrobiologia*, 2006, **570**, 53-59.
- 52 Y. Xu, Q. Cai, X. Han, M. Shao and R. Liu, *Environ. Monit. Assess.*, 2010, **169(1-4)**, 237-248.
- 53 M. Yazgan, B. Armağan and M. Yeşilnacar, International Symposium on water resources and environmental impact assessment, Istanbul, 2001.

A.4 Urban Pollutant Plumes around Wushan and Dachang City in the Three Gorges Reservoir

Andreas Holbach^{1}; Lijing Wang²; Hao Chen²; Nina Schleicher¹; Wei Hu¹; Binghui Zheng²; Stefan Norra^{1,3}*

¹Institute of Mineralogy and Geochemistry, Karlsruhe Institute of Technology, Adenauerring 20b, 76131 Karlsruhe, Germany; *Email: andreas.holbach@kit.edu

²Chinese Research Academy of Environmental Sciences, No.8, Dayangfang, Anwai Beiyuan, Chaoyang District, Beijing, China, 100012

³Institute of Geography and Geoecology, Karlsruhe Institute of Technology, Reinhard-Baumeister-Platz 1, 76128 Karlsruhe, Germany

Abstract

The Three Gorges Reservoir (TGR) in the Yangtze River was among other reasons meant to improve and strengthen socio-economic development of the involved regions. Considerable economic growth and urbanization now pose additional threat to the water quality of the TGR due to urban pollutant inflows. The changed hydrological conditions in the TGR have considerably altered pollutant transport dynamics now causing higher susceptibility of the backwater areas to eutrophication and algal blooms. The Yangtze River is also widely used as a source for drinking water production. The assessment of the urban impact on the water quality in the TGR is, thus, crucial for sustainable future development planning. Measurements with an underwater multi-sensor system (MINIBAT) were performed in the frame of the “Yangtze-Project” (Bergmann et al., 2012) around the cities of Wushan and Dachang on the Daning River in the backwater reaches of the TGR in December 2012. Hydrological conditions were stable at constant water level between 174–175 m a.s.l and low discharge conditions in the TGR during sampling period. 3D distribution patterns of the parameters temperature, conductivity, and turbidity in the water bodies were modeled using geostatistics. Selected water samples from different depths were analyzed for dissolved and particulate constituents using ICP-MS. Results show plumes of higher temperature, conductivity and turbidity in the epilimnion around the investigated urban areas. The range of influence was larger for temperature and conductivity plumes. Significant increase of turbidity was detected around Dachang City during few hours. Urban impacts on the water quality were significant at the encountered conditions and need to be further investigated for risk assessment, especially concerning drinking water production and eutrophication problems.

Introduction

The water quality in the Yangtze River Three Gorges Reservoir (TGR) upstream of the Three Gorges Dam (TGD) is of major concern since the first closure of the dam in 2003. The TGR serves as an

Table 1: Pollutant sources in TGR (MOEP, 2012).

	COD (t)	N (t)	P (t)
Industry	59300	4300	N/A
Urban areas	92600	13300	N/A
Ships	718	340	51
Agriculture	N/A	8700	1800

important drinking water source for the local population. Thus, the increasing nutrient pollution causing eutrophication and algal blooms (Dai et al., 2010; MEP, 2005-2011) as well as pollution with heavy metals and organic compounds need to be carefully monitored. Changed hydrodynamics after the

TGR impoundment may cause serious accumulation of pollutants in critical water bodies making them temporarily inappropriate for safe drinking water production. The very complex interactions in the TGR water bodies include seasonal discharge and water level fluctuations, tributary/main stream mixing dynamics (Ran et al., 2010), density currents (Ji et al., 2010; Luo et al., 2007), thermal stratification development, as well as point and non-point source pollution. The resulting unique dynamics of water quality in TGR and the key driving forces for water quality distribution under different hydrological and ecological conditions are not yet understood. Besides others, discharges from urban areas are the main source for COD and N pollution in the TGR (Table 1). Their consideration for environmental studies in the TGR is, thus, crucial for a holistic understanding of proceeding pollution dynamics. Release of pollutants, e.g. heavy metals, from sediments and inundated former soils and urban areas is likely to occur, especially under the changing oxic conditions caused by water level fluctuations (Ho et al., 2012; Komárek and Zeman, 2004).

The Sino-German environmental research program “Yangtze-Hydro Project” has been established and funded since 2010 (Bergmann et al., 2012) to conduct international and interdisciplinary research on the sustainable utilization and development of the newly created ecosystem in the TGR. Therein, the MINIBAT sub-project aims to monitor water quality distribution dynamics in 3D-space and time in critical areas throughout the TGR region. The data presented in this paper is based on fieldwork conducted from 3rd to 6th December 2011 around the urban areas of Wushan City and Dachang City. Both cities are located in the TGR backwater affected water bodies of the Daning River and its confluence zone with the Yangtze River. The performed in situ MINIBAT measurements and water sample analysis revealed significant pollutant plumes around these urban areas under the very serene hydrological conditions during the measurement period.

Material and methods

Study area and hydrological boundary conditions

The Three Gorges Reservoir (TGR) formed after the impoundment of the Yangtze River by the Three Gorges Dam (TGD) (Ponseti and López-Pujol, 2006). After completion of the TGD in 2009 the TGR

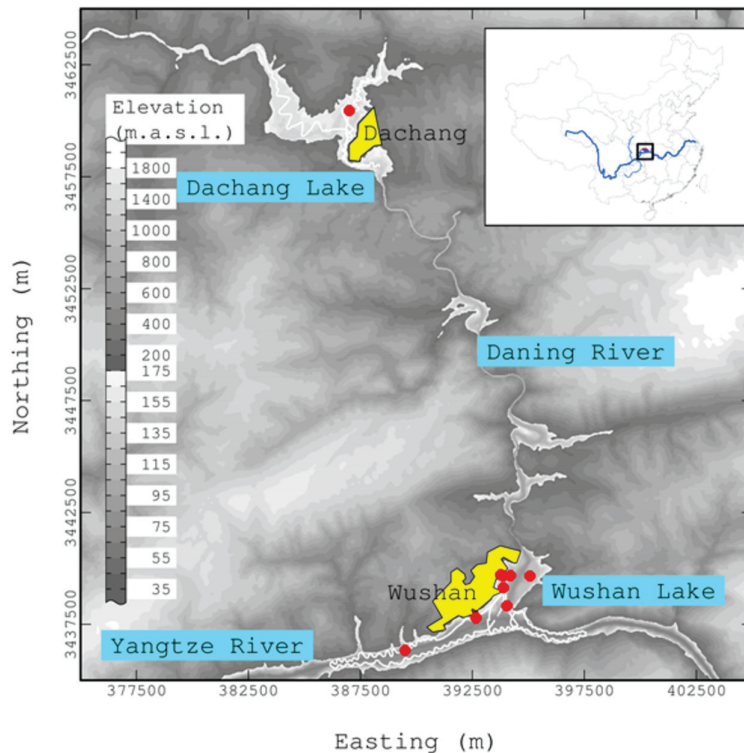


Figure 1: Map of the study area in the TGR backwater reaches of the Daning River and its confluence zone with the Yangtze River. Red points mark water sampling locations. White lines mark MINIBAT measurement cruises. Upper right sketch map shows Yangtze River and outlines of provinces in China.

reservoir water bodies.

The Daning River is a tributary of the TGR entering the Yangtze River main stream through the Wushan Lake, which formed next to Wushan city after the impoundment by the TGD (Figure). The Daning River has a length of 162 km, a watershed of 4170 km², and a mean discharge of 136 m³/s (CQWRB, 2010). The backwater area reaches about 60 km upstream (CCCA, 2007) and comprises the “Little Three Gorges”, a famous National Park and scenic spot in China, and several wide lake-like structures. The two biggest lake-like water bodies are found close to the biggest urban areas in the region. The Wushan Lake formed close to Wushan City and the Dachang Lake close to Dachang City. Frequent algal blooms and low water quality due to high Total Phosphorous (TP) loads threaten the backwater areas of the Daning River since the impoundment of the TGR (MOEP, 2012).

The hydrological boundary conditions were quite stable throughout the measurement period from 3rd to 6th December 2012. Water level did only rise slightly from 174.5 to 174.7 m a.s.l. and the discharge in both the Daning River and the Yangtze River was comparably low with 6.85 – 6.93 m³/s and 6300 – 6700 m³/s, respectively (CQWRB, 2011).

now has a length of more than 600 km at a mean width of 1.1 km, a total storage capacity of 39.3*10⁹ m³ and an annual water level fluctuation between 145 - 175 m a.s.l. caused by the reservoir management. The mean discharge of the Yangtze River is around 30.000 m³/s.

Consequently, the hydrological conditions in the whole involved water bodies changed considerably from a river to a river-style reservoir. Depending on the shape of the riverbed in the backwater reaches and the current hydrological conditions, either lake-like or river-like conditions may form in different

Measurement of physico-chemical water quality parameters with the MINIBAT and data evaluation

The MINIBAT towed underwater multi-sensor system (Casagrande, 1995) is connected to a boat with a data transmission cable. Sensors on the applied instrument measure physico-chemical water quality parameters (temperature (T), conductivity (Cond, normalized to 25°C), turbidity (Turb), chlorophyll a (Chl_a), oxygen saturation ($O_2\%$), and pH) with high spatial and temporal resolution. The MINIBAT can be used while driving the boat and meanwhile be steered to different depths. Vertical depth profiling can be performed when the boat does not move. Positioning and sensor data is recorded online by a computer.

During the measurement campaign in December 2011 measurement cruises were performed densely in the surface waters between 0 – 20 m depth at 40 m cable length using approximately sinusoidal diving course. Depth profiling was done at selected sites. A description of the geostatistical evaluation procedure for MINIBAT datasets can be requested from the authors.

Water sampling, sample preparation, and analysis

A Hydro-Bios FreeFlow Sampler was used for water sampling from different depths in the water column at selected sites. On 3rd–5th December, samples were taken around the Wushan City urban area (Figure). Additionally, samples from two Waste Water Treatment Plant (WWTP1+2) discharge channels and two other untreated sewage water discharge locations (WSS1+2) were taken on 3rd December. The WWTP1 channel contained unmixed water entering the Yangtze River over concrete cascades. Water from the WWTP2 channel was already leveled and mixed with Yangtze water. Samples were filtered (Sartorius stedim CAMembran, 0.45 μ m, 25 mm) to separate dissolved from suspended particulate matter. Filtered water volumes were recorded. For cation and dissolved Phosphorus (DP) analysis, samples of 20 mL were acidified with 50 μ l of 65% HNO_3 (Merck, Suprapur) and stored at 5°C in 20 mL PET bottles. Filters were air dried and sealed.

Prior to analysis, filters were digested using 65% HNO_3 as oxidation agent, 40% HF and 70% $HClO_4$ as digestion agents (all Merck, Suprapur) at 175 – 200°C. HF and $HClO_4$ were fumed off and the residues were dissolved in 10 mL 1% HNO_3 for analysis. DP, dissolved Cu, and dissolved Cd were analyzed from the acidified water samples. Particulate Phosphorus (PP), Cu, and Cd were analyzed from the filter digestions. An X-Series 2 ICP-MS (Thermo Fisher Scientific Inc.) was applied for analysis in collision cell mode to eliminate polyatomic clusters. ^{103}Rh and ^{115}In were used as internal standards and Phosphorus ICP Standard (Merck, CertiPUR) as calibration and cross check standard throughout the analysis procedure. Four blank filters were tested and revealed blank Phosphorus concentrations of $11.66 \pm 0.46 \mu g/L$ in the digestion solution which was subtracted from all analyzed digestion samples.

USGS GXR-2 (Gladney and Roelandts, 1990) and IAEA SL-1 (NOAA, 1995) geochemical standards were also digested four times and revealed Phosphorus recovery rates of $107 \pm 8\%$ for GXR-2 and $118 \pm 13\%$ for SL-1, respectively.

Results and Discussion

Water quality distribution patterns, geostatistically estimated from the in situ and online MINIBAT measurements on 4th and 6th December, revealed plumes of higher T, Cond, and Turb around the urban areas of Wushan City and Dachang City. The plumes were only present in the epilimnion water bodies. Around Wushan City the epilimnion included the upper 65 m water column around Dachang City only 20 m. Pollutant concentrations in the water bodies revealed a similar pattern with higher epilimnetic concentrations around both urban areas.

Wushan City

Plumes around Wushan City

On 4th December, the plume outlines at 5 m depth around Wushan City (Figure 2) appeared very similar for the parameters T, Cond, and Chl_a . However, the highest values for these parameters were found in different locations. T had its maximum values at the western shore within the Wushan Lake. There are parts of the Wushan harbor and untreated waste water discharges in this area. Maximum

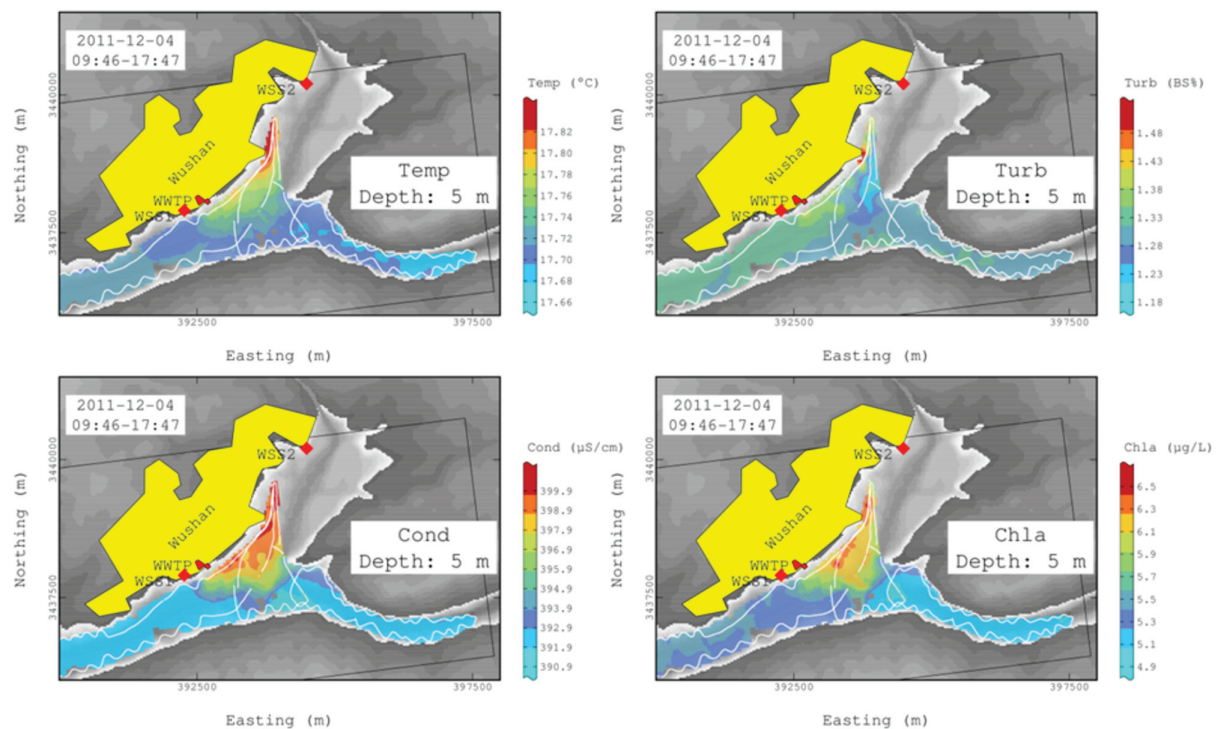


Figure 2: Distribution of T, Turb, Cond (normalized to 25°C), and Chl_a at 5 m depth in the water bodies around Wushan City on 4th December 2012. White lines mark MINIBAT measurement cruises. Waste Water Treatment Plant (WWTP) and sampled discharge locations (WSS) are marked in red.

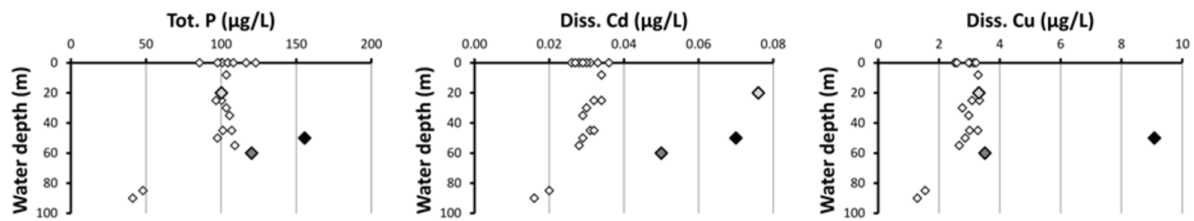


Figure 3: TP, dissolved Cd, and dissolved Cu concentrations in water samples from different depths around Wushan City from 3rd and 5th December 2011. Corresponding samples with outstandingly high concentrations for one or more components are marked accordingly.

values for Cond and Chl_a were also found in the similar area as for T, but additionally in the vicinity of the WWTP discharge location. Turb showed a slightly different pattern and plume outline. Highest Turb values were found in front of the small headland at the Wushan Lake western shore. There was a huge construction site on that headland during the measurement time. A plume with significantly higher Turb around the WWTP discharge location could also be observed. Lowest Turb values were present along the deep central channel in the Wushan Lake. Generally the Turb plume was more concentrated on the water bodies close to the Wushan City shoreline compared to T, Cond, and Chl_a .

Pollutant concentrations in the water bodies around Wushan City

Concentrations of TP as well as dissolved Cd and Cu from sampling locations in the surrounding of Wushan City revealed significantly higher concentrations of these elements in the epilimnion water bodies compared to hypolimnion waters on 3rd and 5th December (Figure 3). Epilimnion TP concentrations ($109 \pm 14 \mu\text{g/L}$) generally had very high levels according to German water quality standards for reservoirs where $> 100 \mu\text{g/L}$ TP account for polytrophic water bodies (LAWA, 2001). Major parts of Cd ($86 \pm 8\%$) and Cu ($92 \pm 4\%$) in the water were present in the dissolved phase. Diss. Cd revealed outstandingly high concentrations ($0.05 - 0.08 \mu\text{g/L}$) in three epilimnion samples, diss. Cu only in one sample ($9.1 \mu\text{g/L}$) (Figure 3). However, measured metal concentrations are very low compared to the threshold values of the WHO (WHO, 2011) and German guidelines (DVGW, 2011) for Cd ($3 \mu\text{g/L}$) and Cu (2 mg/L) in drinking-water. Highest TP and Cu concentrations as well as 2nd highest Cd concentration were all found in the same sample originating from 50 m depth close to the

Table 2: T, Cond (normalized to 25°C), TP, dissolved Cu and dissolved Cd concentrations in water samples from selected Wushan City effluents (for locations see Fig 2).

	T (°C)	Cond ($\mu\text{S/cm}$)	TP ($\mu\text{g/L}$)	Cu ($\mu\text{g/L}$)	Cd ($\mu\text{g/L}$)
WWTP1	16.7	582	1150	1.09	0.012
WWTP2	18.3	467	469	2.17	0.014
WSS1	18.8	489	179	4.90	0.016
WSS2	N/A	N/A	3220	3.39	0.054

river bed in front of the Wushan harbor. Both other samples with outstandingly high Cd concentrations also derived from the Wushan harbor area, one from 20 m depth in the middle of the water column and one from bottom water at 60 m depth.

Pollutant concentrations in Wushan City effluents

Water samples from selected Wushan City effluents revealed both higher and lower T than the ambient water (Table 2). Cond was higher than ambient water in all three measured effluents. The samples contained very different amounts of TP, diss. Cu, and diss. Cd. TP concentrations varied between 2 - 30 fold of the epilimnetic TP concentrations. Both diss. Cu and Cd did not exceed the concentration range measured in the waters around Wushan City. However, concentrations were lowest in the WWTP effluents.

Interpretation of the observed scenario

The plumes of higher T, Cond, and Turb in the water bodies around Wushan City appear to originate from the adjacent urban area. There were very serene hydrological conditions during the sampling period so that only little horizontal transport and mixing of waterborne substances happened. At hydrological conditions with higher discharge and changing water level this kind of plumes could not be observed in August 2011 (Data not shown here; see sections 2.1 and A.1). There was also no effective mixing of epilimnion and hypolimnion water resulting in the enrichment of intruding substances in the epilimnetic water bodies.

MINIBAT observations identified the Wushan harbor as a major source for higher T and higher Cond in the water. However, the source could either be urban effluents but also warm water discharges from ships resting in the harbor. Both sampled WWTP effluents had a higher Cond (Table 2) than the surrounding water body and did, thus, contribute to higher epilimnetic Cond.

The observed higher element concentrations of TP, diss. Cu, and Cd in the epilimnion can partly be explained by the sampled effluents from Wushan City. TP concentrations significantly exceeded the ones of ambient waters in three of four sampled effluents. But still, there are many more discharge locations that could not be sampled, yet, and they might serve as relevant pollution sources. Contaminated sediments and the inundated former urban area of Wushan City could also be a possible source of P, Cu, and Cd in the water (Ho et al., 2012; Komárek and Zeman, 2004). One sample with outstandingly high TP, Cu, and Cd concentrations derived from close to the riverbed. But, highest Cd concentrations were found in the middle of the water column. Water discharge from ships resting in the harbor area or discharged water layering at around 20 m depth might, therefore, also be reasonable Cd pollution sources. High turbidity seemed to be closely related to a huge

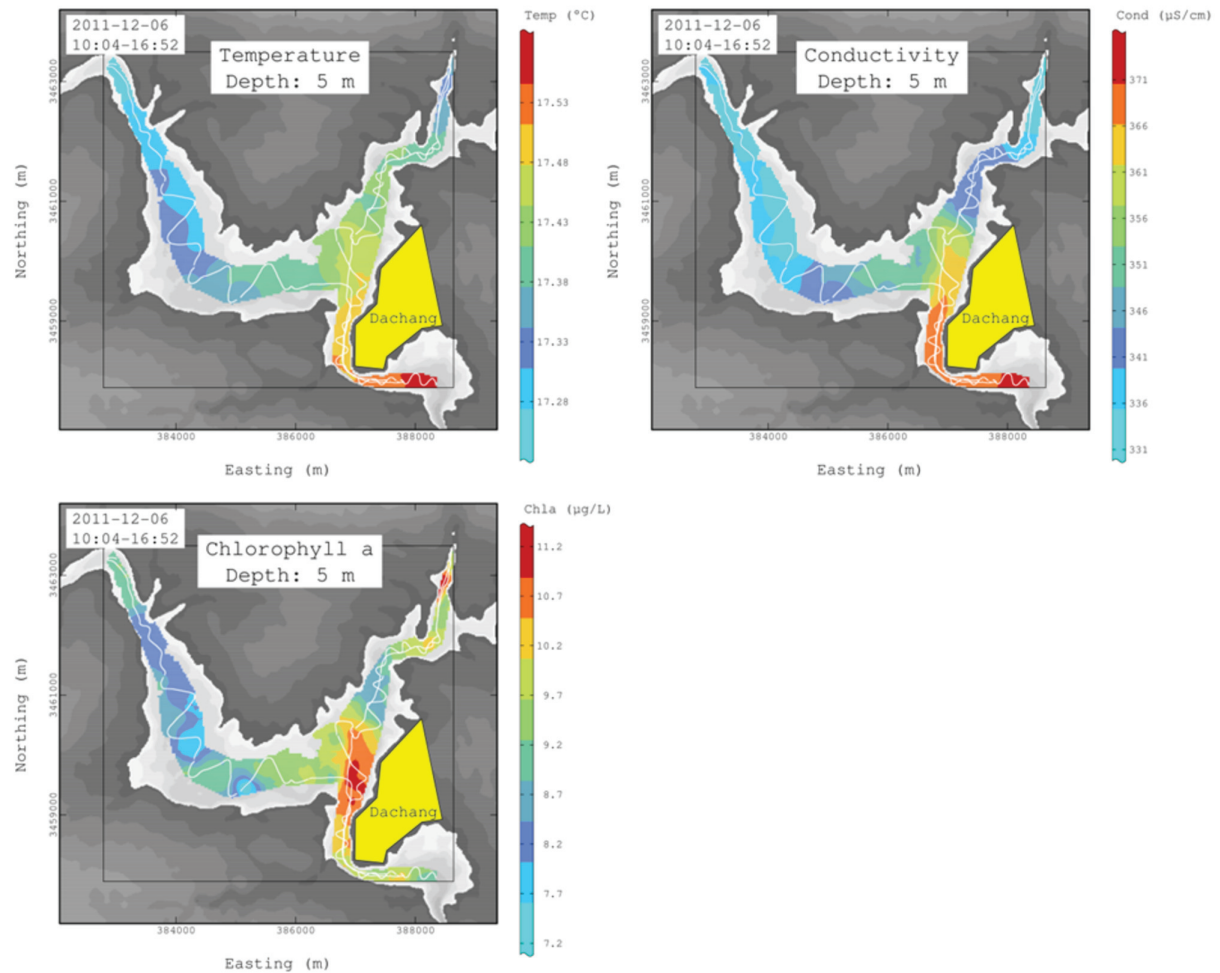


Figure 4: Distribution of T, Cond (normalized to 25°C), and Chl_a at 5 m depth in the water bodies around Dachang City on 6th December 2012. White lines mark MINIBAT measurement cruises.

construction site on the small headland in the Wushan Lake but also to the WWTP effluent. The Chl_a content and, thus, algal activity was positively related to T, and Cond. A significant part of this relation might, however, also be due the higher TP nutrient contents in the epilimnetic water around Wushan City.

Dachang City

On 6th December, plumes were also found around the urban area of Dachang City (Figure 4). T and Cond showed very similar distribution patterns with their maximum values south of Dachang city. Values of both parameters decreased significantly towards the upstream of both meeting rivers. Chl_a on the other hand reached its maximum values north-west of the urban area. Turb values, showed a very significant increase around Dachang City during the course of the day (Figure 5). Three measurement cruises (10:04-11:42; 11:42-13:33; 15:19-16:52) passing Dachang City were performed on 6th December. Initially, the highest Turb was found north-west of Dachang City in similar areas as the highest Chl_a . Subsequently, increasing Turb was found all along the urban area shoreline.

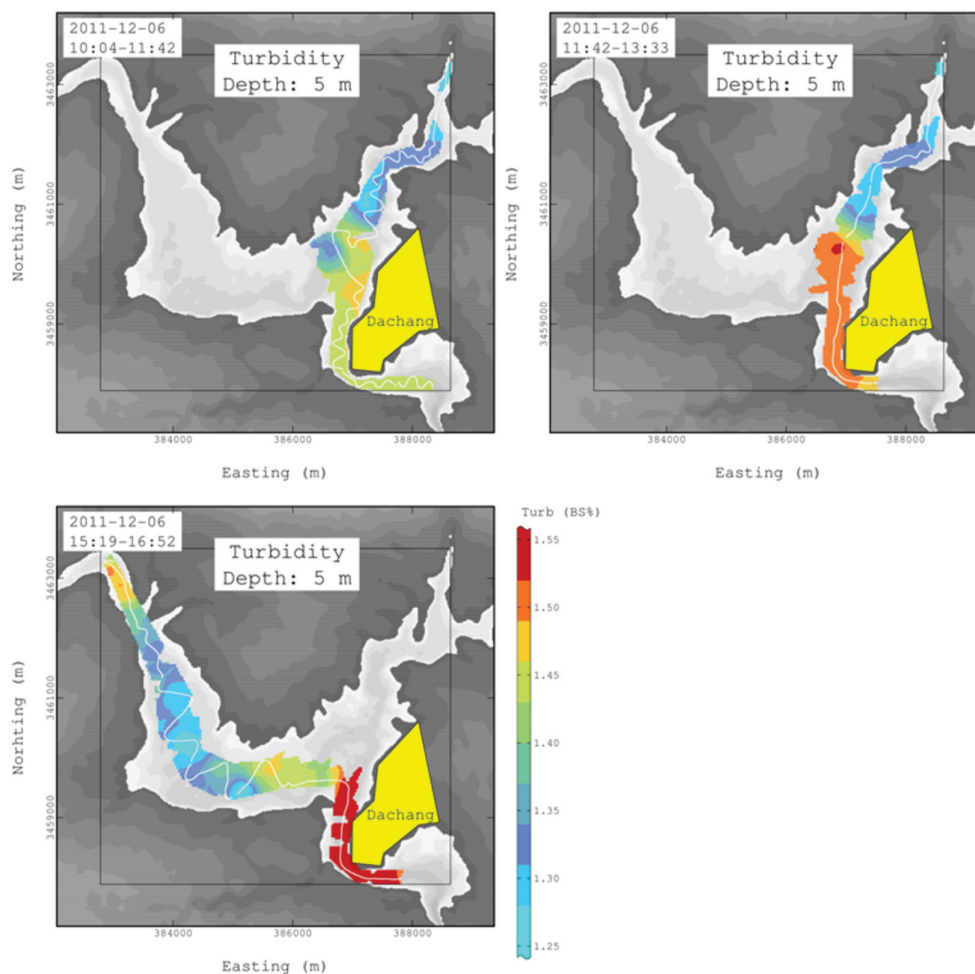


Figure 5: Distribution of Turb at 5 m depth in the water bodies around Dachang City during 3 MINIBAT measurement cruises on 6th December 2012. White lines mark MINIBAT measurement cruises.

Concentrations of TP, Cu, and Cd were also enriched in the epilimnetic water (Table 3) from the Dachang Lake sampling location (Figure). TP concentration is on lower levels compared to the samples from the Wushan area. Diss. Cu is in a similar concentration range, while Cd reaches much higher levels in the epilimnion at Dachang.

Interpretation of the scenario

The main source for higher T and Cond must be in the southern part of Dachang City. There is no big harbor in that area but several urban water discharge locations. The initially highest Turb values were measured in an area where there was active gravel exploitation. Digging in the sediment could also cause nutrient release in this area and explain the highest Chla concentrations, there. However, the significant increase in Turb along the urban shoreline during the day seems to be an impressive result of temporal urban discharge dynamics. The everyday work and water use cycle might be mirrored in the water turbidity.

Table 3: TP, dissolved Cu, and dissolved Cd concentrations in water samples from the Dachang Lake (Figure) on 6th December 2011. Water depth was 42 m.

Depth (m)	TP ($\mu\text{g/L}$)	Cu ($\mu\text{g/L}$)	Cd ($\mu\text{g/L}$)
0	69.8	2.65	0.09
15	66.9	3.22	0.12
40	14.8	0.73	0.02

Conclusion and perspective

Urban pollutant impacts on the water quality in TGR could be successfully monitored with the applied MINIBAT instrument. Pollutants in selected water samples were obviously related to water quality parameter distribution. Consequently, the detection of urban point

source pollution is possible with the applied techniques. Further fieldwork will focus on the coverage of different hydrological and ecological scenarios at different sites in TGR with similar sampling strategy. Evaluation of various impact factors, including urban, hydrological, meteorological, and land-use conditions, on water quality under varying boundary conditions is intended.

Acknowledgments

Thanks to Mrs. Liu, Mr. Wu, and our captain Mr. Ma from the environmental protection agency and the environmental monitoring station in Wushan, Chongqing, China, for their great infrastructural and personal support during the fieldwork. Funding of the Yangtze-Project by the Federal Ministry of Education and Research (BMBF grant no. 02WT1131) of Germany and the International Science and Technology Cooperation Program of China (NO. 2007DFA90510) is gratefully acknowledged.

References

- (Bergmann et al., 2012) Bergmann, A.; Bi, Y.; Chen, L.; et al. The Yangtze-Hydro Project: a Chinese-German environmental program. *Environmental Science and Pollution Research* 2012, 19(4), 1341–1344.
- (Casagrande, 1995) Casagrande, C. The MiniBAT - A miniaturized towed sampling system. *Oceans* 1995, 3, 638-641.
- (CQWRB, 2010) Chongqing Water Resources Bureau, China. Chongqing water function zoning revision report. 2010. <http://www.cqwater.gov.cn/Pages/Home.aspx>. (in Chinese)
- (CQWRB, 2011) Chongqing Water Resources Bureau, China. Hydrological information – Rivers real-time water regime. <http://www.cqwater.gov.cn/swxx/jrbssq/Pages/Default.aspx>. (accessed 21-30 August, 2011; in Chinese)
- (CCCA, 2007) Compilation Committee of Chongqing Atlas, China. Chongqing Atlas 2007, 92-93. Xi'an Cartographic Publishing House. isbn: 978-7-80748-069-3. (in Chinese)
- (Dai et al., 2010) Dai, H.; Zheng, T.; Liu, D. Effects of Reservoir Impounding on Key Ecological Factors in the Three Gorges Region. *Procedia Environmental Sciences* 2010, 2, 15–24.

- (DVGW, 2011) Deutscher Verein des Gas- und Wasserfaches. Erste Verordnung zur Änderung der Trinkwasserverordnung vom 3. Mai 2011 – Nichtamtliche Vollversion. In: Bundesgesetzblatt Jahrgang 2011 Teil Nr. 21. (in German)
- (DLR, 2010) German Aerospace Center. Shuttle Radar Topography Mission, 1 Arc Second scenes E1090000N300000_SRTM_1_DEM – E1100000N310000_SRTM_1_DEM, 2010. <https://centaurus.caf.dlr.de:8443>.
- (Gladney and Roelandts, 1990) Gladney, E.; Roelandts, I. 1988 Compilation of elemental concentration data for USGS Geochemical Exploration Reference Materials GXR-1 to GXR-6. *Geostandards Newsletter* 1990, 14(1), 21-118.
- (Ho et al., 2012) Ho, H.; Swennen, R.; Cappuyns, V.; Vassilieva, E.; Van Gerven, T.; Van Tran, T. Potential release of selected trace elements (As, Cd, Cu, Mn, Pb and Zn) from sediments in Cam River-mouth (Vietnam) under influence of pH and oxidation. *Science of the Total Environment* 2012, 435-436, 487-498.
- (Ji et al., 2010) Ji, D.; Liu, D.; Yang, Z.; Yu, W. Adverse slope density flow and its ecological effect on the algae bloom in Xiangxi Bay of TGR during the reservoir impounding at the end of flood season. *Shuili Xuebao (Journal of Hydraulic Engineering)* 2010, 41, 691–696. (in Chinese)
- (Komárek and Zeman, 2004) Komárek, M.; Zeman, J. Dynamics of Cu, Zn, Cd, and Hg release from sediments at surface conditions. *Bulletin of Geosciences* 2004, 79(2), 99-106.
- (LAWA, 2001) Länderarbeitsgemeinschaft Wasser. Gewässerbewertung – stehende Gewässer: Vorläufige Richtlinie für die Trophieklassifikation von Talsperren. 2001. isbn: 3-88961-237-7. (in German)
- (Luo et al., 2007) Luo, Z.; Zhu, B.; Zheng, B.; Zhang, Y. Nitrogen and phosphorus loadings in branch backwater reaches and the reverse effects in the main stream in Three Gorges Reservoir. *China Environmental Science* 2007, 27(2), 208–212. (in Chinese)
- (MEP, 2005-2011) Ministry of Environmental Protection of China. Three Gorges Bulletin 2005-2011.
- (NOAA, 1995) National Oceanic and Atmospheric Administration. Standard and reference materials for Environmental Science. Technical Memorandum NOS ORCA 94, 1995.
- (Ponseti and López-Pujol, 2006) Ponseti, M.; López-Pujol, J. The Three Gorges Dam project in China: History and consequences. *HMiC: Història Moderna I Contemporània* 2006, 151-188.

(Ran et al., 2010) Ran, X.; Yu, Z.; Yao, Q.; Chen, H.; Mi, T. Major ion geochemistry in the mixing zone of Changjiang (Yangtze) River and its tributaries in the Three Gorges Reservoir. *Hydrological Processes* 2010, 24, 2481–2495.

(USGS, 2006) U.S. Geological Survey. Shuttle Radar Topography Mission, 3 Arc Second scenes SRTM3N30E109 – SRTM3N31E110, 2006. eros.usgs.gov.

(WHO, 2011) World Health Organization. Guidelines for drinking-water quality. 2011, 4th ed. isbn: 978-92-4-154815-1.

© This article was originally published in ‘Rauch, S.; Morrison, G.; Norra, S.; Schleicher, N. (eds.) *Urban Environment*. Springer, 2013, 437-447’ and is reprinted here with kind permission from Springer Science and Business Media.

A.5 Integrated water quality monitoring and modeling in the Three Gorges Reservoir, China

Andreas Holbach¹; Wei Hu¹; Lijing Wang²; Hao Chen²; Nina Schleicher¹; Binghui Zheng²; Bernhard Westrich³; Stefan Norra¹

¹Institute of Mineralogy and Geochemistry, Karlsruhe Institute of Technology, 76128 Karlsruhe, Germany; *Email: andreas.holbach@kit.edu.

²Chinese Research Academy of Environmental Sciences, Beijing 100012, China.

³Institute of Hydraulic Engineering, University of Stuttgart, 70569 Stuttgart, Germany.

⁴Institute of Geography and Geoecology, Karlsruhe Institute of Technology, 76128 Karlsruhe, Germany.

Abstract

Increasing eutrophication and algal bloom events in the Yangtze River Three Gorges Reservoir are widely discussed in relation to hydrodynamics and nutrient transport and distribution processes. Insights into water exchange and interaction dynamics between water masses related to large scale water level fluctuations in the reservoir are crucial to understand water quality and eutrophication dynamics. Therefore, confluence zones of tributaries with the Yangtze River main stream are dedicated key interfaces. In this study, water quality data recorded in situ and online with the MINIBAT towed underwater multi-sensor system is integrated with data obtained from simulations done with TELEMAC hydrodynamic 2D numerical modeling. Key scenario for the current study was a discharge peak and corresponding rising water level in the Yangtze River at its confluence zone with the Daning River following a heavy precipitation event in August 2011.

Water quality data obtained from MINIBAT measurements during this specific period suggest that Yangtze River main stream water flowed upstream into the Daning River. Hydrodynamic 2D numerical modeling supports that hypothesis and enables to specify water and substance origins. Observed algal blooming can only be partly explained by the 2D modeling approach. 3D effects like the stabilization of thermal stratification at the water surface forming good conditions for algal blooming cannot be simulated but were measured with the MINIBAT. However, input of higher nutrient loads from Yangtze River water and from waste water discharges into the Wushan Lake are supported by the model and the field measurements and may have played a key role for the observed algal bloom formation.

Keywords

Water mass mixing; In situ measurement; online measurement; 2D hydrodynamic numerical modeling; algal bloom; Three Gorges Reservoir, China

Introduction

The water quality in the Yangtze River Three Gorges Reservoir (TGR) became a major concern since the first closure of the Three Gorges Dam (TGD) in 2003. Increasing frequency of eutrophication and algal bloom events occur related to the changed hydrodynamics and higher nutrient supply in tributaries (Dai et al., 2010; MOEP, 2012). In this frame a Sino-German environmental research program, the “Yangtze-Hydro Project”, has been established and funded since 2010 (Bergmann et al., 2012) to conduct international and interdisciplinary research on the sustainable utilization and development of the newly created ecosystem in the TGR. Two sub-projects, MINIBAT and Numerical Modeling, aim to monitor and model water quality and pollutant distribution dynamics in space and time throughout the TGR region. In this study, water quality data recorded in situ and online with the MINIBAT towed underwater multi-sensor system is integrated with data obtained from TELEMAC hydrodynamic 2D numerical modeling simulations. Key scenario for the current study was a discharge peak and corresponding rising water level in the Yangtze River at its confluence zone with the Daning River following a heavy precipitation event in August 2011. Observed water quality distribution snapshots on three days during the measurement period are tried to be integrated and explained with calculated flow field and tracer experiments from numerical modeling over the whole period.

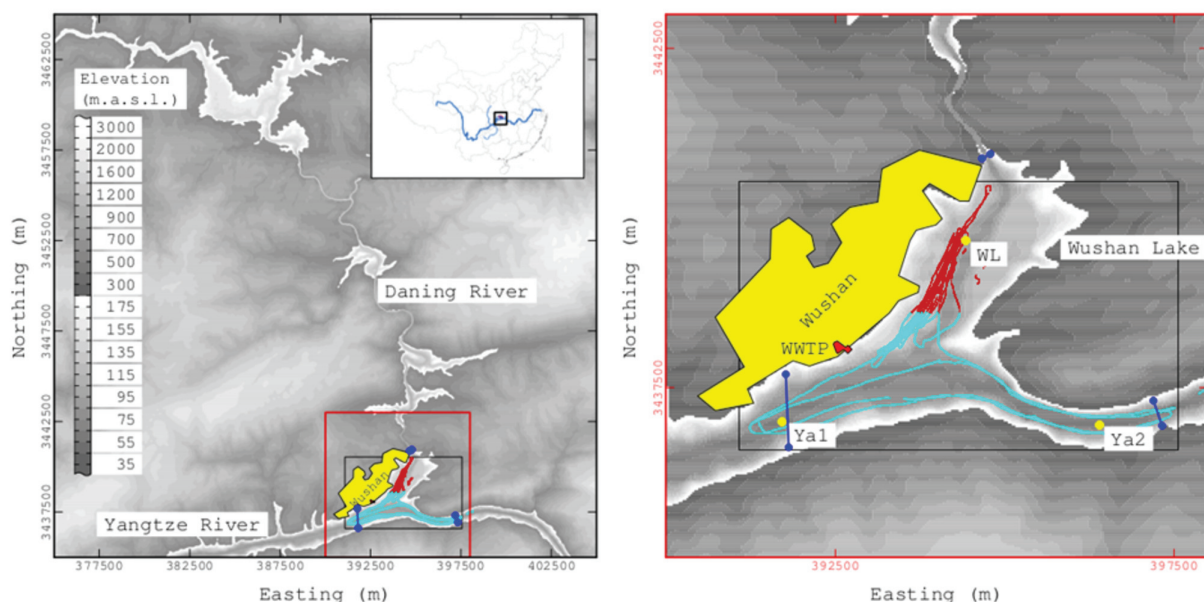


Figure 6: Map of the study area at the confluence zone of the Daning River and the Yangtze River. Right side shows the area zoomed to the red square. Wushan city – Yellow Polygon. WWTP – Red Polygon. Measurement cruises – Blue and Red (Wushan Lake selection see Figure 11) dots. Water sampling locations – Yellow points. Boundaries of model domain – Blue lines. Elevation and Bathymetry data derived from SRTM digital elevation model (DLR, 2010; USGS, 2006) and MINIBAT ground depth measurements.

Material and methods

Study area and hydrological boundary conditions

The Daning River is a tributary of the TGR entering the Yangtze River main stream through the Wushan Lake, which formed next to Wushan city after the impoundment by the TGD (Figure 6). The Daning River has a length of 162 km, a watershed of 4170 km², and a mean discharge of 136 m³/s (CQWRB, 2010). The backwater area reaches about 60 km upstream (CCCA, 2007) and comprises the “Little Three Gorges”, a famous National Park and scenic spot in China, and several wide lake-like structures. Frequent algal blooms and low water quality due to high Total Phosphorous (TP) loads threaten the Daning River since the impoundment of the TGD (MOEP, 2012). There are several discharge locations of different scales for treated and untreated waste water entering the Wushan Lake and upstream water bodies.

Hydrological data was obtained from the Chongqing Water Resources Bureau (CQWRB, 2011). Heavy thunderstorms in the night before 23rd August caused discharge peaks in the upper Daning River at Wuxi and in the Yangtze River. Water level at Wushan was steadily rising with decreasing slope from 146.38 m on 22nd August to 149.89 m on 30th August. Surface air temperature at Fengjie (NOAA, 2012) approximately 40 km west of Wushan rose from 23.4°C on 22nd August to 30.1°C on 30th August.

Measurement of physico-chemical water quality parameters with the MINIBAT and data evaluation

The MINIBAT towed underwater multi-sensor system (Stüben et al., 1994; Casagrande, 1995) is connected to a boat with a data transmission cable. Sensors on the applied instrument measure physico-chemical water quality parameters (Temperature, conductivity, turbidity, chlorophyll *a*, oxygen saturation, pH) with spatial and temporal resolution. Positioning and sensor data is recorded directly by a computer. During the measurement campaign in August 2011 measurement cruises

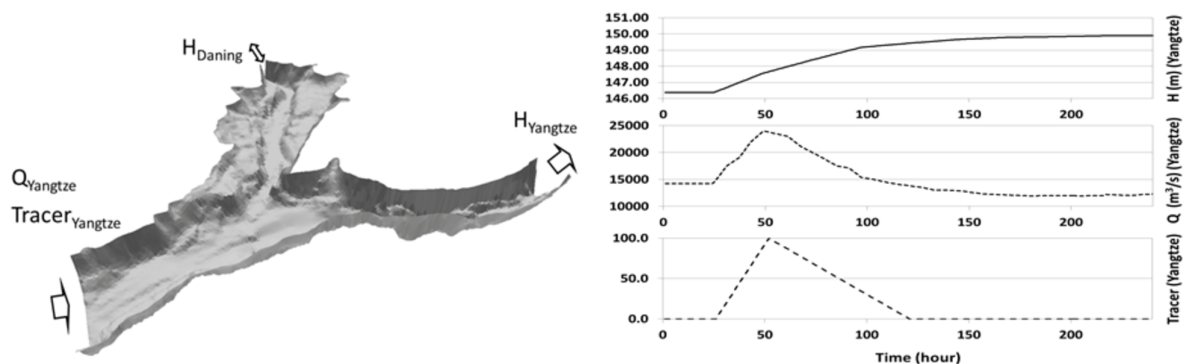


Figure 7: TELEMAC2D model domain in 3D view (left) and boundary conditions (right).

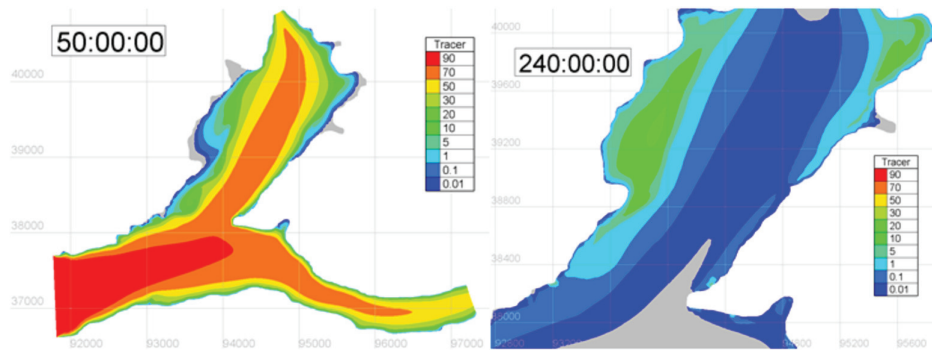


Figure 8: TELEMAC 2D model tracer distribution at 50 hours (left) and detail view of tracer distribution at 240 hours for part of the Wushan Lake (right).

were performed densely in the surface waters between 0 m and 13 m depth at 30 m cable length using approximately sinusoidal diving course. Depth

profiling was done at selected sites. A description of the evaluation procedure for MINIBAT datasets can be requested from the authors.

Hydrodynamic 2D numerical modeling with TELEMAC

The 2D depth-averaged finite element hydrodynamic software TELEMAC (Hervouet, 2007) is used to simulate the water and tracer movement in the confluence zone of the Daning River and the Yangtze River. Model domain (Figure 7) is built based on the bathymetry data derived from the SRTM digital elevation model (DLR, 2010) and MINIBAT ground depth measurements. The boundary conditions are shown in the Figure 7 and resemble the real conditions. The water level H_{Daning} is assumed to be the same as the water level at the downstream of the Yangtze River. To reach stable flow field, upstream discharge Q_{Yangtze} and downstream water level H_{Yangtze} and H_{Daning} are kept constant for the first 24 hours. Then all of them start to rise. After 50 hours, the discharge Q_{Yangtze} decreases but the water level still keeps rising. Tracer concentration ($\text{Tracer}_{\text{Yangtze}}$) is normalized to 0-100 unit range. For a first experiment, the tracer is released at the upstream boundary after 24 hours and reaches peak concentration at 50 hours. At 120 hours, tracer releasing is stopped. The tracer should represent any concentration change of a conservative substance caused by the flood event. In a second experiment the WWTP location is used for tracer release with assumed constant discharge of $0.2 \text{ m}^3/\text{s}$ and normalized tracer concentration of 100 units.

Results and Discussion

During the 10 days simulation period, the flow from the upstream of the Yangtze River is divided into two parts. One flows to the downstream of the Yangtze River and the other one to the upstream of the Daning River. Considerable parts of the simulated tracer released from the upstream of the Yangtze River are transported into the Daning River (Figure 8). After 240 hours, there are still considerable amounts of tracer with concentrations up to 20 units in the low velocity area close to

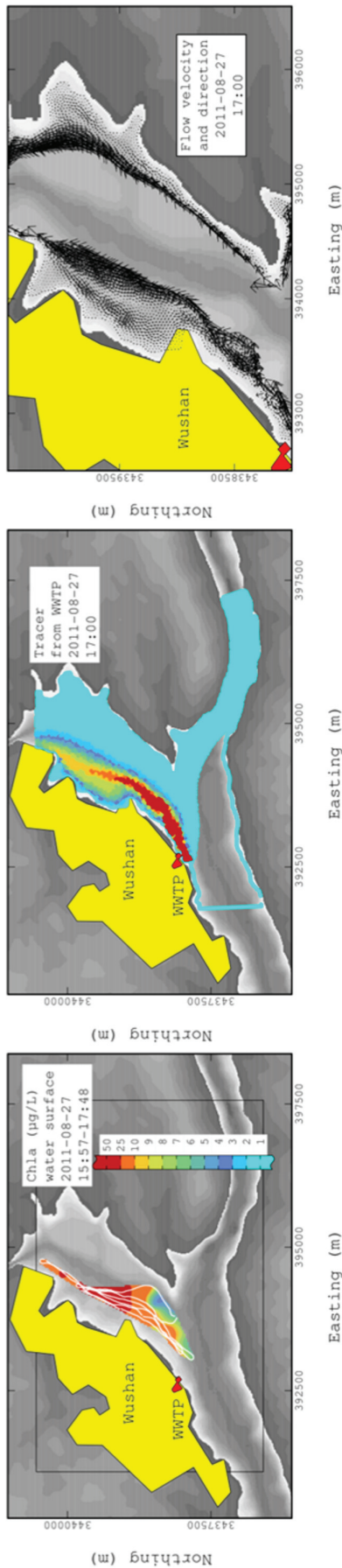


Figure 9: Chlorophyll *a* concentration distribution (left), Tracer released from the WWTP (middle) and flow velocity with direction (right) on 2011-08-27.

the Wushan Lake western shore (Figure 8). Thus, any conservative substance transported into the Wushan Lake by the prior flood event would stay in this area for longer time.

Major parts of the tracer released from the WWTP are transported into the Wushan Lake and the Daning River (Figure 9). Nutrients present in the effluent are favorable for the growth of algae. On 27th August, high Chl_{*a*} concentrations are present in a plume reaching from the WWTP into the Wushan Lake (Figure 9). This could indicate

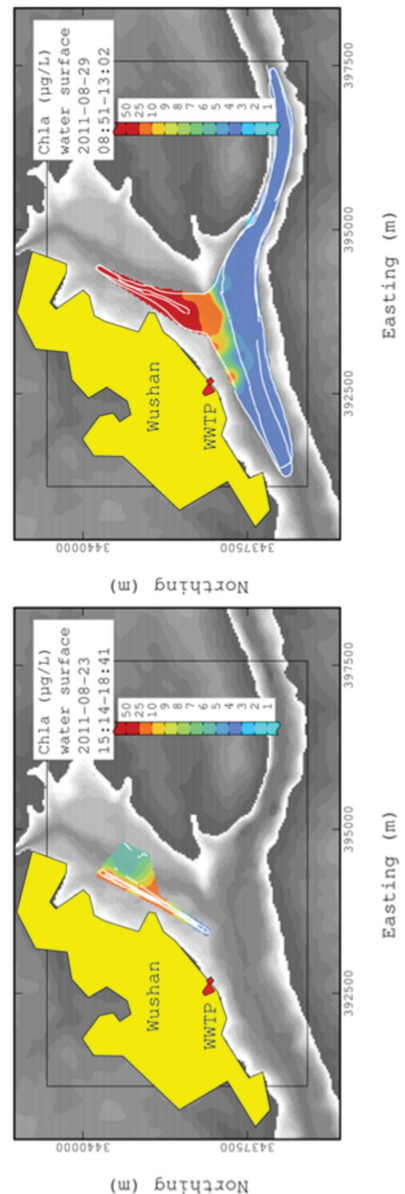


Figure 10: Chlorophyll *a* concentration distribution on 23rd (left) and 29th (right) August.

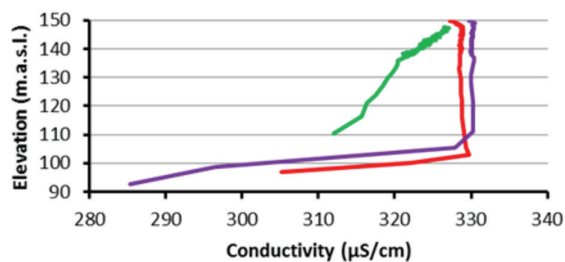


Figure 11: EC₂₅ depth profiles in the Wushan Lake (Selection shown in Figure 6) for 23rd (green), 27th (purple), and 29th (red) August.

Lake from 23rd to 29th August (Figure 10; Figure 11) and replacement of epilimnion water by water with higher conductivity from 23rd to 27th August (Figure 10). Conductivity and nutrient concentrations (data not shown here) were considerably higher in the Yangtze River main stream and the WWTP effluent compared to Wushan Lake water on 23rd August. Hydrodynamic 2D numerical modeling clarifies the question of water origin and explains the nutrient input into the Wushan Lake from the Yangtze River main stream and the WWTP effluent. This is favoring the observed algal growth detected by MINIBAT measurements. Formation of a thermally stratified water surface in the Wushan Lake was measured with the MINIBAT (data not shown here) and can further explain the pronounced algal growth. Small mixing depth is considered one of the most important driving forces for algal blooms in the TGR (Liu et al., 2012). The integrated approach coupling hydrodynamic 2D numerical modeling with in situ online MINIBAT measurements provides very detailed insights into critical processes like algal bloom formation in the TGR.

Conclusion and implications for water quality management

An underwater pipeline with about 500 m length is considered as possible scenario to alleviate the negative impact so that most of the nutrients and pollutants would be transport to the downstream of the Yangtze River (Figure 12). Of course, this would only be a short term measure. It is most important to improve the waste water treatment and release cleaner water into the river.

WWTP effluent driven algal growth and consequently nutrient input from the WWTP into the Wushan Lake and Daning River. A counterclockwise eddy close to the Wushan Lake western shore (Figure 9) causes a circulation, and thus higher retention times, of intruding substances in this low velocity area. MINIBAT datasets clearly show the development of an algal bloom in the Wushan

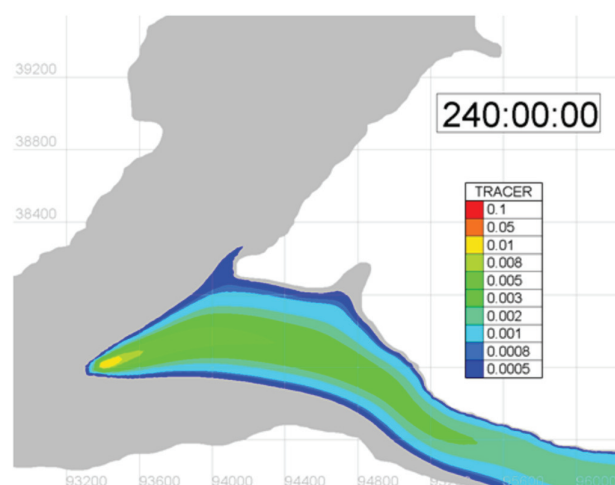


Figure 12: WWTP tracer distribution at 240 hours assuming the water from the WWTP is discharged in the middle of the Yangtze River.

List of Literature

- (Bergmann et al., 2012) Bergmann, A.; Bi, Y.; Chen, L.; et al. The Yangtze-Hydro Project: a Chinese-German environmental program. *Environmental Science and Pollution Research* 2012, 19(4), 1341–1344.
- (Casagrande, 1995) Casagrande, C. The MiniBAT - A miniaturized towed sampling system. *Oceans* 1995, 3, 638-641.
- (CQWRB, 2010) Chongqing Water Resources Bureau, China. Chongqing water function zoning revision report. 2010. <http://www.cqwater.gov.cn/Pages/Home.aspx>. (in Chinese)
- (CQWRB, 2011) Chongqing Water Resources Bureau, China. Hydrological information – Rivers real-time water regime. <http://www.cqwater.gov.cn/swxx/jrbssq/Pages/Default.aspx>. (accessed 21-30 August, 2011; in Chinese)
- (CCCA, 2007) Compilation Committee of Chongqing Atlas, China. Chongqing Atlas 2007, 92-93. Xi'an Cartographic Publishing House. isbn: 978-7-80748-069-3. (in Chinese)
- (Dai et al., 2010) Dai, H.; Zheng, T.; Liu, D. Effects of Reservoir Impounding on Key Ecological Factors in the Three Gorges Region. *Procedia Environmental Sciences* 2010, 2, 15–24.
- (DVGW, 2011) Deutscher Verein des Gas- und Wasserfaches. Erste Verordnung zur Änderung der Trinkwasserverordnung vom 3. Mai 2011 – Nichtamtliche Vollversion. In: *Bundesgesetzblatt Jahrgang 2011 Teil Nr. 21*. (in German)
- (DLR, 2010) German Aerospace Center. Shuttle Radar Topography Mission, 1 Arc Second scenes E1090000N300000_SRTM_1_DEM – E1100000N310000_SRTM_1_DEM, 2010. <https://centaurus.caf.dlr.de:8443>.
- (Hervouet, 2007) Hervouet, J. *Hydrodynamics of Free Surface Flows - modelling with the finite element method*. John Wiley & Sons Ltd. 2007.
- (Liu et al., 2012) Liu, L.; Liu, D.; Johnson, D.; Yi, Z.; Huang, Y. Effects of vertical mixing on phytoplankton blooms in Xiangxi Bay of Three Gorges Reservoir: Implications for management. *Water Research* 2012, 46(7), 2121–2130.
- (MEP, 2005-2011) Ministry of Environmental Protection of China. *Three Gorges Bulletin 2005-2011*.
- (NOAA, 2012) National Oceanic and Atmospheric Administration. Global summary of the day. NOAA Satellite and Information Service. <http://www.ncdc.noaa.gov/cdo-web/#daily>. (accessed 31 July, 2012)

(Stüben et al., 1994) Stüben, D.; Stüben, K.; Haushahn, P. MINIBAT - A new, simple system for in-situ measurement, mapping and sampling of dissolved trace elements in aquatic systems. *Underwater Systems Design* 1994, 16, 5-14.

(USGS, 2006) U.S. Geological Survey. Shuttle Radar Topography Mission, 3 Arc Second scenes SRTM3N30E109 – SRTM3N31E110, 2006. eros.usgs.gov.

© This article was originally published in 'Steusloff, H. (ed.) IWRM 2012—Conference Proceedings. Fraunhofer Verlag, 2012, 132-138' and is reprinted here with kind permission from Fraunhofer Verlag and Fraunhofer-IOSB.

A.6 Dilution of pollution? Processes affecting water quality in the river-style Three Gorges Reservoir

Dilution of pollution? Processes affecting the water quality in the river-style Three Gorges Reservoir

Andreas Holbach · Tilman Floehr · Irene Kranzioch · Anja Wolf

Received: 2 October 2012 / Accepted: 5 October 2012 / Published online: 30 October 2012
© Springer-Verlag Berlin Heidelberg 2012

The Three Gorges Reservoir (TGR) in the Yangtze River is a unique water body. There is no comparative river-style reservoir in the world with similar characteristics and magnitudes of shape, size, water level fluctuation, and discharge. This highly dynamic system is located in a rapidly developing area of China covering parts of the Hubei Province and Chongqing Municipality. Increasing efforts for waste water treatment and pollution management can hardly compete with growing urban areas, industry, and infrastructure. Thus, huge amounts of various pollutants enter the TGR water bodies through point and non-point sources. Serious eutrophication problems manifest themselves in increasing numbers of algal blooms, especially in tributary backwaters of TGR. Besides nutrient loads, absolute concentrations of anthropogenic pollutants like

heavy metals and organic chemical compounds rarely reach critical levels according to the Chinese, German, and WHO water quality guidelines. The massive dilution of these compounds in the mean discharging water of around 30,000 m³/s causes low absolute concentrations. But overall, tremendous total loads are transported further downstream and may remain a threat to connected ecosystems.

At Tongji University in Shanghai, China, the 3rd conference entitled “Workshop on Processes in the Yangtze River System” was held for scientific exchange on the recent cutting edge environmental research in the Yangtze River with a focus on TGR (Fig. 1). The conference marked two important milestones of Sino–German cooperation: (1) the 10-year anniversary of successful scientific Sino–German cooperation on questions related to the newly built Three Gorges Dam and (2) half time of the Yangtze-Hydro Project (Bergmann et al. 2012) funded by the German Federal Ministry of Education and Research (BMBF) from 2010 to 2013. Around 20 Chinese and German research institutions were present and came together with Zhou Wei from the State Council Three Gorges Project Construction Committee, China, Silvia Kettelhut from the German Consulate General in Shanghai, Jijun Xing from the Ministry of Science and Technology (MOST), China, and Philippe Bergeron as representative of the BMBF.

The conference was opened by Daqiang Yin, Dong Qi, Xiahou Dai (Tongji University, China), Guenter Subklew (Research Centre Juelich, Germany), Silvia Kettelhut, and Zhou Wei. They all highlighted the 10 years of successful cooperation between Chinese and German research institutions and the great achievements that were reached on both scientific findings and also socio-cultural mutual understanding.

Zhou Wei gave a detailed introduction on the current status of the establishment and research of the “Major Water Program of China”. He also guaranteed his organization’s support for the ongoing fieldwork of international cooperating institutions for a better understanding of the processes in the Yangtze River and especially in the TGR.

Responsible editor: Philippe Garrigues

This is a report on the conference organized by Tongji University (China), Research Centre Juelich (Germany), Key Laboratory of Yangtze River Water Environment, Ministry of Environmental Protection (China), and State Key Laboratory of Pollution Control and Resource Reuse (China) held at Tongji University, China, on 22–23 September 2012.

A. Holbach (✉)
Institute of Mineralogy and Geochemistry,
Karlsruhe Institute of Technology (KIT),
Karlsruhe, Germany
e-mail: andreas.holbach@kit.edu

T. Floehr
Institute for Environmental Research, RWTH Aachen University,
Aachen, Germany

I. Kranzioch
Department Environmental Biotechnology,
Water Technology Center Karlsruhe (TZW),
Karlsruhe, Germany

A. Wolf
Department of Water Resources Management,
IWW Rhenish-Westfalian Institute for Water Research,
Muelheim a. d. Ruhr, Germany

Fig. 1 Participants of the “Workshop on Processes in the Yangtze River System” at Tongji University, Shanghai, China on 22 September 2012



Guenther Subklew reviewed the history of the Yangtze Project since signing the first cooperation agreement in 2002. Challenging years did follow for the ambitious environmental scientists who waited for political decisions to approve the funding on both sides. The Yangtze Project consists of two sections: (1) the Yangtze-Geo section works on land-use change, soil erosion, mass movements, and diffuse matter inputs, and (2) the Yangtze-Hydro section (Bergmann et al. 2012) focuses on interactions in the pollutant/water/sediment/soil interfaces. In 2008, funding of the project section Yangtze-Geo started for its first 3 years, and recently, the network entered a second phase of funding until 2015. The 3-year funding for the project section Yangtze-Hydro started in 2010.

The scientific program of the conference displayed a diverse spectrum of recent environmental research in the Yangtze River and TGR. Four session topics structured the program into the following: (1) “Yangtze River Water Ecosystem,” (2) “Pollutants in the Water/Soil/Sediment Interface,” (3) “Water Treatment and Management,” and (4) “Monitoring, Modeling and Management.”

Opinions exchanged during discussions and presentations were highly divided on the ecological quality and pollution status of the Yangtze River and TGR. The necessity for further research to objectively reveal the recent status and development of the Yangtze River system became

very obvious and is crucial for scientifically based management implications.

Rolf-Dieter Wilken, coordinator of the Yangtze-HYDRO section, gave a brief conclusion at the end of the workshop: Four overview publications and several others in print or in preparation can already be shown after half-time of the project funding. The priority pollutants N, P, Clopyralid, Picloram, Sulfamethoxazole, Chloroform, MTBE, and Naphtalene could be identified.

After the conference, the German scientists were invited to visit the Taihu Lake and one of the water works of Wuxi City. Besides the Yangtze River and other Chinese rivers and lakes, the seriously polluted and eutrophic Taihu Lake is recently in the focus of the “Major Water Program of China” and the Sino-German “Clean Water” program set up by Chinese MOST and BMBF. This can be a basis for further Sino-German cooperative research for sustainability in the water sector.

References

- Bergmann A, Bi Y, Chen L et al (2012) The Yangtze-Hydro Project: a Chinese-German environmental program. *Environ Sci Pollut R* 19:1341–1344. doi:10.1007/s11356-011-0645-7

B Appendix—Full papers of co-authored scientific publications

B.1 An integrated approach to model the biomagnification of organic pollutants in aquatic food webs of the Yangtze Three Gorges Reservoir ecosystem using adapted pollution scenarios

An integrated approach to model the biomagnification of organic pollutants in aquatic food webs of the Yangtze Three Gorges Reservoir ecosystem using adapted pollution scenarios

Björn Scholz-Starke · Richard Ottermanns · Ursula Rings · Tilman Floehr · Henner Hollert · Junli Hou · Bo Li · Ling Ling Wu · Xingzhong Yuan · Katrin Strauch · Hu Wei · Stefan Norra · Andreas Holbach · Bernhard Westrich · Andreas Schäffer · Martina Roß-Nickoll

Received: 3 November 2012 / Accepted: 17 January 2013 / Published online: 1 February 2013

© Springer-Verlag Berlin Heidelberg 2013

Abstract The impounding of the Three Gorges Reservoir (TGR) at the Yangtze River caused large flooding of urban, industrial, and agricultural areas, and profound land use changes took place. Consequently, substantial amounts of organic and inorganic pollutants were released into the reservoir. Additionally, contaminants and nutrients are entering the reservoir by drift, drainage, and runoff from adjacent

agricultural areas as well as from sewage of industry, aquacultures, and households. The main aim of the presented research project is a deeper understanding of the processes that determines the bioaccumulation and biomagnification of organic pollutants, i.e., mainly pesticides, in aquatic food webs under the newly developing conditions of the TGR. The project is part of the Yangtze-Hydro environmental program, financed by the German Ministry of Education and Science. In order to test combinations of environmental factors like nutrients and pollution, we use an integrated modeling approach to study the potential accumulation and biomagnification. We describe the integrative modeling approach and the consecutive adaption of the AQUATOX model, used as modeling framework for ecological risk assessment. As a starting point, pre-calibrated simulations were adapted to Yangtze-specific conditions (regionalization). Two exemplary food webs were developed by a thorough review of the pertinent literature. The first typical for the flowing conditions of the original Yangtze River and the Daning River near the city of Wushan, and the second for the stagnant reservoir characteristics of the aforementioned region that is marked by an intermediate between lake and large river communities of aquatic organisms. In close cooperation with German and Chinese partners of the Yangtze-Hydro Research Association, other site-specific parameters were estimated. The MINIBAT project contributed to the calibration of physicochemical and bathymetric parameters, and the TRANSMIC project delivered hydrodynamic models for water volume and flow velocity conditions. The research questions were firstly focused on the definition of scenarios that could depict representative situations regarding food webs, pollution, and flow conditions

Responsible editor: Michael Matthies

Björn Scholz-Starke and Richard Ottermanns contributed equally to this work.

B. Scholz-Starke (✉) · R. Ottermanns · U. Rings · T. Floehr · H. Hollert · K. Strauch · A. Schäffer · M. Roß-Nickoll
Institute for Environmental Research, RWTH Aachen University, Aachen, Germany
e-mail: bjoern.scholz-starke@bio5.rwth-aachen.de

J. Hou
East China Sea Fisheries Research Institute, Shanghai, China

B. Li · X. Yuan
College of Resources and Environmental Science,
Chongqing University, Chongqing, China

L. L. Wu
Institute of Environmental Science and Engineering,
Tongji University, Shanghai, China

H. Wei · S. Norra · A. Holbach
Institute of Mineralogy and Geochemistry, Karlsruhe Institute of
Technology, Karlsruhe, Germany

B. Westrich
Institute of Hydraulic Engineering, University of Stuttgart,
Stuttgart, Germany

in the TGR. The food webs and the abiotic site conditions in the main study area near the city of Wushan that determine the environmental preconditions for the organisms were defined. In our conceptual approach, we used the pesticide propanil as a model substance.

Keywords Three Gorges Reservoir · Yangtze food webs · Bioaccumulation · Biomagnification · AQUATOX framework · Regionalization · Simulation · Environmental risk assessment · Integrated environmental modeling

Introduction

The Three Gorges Reservoir area at the Yangtze River

The Chinese people assign a significant portion of their cultural origins to the Yangtze River region nearby and along the Three Gorges Reservoir (TGR; Fig. 1). Since the region has been populated thousands of years ago, nowadays more than 400 million people live there (Müller et al. 2008). The TGR is of major importance

for the economic development of the whole region between Chongqing city and the TGR dam site near the city of Yichang. The TGR serves for the generation of electrical power, the safeguarding of shipping, and the prevention of threatening flood events. The reservoir's appearance is characterized by 30-m water-level fluctuations due to seasonal variations of the discharge rates, natural precipitation, and designated reservoir management (China Three Gorges Corporation 2010). In general, the building of large dams impacts among many other factors the biodiversity of riverine species by altering the ancestral flow conditions, introducing exotic species, and reducing flood plains (McAllister et al. 2001). Caused by the intense resettlements in the area, there is a significant increase in soil surface nitrogen and phosphorous surplus since the time before the first impoundment of the TGR (Xu et al. 2011). In the TGR region, flowing waters became stagnant, periodical changes in water level caused flooding events, and thereby a relocation of contaminated water, particulate matter, and sediment onto agriculturally used areas along the reservoir's shore.

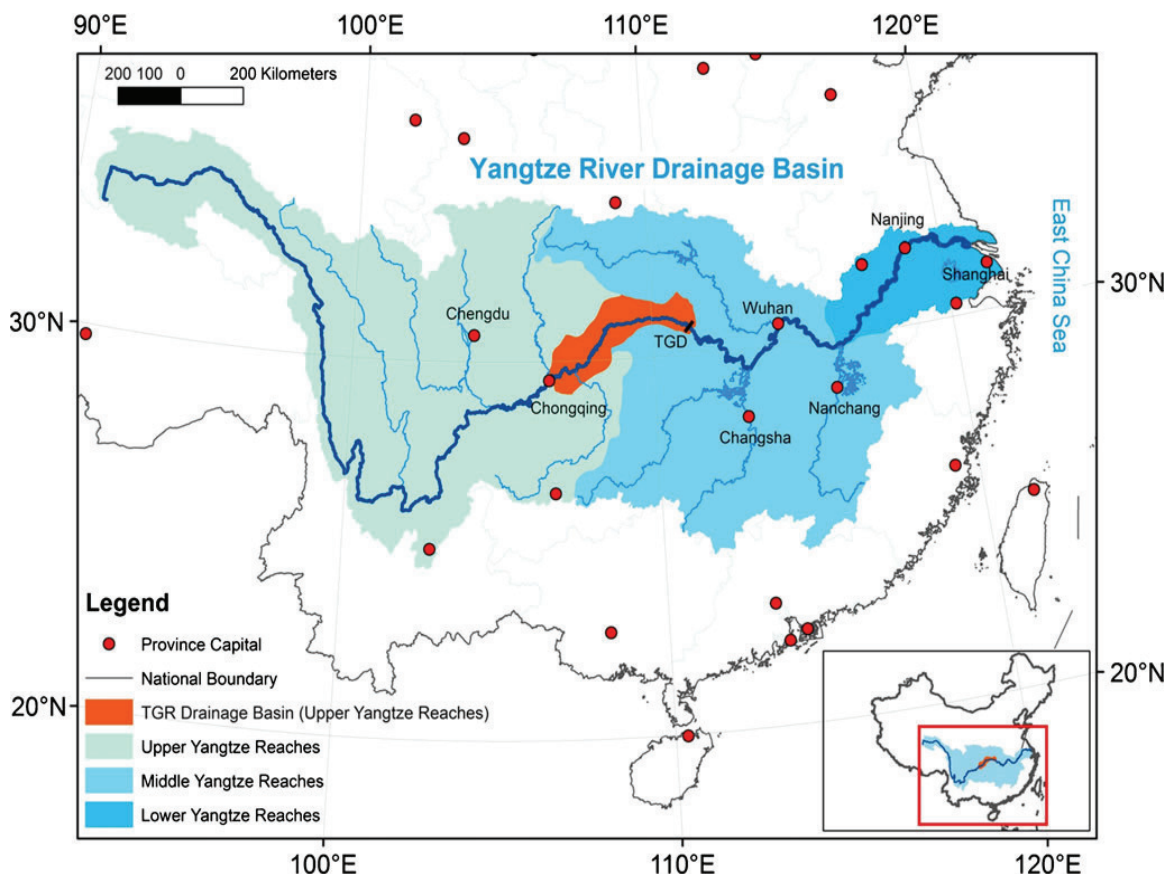


Fig. 1 Map of the Yangtze River Basin (light to dark blue) and the Three Gorges Reservoir (TGR; red). TGD Three Gorges Dam

Dynamics of TGR affect the bioaccumulation of pollutants within aquatic food webs

The loss of arable land after the impoundment of the river has caused an intensification of the agriculture on the remaining fields. In connection with high nonpoint pesticide loads by runoff, direct overspray, and drainage in the area, possible problems with the bioaccumulation along the aquatic food chains of the TGR could arise (Yong 2010). It is well known that an alteration of the flow regimen of a river from flowing to stagnant conditions entails manifold biotic alterations (Bunn and Arthington 2002). Organic pollutants pose a major threat to the ecosystems of the newly built reservoir, with many of them showing remarkable potential to accumulate in organisms. Among them, polycyclic aromatic hydrocarbons, polychlorinated biphenyls, and organochlorine pesticides (OCP) have been detected in the water column of the TGR (measured, e.g., by Wang et al. 2009). From the group of OCP, the herbicide propanil has been identified as highly relevant because of its intense use in the TGR region (Zhang 2000).

Aims of the study

The main aim of our studies is a deeper understanding of the processes that determine the bioaccumulation of organic pollutants, mainly pesticides, within aquatic food chains under the newly developing conditions of the huge reservoir. For this purpose, we quantify the internal concentrations of chosen model pollutants in ecological and economical key species, i.e., mainly fish, under the influence of TGR-representative pollution scenarios. We analyze different agricultural land use patterns and nutrient loads under the fluctuating water level regimen caused by the mode of operation of the dam. The concept of this integrated modeling procedure requires input data from various scientific disciplines such as ecotoxicology, environmental analysis, ecology, and hydrology. Therefore, this paper describes in detail the approach to compare the environmental risks in an exemplified season under the new operating conditions of the dam and give recommendations for risk management procedures.

Model structure—conceptual approach

Integrated modeling

In this study, we follow an integrated modeling approach to gain a comprehensive overview on factors and mechanisms that trigger the bioaccumulation of organic pollutants in aquatic ecosystems. *Integrated Environmental Modeling* (IEM; Argent 2004) is of increasing importance in environmental

management, decision-making, and risk assessment. This interdisciplinary approach allows for a gainful aggregation of knowledge and data from different disciplines and the handling of the complexity of environmental systems (Jopp et al. 2011). It is based on the idea of an integrated assessment (Hisschemöller et al. 2001). To account for the complexity of the TGR situation concerning hydrological, biological, and ecotoxicological factors, we combine and couple several specialized modules to focus on TGR-specific environmental and ecological conditions (Fig. 2). The AQUATOX model suite (Park et al. 2008) is used as an interconnected modeling framework. It links the eight modules exposition module (EXM), food-web module (FWM), hydrodynamic module (HDM), particle transport module (PTM), site-descriptor module (SDM), bioaccumulation module (BAM), ecotoxicological module (ETM), and risk-assessment module (RAM) of our approach seamlessly. The modules are implemented either as integrated submodels within the AQUATOX modeling environment or as external models. Adequate input values are provided by literature data, expert knowledge, or available empirical data (e.g., in the case of FWM). In some cases, e.g., for HDM, results of external models have been used. Thereby, this modular approach fulfills the requirements for an aquatic environmental risk assessment, as evaluated by Echeverría et al. (2003) for AQUATOX.

Exposition module The exposition module estimates environmental concentrations of xenobiotics under different pollution scenarios specifically for the TGR region. Here, we rely on the standard assumptions from the EU environmental risk assessment (ERA) which is based on realistic worst-case scenarios. Spatial aspects of exposition are considered by the distribution of relevant model substances. In particular, the rice herbicide propanil, which is a widely used crop protection substance in Asia (Labrada 2003) and its main metabolites 3,4-dichloroaniline (3,4-DCA) and 3,4,3',4'-tetrachloro-azobenzene (TCAB) will be modeled by the HDM and the PTM. Estimated concentrations of these model substances are handed over to the chemical fate module of AQUATOX.

Food-web module The food web module describes the composition, interactions and dynamics of the communities of aquatic organisms in the TGR. This module is integrated within the AQUATOX environment. The AQUATOX model provides validated surrogate simulations with all biotic and abiotic properties. These simulations are subsequently modified to regionalize the standard site (river scenarios) or are compiled from the scratch (reservoir scenarios) if necessary.

Hydrodynamic module The hydrodynamic module is used to generate flow conditions of the given water bodies according to the normal operation mode of the Three Gorges Dam (TGD). The module describes changes in water

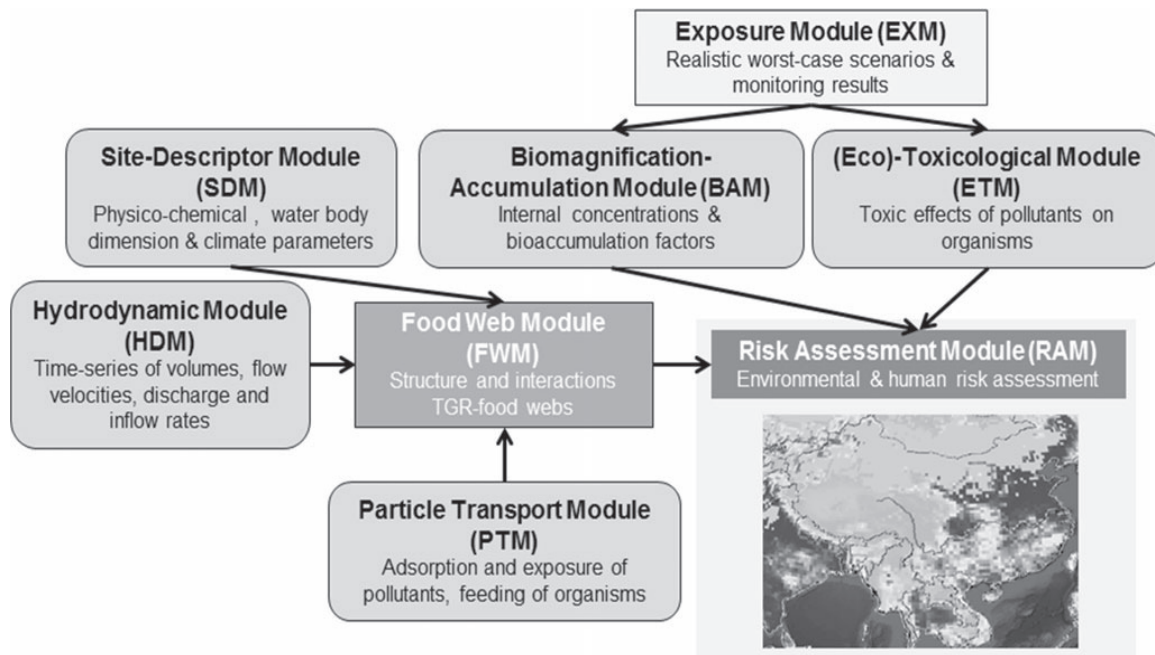


Fig. 2 Integrated environmental modeling approach of the bioaccumulation module within the MICROTOX project. TGR-specific scenarios are adapted to describe the potential bioaccumulation under the

altered land use and water-level regimen in the TGR region by linking specialized submodules

volume, flow velocity, discharge and inflow rates delivered by the external 1D model HEC-RAS (U.S. Army Corps of Engineers 2001). These flow conditions are provided to the AQUATOX environment as time series data in the water volume module.

Particle transport module The particle transport module simulates the distribution of contaminated particles within the TGR water bodies (TELEMAC 2-D, Hervouet 2007). These particles are of particular importance in the TGR as they absorb the pollutants, feed the organisms, expose the organisms to the pollutants and distribute the pollutants over the water body. Detritus particles as well as algae can act in such a way. The simulations provide spatially explicit time series of pollutant concentrations, which are provided to the AQUATOX environment via the toxicity module to define site-specific expositions. The sampling sites are defined according to the general pollution scenarios that correspond to specific sites at the TGR where samples for sediment toxicity characterization within the MICROTOX project have been taken.

Site-descriptor module The site descriptor module provides the site-specific environmental conditions, such as water temperatures, nutrients and radiation energy. These variables have been measured in the field, taken from literature or provided by external models. They are used as fixed site-specific state variables for the internal module in AQUATOX.

Bioaccumulation module The bioaccumulation module describes the adsorption of the model pollutants (e.g., TCAB) to detritus particles by chemical characteristics. An adsorption coefficient can be modeled via adsorption isotherms (Foo and Hameed 2010). In case of substances with unknown chemical properties, the adsorption characteristics have been estimated by external QSAR-based chemical properties estimation software (CHEMPROP; Schüürmann et al. 1997). In case of algae as transporting particles, the accumulation of model substances within the algae is modeled via uptake factors in the AQUATOX environment and exported as bioconcentration factors. Based on the loading of pollutants on the surfaces of detritus particles or concentrations within the algae, the BAM models the accumulation of these substances in the higher aquatic surrogate species of the TGR food web (especially fish) also via uptake factors.

Ecotoxicological module Based on the estimated internal pollutant concentrations provided by BAM, ecotoxicological effects of the model substances are estimated in the ETM using literature data on toxic effects to aquatic organisms, sediment toxicity information generated in the MICROTOX project and interpolation by inter-species correlation estimates (Web ICE) within AQUATOX (Raimondo et al. 2010). Due to the outstanding importance of fish as humans' food resource in the TGR region, the adaptation of the food webs focuses on carps that pose the main target species for our environmental risk assessment.

Risk-assessment module We assess the risk for the environment by comparing the effects of different doses of pollutants that are predicted by the AQUATOX model on the level of individuals, populations and aquatic communities. For the estimate of risks to humans, we compare the internal pollutant concentrations of important food source fishes with acceptable daily intake rates (ADI).

The AQUATOX model and its adaptation

Since the analysis of organic traces in environmental samples and organisms tissues is very labor and cost intensive, we use deterministic modeling approaches for the prediction of the potential accumulation and biomagnification of model pollutants. The whole complexity and the basic mechanism of the unique hydrological, biological and ecotoxicological situation of the TGR can be best reflected by an ecological model for environmental risk assessment, as shown by the reviews cited in Lei et al. (2008). We use an AQUATOX-based simulation model that has been adapted to the local conditions at the TGR to predict the fate of pollutants, such as pesticides or nutrients, and to describe the potential accumulation within the food webs of the reservoir. The AQUATOX model has been developed for the US Environmental Protection Agency for the purpose of environmental risk assessment (Park and Clough 2010). It is a general, mechanistic model that can be used to predict the fate, behavior, and effects of various stressors, such as toxic chemicals, nutrients, or environmental variables in an environmental risk assessment context for aquatic ecosystems (Park et al. 2008). Lei et al. (2008) described a successful example of an adaptation of the AQUATOX simulation

environment to the situation of a Chinese river. In our study, already existing simulations are adapted to the specific requirements of the recent study by detailed knowledge on the structure of the river and the reservoir biocoenoses. We describe the consecutive adaptation steps that are necessary to change the pre-defined simulations of AQUATOX to “Yangtze-specific” conditions (“regionalization”). A scenario-based procedure is preferred over the best possible representation of real sites because an understanding of the underlying processes that determine the effects and the bioaccumulation of pollutants is desired. The definition of scenarios includes the status of agricultural and industrial pollution, the hydrology, the mode of operation of the TGD and further aspects. Our research is focused on the influence of high concentrations of nutrients on food web structures. Two different types of simulations, “reservoir” and “river,” have been adapted in AQUATOX based on the “Cheney reservoir” data that are marked by lake species (USGS 2008) and the predefined “Rum River” scenario (Park et al. 2005) marked by flowing water specialists, respectively.

Definition of scenarios

The main scenarios of pollution (compare step 1 “definition of scenarios” in the flow chart of Fig. 3) have been derived in an incremental procedure. Firstly, a study area near Wushan city has been chosen because of its exemplary pattern of landscape features and pollution sources. Secondly, the hydrodynamic situation in the designated study area has been estimated by simulating the yearly patterns of flow conditions and water volumes of Daning River sections. Thirdly, based on the patterns of agricultural practice and land use, segments with

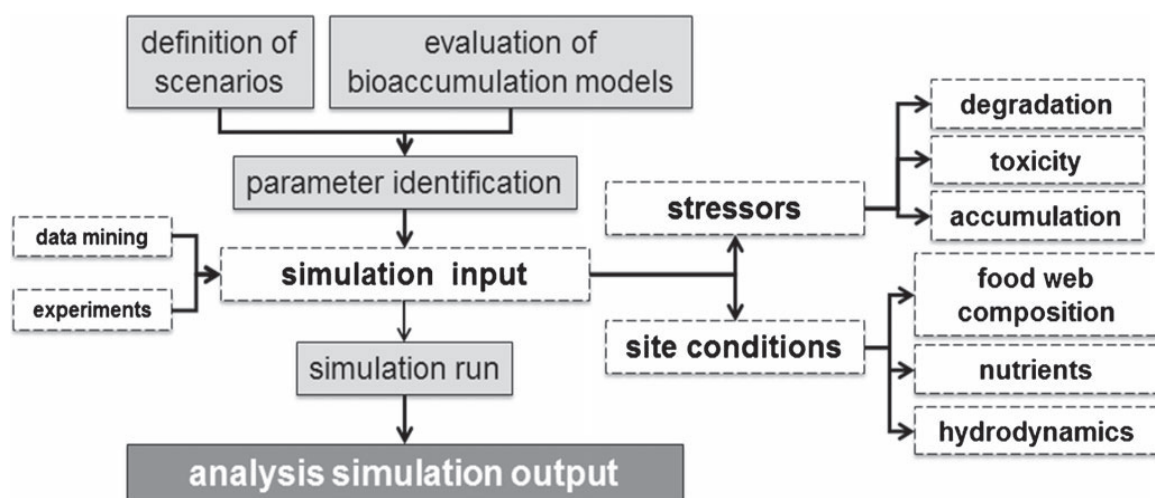


Fig. 3 Set up of the adapted simulations. Workflow of bioaccumulation studies. A step-wise procedure for the definition of necessary input data to conduct sound simulation experiments is established

high and low pesticide loads have been determined. The assumptions and predictions of a standard environmental risk assessment are used to define maximum loads of pesticides according to expectable application procedures and additional massive overuse. The study area is marked by a “unique” hydrodynamic situation at the mouth of the Daning River where a huge whirlpool with high-residence time of Wushan Lake water is located. The segment definition procedure in the MICROTOX project includes that “reservoir” and “river” segments are linked. Feedback links are incorporated in case the hydrodynamic model predicts a backflow of water to upstream or the respective segment is directly connected to stagnant waters. The supposed “area-of-exposition” is marked by rice cultures on terraces. Hence, intense nutrient and pesticide use can be expected. The main branch of the Yangtze River is assumed to contribute minor pollution loads and is hence a “diluting agent.” Segments have been defined and their characteristics of the area studied have been implemented into the simulation environment of AQUATOX. The segments are linked in a feed-back and feed-forward way to adjacent ones according to requirements of the AQUATOX simulation environment (Park and Clough 2010). The linkages between segments may be unidirectional or bidirectional. (1) All of the linked segments have an identical set of state variables; (2) each segment is assumed to be well mixed. Hence, a dynamic stratification of water layers does not apply. The stratified pairs of segments must be specified by the user. In a simulation, nutrients, biota, and other state variables “pass” from segment to segment through active migration, passive drift, diffusion, or bed-load. Four segments representing different pollution scenarios have been defined.

HDM—hydrological characteristics of the study area water bodies

The study area near the city of Wushan includes the Daning River up to Dachang Lake, as well as adjacent upstream and downstream parts of the Yangtze River in western and eastern direction. It has been chosen as the model region to show basic patterns of bioaccumulation under unique hydrodynamic conditions in the confluence of the Yangtze River and the Daning River into the Wushan Lake. The Wushan district is located at the eastern boarder of the Chongqing municipality in a subtropical area in central China. Depending on the water level of the TGR and the actual flood conditions, a massive backflow of water from the Yangtze into the Daning River is often observed. This leads to the rare situation that a large mixing zone alters the normal exchange rates in the huge “whirlpool” in front of Wushan city. The area is divided in several sections according to the basic river geometry. “Fast-flowing gorges” are assumed equipped with a typical river food web and “slow-flowing basins” with reservoir food webs. Several segments

of significantly differing flow conditions and probable pollution patterns are intended to be modeled (as schematically shown by Fig. 4). The predefined segments have been refined and re-defined by the results of the one-dimensional HDM HEC-RAS (U.S. Army Corps of Engineers 2001) considering the water level alterations, realistic flow conditions in an annual cycle and the volumes of the different water bodies. The model HEC-RAS has been developed by the Hydrologic Engineering Center as a River Analysis System. It models the one-dimensional flow disregarding the shape of a river cross-section. It has a graphical user interface integrated in ArcGIS for the pre- and post-processing for the modeling and models the hydrodynamic situation based on available spatial data. The water channels of the Daning River between the Dachang Lake and the bridge near Wushan, and the Wushan Lake are first divided in sectors by drawing 125 cutlines (Fig. 5). The model has been calibrated to the specific conditions in the regarded region; the geometry of the river system has been built by the worldwide digital elevation model (DEM) and water depth measurement of the MINIBAT project. Data for water level fluctuations have been taken from the gauging station Wushan in the mainstream of the Yangtze River as the downstream boundary condition. Discharge data have been taken from the Wuxi gauging station in the Daning River mainstream. Inflows have been estimated from smaller tributaries as the upstream boundary condition. The DEM data are available in the public domain (DLR-German Aerospace Center 2000). After calibration, the HDM models the volume, inflow, and discharge rates as well as the actual water levels of each of the sections in a daily time-step. The data delivered by the HEC-RAS model have been used to define homogenous segments within the study area that show flowing or stagnant characteristics and to calculate relevant input values for the AQUATOX *site descriptors*. Seasonal changes in the water level and the operation mode of TGD take effect in the AQUATOX model through water volume and inflow and/or discharge rates in a given cross-section of the river.

EXM—exposure

Estimation of pollution loads

The next step in setting up pollution scenarios is the estimation of the most probable exposition to the organisms of the Yangtze food webs. Several Yangtze-Hydro sub-projects occasionally identified increased pesticide concentrations in the past, particularly in TGR tributary water bodies (Wolf et al. 2012). However, the exposition has been assessed mainly by using the standard environmental risk assessment procedures for the registration of plant protection products within the European Union. Scenarios for example applications of

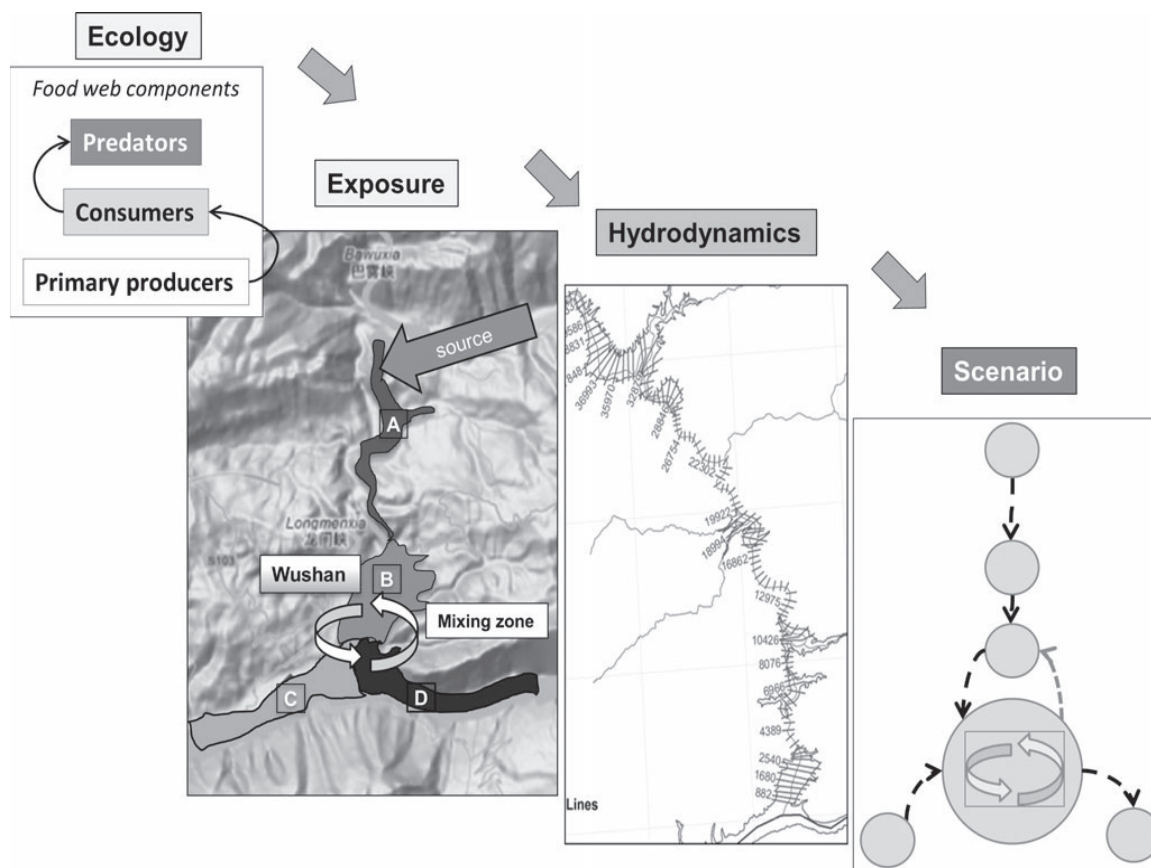


Fig. 4 The derivation of relevant scenarios (i.e., segments of the Yangtze River or its tributaries) for simulation experiments in the MICROTOX project combining the ecological, exposure, and hydrodynamic situation at the TGR. Four schematic pollution scenarios near the city of Wushan, Hubei province. Ecological assumptions on typical biocoenoses led to the definition of TGR food webs, separately for

“rivers” and “reservoir” intercepts. The exposure situation is characterized by *A* a high risk of agricultural pollution due to adjacent fields, by *B* pollution from urban waste water and a water body mixing zone with high residence times, by *C* highly diluted urban and agricultural pollution, and by *D* an intermediate burden of contamination after confluence. Flow conditions are modeled by the HEC-RAS model

the model substances proposed by Forum for the Coordination of Pesticide Fate Models and their Use (FOCUS (2001)) and Med-Rice (2003) helped to identify the worst-case surface water concentrations, mainly caused by drift events. In our studies, we concentrate on fate, effects, bioaccumulation and biomagnification of the parent compound propanil, its main and primary metabolite 3,4-DCA within the components of the aquatic food webs, and a supposedly lipophilic and thus accumulative secondary metabolite TCAB. The surface water concentrations of propanil and 3,4-DCA are taken from the literature, particularly from the draft assessment report (DAR) of propanil that has been written by the rapporteur member state Italy, which is again the most important rice producer within the European Union (Ministry of Health of Italy 2006). The DAR has been written for the environmental risk assessment prior the decision to list propanil in Annex I of Commission Directive 91/414/EEC as a post-emergence, foliar-applied rice

herbicide and is thus relevant for Chinese use patterns. Propanil is intended to be used on drained paddy fields with a maximum of two sequencing spray applications within a 14-day interval. In the DAR of propanil, a single application of 4-kg active ingredient (a.i.)/ha has been assumed, because of its very short degradation half-time (DT_{50}) of 0.5–3 days. For 3,4-DCA, the $DT_{50} > 26$ days leads to the assumption of a 2-fold application with 14 days time lag. The Predicted Environmental Concentrations in surface waters (PEC_{SW}) of propanil from realistic worst-case standard scenarios are calculated by the MED-RICE model Standard scenario 1b (degradation, no sorption). The PEC has been assumed to appear and affect the communities directly after application as initial concentrations (PEC_{SWini}). Thus, the PEC_{SWini} for propanil is then 0.0022 mg a.i./L, the PEC_{SWini} for 3,4-DCA has been 0.094 mg a.i./L, respectively.

The formation rate of TCAB from the parent substance is about 0.5 %. However, no PEC-calculations for TCAB are

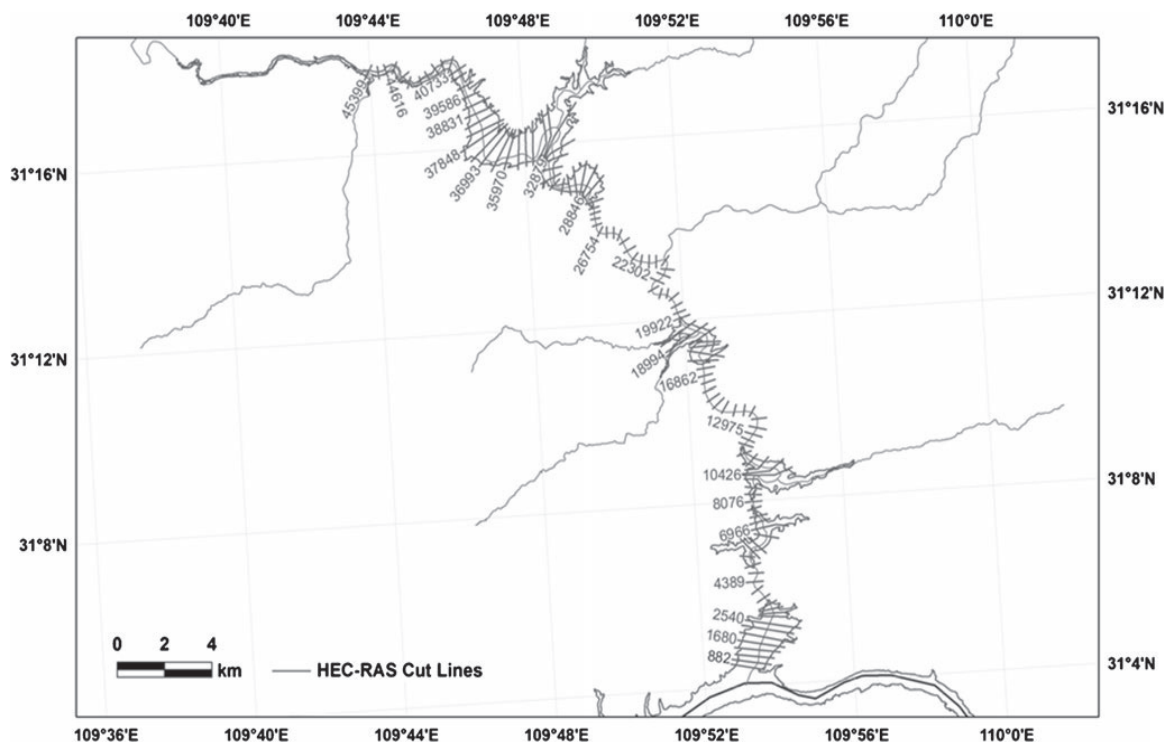


Fig. 5 Map of the Daning River including the Dachang Lake divided by 125 cutlines that are interconnected but modeled separately

available; the maximum formation rates are known to reach approximately 26 % of the concentration of the parent substance in rice paddy soils (Chisaka and Kearney 1970). Having fixed the initial surface water concentration of the three model substances, the concentrations have been multiplied by a factor of 100 to reflect heavy overuse. Overuse of pesticides is known to be a common problem in rural areas of China (Yang et al. 2008).

Chemical properties of the parent pollutant and its metabolites

Like other dichloropropionanilide pesticides, propanil is readily cleaved to release 3,4-DCA which subsequently, catalyzed by oxidative enzymes, such as lignin peroxidase in soils, forms TCAB (Pieper et al. 1992). 3,4-DCA is also formed by degradation of phenyl-carbamates, phenylureas, and other acylanilides and represents a “priority pollutant” (Ashauer et al. 2010). Although the formation rate of TCAB in soils varies greatly, probably due to different oxidation states of the soils, many studies revealed quite high TCAB concentrations in soils. Chisaka and Kearney (1970) reported the percent conversion of propanil to TCAB in five soils with similar physico-chemical properties varied between 1.3 and 26.2 %. This was if propanil has been applied at 850 ppm. At lower application rates of propanil (85 ppm), the TCAB conversion rate varied between 1.0 and 18.6 %. TCAB seems to be

persistent in the environment. During the incubation period of 105 days in the latter experiment, TCAB was not degraded. However, specific information of the fate of TCAB in soils and sediment is not available. TCAB in nutrient solution is absorbed by rice plants (5–6 % of the amount applied to soil of which less than 10 % is transported to the shoots). From rice treated with propanil and with 3,4-DCA, however, no TCAB can be isolated (Still 1969). Soya beans resorb TCAB from soils. Roots of plants grown in a soil with 1.7 % organic matter and treated with 10 mg/kg TCAB reach levels above 50 mg/kg, while in the shoots TCAB concentrations are lower (<1 mg/kg) (Worobey 1984). Trans-TCAB is taken up from soils by carrots (Worobey 1988) that has been incubated with 0.02 and 10 mg/kg a.i. Residues in the plants are highest in the carrot peels (1.9 and 375 µg/kg, respectively). Many reports are available that prove the high mutagenic, cancerogenic and toxic activity of TCAB for which a reactive arene oxide intermediate mediated by oxidative enzymes has been proposed as responsible mediator (Witt et al. 2000; Van Birgelen et al. 1999; Allison and Morita 1995; Hsia and Kreamer 1981). Polychlorinated trans-azobenzenes in their stereo configuration and toxicity resemble some of highly toxic planar polychlorinated dibenzo-*p*-dioxins. It is interesting to note that the chemical stability and toxicity of the chlorinated trans-azobenzenes are considered more relevant than that of the corresponding *cis*-analogues (Wilczynska et al. 2006). Our own experiments in

synthesizing TCAB by both enzymatic reaction (horse-radish peroxidase) and chemical oxidation (MnO_2) reveal that both isomers are formed in various ratios, most often in favor of the trans-product (Fig. 6).

3,4-DCA is quite well water soluble (0.58 g/L at 20 °C; $\log P_{\text{OW}}=2.7$, European Chemicals Bureau 2006). The compound has a low Henry's law constant ($0.05 \text{ Pa}\times\text{m}^3\times\text{mol}^{-1}$), a low potential for abiotic hydrolysis but is prone to be degraded by photolysis in surface waters. The biodegradation rate of 3,4-DCA is low but the reactivity to form covalent bonds in humic matter is high. Thus, the concentration of 3,4-DCA residues in soil and sediment is expected to be high (e.g., in milligrams per kilogram quantities as calculated from typical application and production rates of 3,4-DCA and corresponding pesticides). 3,4-DCA releasing pesticides therefore form high amounts of nonextractable residues (NER), probably due to the binding of chloroaniline to humic matter. However, there is no experimental proof for this hypothesis. Neither is it known whether NER in soils and sediments contain incorporated TCAB. In Table 1, the physicochemical properties of propanil, 3,4-DCA and TCAB are summarized as calculated by the structure activity model ChemProp (Schüürmann et al. 1997, 2007). It is obvious, that bioaccumulation of the final metabolite TCAB is most relevant while that of propanil and 3,4-DCA is low. However, bioaccumulation data for aquatic and terrestrial organisms, the ecotoxicological profile and the fate of TCAB in the environment are largely unknown.

Data input for simulation setup (localization)

SDM—localized site properties

Site-specific variables as surface water temperatures have been measured in time-series during the MINIBAT (Stüben et al. 1998; Casagrande 1995) sampling campaigns combined with point estimates of own sampling campaigns. The data serve as input for the modified AQUATOX model (Table 2). The joint MINIBAT project contributed nutrient measures also (NO_3^- , total phosphorus). For each of the pollution scenarios in the Wushan region, the parameters have been calculated separately. For each scenario segment, the corresponding MINIBAT measurements are averaged

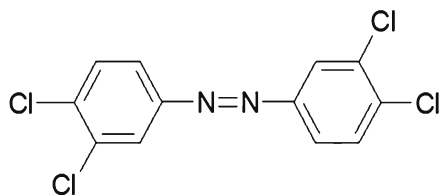


Fig. 6 Isomers of TCAB formed by enzymatic and chemical dimerization of 3,4-DCA

for the upper 1-m water layer. The data are partly imported into the AQUATOX simulation as fixed site-specific state variables directly, and partly converted into compatible units (i.e., chlorophyll *a* concentration is converted to primary producer's biomass (Desortova 1981)). State variables like annual mean radiation and the limits of air and water temperature variation determine the maximum rates of photosynthesis in the AQUATOX model. The annual radiation has been taken from Chen et al. (2001).

FWM—food web

The food-related interactions within a community can be represented by a simple food chain. The energy fixed by primary producers is transferred to the highest trophic level in distinct steps. All organisms of a “trophic level” in a food web share the same number of transfer processes their diet passed through (Schwoerbel 1999). In our approach, for each of the trophic levels only one species or guild is listed (Figs. 7 and 8). In our studies, we use a food web with four trophic levels. The composition of the TGR biocoenoses is expected to be a mixture of the typical coenoses of flowing and stagnant waters. According to a time scale for the succession of communities of aquatic organisms with relatively short generation times, the recently impounded reservoir is assumed to be in a steady state already. Clear changes of, e.g., the nutrient status and the algal communities have been recorded immediately after impounding within a period of one year (Dai et al. 2010). For this reason *two basic simulations*, one representative for a “reservoir” and one for “river,” including different food webs and flow conditions have been set up. A food web consists of a typical structure marked by hierarchical guilds. The energy flows from the primary producers (algae and macrophytes) to the primary consumers (invertebrate feeders and planktivorous fishes), and then to the first order predators (predatory or omnivorous fishes). The arrows in Figs. 7 and 8 point from predator to prey, as indicated. Second order predatory fishes or mammals are not included in our sketches of the TGR food webs, because it is not expected that typical predators like the Chinese Sturgeon (*Acipenser sinensis*) or the Yangtze Dolphin (*Lipotes vexillifer*) have a significant influence on the Yangtze ecosystems. These species are critically endangered and close to extinction since a long time (Xie 2003; IUCN 2012). In our system, secondary predator-like effects are represented by human fishing and piscivorous birds. Species names are meant to be common representatives of a trophic guild, combined with a distinct taxonomical group. The trophic group of primary producers is represented in Fig. 8 by the green algae *Scenedesmus arctuatus*. The predefined food web has thus been simplified in the way that information has been reduced from “species level” to “guild level” and typical surrogate species for the TGR have been chosen.

Table 1 Chemical properties of model substances

Property	Propanil	3,4-DCA	TCAB
CAS No.	709-98-8 ^e	95-76-1 ^c	14047-09-7
Molecular weight (g/mol)	218.1	162.02	320
Octanol (oc)–water partitioning coefficient log K_{ow} (mol/mol)	2.29 ^c	2.69 ^c	5.84 ^a
Henry law constant log K_{aw} (dimensionless)	-7.53 ^j	-4.47 ^j	-3.74 ^k
Soil sorption log K_{OC} (L (water)/kg (oc))	2.17 ^c	2.68 ^c	4.47 ^b
Water solubility (mg/L) at 20°C	95 ^c	580 ^c	0.04 ^d
Bioconcentration factor (log BCF)	1.75 (uncertainty 0.25) ^f	1.37 (uncertainty 0.2) ^f	4.52 (uncertainty 0.5) ^f
Bioaccumulation factor (log BAF)	1.66 ^g	1.56 ^g	5.74 ^g
Fish toxicity fathead minnow (log LC_{50} mol ⁻¹ l ⁻¹)	-4.60 ^c	-4.57 ^c	-7.04 ^h
Mutagenicity	No ^c	No ^c	Yes ⁱ

Values set in italics are estimated by ChemProp Ver. 5.2.8, UFZ Department of Ecological Chemistry (2012), basically described by Schüürmann et al. (1997, 2007)

^a Estimated by class-based model selection, selected model: Hou and Xu (2003)

^b Estimated as mean value via decision tree by Sabljic et al. and according to LSER Poole and Poole (1999)

^c Read across from ACF (UFZ set, ACF similarity=1)

^d Estimated by ACF-based model selection, selected model: Klopman and Zhu (2001)

^e Source: PPDB (2009)

^f Estimated for fish from K_{ow} according to Mackay (1982)

^g Estimated according to Arnot and Gobas (2003)

^h Estimated from ECOSAR type model: 96-h log LC_{50} for fish according to Nabholz and Mayo-Bean (2009)

ⁱ Predicted according to Kazius et al. (2005) and Benigni and Bossa (2008)

^j Read across from ACF (UFZ set, chemical domain=in)

^k Estimated according to Meylan and Howard (1991) (bond 2.6)

Fishes

The fish surrogate species are chosen according to the number of relevant literature entries and their economic importance. Many references mention the four main “Asian carp” species (Wanner and Klumb 2009; Kocovsky et al. 2012), which shows the particular commercial meaning of those species in the TGR region (Zhang et al. 2012; Duan et al. 2009; Yi et al. 2010). Namely, these are *Ctenopharyngodon idella* (grass carp), *Mylopharyngodon piceus* (black carp), *Hypophthalmichthys molitrix* (silver carp), and *Hypophthalmichthys nobilis* (bighead carp).

Although the four species belong to the family of cyprinids (order cypriniformes), they show different behaviors and body masses (Table 3). While the grass carp is herbivorous and prefers to live near the river bank, silver and bighead carp stay in deeper waters where they feed on plankton. The black carp lives near the bottom and its diet mainly consists of molluscs (Yi et al. 2010; Duan et al. 2009). Additionally, two further common non-cyprinid fish species are chosen, namely *Tachysurus fulvidraco* (yellowhead catfish) and *Monopterus albus* (Asian swamp or rice field eel). The two latter species have been integrated in the simulations for having at least one bottom dwelling fish species with close contact to the sediment and thus connected to the resuspension of toxicants from the sediment. Secondary predatory fishes have been substituted by fishing pressure (approximately 100 kg fish/fisherman in the Kaixian area) and by piscivorous birds as mentioned above.

Algae and macrophytes

The feeding preferences of fishes and invertebrates have been analyzed for the identification of the most important groups of algae and macrophytes as primary producers. The occurrence of the above species in the study area, the

Table 2 Physicochemical variables measured by the MINIBAT

Endpoint	Unit
Water level	Meter
Water temperature	°C
Water depth	Meter
Conductivity	μS/cm
Turbidity	% base saturation
Chlorophyll <i>a</i>	μg/L
pH	Unitless
Oxygen	Backscatter %

Units have been converted to AQUATOX-compatible values where necessary

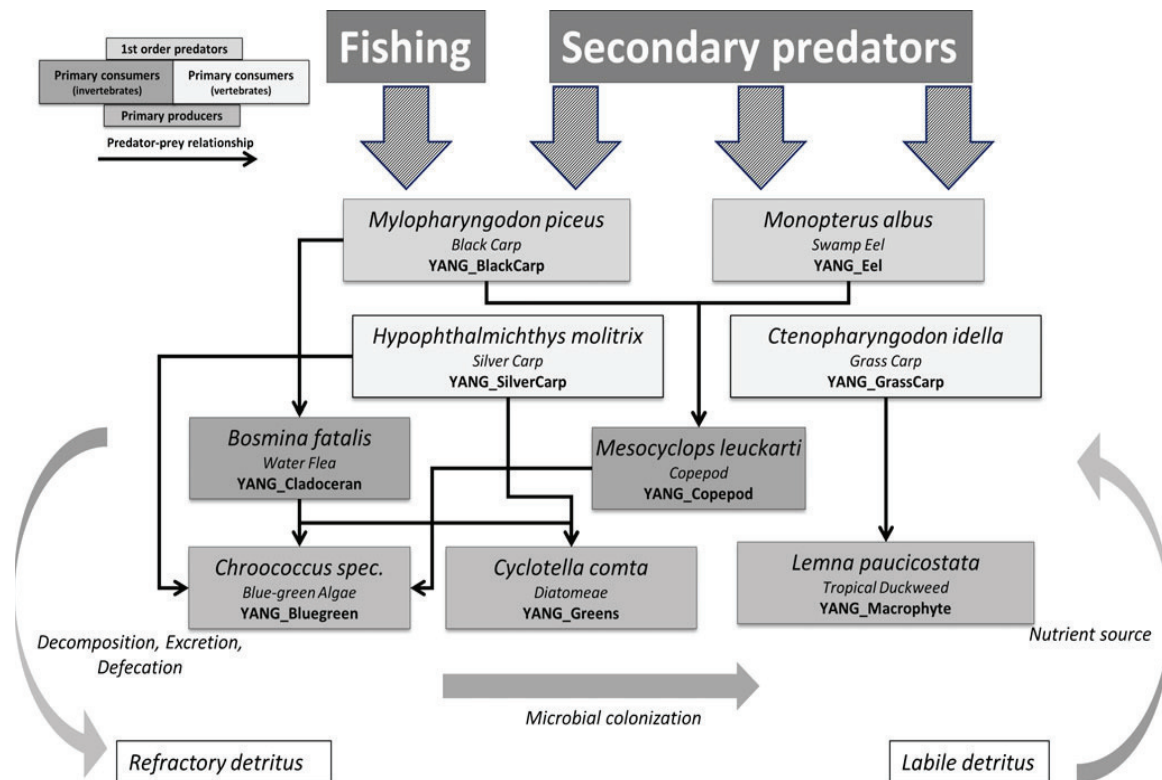


Fig. 7 The simplified “connectedness” food web of the reservoir simulation as implemented in the AQUATOX model. Arrows point from predators to prey

Yangtze River and its tributaries has been acquired. For each of the taxonomic groups and for each of the pollution scenarios, one representative has been chosen and implemented into the AQUATOX simulations. The green algae are represented by *S. arcutatus*, the diatoms by *Cyclotella comta* (reservoir scenario) and *Melosira granulata* (river scenario). The surrogate species for the group of cyanobacteria that cause particular problems in the region associated with progressing eutrophication are *Microcystis* sp. (river scenario) and *Chroococcus* sp. (reservoir scenario) (Kawanabe 1996). In the food web, the algae are fed upon by phyto-planktivorous fishes, e.g., silver carp and by invertebrates (Liu and Wang 2008; Calkins et al. 2012). The macro-herbivorous grass carp needs macrophytes, in this case *Lemna paucicostata* in its diet.

Zooplankton and molluscs

Zooplankton organisms are chosen by their occurrence in the lakes and rivers of the study area as well as by the food preferences of the fishes. One surrogate species that can stand for the focused taxonomic groups has been integrated in the model food webs. The cladocerans *Daphnia magna*

(river scenario) and *Bosmina fatalis* (reservoir scenario) serve as food for the zooplanktivorous fishes (Kawanabe 1996). *Corbicula fluminea* is a common mollusc species in the study area (Xia et al. 2006). Additionally, insect larvae (*Chironomus* sp.) and copepods (*Mesocyclops leuckarti*) are introduced as food, e.g., the swamp eel (Yang et al. 1997).

Interactions

After identifying surrogate species for the set up of the specific food webs “river” and “reservoir,” predator–prey relationships and food intake rates have been estimated from literature (e.g., Cui et al. 1992). The grass carp has been artificially introduced in the past into Chinese surface waters to reduce the densities of macrophytes (Kirkağac and Demir 2006; Krupska et al. 2012). For this reason, in our approach it is assigned to feed exclusively on the macrophyte *L. paucicostata*. Several studies have shown that silver carps feed on more than one trophic level and the species has already been deployed to control algal growth in experimental ponds (Kocovsky et al. 2012; Calkins et al. 2012). This information is used to connect the silver carp to the trophic levels of primary producers and

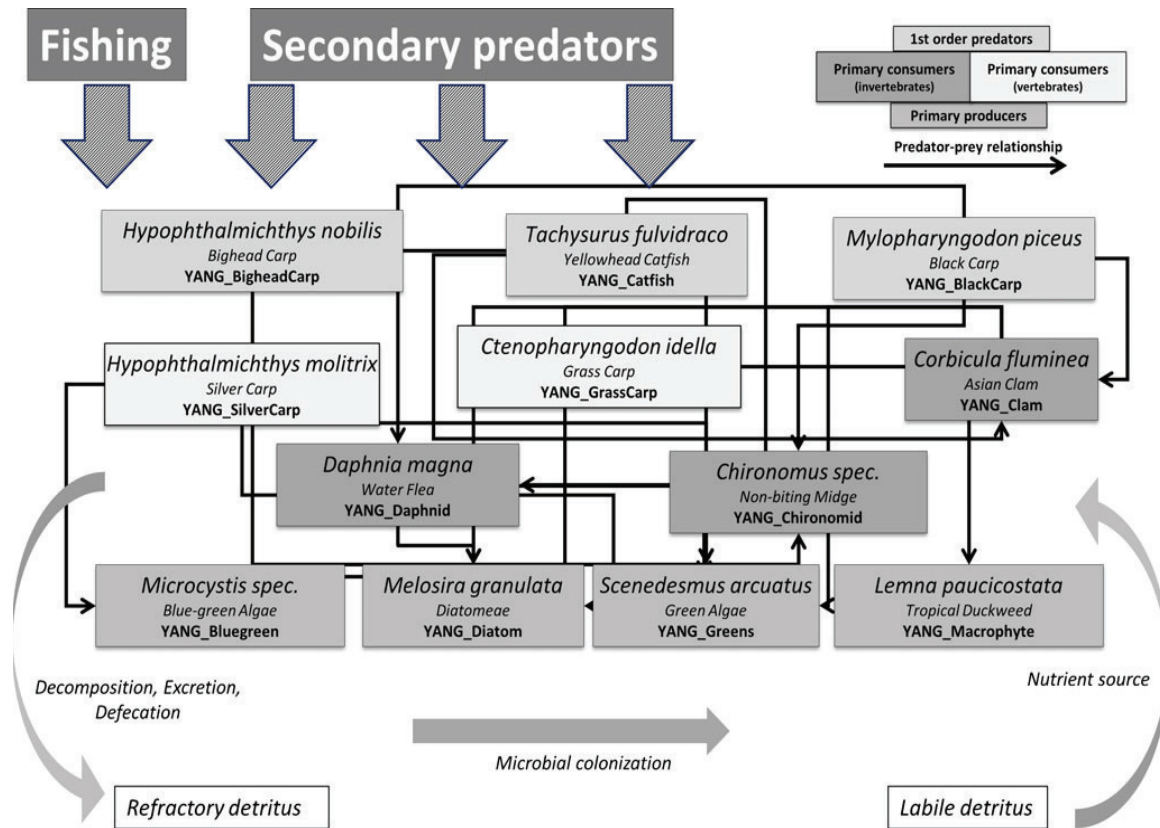


Fig. 8 The simplified “connectedness” food web of the river simulation as implemented in the AQUATOX model. Arrows point from predators to prey

primary consumers within the food webs. The bighead carp shows a similar behavior as it feeds on zooplankton organisms also. However, alternatively it can use phytoplankton and cyanobacteria as food sources in case of zooplankton deficiency (Kocovsky et al. 2012; Zhou et al. 2009). The black carp mainly feeds on mussels and molluscs. At some places, it is used as a pest control against molluscs (Wui and Engle 2007). *T. fulvidraco* feeds mainly on mussels and bottom-bound insect larvae (trichopterans, chironomids, referred to Froese and Pauly 2012). The carnivorous swamp eel feeds on worms and crustaceans, in our model represented by the copepod *M. leuckarti* (Yang et al. 1997). A complex detrital

side chain is implemented in the model. Physiological parameters that could not be estimated from literature data are taken from the original AQUATOX model environment for similar closely related species.

Bioaccumulation and ecotoxicity

The chemical properties of the model substance, as well as the (initial) concentrations of the pollutants (propanil and its metabolites) have been described according to the procedures of module EXM. The way how pollutants enter the (species) components of food webs, how they distribute

Table 3 Characteristics of fish species represented in the food webs of the river and reservoir simulation scenarios

Species	Habitat	Food preferences
<i>Ctenopharyngodon idella</i> (grass carp)	Litoral zone	Herbivorous (macrophytes)
<i>Hypophthalmichthys molitrix</i> (silver carp)	Upper water layer	Phyto- and zooplanktivorous
<i>Hypophthalmichthys nobilis</i> (bighead carp)	Upper water layer	Phyto- and zooplanktivorous
<i>Mylopharyngodon piceus</i> (black carp)	Deeper water layer	Molluscs
<i>Tachysurus fulvidraco</i> (yellowhead catfish)	Bottom layer	Molluscs and insects
<i>Monopterus albus</i> (Asian swamp eel)	Bottom layer	Worms and crustaceans

within the organisms and how they are eliminated from the tissues, crucially affects the biomagnification on the organism level in the module Toxic effects from the ETM module can veil the bioaccumulation procedures of BAM and reduce the individual fitness of the focused species.

BAM—bioaccumulation

The bioaccumulation mainly depends on the chemical properties of the model substances, mainly the octanol–water coefficient ($\log K_{OW}$) and the organism-specific routes of exposure and uptake. Park and Clough (2010) estimated the bioaccumulation by empirical regressions, which highly depends on the lipid content of an organism and varies greatly between algae, detritus, macrophytes, invertebrates, and fish. Under *steady-state conditions*, the AQUATOX model uses bioconcentration factors BCF (synonym: bioaccumulation factor BAF) to describe the partition between the organism tissues and the surrounding water. These factors are in particular used here to describe the internal toxicity of pollutants in aquatic organisms. Empirical regression equations and the $\log K_{OW}$ serve as the predictors of bioaccumulation. The coefficients are taken from literature, or they are calculated by the AQUATOX model based on the chemical properties of the model substances. The partition coefficients for detritus are estimated based on assumptions by Abbott et al. (1995) and Schwarzenbach et al. (1993). The partition coefficients used in AQUATOX for macrophytes and algae are taken from Gobas et al. (1991) and Koelmans and Heugens (1998), respectively. Coefficients for invertebrates are derived from Southworth et al. (1978) and Lyman et al. (1982). In the case of short exposure times, no equilibrium can be assumed and thus no steady-state partition coefficients are used but the kinetic processes are modeled. In our studies, we focus on the bioaccumulation in fish. Uptake pathways via gills and diet are considered by the model, using respiration and ingestion rates. The basic equations for fishes are taken from Park and Clough (2010).

ETM—ecotoxicity

The MICROTOX project focuses on the herbicidal model substance propanil. The ecotoxicological properties of the parent and its metabolites 3,4-DCA and TCAB are evaluated because of their relevance for the environmental risk assessment (propanil and 3,4-DCA) and the assumptive persistence (TCAB). While 3,4-DCA is very well described and a number of data are available in the public domain, studies on propanil have been mainly filed in the context of the Annex-I inclusion during the registration process of propanil for the use as a herbicidal substance in the European Union. For the estimation of toxic effects from

exposure to propanil, 3,4-DCA and TCAB, the most sensitive endpoints have been taken from the DAR of propanil (Ministry of Health of Italy 2006; Table 4). The rationale behind the choice is not to find the most relevant effect concentration regarding taxonomical or distributional characteristics of the species that are found to fit our Yangtze food web but to depict a worst-case threshold. In case the pollution scenarios deliver very high concentrations, it is assumed that complete extinctions of sensitive species could occur. As propanil inhibits the photosynthesis of higher plants and algae (disruption of Hill's reaction as herbicidal mode of action, Corbett et al. 1984), it is expected that aquatic plants, algae or macrophytes are the most sensitive species. Some different modes of action of 3,4-DCA are known from human risk assessments, referring to *in vitro* and *in vivo* experiments with mammals other than humans. Beyond its unspecific polar narcotical mechanism of action, it acts as an antagonist of the androgynous receptor of rats, thus being an endocrine disruptor (Cook et al. 1993). A further specific mechanism of action of 3,4-DCA is the formation of methaemoglobin based on hydroxylated compounds (compare, e.g., Lenk and Sterzl 1984).

Outlook

Improvement of scenarios

The simulation environment will be improved in the future for all modules of the integrative modeling approach. Further regionalization, e.g., by using real initial biomasses other than the default assumptions (validated scenarios of “Cheney Reservoir” and “Rum River”), will be achieved in cooperation with sub-projects of the German Yangtze environmental program and the Chinese project partners. Up to now, initial algal biomasses are derived from measured chlorophyll *a* concentrations using the empirical relationships described by Desortova (1981). Nevertheless, consultations with Chinese experts at a project related workshop in Shanghai 2012 already revealed the high degree of accuracy and relevance of the abstracted food webs, which contain surrogate species for trophic guilds.

In the course of further studies, we will also broaden the sub-model implementation beyond the scope of the data included in the manuscript at hand. For example, the spatial distribution of tracer particles, predicted by the particle transport module (PTM), will be used to provide spatially explicit information about the distribution of pollutants within the water bodies. Tracer particles thereby represent detritus particles or plankton organisms that are subjected to passive drift even under the new and reduced TGR flow conditions and thus constantly loaded with organic (model) substances. Using this approach, we are able to describe the

Table 4 Toxicity endpoints for aquatic species relevant for the toxicity of individual surrogate species of the “river” and “reservoir” scenarios and for ERA of the model substances propanil, 3,4-DCA and TCAB

Test species	Endpoint	Effect measure (exposure period)	Effect concentration	Unit
Propanil				
Acute				
<i>Cyprinodon variegatus</i> (sheepshead minnow)	Mortality	LC ₅₀ (96 h)	4.6	mg/L
<i>Navicula pelliculosa</i>	Growth rate	EC ₅₀ (72 h)	0.025	mg/L
<i>Anabaena flos-aquae</i>	Growth rate	EC ₅₀ (96 h)	0.070	mg/L
<i>Lemna gibba</i>	Growth rate	EC ₅₀ (14 days)	0.11	mg/L
<i>Daphnia magna</i>	Immobilization	LC ₅₀ (48 h)	6.7	mg/L
Long term				
<i>Pimephales promelas</i> (fathead minnow)	Weight and length of fry	NOEC (35 days; early life stage)	0.019	mg/L
<i>Daphnia magna</i>	Immobilization	NOEC (21 days)	0.086	mg/L
<i>Chironomus riparius</i>	Emergence	NOEC (28 days; full life cycle (spiked sediment))	16	mg as/kg dw sediment
<i>C. riparius</i>	Emergence	NOEC (28 days; full life cycle (spiked water))	1.9	mg/L
3,4-DCA				
Acute				
<i>Oncorhynchus mykiss</i> (rainbow trout)	Mortality	LC ₅₀ (96 h)	1.9	mg/L
<i>D. magna</i> (water flea)	Immobilization	LC ₅₀ (48 h; acute)	0.012	mg/L
<i>Pristina longiseta</i>	Mortality	LC ₅₀ (96 h)	2.5	mg/L
<i>Phaeodactylum tricornutum</i>	Growth rate	E _r C ₅₀ (96 h)	0.45	mg/L
<i>C. riparius</i>	Growth and mortality	LC ₅₀ (10 days)	450	mg/kg dw sediment
Long term				
<i>Peocilia reticulata</i> (guppy)	Number of offspring in F1	NOEC (42 days)	<0.002	mg/L
<i>Ceriodaphnia quadrangula</i>	Reproduction	NOEC (21 days)	0.002	mg/L

Data taken from Ministry of Health of Italy (2006). For results of QSAR estimations for the propanil metabolite TCAB, refer to Table 1

toxic effects of model pollutants on populations and aquatic communities. The realistic worst-case exposition is estimated in the EXM and can flexibly be used to conduct dose–response experiments using simulation output data. First numerical experiments reveal that the surface water concentrations vary between very low loads, in particular at sites where the pollutants are suspected to be diluted, to very high concentrations in scenarios where heavy overuse is assumed and the water is stagnant.

Statistical analysis of simulation outputs

After completion of scenarios and running the final simulations (according to Fig. 3), the output of simulations will be analyzed statistically (Fig. 9). The effects on populations will be described by univariate test statistics, e.g., by fitting dose response curves and deriving EC₅₀ effect concentrations. Multivariate statistics will be used to calculate community-based effect thresholds from the time series, e.g., by principal

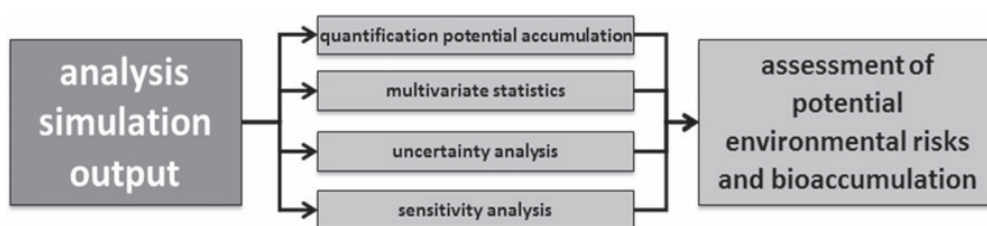


Fig. 9 Analysis of the model output. Workflow of bioaccumulation studies. A step-wise procedure for the definition of necessary input data to conduct sound simulation experiments is established

response curve analysis (Van den Brink and Ter Braak 1999). Furthermore, the AQUATOX model provides the opportunity to estimate uncertainties of simulation outputs and to quantify the most sensitive variables within the model. Using sensitivity analysis, the hypothesis that altered nutrient regimes or flow conditions of the newly built TGR severely and significantly affect the composition of the aquatic communities and the bioaccumulative processes will be tested. The food web will be further analyzed according to the proposal of Preziosi and Pastorok (2008).

Specification of ecological and human risk assessment

The indicators of environmental and consumer risks from the model pollutants will be further defined in RAM. This includes the definition of risk management measures, suitable for the overall aims of the Yangtze-Hydro environmental program, i.e., giving purposeful recommendations for the melioration of the TGR's water quality where appropriate. At this stage of our studies, it can already be stated that the criteria and parameters used in the model are suitable to distinguish between realistic ecological, toxicological and hydrological scenarios for the TGR situation possibly posing risks to communities of aquatic organisms as well as to consumers. Having finally identified the most critical scenarios, our approach can be used to recommend specific management actions to reduce the pollution loads in sensitive areas, e.g., by the prevention of pesticide overuse and establishment of waste water treatment plants. Furthermore, the emphasis of the risk assessment procedures is on concrete recommendations for consumers, e.g., to give advice how to avoid excess exposure by high pollutant burdens of food, especially fish.

In case of exceeded triggers, appropriate risk management measures will be subjected. In the above context, the use of internal concentrations in the AQUATOX program enables to calculate probabilities of toxic effects and risk.

The potential bioaccumulation of important food sources (e.g., the “Chinese carps”) will be compared with ADI for chronic exposure as deduced from the ERA of the model substance propanil and its metabolites under the different pollution scenarios and under the regulation 91/414/EEC regarding the registration of plant protection products in the European Union. Finally, risk maps of a regarded region will be drawn based on time series data from the PTM.

Integrated environmental modeling

The integrated modeling approach can be described as a hybrid model as it combines and couples several methodologies under the AQUATOX framework. The modules are

either of general static nature and defined by expert knowledge to provide suitable input values for existing submodel structures (e.g., species composition and interaction matrices within the food web model), spatially explicit and dynamical (like the hydrodynamic model providing time-variant flow conditions as simulation input) or theory-based and mechanistic (e.g., the bioaccumulation model to calculate the uptake). They are also statistical and probabilistic (like the regression or classification-based QSAR models within the ecotoxicological model to estimate chemical properties of metabolites) or synthetic (like the risk assessment module).

As this modeling approach combines theoretical models, empirical data, and expert knowledge to describe the TGR ecosystem, it is in accordance with the concept of IEM, which is of increasing importance in modern environmental management and decision-making (Jopp et al. 2011). It allows for the interpolation of information on ecosystem behavior on a local level, as well as for the extrapolation and transfer of results to other locations, to different scenarios and into the future.

Acknowledgments Our study has been carried out as part of the project MICROTOX (“Transformation, Bioaccumulation and Toxicity of Organic Micropollutants in the Yangtze Three Gorges Reservoir” which is integrated into the joint environmental research program “Yangtze-Hydro-sustainable Management of the Newly Created Ecosystem at the Three Gorges Dam” (Bergmann et al. 2012, www.yangtze-project.de). The project has been financed by the Federal Bureau of Education and Science of Germany (BMBF) as part of the research cluster “Pollutants/Water/Sediment—Impacts of Transformation and Transportation Processes on the Yangtze Water Quality.”

References

- Abbott JD, Hinton SW, Borton DL (1995) Pilot scale validation of the river/fish bioaccumulation modeling program for non-polar hydrophobic organic compounds using the model compounds 2,3,7,8-TCDD and 2,3,7,8-TCDF. *Environ Toxicol Chem* 14:1999–2012
- Allison G, Morita M (1995) Bioaccumulation and toxic effects of elevated levels of 3,3',4,4'-tetrachloroazobenzene (33'44'-TCAB) towards aquatic organisms. II: Bioaccumulation and toxic effects of dietary 33'44'-TCAB on the Japanese medaka (*Oryzias latipes*). *Chemosphere* 30:223–232
- Argent RM (2004) An overview of model integration for environmental applications—components, frameworks and semantics. *Environ Modell Softw* 19:219–234
- Arnot JA, Gobas FAPC (2003) A generic QSAR for assessing the bioaccumulation potential of organic chemicals in aquatic food-webs. *QSAR Comb Sci* 22:337–345
- Ashauer R, Caravatti I, Hintermeister A, Escher BI (2010) Bioaccumulation kinetics of organic xenobiotic pollutants in the freshwater invertebrate *Gammarus pulex* modeled with prediction intervals. *Environ Toxicol Chem* 28:1625–1636
- Benigni R, Bossa C (2008) Predictivity of QSAR. *J Chem Inf Model* 48:971–980

- Bergmann A, Bi Y, Chen L, Floehr T, Henkelmann B, Holbach A, Hollert H, Hu W, Kranzloch I, Klumpp E, Küppers S, Norra S, Ottermanns R, Pfister G, Roß-Nickoll M, Schäffer A, Schleicher N, Schmidt B, Scholz-Starke B, Schramm KW, Subklew G, Tiehm A, Temoka C, Wang J, Westrich B, Wilken RD, Wolf A, Xiang X, Yuan Y (2012) The Yangtze-Hydro Project: a Chinese-German environmental program. *Environ Sci Pollut Res* 19:1341–1344
- Bunn SE, Arthington AH (2002) Basic principles and ecological consequences of altered flow regimes for aquatic biodiversity. *Environ Manag* 30:492–507
- Calkins HA, Tripp SJ, Garvey JE (2012) Linking silver carp habitat selection to flow and phytoplankton in the Mississippi river. *Biol Invasions* 14:949–958
- Casagrande CE (1995) The MiniBAT—a miniaturized towed sampling system. *OCEANS '95. MTS/IEEE. Challenges of our changing global environment. Conference Proc* 1:638–641
- Chen Z, Li J, Shen H, Zhanghua W (2001) Yangtze River of China: historical analysis of discharge variability and sediment flux. *Geomorphology* 41:77–91
- China Three Gorges Corporation (2010) Annual Report 2009. Available from http://www.ctgpc.com/file/Annual_Report_2009.pdf. Accessed August 2012
- Chisaka H, Kearney PC (1970) Metabolism of propanil in soils. *J Agric Food Chem* 18:854–858
- Cook JC, Mullin LS, Frame SR, Biegel LB (1993) Investigation of a mechanism for Leydig cell tumorigenesis by linuron in rats. *Toxicol Appl Pharmacol* 119:195–204
- Corbett JR, Wright K, Baillie AC (1984) The biochemical mode of action of pesticides. Academic, London
- Cui Y, Liu X, Wang S, Che S (1992) Growth and energy budget in young grass carp, *Ctenopharyngodon idella* Val., fed plant and animal diets. *J Fish Biol* 41:231–238
- Dai H, Zheng T, Liu D (2010) Effects of reservoir impounding on key ecological factors in the Three Gorges Region. *Procedia Environ Sci* 2:15–24
- Desortova B (1981) Relationship between chlorophyll-*a* concentration and phytoplankton biomass in several reservoirs in Czechoslovakia. *Int Rev Ges Hydrobiol* 66:153–169
- DLR-German Aerospace Center (2000) Global land survey digital elevation model. Available from http://www.dlr.de/eoc/en/desktopdefault.aspx/tabid-5515/9214_read-17716/. Accessed October 2012
- Duan X, Liu S, Huang M, Qiu S, Li Z, Wang K, Chen D (2009) Changes in abundance of larvae of the four domestic Chinese carps in the middle reach of the Yangtze river, China, before and after closing of the Three Gorges Dam. *Env Biol Fish* 86:13–22
- Echeverría M, Wellman M, Park R, Clough J (2003) Evaluation of AQUATOX for ecological risk assessments in the U.S. EPA Office of Pesticide Programs. SETAC NA 24th Annual Meeting in North America, Austin, Texas.
- European Chemicals Bureau (2006) European Union risk assessment report—3,4-dichloroaniline (3,4-DCA). 3rd priority list. Volume 65. ISSN 1018-5593.
- FOCUS (2001) FOCUS surface water scenarios in the EU evaluation process under 91/414/EEC. Report of the FOCUS Working Group on Surface Water Scenarios, EC Document Reference SANCO/4802/2001—rev.2.
- Foo KY, Hameed BH (2010) Insights into the modeling of adsorption isotherm systems. *Chem Eng J* 156:2–10
- Froese R, Pauly D (eds.) (2012) FishBase. World Wide Web electronic publication. <http://www.fishbase.org>, update ver. (accessed October 2012).
- Gobas FAPC, McNeil EJ, Lovett-Doust L, Haffner GD (1991) Bioconcentration of chlorinated aromatic hydrocarbons in aquatic macrophytes (*Myriophyllum spicatum*). *Environ Sci Technol* 25:924–929
- Hervouet JM (2007) Hydrodynamics of free surface flows: modelling with the finite element method. Wiley, New York
- Hisschemöller M, Tol RSJ, Vellinga P (2001) The relevance of participatory approaches in integrated environmental assessment. *Integr Assess* 2:57–72
- Hou TJ, Xu XJ (2003) ADME evaluation in drug discovery. 2. Prediction of partition coefficient by atom-additive approach based on atom-weighted solvent accessible surface areas. *J Chem Inf Comp Sci* 43:1058–1067
- Hsia MT, Kreamer BL (1981) Metabolism studies of 3,3',4,4'-tetrachloroazobenzene. I. In vitro metabolic pathways with rat liver microsomes. *Chem-Biol Interact* 34:19–29
- IUCN (2012) The IUCN red list of threatened species. Version 2012.2. Available from <http://www.iucnredlist.org>. Accessed October 2012
- Jopp F, Breckling B, Reuter H, DeAngelis DL (2011) Perspectives in ecological modelling. In: Jopp F, Reuter H, Breckling B (eds) *Modelling complex ecological dynamics*. Springer, Berlin, pp 341–347
- Kawanabe H (1996) Asian great lakes, especially lake Biwa. *Env Biol Fish* 47:219–234
- Kazius J, McGuire R, Bursi R (2005) Derivation and validation of toxicophores for mutagenicity prediction. *J Med Chem* 48:312–320
- Kirkağac MU, Demir N (2006) The effects of grass carp (*Ctenopharyngodon idella* Val., 1844) on water quality, plankton, macrophytes and benthic macroinvertebrates in a spring pond. *Turk J Fish Aquat Sci* 6:7–15
- Klopman G, Zhu H (2001) Estimation of the aqueous solubility of organic molecules by the group contribution approach. *Journal of Chemical Information and Computer Science* 41: 439–445. Errata: 2001, 41: 1096–1097.
- Kocovsky PM, Chapman DC, McKenna JE (2012) Thermal and hydrologic suitability of Lake Erie and its major tributaries for spawning of Asian carps. *J Great Lakes Res* 38:159–166
- Koelmans AA, Heugens EHW (1998) Binding constants of chlorobenzenes and polychlorobiphenyls for algal exudates. *Water Sci Technol* 37:67–73
- Krupska J, Pelechaty M, Pukacz A, Ossowski P (2012) Effects of grass carp introduction on macrophyte communities in a shallow lake. *Oceanol Hydrobiol Stud* 41:35–40
- Labrada R (2003) The need for improved weed management in rice. FAO: Proceedings of the 20th Session of the International Rice Commission (Bangkok, Thailand, 23–26 July 2002). Available from <http://www.fao.org/docrep/006/y4751e/y4751e00.htm>. Accessed October 2012
- Lei B, Huang S, Qiao M, Li T, Wang Z (2008) Prediction of the environmental fate and aquatic ecological impact of nitrobenzene in the Songhua River using the modified AQUATOX model. *J Environ Sci* 20:769–777
- Lenk W, Sterzl H (1984) Peroxidase activity of oxyhaemoglobin in vitro. *Xenobiotica* 14:581–588
- Liu XQ, Wang HZ (2008) Food web of benthic macroinvertebrates in a large Yangtze River-connected lake: the role of flood disturbance. *Fund Appl Limnol (Archiv für Hydrobiologie)* 171:297–309
- Lyman WJ, Reehl WF, Rosenblatt DH (1982) Handbook of chemical property estimation methods. McGraw-Hill, New York
- Mackay D (1982) Correlation of bioconcentration factors. *Environ Sci Technol* 16:274–278
- McAllister DE, Craig JF, Davidson N, Delany S, Seddon M (2001) Biodiversity Impacts of Large Dams. Background Paper Nr. 1. Prepared for IUCN/UNEP/WCD.
- Med-Rice (2003) Guidance document for environmental risk assessments of active substances used on rice in the EU for Annex-I-

- inclusion. Final Report of the Working Group 'MED-RICE' prepared for the European Commission 1 in the framework of Council Directive 91/414/EEC. Sanco/1090/2000-rev.1.
- Meylan WM, Howard PH (1991) Bond contribution method for estimating Henry's law constants. *Environ Toxicol Chem* 10:1283–1293
- Ministry of Health of Italy (2006) Propanil—report and proposed decision of Italy made to the European Commission under 91/414/EEC. European Commission, Brussels. Volumes 1–9.
- Müller B, Berg M, Yao ZP, Zhang XF, Wang D, Pfluger A (2008) How polluted is the Yangtze river? Water quality downstream from the Three Gorges Dam. *Sci Total Environ* 402:232–247
- Nabholz V, Mayo-Bean K (2009) ECOWIN. ECOSAR Classes for Microsoft Windows. v.1.00. USEPA OPPT Risk Assessment Division.
- Park RA, Clough JS (2010) Aquatox (Release 3.1 Beta) Modeling environmental fate and ecological effects in aquatic ecosystems. Draft Volume 2: technical documentation. United States Environmental Protection Agency. Office of Water (4305). EPA-823-R-09-004. DRAFT October 2010.
- Park RA, Clough JS, Coombs Wellman M (2008) AQUATOX: Modeling environmental fate and ecological effects in aquatic ecosystems. *Ecol Model* 213:1–15
- Park RA, Clough JS, Wellman MC, Donigan AS (2005) Nutrient criteria development with a linked modeling system: calibration of AQUATOX across a nutrient gradient. TMDL 2005. Water Environment Federation, Philadelphia, pp 885–902
- Pieper DH, Winkler R, Sandermann H (1992) Formation of a toxic dimerization product of 3,4-dichloroaniline by lignin peroxidase from *Phanerochaete chrysosporium*. *Angew Chem Int Ed* 31:68–69
- Poole SK, Poole CF (1999) Chromatographic models for the sorption of neutral organic compounds by soil from water and air. *J Chromatogr A* 845:381–400
- PPDB (2009) The Pesticide Properties Database (PPDB). Agriculture and Environment Research Unit (AERU), University of Hertfordshire, funded by UK national sources and the EU-funded FOOTPRINT project (FP6-SSP-022704).
- Preziosi DV, Pastorok RA (2008) Ecological food web analysis for chemical risk assessment. *Sci Total Environ* 406:491–502
- Raimondo S, Vivian DN, Barron MG (2010) Web-based Interspecies Correlation Estimation (Web-ICE) for acute toxicity: user manual. Version 3.1. EPA/600/R-10/004. Office of Research and Development, U. S. Environmental Protection Agency. Gulf Breeze, FL.
- Schüürmann G, Ebert RU, Nendza M, Dearden JC, Paschke A, Kuehne R (2007) Prediction of fate-related compound properties. In: van Leeuwen K, Vermeire T (eds) Risk assessment of chemicals. An introduction. Springer, Dordrecht, pp 375–426
- Schüürmann G, Kuehne R, Kleint F, Ebert RU, Rothenbacher C, Herth P (1997) A software system for automatic chemical property estimation from molecular structure. In: Chen F, Schüürmann G (eds) Quantitative structure-activity relationships in environmental sciences. VII SETAC Press, Pensacola, pp 93–114
- Schwarzenbach RP, Gschwend PM, Imboden DM (1993) Environmental organic chemistry. Wiley, New York
- Schwoerbel J (1999) Einführung in die Limnologie, 8th edn. Gustav Fischer, Stuttgart
- Southworth GR, Beauchamp JJ, Schmieder PK (1978) Bioaccumulation potential of polycyclic aromatic hydrocarbons in *Daphnia pulex*. *Water Res* 12:973–977
- Still GG (1969) 3,4,3',4'-tetrachloroazobenzene its translocation and metabolism in rice plants. *Weed Sci* 9:211–217
- Stüben D, Walpersdorf E, Voss K, Baborowski M, Luther G, Elsner W, Rönicke H, Schimmele M (1998) Application of Lake Marl at Lake Arendsee, NE Germany: first results of a geochemical monitoring during the restoration experiment. *Sci Total Environ* 218:33–44
- U.S. Army Corps of Engineers (2001) HEC-RAS river analysis system user's manual. US Army Corps of Engineers, Davis, CA
- UFZ Department of Ecological Chemistry (2012) ChemProp 5.2.8. Available from <http://www.ufz.de/index.php?en=6738>. Accessed October 2012
- US Geological Survey (USGS) (2008) The Cheney Reservoir and Watershed Study. Available from <http://ks.water.usgs.gov/studies/qw/cheney/>. Accessed October 2012
- Van Birgelen APJM, Hebert CD, Wenk ML, Grimes LK, Chapin RE, Mahler J, Trevlos GS (1999) Toxicity of 3,3',4,4'-tetrachloroazobenzene in rats and mice. *Toxicol Appl Pharmacol* 156:147–159
- Van den Brink PJ, Ter Braak CJF (1999) Principal response curves: analysis of time-dependent multivariate responses of biological community to stress. *Environ Toxicol Chem* 18:138–148
- Wang J, Bi Y, Pfister G, Henkelmann B, Zhu K, Schramm KW (2009) Determination of PAH, PCB, and OCP in water from the Three Gorges Reservoir accumulated by semipermeable membrane devices (SPMD). *Chemosphere* 75:1119–1127
- Wanner GA, Klumb RA (2009) Length-weight relationships for three Asian carp species in the Missouri River. National Invasive Species Council materials, Paper 31
- Wilczynska AJ, Puzyn T, Piliszek S, Falandysz J (2006) Selection of representative congener for polychlorinated transazobenzenes (PCT-ABs) based on comprehensive thermodynamical and quantum-chemical characterization. *J Environ Sci Heal B* 41:1131–1142
- Witt KL, Zeiger E, Tice RR, Van Birgelen APJM (2000) The genetic toxicity of 3,3',4,4'-tetrachloroazobenzene and 3,3',4,4'-tetrachloroazoxybenzene: discordance between acute mouse bone marrow and subchronic mouse peripheral blood micronucleus test results. *Mutat Res Genet Toxicol Environ Mutagen* 472:147–154
- Wolf A, Bergmann A, Wilken RD, Gao X, Bi Y, Chen H, Schüth C (2012) Spatial and temporal distribution of organic trace substances in the Three Gorges Reservoir, China. Submitted to Environmental Science and Pollution Research October 2012
- Worobey BL (1984) Fate of 3,3',4,4'-tetrachloroazobenzene in soybean plants grown in treated soils. *Chemosphere* 13:1103–1111
- Worobey BL (1988) Translocation and disposition of [14C] trans 3,4,3',4'-tetrachloroazobenzene into carrots grown in treated soil. *Chemosphere* 17:1727–1734
- Wui YS, Engle CR (2007) The economic impact of restricting use of black carp for snail control on hybrid striped bass farms. *N Am J Aquacult* 69:127–138
- Xia AJ, Chen XH, Cai YX, Peng G, Wang MH (2006) The status of zoobenthos community structure and preliminary evaluation of water quality in the Jiangsu section of the Yangtze river. *Mar Fish* 28:272–277
- Xie P (2003) Three-Gorges Dam: risk to ancient fish. *Science* 302:1149
- Xu X, Tan Y, Yang G, Li H (2011) Three Gorges Project: effects of resettlement on nutrient balance of the agroecosystems in the reservoir area. *J Environ Plan Manag* 54:517–537
- Yang D, Chen F, Li D, Liu B (1997) Preliminary study on the food composition of mud eel, *Monopterus albus*. *Acta Hydrobiologica Sinica* 1.
- Yang G, Weng L, Li L (2008) Yangtze conservation and development report 2007. Science Press, Beijing
- Yi Y, Wang Z, Yang Z (2010) Impact of the Gezhouba and Three Gorges Dams on habitat suitability of carps in the Yangtze River. *J Hydrol* 387:283–291

- Yong Z (2010) Pesticide Pollution to Water Environment of Three Gorges Reservoir Area. International Conference on Challenges in Environmental Science and Computer Engineering.
- Zhang C (2000) Wild and Weedy Rice in China. In: Baki B, Chin D, Mortimer M (eds) Wild and weedy rice in rice ecosystems in Asia—a review. International Rice Research Institute, Los Banos, Philippines
- Zhang G, Wu L, Li H, Liu M, Cheng F, Murphy BR, Xie S (2012) Preliminary evidence of delayed spawning and suppressed larval growth and condition of the major carps in the Yangtze River below the Three Gorges Dam. *Environ Biol Fish* 93:439–447
- Zhou Q, Xie P, Xu J, Ke Z, Guo L (2009) Growth and food availability of silver and bighead carps: evidence from stable isotope and gut content analysis. *Aquac Res* 40:1616–1625

B.2 Dechlorination and organohalide-respiring bacteria dynamics in sediment samples of the Yangtze Three Gorges Reservoir

Dechlorination and organohalide-respiring bacteria dynamics in sediment samples of the Yangtze Three Gorges Reservoir

Irene Kranzioch · Claudia Stoll · Andreas Holbach ·
Hao Chen · Lijing Wang · Binghui Zheng · Stefan Norra ·
Yonghong Bi · Karl-Werner Schramm · Andreas Tiehm

Received: 30 September 2012 / Accepted: 3 February 2013
© Springer-Verlag Berlin Heidelberg 2013

Abstract Several groups of bacteria such as *Dehalococcoides* spp., *Dehalobacter* spp., *Desulfomonile* spp., *Desulfuromonas* spp., or *Desulfitobacterium* spp. are able to dehalogenate chlorinated pollutants such as chloroethenes, chlorobenzenes, or polychlorinated biphenyls under anaerobic conditions. In order to assess the dechlorination potential in Yangtze sediment samples, the presence and activity of the reductively dechlorinating bacteria were studied in anaerobic batch tests. Eighteen sediment samples were taken in the Three Gorges Reservoir catchment area of the Yangtze River, including the tributaries Jialing River, Daning River, and Xiangxi River. Polymerase chain reaction analysis indicated the presence of dechlorinating bacteria in most samples, with

varying dechlorinating microbial community compositions at different sampling locations. Subsequently, anaerobic reductive dechlorination of tetrachloroethene (PCE) was tested after the addition of electron donors. Most cultures dechlorinated PCE completely to ethene via *cis*-dichloroethene (*cis*-DCE) or *trans*-dichloroethene. Dehalogenating activity corresponded to increasing numbers of *Dehalobacter* spp., *Desulfomonile* spp., *Desulfitobacterium* spp., or *Dehalococcoides* spp. If no bacteria of the genus *Dehalococcoides* spp. were present in the sediment, reductive dechlorination stopped at *cis*-DCE. Our results demonstrate the presence of viable dechlorinating bacteria in Yangtze samples, indicating their relevance for pollutant turnover.

Responsible editor: Robert Duran

Electronic supplementary material The online version of this article (doi:10.1007/s11356-013-1545-9) contains supplementary material, which is available to authorized users.

I. Kranzioch · C. Stoll · A. Tiehm (✉)
Department Environmental Biotechnology,
DVGW-Technologiezentrum Wasser (TZW), Karlsruher Straße 84,
76139 Karlsruhe, Germany
e-mail: andreas.tiehm@tzw.de

A. Holbach
Institute of Mineralogy and Geochemistry, Karlsruhe Institute
of Technology (KIT), Adenauerring 20b, Bldg. 50.40,
76131 Karlsruhe, Germany

H. Chen · L. Wang · B. Zheng
Institute of Water Environment Research, Chinese Research
Academy of Environmental Sciences (CRAES),
AnWai Dayangfang 8, Chaoyang District Beijing 100012,
People's Republic of China

S. Norra
Institute of Geography and Geoecology, Karlsruhe Institute
of Technology, 76128 Karlsruhe, Germany

Y. Bi
Institute of Hydrobiology, Chinese Academy of Sciences,
Donghuan Road 7, Wuhan,
Hubei Province 430072, People's Republic of China

Y. Bi · K.-W. Schramm
Department Biosciences, Technische Universität München
(TUM), Weihenstephaner Steig 23,
85350 Freising, Germany

K.-W. Schramm
Molecular EXposomics (MEX), Department of Environmental
Sciences, Helmholtz Zentrum München–German Research Center
for Environmental Health, Ingolstädter Landstr. 1,
85764 Neuherberg, Germany

Keywords Yangtze · Tetrachloroethene · Reductive dechlorination · *Desulfitobacterium* spp. · *Dehalococcoides* spp. · qPCR

Introduction

The Yangtze River is the third largest river in the world, with a mean annual water discharge of 29,400 m³/s and a sediment load of 500 million tons/year (Zhang 1995). In the last decades, pollutant discharge into Chinese rivers has increased because of growing industrial development and the widespread application of fertilizers, pesticides, and herbicides in agriculture (Müller et al. 2008). Additionally, changes in water quantity, water quality, and the aquatic ecosystems have to be expected from large dam constructions, e.g., the Three Gorges Dam (TGD) at the Yangtze. A joint Sino-German research project was initiated to obtain more insight into the environmental processes under these highly dynamic conditions (Bergmann et al. 2012).

In this study, the dehalogenation of chlorinated pollutants and monitoring the growth of dechlorinating bacteria are reported. Chlorinated contaminants such as polychlorinated biphenyls (PCBs) and chlorinated benzenes (CBs) have been detected in the Yangtze River water and sediments in low concentrations (Jiang et al. 2000; Wang et al. 2009). PCBs are anthropogenic environmental pollutants, which originate from the recycling procedures or dumping of electronic wastes (Shen et al. 2009; Liu et al. 2008). CBs, especially hexachlorobenzene, had a lot of applications in industry and agriculture (Barber et al. 2005). In China, it was used as a cheap broad spectrum insecticide (Jiang et al. 2000). Chlorinated ethenes belong to the most commonly found contaminants in the groundwater worldwide, because they had been widely used as cleaning and degreasing agents (Schmidt and Tiehm 2008; Tiehm and Schmidt 2011). There are several groups of bacteria which are able to dehalogenate chlorinated aliphatic and aromatic hydrocarbons under anaerobic conditions. Remarkably, similar groups of bacteria have been reported to be capable of dechlorination of CBs (Field and Sierra-Alvarez 2008; Taş et al. 2011), PCBs (Bedard 2008), and chlorinated ethenes (Löffler et al. 2000; Schmidt et al. 2006). In this study, chloroethenes were used as model compounds. Microorganisms which are known to be able to reductively dechlorinate pollutants are *Desulfomonile* spp., *Desulfitobacterium* spp., *Dehalobacter* spp., *Desulfuromonas* spp., and *Dehalococcoides* spp., but only bacteria belonging to *Dehalococcoides* spp. are capable of complete dehalogenation of tetrachloroethene (PCE) to ethene (Holliger et al. 1993; Smidt and de Vos 2004; Schmidt et al. 2006; Aktaş et al. 2012; Löffler et al. 2012).

Previously, in most laboratory studies on anaerobic dechlorination, only one or two groups of bacteria were

investigated and monitored by polymerase chain reaction (PCR) analysis, e.g., *Desulfitobacterium* sp. and *Dehalococcoides* spp. (Lohner and Tiehm 2009), *Desulfitobacterium dehalogenans* and *Desulfomonile tiedjei* (El Fantroussi et al. 1997), *Desulfuromonas* spp. and *Dehalococcoides mccartyi* (Löffler et al. 2000; Löffler et al. 2012), *Dehalobacter* spp. and *Dehalococcoides* spp. (Smits et al. 2004; Grostern and Edwards 2006) or *Dehalococcoides* bacteria (Schmidt et al. 2006; Aktaş et al. 2012). It has been shown recently that in the field, often several dechlorinating bacteria are present simultaneously (Rouzeau-Szynański et al. 2011). In the environment, the reductively dechlorinating bacteria have been detected in different compartments, mainly in contaminated soil (Löffler et al. 2000; Hendrickson et al. 2002) and polluted groundwater (Schmidt et al. 2006; Schmidt and Tiehm 2008; Vancheeswaran et al. 1999). For river sediments, their occurrence in the Dutch part of the Rhine River (Holliger et al. 1993), the Red Cedar, Père Marquette (Löffler et al. 2000), Tahquamenon and Pine Rivers in the USA, and the Perfume River in Vietnam (Griffin et al. 2004) was reported. However, no reports were available addressing the anaerobic dechlorination potential in the Yangtze River. The objectives of this study are (1) to assess the dechlorination potential in Yangtze sediment samples and (2) to monitor the changes of the dechlorinating microbial community during PCE dechlorination.

Materials and methods

Sampling and sample storage

Eighteen sediment samples were taken in the Three Gorges Reservoir (TGR) catchment area (Fig. 1). Seven samples (MP1, MP2, MP3, MP4, MP5, MP6, and MP7) are from a sediment core with a total length of 0.7 m taken 76.5 m below the water level in the Yangtze River near the TGD. The sediment core was collected with a stainless gravity sediment core sampler (100 cm in length and 25 cm in diameter). Three samples (YCQ1, YCQ4, and YEND) originate from the Yangtze River close to and within Chongqing city, and another sample was also taken within Chongqing from the tributary Jialing River (JL1). These four samples are surface sediment samples from the littoral zone and were collected manually. Six samples (XX01, XX02, XX04, XX07, PYK, and WJW) were taken from the tributary Xiangxi River in a depth between 3 and 71 m below the water level, and another sample (DH2) originated from the tributary Daning River (depth 35 m). These samples have been collected with a sediment grabber. All samples were stored in plastic bags, which were put into gastight tins. After sampling, the sediments were stored at 4 °C until usage.

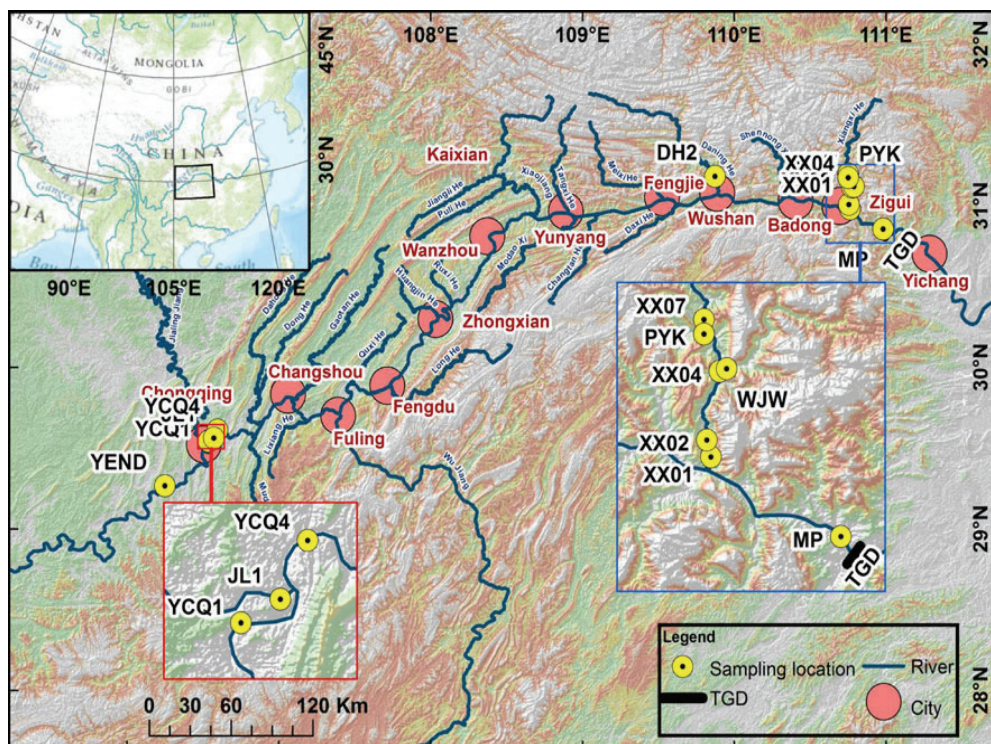


Fig. 1 Map of sampling points within the Three Gorges Reservoir

Biodegradation studies

Experiments were performed in 2-L laboratory glass bottles capped with teflon-coated septa, held in place with screw caps. The mineral medium contained the following mineral salts (analytical grade, Merck, Darmstadt, Germany) per liter of demineralized water: 3.17 g of KH_2PO_4 , 14.33 g of $\text{Na}_2\text{HPO}_4 \cdot 12\text{H}_2\text{O}$, 0.45 g of $(\text{NH}_4)_2\text{HPO}_4$, 0.12 g of $\text{MgHPO}_4 \cdot 3\text{H}_2\text{O}$, 5 mL of trace element solution 1 (200 mg of $\text{FeSO}_4 \cdot 7\text{H}_2\text{O}$, 20 mg of $\text{MnSO}_4 \cdot 5\text{H}_2\text{O}$, 4 mg of CoCl_2 , 20 mg of $\text{ZnSO}_4 \cdot 7\text{H}_2\text{O}$, 20 mg of $\text{CuSO}_4 \cdot 5\text{H}_2\text{O}$, 530 mg of CaCl_2 , 3 mg of H_3BO_3 , 4 mg of $\text{NaMoO}_4 \cdot 2\text{H}_2\text{O}$, and 1 mL of concentrated H_3PO_4 per liter), and 100 μL of trace element solution 2 (50 mg of $\text{Na}_2\text{WO}_4 \cdot 2\text{H}_2\text{O}$, 50 mg of $\text{Na}_2\text{SeO}_3 \cdot 5\text{H}_2\text{O}$, and 250 mg of NiCl_2 per liter). The medium was adjusted to $\text{pH} 7.2 \pm 0.2$ and autoclaved at 121°C for 20 min. Oxygen was removed by repeatedly applying vacuum and flushing with nitrogen. Additionally, all cultures received filter-sterilized 1 mL vitamin solution (2 mg of biotin, 2 mg of folic acid, 10 mg of pyridoxamine, 5 mg of riboflavin, 5 mg of thiamine, 0.1 mg of cyanocobalamin, 5 mg of nicotinamide, 5 mg of *p*-amino benzoic acid, 5 mg of lipoic acid, 5 mg of pantothenic acid per 100 mL). Sodium acetate (40 mg), 40 mg of sodium pyruvate, 0.5 g of yeast extract, and 10 mL H_2 per liter were added in order to provide the electron donors required for reductive

dechlorination. Depletion of acetate and pyruvate was followed by ion chromatographic analysis. All handling, except H_2 addition, was performed inside the anaerobic gas chamber flushed with nitrogen. All bottles were amended with 50 μM (8.3 mg/L) PCE (99 %, Fluka, Steinheim, Germany). Each batch test was inoculated with 20 g of wet sediment. According to the dehalogenation of chloroethenes and consumption of electron donors, the cultures have been repeatedly spiked with 50 μM (8.3 mg/L) PCE and amended with acetate, pyruvate, and hydrogen. Bottles were kept at room temperature ($22\text{--}24^\circ\text{C}$) in the dark. In order to avoid volatilization of chloroethenes during sampling, the teflon-coated septa were pierced with stainless steel needles. Aqueous phase samples were taken using glass syringes, and septa were quickly changed subsequently. Chlorinated ethenes and ethene were analyzed by gas chromatography. Chloride formation was monitored via ion chromatography. Samples for gas chromatographic analyses were acidified to $\text{pH} 2$ with phosphoric acid in order to stop biological reactions and stored at 4°C until analysis.

Analytical methods

Chloroethene and ethene concentrations were determined using a gas chromatograph (Series II 5890, Hewlett Packard, Waldbronn, Germany) equipped with headspace

sampler, flame ionization detector, and electron capture detector. Separation was accomplished in a capillary column (Hewlett Packard PONA, 50 m, 0.2 mm inside diameter, crosslinked methyl siloxane, 0.5- μ m film thickness). The injector and detector temperatures were 180 and 220 °C, respectively, and the following temperature program was used: held at 35 °C for 15 min, heated gradually to 60 °C (1.5 °C/min), heated gradually to 130 °C (15 °C/min), held for 7 min, heated gradually to 200 °C (30 °C/min), and held at 200 °C for 5 min. Concentrations were determined using external standards ($R^2=0.998$). Reproducibility on standard analyses was ± 6 %. Each reported value was the average of at least duplicate samples and represents the aqueous phase concentration.

Chloride concentrations were determined via ion chromatograph (Metrohm 761 compact IC, Metrohm, Filderstadt, Germany) equipped with a Metrohm A-Supp-5 column conductivity detector. Concentrations were determined using external standards ($R^2=0.996$). Reproducibility on standard analyses was ± 1 %.

All samples were taken from the aqueous phase. At each time point, oxidation–reduction potential (ORP) and pH were determined with a multimeter WTW Multiline P4 (Weilheim, Germany), and oxygen was measured using a WTW oximeter Oxi 330.

Polymerase chain reaction

For the analysis of total DNA from the sediment, the gas-tight tins were opened in the anaerobic gas chamber. Per sample, 1 g of soil was removed and extracted using the Ultra Clean Soil DNA Kit (MoBio Laboratories, Carlsbad, USA) according to the manufacturer's protocol. For PCR analysis of the culture liquid, 50 mL of the culture was transferred to a conical centrifuge tube (VWR, Darmstadt, Germany) and afterwards filtered through a 0.2 μ m membrane filter (47 mm diameter) (PALL, Michigan, USA). The membrane was stored at -20 °C until DNA extraction and analysis. The DNA of the frozen filters was extracted using the Fast DNA[®] Spin Kit for soil (MP Biomedicals, OH, USA).

The pre-screening of sediment samples for the *16S* rRNA gene sequences specific for dechlorinating microorganisms *Desulfomonile* spp., *Desulfitobacterium* spp., *Dehalobacter* spp., *Desulfuromonas* spp., and *Dehalococcoides* spp. was done with nested PCR containing 2 μ L of the template, 13.4 μ L of DNase free water, 2 μ L of $10\times$ reaction buffer, 0.2 μ L of Taq polymerase, 200 μ M of each nucleotide, and 500 nM of each primer, using a Biometra thermocycler (Biometra, Goettingen, Germany). First, a PCR with bacterial primers was performed using different dilutions of DNA extracts as templates. Thus, false negative results caused by PCR inhibitors could be precluded. Second, a 1 to 10 dilution of the bacterial PCR product was used as template

for a second PCR with primers specific for the five dechlorinating groups. The used primers and temperature programs are listed in Table 1. Amplicons were tested with agarose gel electrophoresis, and gels were documented with a GeneFlash camera (Syngene, Cambridge, UK).

For enumeration of the *16S* RNA gene copies in the degradation experiments, quantitative PCR (qPCR) was performed in an Eppendorf Realplex² qPCR machine (Eppendorf, Hamburg, Germany) with primers and temperature profiles listed in Table 1. The qPCR was done with a Master Mix containing 8.5 μ L of RNase and DNase free water (Invitrogen, Carlsbad, USA), 12.5 μ L of $2\times$ Sensi Mix including Hot Start Taq Polymerase (Bioline, Luckenwalde, Germany), and 500 nM of each primer. All samples and standards were analyzed in duplicates, and gene concentrations were reported as gene copies per liter of culture liquid. Calibration was performed with serial dilutions of a known quantity of linearized plasmid containing *16S* gene fragments. The quantification limits (QL) for all qPCR assays were $1E+5$ *16S* RNA gene copies/L.

Results

The pre-screening of the sediment samples revealed that dechlorinating bacteria were present in most of the samples. In 16 of the 18 sediment samples, positive PCR signals for at least one of the 5 different dechlorinating groups were detected (see supplementary data Table T1). For subsequent dehalogenation studies, nine sediment samples from different areas and with different dechlorinating microbial communities were selected.

All nine batch cultures were able to reductively dechlorinate PCE, thus demonstrating the viability of the bacteria. During 28 weeks, in all batch cultures, the pH stayed at a constant level between 7.0 and 7.4. The oxygen concentration in the medium never exceeded the limit of detection (0.2 mg/L), and the ORP values decreased at the beginning and afterwards remained between -24 and -124 mV (supplementary Figs. S1 and S2). Thus, the O_2 , pH, and ORP values confirmed suitable conditions for reductive dechlorination. All batch cultures were spiked at least two times with PCE and showed repeatedly reductive dechlorination. qPCR analysis showed different patterns of dechlorinating microorganisms during the dehalogenation tests (Table 2). The growth of *Dehalococcoides* spp. was observed in all cultures showing complete dechlorination of PCE to ethene. Three of the batch experiments are shown exemplarily in Figs. 2, 3 and 4. The remaining six batch experiments are shown in the supplementary data Figs. S3–S8.

The culture MP1 transformed PCE after the first addition of PCE mainly to trichloroethene (TCE). Initially, only a small amount of about 5 μ M *cis*-DCE was formed (Fig. 2a).

Table 1 Primers and temperature programs used for the nested PCR and qPCR

Detection of	Primer sequence (5'-3')	Amplicon size (bp)	Reference for primer sequence	Temperature program nested PCR	Temperature program qPCR
Bacteria (16S)	F-AGAGTTTGATCCTGGCTCAG R-GGTTACCTTGTACGACTT	1,500	Hendrickson et al. (2002)	3 min 95 °C 35 cycles: 30 s 94 °C/30 s 55 °C/90 s 72 °C 10 min 72 °C	–
<i>Dehalococcoides</i> spp. (16S)	F-GATGAACGCTAGCGGCG R-TCAGTGACAACCTAGAAAAC	690	Hendrickson et al. (2002)	3 min 95 °C 35 cycles: 30 s 94 °C/30 s 55 °C/60 s 72 °C 10 min 72 °C	–
<i>Dehalococcoides</i> spp. (16S)	F-AAGGCGGTTTTCTAGGTTGTAC R-CTTCATGCAATGCAAAAT	215	Smits et al. (2004)	–	15 min 95 °C 45 cycles: 15 s 94 °C/20 s 55 °C/20 s 72 °C Melt
<i>Desulfomonile</i> spp. (16S)	F-GGGTCAAAGTCGGCCTCTCGACG R-GCTTTCACATTCGACTTATCG	360	El Fantroussi et al. (1997)	3 min 95 °C 35 cycles: 30 s 94 °C/30 s 55 °C/60 s 72 °C 10 min 72 °C	15 min 95 °C 45 cycles: 15 s 94 °C/ 55 °C/30 s 72 °C Melt
<i>Dehalobacter</i> spp. (16S)	F-GTTAGGGAAGAACGGCAICTGT R-CCTCTCCTGTCTCAAGCCATA	250	Smits et al. (2004)	3 min 95 °C 35 cycles: 30 s 94 °C/30 s 58 °C/40 s 72 °C 10 min 72 °C	15 min 95 °C 45 cycles: 15 s 94 °C/30 s 55 °C/30 s 72 °C Melt
<i>Desulfuromonas</i> spp. (16S)	F-AACTTCGGGTCCTACTGTC R-GCCGAACCTGACCCCTATGTT	820	Löffler et al. (2000)	3 min 95 °C 35 cycles: 30 s 94 °C/ 30 s 55 °C/ 60 s 72 °C 10 min 72 °C	–
<i>Desulfitobacterium</i> spp. (16S)	F-CTACGACGAAGGCCTTCGGGT R-CCCAGGGTTGAGCCCTAGGT	210	Smits et al. (2004)	3 min 95 °C 35 cycles: 30 s 94 °C/ 30 s 58 °C/ 40 s 72 °C 10 min 72 °C	15 min 95 °C 45 cycles: 15 s 95 °C/ 30 s 58 °C/30 s 72 °C Melt

Table 2 qPCR results after 28 weeks of incubation and dechlorination products

	TGD area			Xiangxi River			Yangtze River		Yangtze River
	MP1 Gene copies/L	MP3 Gene copies/L	MP7 Gene copies/L	XX01 Gene copies/L	XX04 Gene copies/L	XX07 Gene copies/L	YCQ1 Gene copies/L	YCQ4 Gene copies/L	DH2 Gene copies/L
qPCR analysis after 28 weeks									
<i>Dehalococcoides</i> spp.	<QL	2.45E+10	8.59E+10	4.15E+10	4.76E+10	4.10E+10	7.18E+10	6.50E+10	3.17E+10
<i>Desulfomonile</i> spp.	2.25E+06	1.93E+06	1.41E+06	7.79E+06	8.74E+06	4.10E+06	2.29E+06	1.99E+06	3.93E+06
<i>Dehalobacter</i> spp.	1.58E+07	2.57E+06	8.31E+06	6.18E+06	1.56E+06	1.61E+06	2.05E+06	2.62E+06	1.92E+06
<i>Desulfitobacterium</i> spp.	1.11E+09	<QL	3.62E+07	9.00E+07	2.14E+08	2.58E+08	5.58E+07	5.07E+09	6.70E+06
Dechlorinating activity to									
<i>cis</i> -DCE	+	+	+	+	+	+	+	+	+
<i>trans</i> -DCE	-	-	-	-	+	+	-	-	+
VC	-	+	+	+	+	+	+	+	+
Ethene	-	-	+	+	+	+	+	+	+

All values are in copies/L

Plus sign (+) detected, minus sign (-) not detected, QL (quantification limit = 1E+5 16S RNA gene copies/L)

No further dechlorination of TCE to *cis*-DCE was observed within the first 15 weeks. After addition of PCE and electron donors, the dehalogenation of TCE started also, and TCE was completely dechlorinated to *cis*-DCE after 22 weeks.

Repeated spiking with PCE resulted in an accumulation of *cis*-DCE. No further dechlorination products such as vinylchloride (VC) or ethene were measured. In this culture, a nearly stoichiometric chloride formation was observed.

Fig. 2 PCE dechlorination and growth of dechlorinating bacteria in culture MP1. **a** Aqueous phase concentrations of chloroethenes and ethene; **b** results of qPCR (*n.d.* not detected)

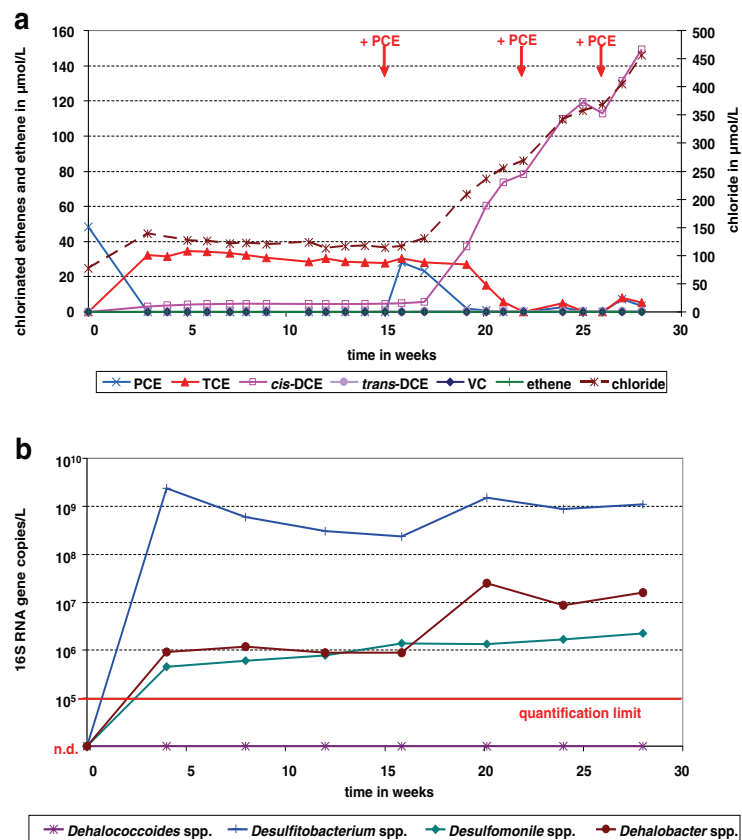
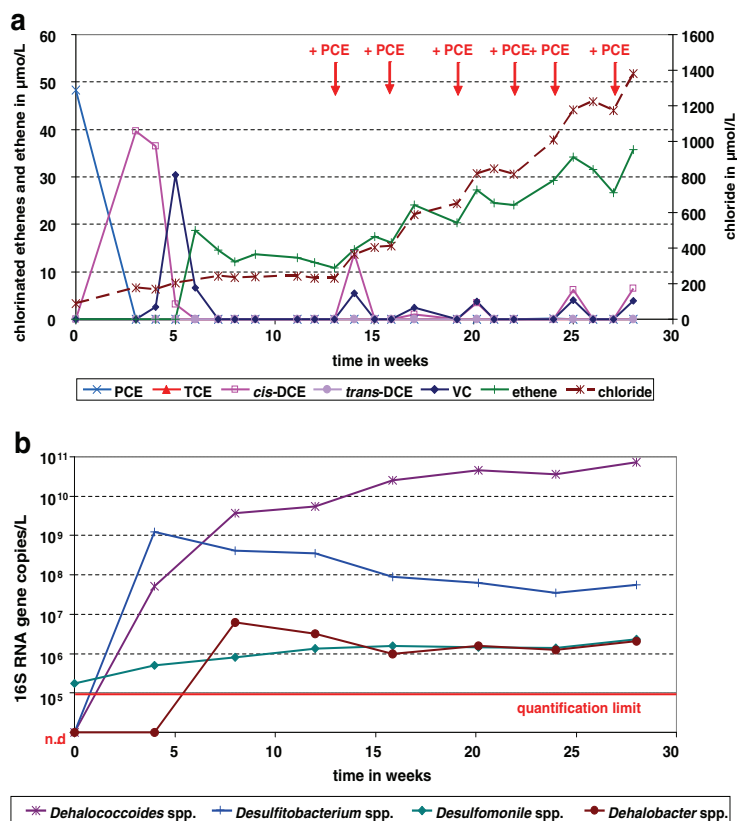


Fig. 3 PCE dechlorination and growth of dechlorinating bacteria in culture YCQ1. **a** Aqueous phase concentrations of chloroethenes and ethene; **b** results of qPCR (*n.d.* not detected)



The dechlorinating microbial community analysis is shown in Fig. 2b. The main increase in bacterial genes was detected for *Desulfitobacterium* spp. within the first 16 weeks. During this time, the gene copies per liter of *Desulfitobacterium* spp. increased about four orders of magnitude. In the case of *Dehalobacter* spp., the main growth of one order of magnitude occurred in the first 4 weeks. After the second spiking, again a growth of about one order of magnitude to $10E+7$ 16S RNA gene copies/L was observed. *Desulfomonile* spp. showed a weak growth, and *Dehalococcoides* spp. was below the quantification limit during the whole investigation period.

One culture (YCQ1) which completely dechlorinated PCE via TCE, *cis*-DCE, and VC to ethene is shown in Fig. 3a. The culture was spiked six times with PCE and showed a complete dehalogenation to ethene each time. The dechlorination of PCE started quickly, and after 3 weeks, PCE was completely transformed to *cis*-DCE. At the end of the experiment, the time for complete dechlorination of 48 µM PCE via *cis*-DCE and VC to ethene was less than 2 weeks.

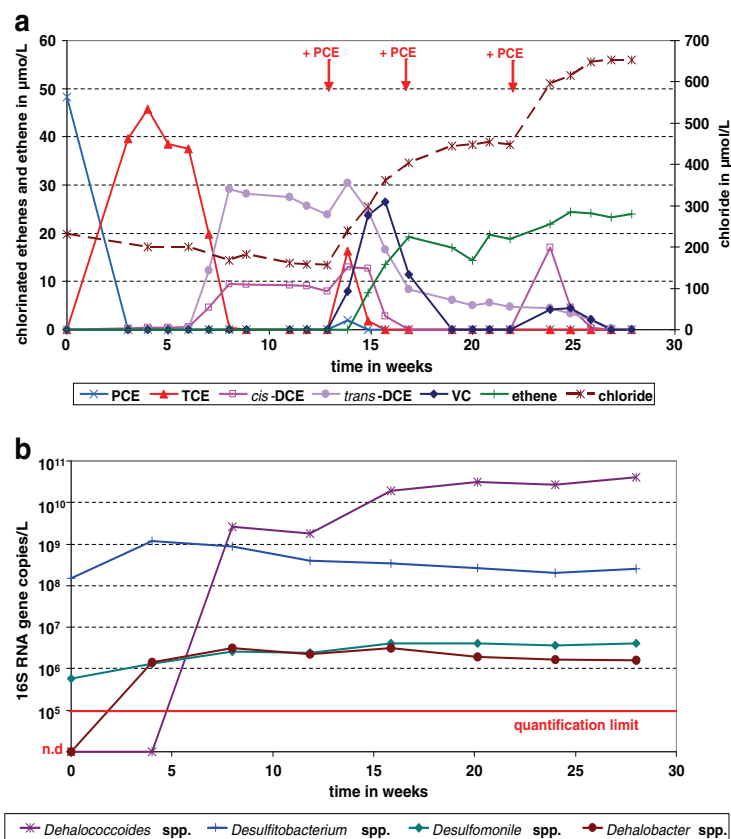
The growth of the dechlorinating microorganisms is shown in Fig. 3b. Within 4 weeks, the number of *Dehalococcoides* spp. increased by at least three orders of magnitude, and in the following 24 weeks, it increased by another

three orders of magnitude. Finally, $10E+11$ gene copies/L was reached. In the case of *Desulfitobacterium* spp., first, an increase of four orders of magnitude was observed, and then a slow decline to about $10E+8$ 16S RNA gene copies/L occurred. *Dehalobacter* spp. and *Desulfomonile* spp. showed a small incline of about 1 and two orders of magnitude.

In Fig. 4a, the results for the culture XX07 are shown. In contrast to the other cultures, the dehalogenation of PCE to *trans*- and *cis*-DCE in a ratio of 3:1 was observed. After repeated addition of PCE and electron donors, a complete dechlorination of PCE and the lower chlorinated metabolites to ethene and stoichiometric chloride formation were observed.

The growth of *Dehalococcoides* spp. was observed concomitantly with the reduction of TCE to *cis*- and *trans*-DCE (Fig. 4b). The gene copy number per liter increased at least four orders of magnitude within 8 weeks. After 28 weeks, a value of approximately $1E+10$ 16S RNA gene copies/L was reached. The gene copy numbers of *Desulfitobacterium* spp. were already high initially and increased about one order of magnitude. *Desulfomonile* spp. and *Dehalobacter* spp. showed growth in the first 4 weeks about one order of magnitude, but afterwards remained constant until the end of the experiment.

Fig. 4 PCE dechlorination and growth of dechlorinating bacteria in culture XX07. **a** Aqueous phase concentrations of chloroethenes and ethene; **b** results of qPCR (*n.d.* not detected)



The results of the batch studies are summarized in Table 2 (for more detailed information see supplementary data Figs. S3–S8). Obviously, different bacteria known for their organohalide respiring potential developed during the incubation of Yangtze sediment samples. In particular, increase of gene copy numbers over four orders of magnitude was observed for *Desulfitobacterium* spp. (Figs. 2 and 3, Fig. S5), *Dehalobacter* spp. (Figs. S4 and S6), and *Dehalococcoides* spp. (Figs. 3 and 4, Figs. S3–S8). If bacteria of the *Dehalococcoides* group were not present, the reductive dechlorination stopped at *cis*-DCE. In the presence of *Dehalococcoides* spp., in all samples except one, a complete reductive dechlorination to ethene occurred. Only in one sediment sample (MP3), VC was observed as the end product of reductive dechlorination (Fig. S3).

Discussion

In all batch tests incubated with sediments from the TGR catchment area, anaerobic biological dechlorination was demonstrated (Table 2). Although *Dehalococcoides* spp. were below the limit of detection in the initial nested PCR screening (Table T1), these bacteria were detected in most of the batch dechlorination tests. However, differences in the

biochemical pathways and end-products of reductive dechlorination were observed, most probably due to different halo-respiring bacteria community compositions. In nearly all sediment samples, *Desulfuromonas* spp. was detected with the nested PCR approach (Table T1). However, growth of *Desulfuromonas* spp. was not studied by qPCR in the batch tests because of the lack of suitable primers.

The culture MP1 repeatedly dechlorinated PCE via TCE to *cis*-DCE (Fig. 2a). In this culture, *Dehalococcoides* spp. was below the quantification limit during the whole incubation time. In contrast, *Dehalococcoides* spp. were detected with increasing numbers over investigation time in the YCQ1 (Fig. 3b) and the XX07 cultures (Fig. 4b). These cultures showed complete dechlorination, thus confirming previous reports that bacteria of the *Dehalococcoides* group are the only known microorganism to completely dehalogenate PCE to ethene (Holliger et al. 1999; Löffler et al. 2000; Maymó-Gatell et al. 2001; Hendrickson et al. 2002; Smidt and de Vos 2004; Schmidt et al. 2006). During 28 weeks and anaerobic transformation of approximately 60 mg/L PCE, the *Dehalococcoides* spp. gene copies/L increased by five orders of magnitude. Also, Aktaş et al. (2012) reported a several orders of magnitude increase of gene numbers during the reductive dechlorination of approximately 100 mg/L PCE to ethene.

Although in both cultures, YCQ1 and XX07, complete dechlorination to ethene was observed, the temporarily detected metabolites differed. As in most previous studies (Löffler et al. 2000; Schmidt and Tiehm 2008; Aktaş et al. 2012), dechlorination via *cis*-DCE without any detection of *trans*-DCE was observed in culture YCQ1 (Fig. 3a). The culture XX07 dechlorinated PCE via TCE to *trans*-DCE and *cis*-DCE in a ratio of 3:1. Similar ratios were already reported in some other studies (Griffin et al. 2004; Kittelmann and Friedrich 2008; Cheng and He 2009; Cheng et al. 2009; Marco-Urrea et al. 2011). Chow et al. (2010) and Marco-Urrea et al. (2011) found that the *Dehalococcoides* strains MB and CBDB1 dechlorinate PCE and TCE to mainly *trans*-DCE. In our study, mainly the growth of *Dehalococcoides* spp. and smaller increases of *Desulfitobacterium* spp., *Desulfomonile* spp., and *Dehalobacter* spp. were observed. The *D. mccartyi* group encompasses the six bacterial isolates of strains 195, BAV1, CBDB1, FL2, GT, and VS (Löffler et al. 2012). Most probably, different strains of the genus *Dehalococcoides* spp. with different dechlorinating abilities were present in the cultures YCQ1 and XX07. In order to obtain more insight into the dechlorinating strains of *Dehalococcoides* spp. within the Yangtze samples, further investigation focusing on chloroethene reductive dehalogenase genes such as *pceA*, *tceA*, *vcrA*, and *bvcA* are promising (Behrens et al. 2008; Maphosa et al. 2010).

In culture MP1, *Desulfitobacterium* spp. was the predominant growing bacterium in the absence of *Dehalococcoides* spp. The transformation of approximately 50 mg/L PCE to *cis*-DCE resulted in an increase of *Desulfitobacterium* spp. over four orders of magnitude, and an increase of *Dehalobacter* spp. over two orders of magnitude (Fig. 2b). Obviously, the addition of PCE and the electron donors acetate/pyruvate and H₂ could stimulate the growth of the different dechlorinating bacteria. However, a small amount of sulphate and Fe(III) was available in the mineral medium, and it is also possible that fermentation of the yeast extract resulted in the formation of fumarate. As reviewed recently by Maphosa et al. (2010), these compounds might also have been used as electron acceptors by *Desulfitobacterium* spp. or *Desulfomonile* spp. in the cultures.

Mass balance calculations revealed that the formation of chloride corresponded to the dechlorination of PCE to DCE or ethene (Figs. 2, 3 and 4). Also, the amount of *cis*-DCE detected in the aqueous phase samples of the culture MP1 reflected the amount of PCE added to the flask in total, i.e., by several spikings. However, in all cultures with complete dechlorination, less ethene formation was observed than calculated from the total amount of spiked PCE. As discussed previously (Aktaş et al. 2012), the repeated aqueous phase sampling results in an increase of the gas/liquid ratio in the bottles. Therefore, the high volatility, in particular, of ethene leads to a transfer into the gas phase resulting in lower concentrations in the aqueous phase.

In the case of incomplete dechlorination of PCE to the end-product *cis*-DCE, as observed in culture MP1, bioaugmentation with a *Dehalococcoides* spp.-containing culture can stimulate further dechlorination to ethene (Ritalahti et al. 2005). On the other hand, sequential anaerobic/aerobic degradation (Tiehm and Schmidt 2011) might be important in the field. Higher chlorinated compounds like PCE and TCE are more easily dechlorinated in an anaerobic reductive environment (Schmidt et al. 2010; Tiehm and Schmidt 2011). Lower chlorinated compounds like DCE and VC also can be degraded by aerobic degradation (Tiehm et al. 2008; Schmidt et al. 2010; Zhao et al. 2010; Zhao et al. 2011). At contaminated field sites, anaerobic dechlorination could stop at *cis*-DCE or VC, followed by aerobic mineralization of the lower chlorinated metabolites (Schmidt and Tiehm 2008; Lohner et al. 2011; Tiehm and Schmidt 2011). A similar sequential anaerobic/aerobic degradation might be possible also in the Yangtze TGR, taking into consideration the periodical water level fluctuations and expected spatio-temporal dynamics of the hydrochemical parameters (Bergmann et al. 2012; Kranzioch and Tiehm 2012). However, additional studies are required to prove this hypothesis.

Conclusions and outlook

In this study, the presence of viable dechlorinating bacteria in Yangtze sediment samples was demonstrated, thus indicating their relevance for pollutant turnover in the catchment area. The applied PCR methods proved to be suitable for the detection and quantification of the different dechlorinating bacteria. The qPCR analysis showed, in several samples, that the dehalogenation of PCE corresponded to the increasing numbers of *Dehalococcoides* spp., *Desulfitobacterium* spp., *Desulfomonile* spp., or *Dehalobacter* spp. In this study, the focus was on different bacteria, which are capable growing on chlorinated ethenes as electron acceptor. Studies focusing on the dehalogenase genes and dynamic environmental conditions are in progress.

Acknowledgments The authors gratefully acknowledge the financial support from the German Ministry of Education and Research (BMBF, grant no.: 02WT1130). This study is part of the Sino-German Yangtze-Hydro Project (www.yangtze-project.de).

References

- Aktaş Ö, Schmidt KR, Mungenast S, Stoll C, Tiehm A (2012) Effect of chloroethene concentrations and granular activated carbon on reductive dechlorination rates and growth of *Dehalococcoides* spp. *Biores Technol* 103:286–292. doi:10.1016/j.biortech.2011.09.119
- Barber JL, Sweetman AJ, van Wijk D, Jones KC (2005) Hexachlorobenzene in the global environment: emissions, levels,

- distribution, trends and processes. *Sci Total Environ* 349:1–44. doi:10.1016/j.scitotenv.2005.03.014
- Bedard DL (2008) A case study for microbial biodegradation: anaerobic bacterial reductive dechlorination of polychlorinated biphenyls from sediment to defined medium. *Annu Rev Microbiol* 62:253–270. doi:10.1146/annurev.micro.62.081307.162733
- Behrens S, Azizian MF, McMurdie PJ, Sabalowsky A, Dolan M, Semprini L, Spormann AM (2008) Monitoring abundance and expression of *Dehalococcoides* species chloroethene-reductive dehalogenases in a tetrachloroethene-dechlorinating flow column. *Appl Environ Microb* 74:5695–5703. doi:10.1128/AEM.00926-08
- Bergmann A, Bi Y, Chen L, Floehr T, Henkelmann B, Holbach A et al (2012) The Yangtze-Hydro Project: a Chinese-German environmental program. *Environ Sci Poll Res* 19:1341–1344. doi:10.1007/s11356-011-0645-7
- Cheng D, He J (2009) Isolation and characterization of *Dehalococcoides* sp. strain MB, which dechlorinates tetrachloroethene to trans-1,2-dichloroethene. *Appl Environ Microb* 75:5910–5918. doi:10.1128/AEM.00767-09
- Cheng D, Chow WL, He J (2009) A *Dehalococcoides*-containing coculture that dechlorinates tetrachloroethene to trans-1,2-dichloroethene. *ISME J* 4:88–97. doi:10.1038/ismej.2009.90
- Chow WL, Cheng D, Wang S, He J (2010) Identification and transcriptional analysis of trans-DCE-producing reductive dehalogenases in *Dehalococcoides* species. *ISME J* 4:1020–1030. doi:10.1038/ismej.2010.27
- El Fantroussi S, Mahillon J, Naveau H, Agathos SN (1997) Introduction of anaerobic dechlorinating bacteria into soil slurry microcosms and nested-PCR monitoring. *Appl Environ Microb* 63:806–811
- Field JA, Sierra-Alvarez R (2008) Microbial degradation of chlorinated benzenes. *Biodegradation* 19:463–480. doi:10.1007/s10532-007-9155-1
- Griffin BM, Tiedje JM, Löffler FE (2004) Anaerobic microbial reductive dechlorination of tetrachloroethene to predominately trans-1,2-dichloroethene. *Environ Sci Technol* 38:4300–4303. doi:10.1021/es035439g
- Grosten A, Edwards EA (2006) Growth of *Dehalobacter* and *Dehalococcoides* spp. during degradation of chlorinated ethanes. *Appl Environ Microb* 72:428–436. doi:10.1128/AEM.72.1.428-436.2006
- Hendrickson ER, Payne JA, Young RM, Starr MG, Perry MP, Fahnestock S et al (2002) Molecular analysis of *Dehalococcoides* 16S ribosomal DNA from chloroethene-contaminated sites throughout North America and Europe. *Appl Environ Microb* 68:485–495. doi:10.1128/AEM.68.2.485-495.2002
- Holliger C, Schraa G, Stams AJ, Zehnder AJ (1993) A highly purified enrichment culture couples the reductive dechlorination of tetrachloroethene to growth. *Appl Environ Microb* 59:2991–2997
- Holliger C, Wohlfarth G, Diekert G (1999) Reductive dechlorination in the energy metabolism of anaerobic bacteria. *FEMS Microbiol Rev* 22:383–398. doi:10.1111/j.1574-6976.1998.tb00377.x
- Jiang X, Martens D, Schramm KW, Kettrup A, Xu SF, Wang LS (2000) Polychlorinated organic compounds (PCOCs) in waters, suspended solids and sediments of the Yangtze River. *Chemosphere* 41:901–905. doi:10.1016/s00456535(99)00435-x
- Kittelmann S, Friedrich MW (2008) Novel uncultured *Chloroflexi* dechlorinate perchloroethene to trans-dichloroethene in tidal flat sediments. *Environ Microbiol* 10:1557–1570. doi:10.1111/j.1462-2920.2008.0157.x
- Kranzloch I, Tiehm A (2012) Assessment of pollutant biodegradation at the Yangtze Three Gorges Dam, China. *Int J Water Management* “blue facts” 2012:70–77
- Liu H, Zhou Q, Wang Y, Zhang Q, Cai Z, Jiang G (2008) E-waste recycling induced polybrominated diphenyl ethers, polychlorinated biphenyls, polychlorinated dibenzo-*p*-dioxins and dibenzofurans pollution in the ambient environment. *Environ Int* 34:67–72. doi:10.1016/j.envint.2007.07.008
- Löffler FE, Sun Q, Li J, Tiedje JM (2000) 16S rRNA gene-based detection of tetrachloroethene-dechlorinating *Desulfuromonas* and *Dehalococcoides* species. *Appl Environ Microb* 66:1369–1374. doi:10.1128/AEM.66.4.1369.1374.2000
- Löffler FE, Yan J, Ritalahti KM, Adrian L, Edwards EA, Konstantinidis KT et al (2012) *Dehalococcoides mccartyi* gen. nov., sp. nov., obligate organohalide-respiring anaerobic bacteria, relevant to halogen cycling and bioremediation, belong to a novel bacterial class, *Dehalococcoidetes classis* nov., within the phylum *Chloroflexi*. *Int J Syst Evol Microbiol*. doi:10.1099/ijs.0.034926-0
- Lohner ST, Tiehm A (2009) Application of electrolysis to stimulate microbial reductive PCE dechlorination and oxidative VC biodegradation. *Environ Sci Technol* 43:7098–7104. doi:10.1021/es900835d
- Lohner ST, Becker D, Mangold K-M, Tiehm A (2011) Sequential reductive and oxidative biodegradation of chloroethenes stimulated in a coupled bioelectro-process. *Environ Sci Technol* 45:6491–6497. doi:10.1021/es200801r
- Maphosa F, de Vos WM, Smidt H (2010) Exploiting the ecogenomics toolbox for environmental diagnostics of organohalide-respiring bacteria. *Trends Biotechnol* 28:308–316. doi:10.1016/j.tibtech.2010.03.005
- Marco-Urrea E, Nijenhuis I, Adrian L (2011) Transformation and carbon isotope fractionation of tetra- and trichloroethene to trans-dichloroethene by *Dehalococcoides* sp. strain CBDB1. *Environ Sci Technol* 45:1555–1562. doi:10.1021/es1023459
- Maymó-Gatell X, Nijenhuis I, Zinder SH (2001) Reductive dechlorination of cis-1,2-dichloroethene and vinyl chloride by *Dehalococcoides ethenogenes*. *Environ Sci Technol* 35:516–521. doi:10.1021/es001285i
- Müller B, Berg M, Yao ZP, Zhang XF, Wang D, Pfluger A (2008) How polluted is the Yangtze river? Water quality downstream from the Three Gorges Dam. *Sci Total Environ* 402:232–247. doi:10.1016/j.scitotenv.2008.04.049
- Ritalahti KM, Löffler FE, Rasch EE, Koenigsberg SS (2005) Bioaugmentation for chlorinated ethene detoxification: bioaugmentation and molecular diagnostics in the bioremediation of chlorinated ethene-contaminated sites. *Ind Biot* 1:114–118. doi:10.1089/ind.2005.1.114
- Rouzeau-Szynalski K, Maillard J, Holliger C (2011) Frequent concomitant presence of *Desulfitobacterium* spp. and *Dehalococcoides* spp. in chloroethene-dechlorinating microbial communities. *Appl Microbiol Biot* 90:361–368. doi:10.1007/s00253-010-3042-0
- Schmidt KR, Tiehm A (2008) Natural attenuation of chloroethenes: identification of sequential reductive/oxidative biodegradation by microcosm studies. *Water Sci Technol* 58:1137–1145. doi:10.2166/wst.2008.729
- Schmidt KR, Stoll C, Tiehm A (2006) Evaluation of 16S-PCR detection of *Dehalococcoides* at two chloroethene-contaminated sites. *Water Sci Technol* 6:129–136. doi:10.2166/ws.2006.787
- Schmidt KR, Augenstein T, Heidinger M, Ertl S, Tiehm A (2010) Aerobic biodegradation of cis-1,2-dichloroethene as sole carbon source: stable carbon isotope fractionation and growth characteristics. *Chemosphere* 78:527–532. doi:10.1016/j.chemosphere.2009.11.033
- Shen C, Tang X, Cheema SA, Zhang C, Khan MI, Liang F et al (2009) Enhanced phytoremediation potential of polychlorinated biphenyl contaminated soil from e-waste recycling area in the presence of randomly methylated-beta-cyclodextrins. *J Hazard Mater* 172:1671–1676. doi:10.1016/j.jhazmat.2009.08.064
- Smidt H, de Vos WM (2004) Anaerobic microbial dehalogenation. *Annu Rev Microbiol* 58:43–73. doi:10.1146/annurev.micro.58.030603.123600
- Smits THM, Devenoges C, Szynalski K, Maillard J, Holliger C (2004) Development of a real-time PCR method for quantification of the three genera *Dehalobacter*, *Dehalococcoides*, and *Desulfitobacterium* in microbial communities. *J Microbiol Meth* 57:369–378. doi:10.1016/j.mimet.2004.02.003

- Taş N, van Eekert MHA, Wagner A, Schraa G, de Vos WM, Smidt H (2011) Role of *Dehalococcoides* spp. in the anaerobic transformation of hexachlorobenzene in European rivers. *Appl Environ Microbiol* 77:4437–4445. doi:10.1128/AEM.01940-10
- Tiehm A, Schmidt KR (2011) Sequential anaerobic/aerobic biodegradation of chloroethenes-aspects of field application. *Curr Opin Biotech* 22:415–421. doi:10.1016/j.copbio.2011.02.003
- Tiehm A, Schmidt KR, Pfeifer B, Heidinger M, Ertl S (2008) Growth kinetics and stable carbon isotope fractionation during aerobic degradation of cis-1,2-dichloroethene and vinyl chloride. *Water Res* 42:2431–2438. doi:10.1016/j.watres.2008.01.029
- Vancheeswaran S, Hyman MR, Semprini L (1999) Anaerobic biotransformation of trichlorofluoroethene in groundwater microcosms. *Environ Sci Technol* 33:2040–2045. doi:10.1021/es9811952
- Wang J, Bi Y, Pfister G, Henkelmann B, Zhu K, Schramm KW (2009) Determination of PAH, PCB, and OCP in water from the Three Gorges Reservoir accumulated by semipermeable membrane devices (SPMD). *Chemosphere* 75:1119–1127. doi:10.1016/j.chemosphere.2009.01.016
- Zhang J (1995) Geochemistry of trace metals from Chinese river/estuary systems: an overview. *Estuar Coast Shelf S* 41:631–658. doi:10.1006/ecss.1995.0082
- Zhao HP, Schmidt KR, Tiehm A (2010) Inhibition of aerobic metabolic cis-1,2-di-chloroethene biodegradation by other chloroethenes. *Water Res* 44:2276–2282. doi:10.1016/j.watres.2009.12.023
- Zhao HP, Schmidt KR, Lohner S, Tiehm A (2011) Robustness of an aerobic metabolically vinyl chloride degrading bacterial enrichment culture. *Water Sci Technol* 64:1796–1803. doi:10.2166/wst.2011.752

B.3 The Yangtze-Hydro Project: a Chinese–German environmental program

The Yangtze-Hydro Project: a Chinese–German environmental program

A. Bergmann · Y. Bi · L. Chen · T. Floehr · B. Henkelmann · A. Holbach · H. Hollert · W. Hu · I. Kranzioch · E. Klumpp · S. Küppers · S. Norra · R. Ottermanns · G. Pfister · M. Roß-Nickoll · A. Schäffer · N. Schleicher · B. Schmidt · B. Scholz-Starke · K.-W. Schramm · G. Subklew · A. Tiehm · C. Temoka · J. Wang · B. Westrich · R.-D. Wilken · A. Wolf · X. Xiang · Y. Yuan

Received: 5 October 2011 / Accepted: 10 October 2011 / Published online: 20 October 2011
© Springer-Verlag 2011

Abstract Water of good quality is one of the basic needs of human life. Worldwide, great efforts are being undertaken for an assured water supply. In this respect, one of the largest water technology projects worldwide is the Yangtze Three Gorges Dam in China. There is a need for extensive scientific and technical understanding of the challenges arising from this large

hydrological engineering project. German and Chinese groups from various scientific fields are collaborating to provide knowledge for the sustainable management of the reservoir. In this project description, the Yangtze Three Gorges Dam Project, its goals and challenges, are described in brief, and the contributions of the German research projects are presented.

Responsible editor: Philippe Garrigues

A. Bergmann · R.-D. Wilken · A. Wolf
IWW Water Centre, Water Resources Management,
45476 Mülheim/Ruhr, Germany

Y. Bi · J. Wang
State Key Laboratory of Freshwater Ecology and Biotechnology,
Institute of Hydrobiology, Chinese Academy of Sciences,
Wuhan 430072, People's Republic of China

L. Chen
College of Environmental and Resource Sciences,
Zhejiang University,
Hangzhou 310058, People's Republic of China

L. Chen · S. Küppers · X. Xiang
Central Division of Analytical Chemistry, Research Centre Jülich,
52425 Jülich, Germany

T. Floehr · H. Hollert (✉) · R. Ottermanns · M. Roß-Nickoll ·
A. Schäffer · B. Schmidt · B. Scholz-Starke · Y. Yuan
Institute of Biology V, RWTH Aachen University,
52074 Aachen, Germany
e-mail: henner.hollert@bio5.rwth-aachen.de

B. Henkelmann · G. Pfister · K.-W. Schramm
Institute of Ecological Chemistry,
Helmholtz Zentrum München–German Research Center
for Environmental Health,
85764 Neuherberg, Germany

A. Holbach · W. Hu · S. Norra · N. Schleicher
Institute for Mineralogy and Geochemistry,
Karlsruhe Institute of Technology,
76128 Karlsruhe, Germany

I. Kranzioch · A. Tiehm
Water Technology Center,
76139 Karlsruhe, Germany

E. Klumpp
Institute of Bio- and Geosciences, Agrosphere,
Research Centre Jülich,
52425 Jülich, Germany

Y. Bi · K.-W. Schramm · C. Temoka · J. Wang
Center of Life and Food Sciences Weihenstephan, Biosciences,
Technische Universität München,
85350 Freising, Germany

G. Subklew
Institute of Bio- and Geosciences, Plant Sciences,
Research Centre Jülich,
52425 Jülich, Germany

B. Westrich
Institute of Hydraulic Engineering, University of Stuttgart,
70569 Stuttgart, Germany

X. Xiang
School of Geographical Sciences, Southwest University,
Chongqing 400715, People's Republic of China

Keywords Water quality · Human impact · Research cooperation · Yangtze River

1 Introduction

Under normal conditions, obtaining water of high quality is not a concern in Western Europe. However, in view of climate change, additional efforts are necessary to assure a permanent supply of high-quality drinking water.

The situation is quite different in China. Due to a growing demand for water in households and industry, more and more people are suffering from water scarcity. The Chinese authorities regard the diversion of water from the southern areas in China to the North by water channels as a promising alternative to mitigate this problem (Subklew et al. 2010). Closely linked to these challenging planning and engineering activities are numerous dam construction projects in the southern part of China. The largest dam in China—and one of the largest worldwide—is the Three Gorges Dam, which dams the Yangtze River between Sandouping (near Yichang) and Chongqing along a length of about 660 km (<http://www.yangtze-project.de/wasser/>, accessed on 6 July 2011).

As there are many technical, ecological, and social challenges linked with such a large project, the German Federal Ministry of Education and Research has been providing financial support for five German research institutions to perform applied research on changing land use, soil erosion, mass movements, and matter fluxes in a highly dynamic ecosystem since 2008/2009. Since August 2010, another six German partners receive funding for research on sustainable water management (Yangtze-Hydro).

Within Yangtze-Hydro, they cooperate with Chinese research groups from a number of universities, institutes of the Chinese Academy of Sciences, the China Research Academy of Environmental Sciences, and other research centres. In this presentation, the objectives of the joint project are introduced.

2 Background

The People's Republic of China has an area of about 9.6 million square kilometres, making it one of the biggest countries on earth with some of the largest rivers on the planet. The 6,300-km-long Yangtze, which rises in the Qinghai-Tibetan Plateau, passes through 11 Chinese provinces with a population of about 400 million including the city of Shanghai, where it flows into the East China Sea. The upper Yangtze down to Yichang (with a catchment area of about 100,104 km²) is more than 4,300 km in length, the central section down to Hu-kou (outlet of Lake Poyang) more than 950 km (catchment area roughly 68,104 km²)

and the lower section down to the estuary is about 930 km long (catchment area, 12,104 km²).

Over the past 100 years, the annual water discharge of the upper Yangtze at Yichang has varied between 5,000 m³/s in January and 40,000 m³/s in the rainy summer months. In the months from June to September, there are also considerable amounts of suspended matter transported. In the course of the last few decades, the periods of both low and high discharges have become more and more extreme so that by the end of the 1970s, the saltwater intrusion from the East China Sea combined with a very low water level had already severely affected the water supply of the city of Shanghai.

The first plans for damming the Yangtze in the region of the Three Gorges and regulating its flow were put forward in 1919, the National People's Congress finally approved the construction plans in 1992 and the dam was completed in 2009. With this gigantic project, the national executive is pursuing the aims of:

- Preventing flooding
- Safeguarding the water supply
- Enhancing navigation and
- Generating electric energy

In the future, fluctuations of the water level of up to 30 m will be deliberately applied in the dammed-up section of the river. Up to the start of the rainy period, from the end of May until early June, the water level is lowered to 145 m above sea level in order to provide storage volume for the peak discharge during the following months and to allow sediment flushing. After the maximum water volume has passed, the water level is raised in October to the highest level of 175 m above sea level. Peak energy production then begins. In the months from January to May, the water level is then gradually reduced again to 145 m in order to compensate for the lack of precipitation during the dry winter and thus to increase the flow downstream of the dam. This is intended to combat sediment formation in the reservoir in the months from June to September and to wash away some of the existing deposits.

The Yangtze-Hydro Project is related to the most relevant changes in water and sediment quality as:

- Eutrophication by wastewater and agrochemicals, which may lead to algae blooming and water hyacinth growth
- Re-solution of pollutants from flooded urban, industrial and agricultural areas
- Sediment accumulation along the reservoir and especially in front of the dam
- Possibly unknown contamination of toxic inorganic and organic trace compounds from industry, municipal wastewater discharge, landfill deposits, and waste (Müller et al. 2008)

3 The Yangtze-Hydro Consortium and the aims of the joint research

The German Consortium consists of four work packages and the project coordination:

1. Dynamics of physico-chemical parameters within the new reservoir
 - Karlsruhe Institute of Technology in collaboration with the China Research Academy of Environmental Sciences (CRAES) has two tasks. One task is to analyse the spatio-temporal dynamics of physico-chemical parameters within the reservoir by means of a towed underwater sensor system (called MiniBAT). This sensor system is able to detect online and in situ parameters such as temperature, turbidity, chlorophyll a, pH, electrical conductivity, oxygen and hydrogen sulphide. The sensor system will be extended to include a TOC sensor and a sampling system during the project (Casagrande 1995; Stüben et al. 1998). Furthermore, a free flow sampler will be used to monitor water quality at various depths. The other task is the numerical modelling of transport dynamics supported by the data obtained in task one and from further German and Chinese partners (Westrich and Förstner 2007).
2. Concentration of substances
 - IWW Water Centre, Water Resources Management, will perform a contaminant survey focusing on organic pollutants on the Yangtze River as they do on the River Rhine and a comparison of Chinese and German standards for water quality aspects (Ministry of Environmental Protection of the PR of China 1999) and will investigate suitable water technologies to obtain clean and safe drinking water (Wateruse) (Bergmann 2011).
3. Behaviour and transformation of contaminants
 - RWTH Aachen University, Biology V, is a project partner with strong connections to Chinese groups, especially to Nanjing University, Chongqing University and Tongji University in Shanghai. They will work on the process understanding of biological transformation, bioaccumulation and ecotoxicological evaluation of pollutants (Wolz et al. 2009).
 - Technische Universität München (TUM) has developed a monitoring tool for evaluating the bioaccumulation of non-polar organic compounds. The so-called “Biovirtous”, a virtual passive sampling fish, will be installed at different places in the reservoir, thus obtaining information on the contamination of the reservoir with non-polar persistent pollutants

such as pesticides in fish, other lipophilic biota and sediments (Wang et al. 2009).

- Research Center Jülich with IBG-3 Agrosphere and the Central Division of Analytical Chemistry (ZCH) addresses the physico-chemical processes of pollutant evaluation at the sediment/water interface (Zhang et al. 2010) and the modelling of their chemical degradation (Hoffmann et al. 2011).
4. Degradation of contaminants
 - Water Technology Center, Karlsruhe (TZW), will study microbiological processes to understand the degradation of chlorinated hydrocarbons under oxidative and reductive conditions in the water phase and the sediment (Schmidt and Tiehm 2008; Tiehm and Schmidt 2011).
 5. Project coordination

The project coordination of the Yangtze projects is performed in Jülich by Günter Subklew. The coordination of Yangtze-Hydro is performed by Rolf-Dieter Wilken from IWW.

4 Chinese partners (in alphabetical order of the home town of the institution) complement the German projects:

- Chinese Research Academy of Environmental Sciences, Beijing
- Standing Office of the State Council Three Gorges Project Construction Committee, Beijing
- Chinese Research Academy of Environmental Sciences, Beijing
- Chongqing University, Chongqing
- Zhejiang University, Hangzhou
- Nanjing University, Nanjing
- Tongji University, Shanghai
- Yangtze Water Resources Protection Institute, Wuhan
- Chinese Academy of Sciences, Institute of Hydrobiology/ Institute of Hydroecology, Wuhan
- China Three Gorges University, Yichang

In the future, additional partners are expected to join the project network.

The overall aims of the German Yangtze-Hydro projects is to support the Chinese partners in the field of sustainable management of the Yangtze Three Gorges Dam ecological system, where the Chinese partners have already obtained a great deal of experience and have developed a variety of strategies to deal with the upcoming challenges caused by the dam project.

References

- Subklew G, Ulrich J, Fürst L, Höltkemeier A (2010) Environmental impacts of the Yangtze Three Gorges project: an overview of the Chinese-German research cooperation. *J Earth Sci* 21:817–823
- Müller B, Berg M, Ping Yao Z, Feng Zhang X, Wang D, Pfluger A (2008) How polluted is the Yangtze River? Water quality downstream from the Three Gorges Dam. *Sci Total Environ* 402:232–247
- Casagrande CE (1995) The MiniBAT-a miniaturized towed sampling system. *OCEANS '95. MTS/IEEE. Challenges of our changing global environment. Conference Proceedings* 1:638–641
- Stüben D, Walpersdorf E, Voss K, Röncke H, Schimmele M, Baborowski M, Luther G, Elsner W (1998) Application of lake marl at Lake Arendsee, NE Germany: first results of a geochemical monitoring during the restoration experiment. *Sci Total Environ* 218:33–44
- Westrich B, Förstner U (eds) (2007) *Sediment dynamics and pollutant mobility in rivers—an interdisciplinary approach*. Springer, Heidelberg
- Ministry of Environmental Protection of the PR of China (1999) Environmental quality standard for surface water (1999) GHZB1-1999. Available at: www.zhb.gov.cn/eic/650208300025053184/20050512/7546.shtml. Accessed on 17 Oct 2005
- Bergmann A (2011) IWW forscht im Auftrag des BMBF am Drei-Schluchten-Staudamm in China. *IWW-Journal* 35:13
- Wolz J, Cofalla C, Hudjetz S, Roger S, Brinkmann M, Schmidt B, Schaffer A, Kammann U, Lennartz G, Hecker M, Schuttrumpf H, Hollert H (2009) In search for the ecological and toxicological relevance of sediment re-mobilisation and transport during flood events. *J Soils Sed* 9:1–5
- Wang J, Bi Y, Pfister G, Henkelmann B, Zhu K, Schramm KW (2009) Determination of PAH, PCB, and OCP in water from the Three Gorges Reservoir accumulated by semipermeable membrane devices (SPMD). *Chemosphere* 75:1119–1127
- Zhang J, Sequaris JM, Narres HD, Vereecken H, Klumpp E (2010) Effect of organic carbon and mineral surface on the pyrene sorption and distribution in Yangtze River sediments. *Chemosphere* 80:1321–1327
- Hoffmann Th, Hofmann D, Klumpp E, Küppers S (2011) Electrochemistry-mass spectrometry for mechanistic studies and simulation of oxidation processes in the environment. *Anal Bioanal Chem* 399:1859–1868
- Schmidt KR, Tiehm A (2008) Natural attenuation of chloroethenes: identification of sequential reductive/oxidative biodegradation by microcosm studies. *Water Sci Techn* 58(5):1137–1145
- Tiehm A, Schmidt KR (2011) Sequential anaerobic/aerobic biodegradation of chloroethenes-aspects of field application. *Curr Opin Biotechnol* 22(3):415–421